

JUN 18 1998

SANDIA REPORT

SAND98-1171/2 • TTC 1525/2

Unlimited Release

Printed May 1998

RECEIVED

JUN 23 1998

OSTI

Data and Methods for the Assessment of the Risks Associated with the Maritime Transport of Radioactive Materials Results of the SeaRAM Program Studies

Volume 2: Appendices

Jeremy L. Sprung, Stephen J. Bepalko, Francis L. Kanipe, Sieglinde Neuhauser,
James D. Smith, Richard Yoshimura, Philip C. Reardon, Clinton J. Shaffer, Rod Fisk,
Holly Tomasik, Robert J. Heid

Prepared by
Sandia National Laboratories
Albuquerque, New Mexico 87185 and Livermore, California 94550

Sandia is a multiprogram laboratory operated by Sandia Corporation,
a Lockheed Martin Company, for the United States Department of
Energy under Contract DE-AC04-94AL85000.

Approved for public release; further dissemination unlimited.



Sandia National Laboratories

REPRODUCTION QUALITY NOTICE

This document is the best quality available. The copy furnished to DTIC contained pages that may have the following quality problems:

- **Pages smaller or larger than normal.**
- **Pages with background color or light colored printing.**
- **Pages with small type or poor printing; and or**
- **Pages with continuous tone material or color photographs.**

Due to various output media available these conditions may or may not cause poor legibility in the microfiche or hardcopy output you receive.



If this block is checked, the copy furnished to DTIC contained pages with color printing, that when reproduced in Black and White, may change detail of the original copy.

Issued by Sandia National Laboratories, operated for the United States Department of Energy by Sandia Corporation.

NOTICE: This report was prepared as an account of work sponsored by an agency of the United States Government. Neither the United States Government nor any agency thereof, nor any of their employees, nor any of their contractors, subcontractors, or their employees, makes any warranty, express or implied, or assumes any legal liability or responsibility for the accuracy, completeness, or usefulness of any information, apparatus, product, or process disclosed, or represents that its use would not infringe privately owned rights. Reference herein to any specific commercial product, process, or service by trade name, trademark, manufacturer, or otherwise, does not necessarily constitute or imply its endorsement, recommendation, or favoring by the United States Government, any agency thereof, or any of their contractors or subcontractors. The views and opinions expressed herein do not necessarily state or reflect those of the United States Government, any agency thereof, or any of their contractors.

Printed in the United States of America. This report has been reproduced directly from the best available copy.

Available to DOE and DOE contractors from
Office of Scientific and Technical Information
P.O. Box 62
Oak Ridge, TN 37831

Prices available from (615) 576-8401, FTS 626-8401

Available to the public from
National Technical Information Service
U.S. Department of Commerce
5285 Port Royal Rd
Springfield, VA 22161

NTIS price codes
Printed copy: A21
Microfiche copy: A01



SAND98-1171/2
Unlimited Release
Printed May 1998

TTC-1525

**Data and Methods for the Assessment of the Risks
Associated with the Maritime Transport of Radioactive Materials
Results of SeaRAM Program Studies
Volume II--Appendices**

Jeremy L. Sprung, Stephen J. Bepalko, Francis L. Kanipe, Sieglinde Neuhauser,
James D. Smith, and Richard Yoshimura
Transportation Systems Analysis Department
Sandia National Laboratories
P.O. Box 5800
Albuquerque, NM 87185

Philip C. Reardon
PCRT Technologies
8416 Yeager Drive NE
Albuquerque, NM 87109

Clinton J. Shaffer
Science and Engineering Associates, Inc.
6100 Uptown Boulevard NE
Albuquerque, NM 87190

Rod Fisk and Holly Tomasik
Edlow International Co.
1666 Connecticut Avenue NW, Suite 201
Washington, DC 20009

Robert J. Heid
Engineering Computer Optecnomics, Inc.
1356 Cape St. Claire Road
Annapolis, MD 21401

Abstract**MASTER**

This report describes ship accident event trees, ship collision and ship fire frequencies, representative ships and shipping practices, a model of ship penetration depths during ship collisions, a ship fire spread model, cask-to-environment release fractions during ship collisions and fires, and illustrative consequence calculations.

DISTRIBUTION OF THIS DOCUMENT IS UNLIMITED

MEAN

DISCLAIMER

This report was prepared as an account of work sponsored by an agency of the United States Government. Neither the United States Government nor any agency thereof, nor any of their employees, makes any warranty, express or implied, or assumes any legal liability or responsibility for the accuracy, completeness, or usefulness of any information, apparatus, product, or process disclosed, or represents that its use would not infringe privately owned rights. Reference herein to any specific commercial product, process, or service by trade name, trademark, manufacturer, or otherwise does not necessarily constitute or imply its endorsement, recommendation, or favoring by the United States Government or any agency thereof. The views and opinions of authors expressed herein do not necessarily state or reflect those of the United States Government or any agency thereof.

Contents

| | | |
|---------|--|------|
| Part A. | Charter Freighters | I-1 |
| Part B. | Break-Bulk Freighters..... | I-9 |
| Part C. | Picture of Container Ship with Ro-Ro Ramp..... | I-12 |
| Part D. | Purpose-Built Ship | I-14 |
| Part E. | Transport Index and Segregation Requirements | I-23 |
| Part F. | Ocean Containers | I-25 |
| Part G. | Secured Cell Slots | I-34 |
| Part H. | Lashings and Securements..... | I-47 |
| Part I. | IMDG Segregation Requirements | I-76 |
| Part J. | DOT Segregation Requirements..... | I-87 |
| Part K. | Presentations from the IMO Special Consultative Meeting, March 4-6, 1996 | I-90 |

APPENDIX I. REPRESENTATIVE SHIPS AND SHIPPING PRACTICES

Contents

| | |
|---------------|---|
| Appendix I. | Representative Ships and Shipping Practices |
| Appendix II. | Input Data for Minorsky Calculations |
| Appendix III. | Port Ship Speed Distribution |
| Appendix IV. | Cask-to-Environment Release Fractions |

APPENDIX I. REPRESENTATIVE SHIPS AND SHIPPING PRACTICES

Part A. Charter Freighters

Radioactive materials are frequently shipped in small freighters chartered to carry the radioactive materials with other compatible materials or without other cargo. Part A of this appendix presents data (facts, figures, photographs) for two small freighters like those that have been chartered to transport radioactive materials. The first ship (*Le Bouguenais*) is a 4,800-metric-ton freighter equipped to comply with INF-2 standards. The second ship is a 2,515-ton, multi-purpose INF-2 Ro/Lo/So vessel.

Sandia National Laboratories gratefully acknowledges **Nuclear Cargo & Service** and **Transkem Spedition GmbH** for providing information on typical INF-2 multi-purpose Ro-Ro vessels.

**M/V "BOUGUENAI" EN QUELQUES CHIFFRES
FACTS AND FIGURES ON *LE BOUGUENAI***

| OFFICIAL DESCRIPTION | |
|----------------------|--------|
| Nationality | French |

| TECHNICAL CHARACTERISTICS | |
|----------------------------|---|
| Length | 90 meters |
| Width | 16 meters |
| Summer draft | 6.45 meters |
| Dead weight | 4,800 metric tons |
| Twin screws (twin engines) | 2 x 1,625 HP |
| Speed | 12.6 knots (23 km/hr) |
| Dimensions of the hold | length: 50.00 meters width: 12.65 meters height: 08.10 meters volume: 5,235 m ³ |
| Ventilation of cargo areas | 4 x 40,000 m ³ /hr ventilators |

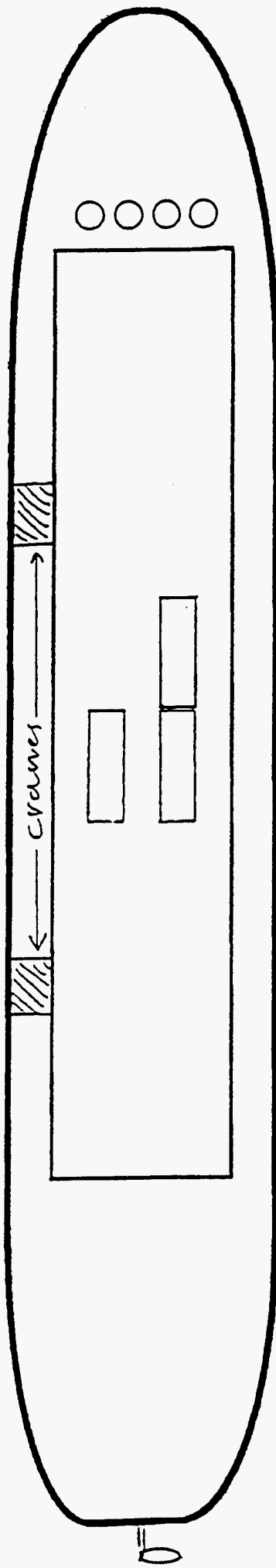
| FEATURES COMPLYING WITH INF2 STANDARDS | |
|--|--|
| Temperature control system linked to powerful cargo cooling system | |
| Extra backup electrical systems | |
| Fire detection and protection systems | |
| Radiation protection equipment | |
| Compliance with standards for stability after damage (INF2 classification) | |
| Radiation protection training program for crew | |
| Development of National Maritime Code emergency shipping plan | |

| FICHE SIGNALÉTIQUE | |
|--------------------|--------|
| Pavillon | France |

| CARACTERISTIQUES TECHNIQUES | |
|-------------------------------------|--|
| Longueur | 90 mètres |
| Largeur | 16 mètres |
| Tirant d'eau d'été | 6,45 mètres |
| Dead weight | 4 800 tonnes |
| Double motorisation | 2 X 1.625 HP |
| Vitesse | 12,6 noeuds (23 km/h) |
| Dimensions de la cale | longueur : 50,00 mètres largeur : 12,65 mètres hauteur : 08,10 mètres volume : 5 235 m ³ |
| Ventilation des espaces à cargaison | 4 ventilateurs de 40 000 m ³ /h chacun |

| SPECIFICITES PROPRES A LA MISE AUX NORMES INF2 | |
|--|--|
| Système de régulation de la température associé à un système puissant de refroidissement de la cargaison | |
| Systèmes électriques de secours renforcés | |
| Systèmes de protection et de détection incendie | |
| Équipement de matériel de radioprotection | |
| Réponse aux normes de stabilité après avarie (classe INF2) | |
| Organisation d'un plan de formation à la radioprotection du personnel de bord | |
| Elaboration d'un plan d'urgence transport CMN/TN | |

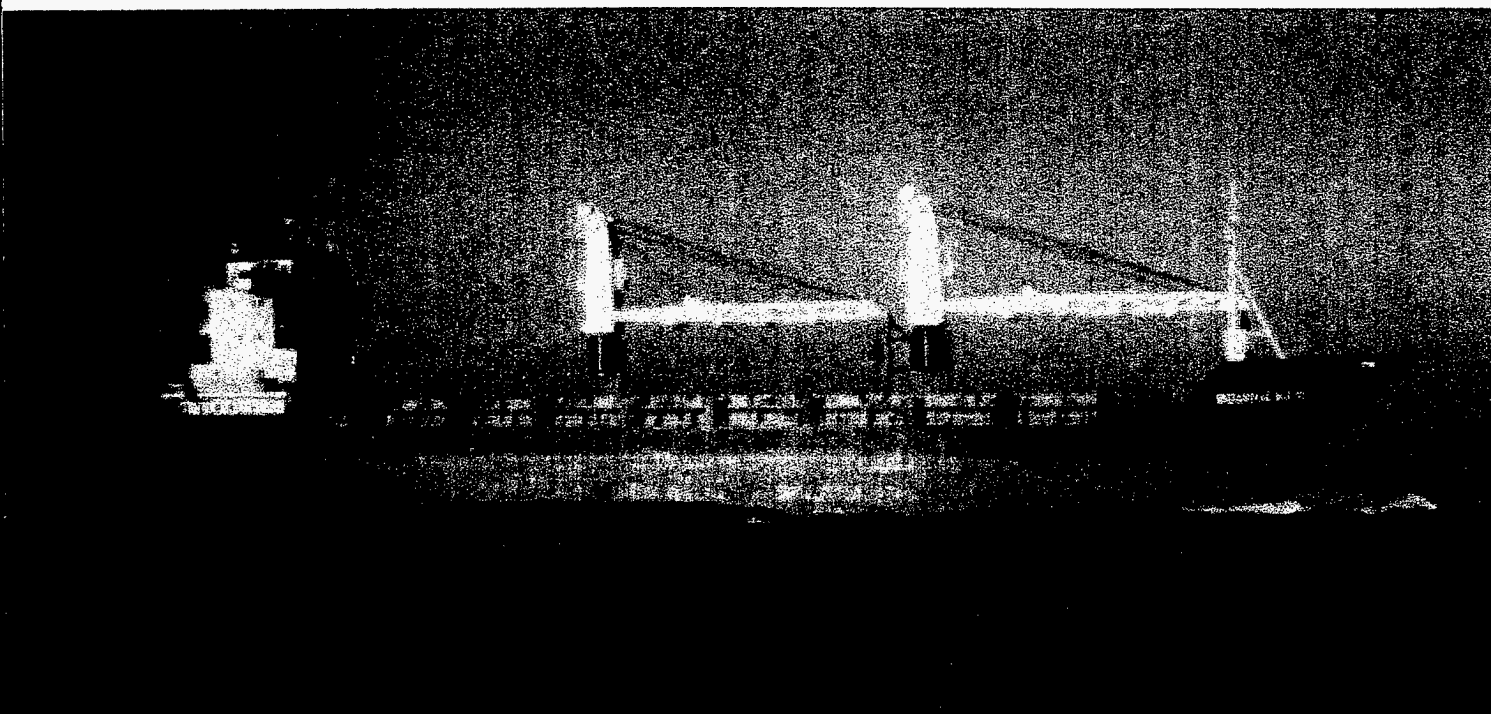
LOADING PLAN



Remarks : - Loading : 3 containers 20' each containing radioactives materials :

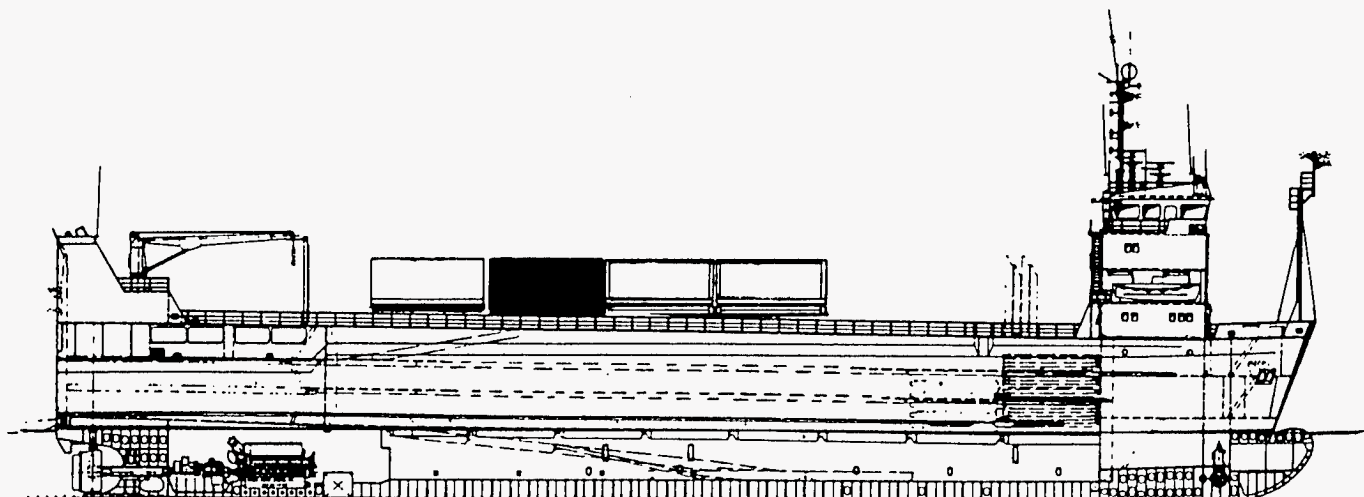
"2918, RADIOACTIVE MATERIAL, FISSILE, N.O.S, in type B(U)I' package, 7, schedule 12."

| TRANSNUCLÉAIRE | DATE | SIGNATURE | CAPTAIN | DATE | SIGNATURE |
|----------------|----------|-----------|------------|----------|-----------|
| M. DEGUETTE | 22/08/95 | | D. DUHAYON | 28/09/95 | |



Le Bouguenais Charter Freighter.

MULTI-PURPOSE VESSEL



| | | |
|--|--|--|
| Type | Ro/Lo/So Ship | Equipment |
| Classification | GL+100 A 4 E 1 Ro-Ro-vessel, meets INF-2 requirements | 2 radars, gyro compass, autopilot, direction finder, echo sounder SATNAV, NAVTEX, telex, weather FAX Hyperbel navigator, wireless station, 2 VHF-units |
| Tonnage | 999.89 GRT / 536.28 NRT | electr.-hydr. steering gear |
| Deadweight | 2515 t | 2 electr. mooring winches, each 30/15 kN |
| Length o.a. | 88.63 m | 2 electr. mooring winches, each 45/22 kN |
| Length b.p. | 83.10 m | bow thruster, 260 kW |
| Moulded breadth | 13.60 m | |
| Draught | 5.11 m | |
| Speed | 13.00 kn | |
| Propelling machinery | | stern ramp, strengthened for up to 400 t; adjustable in length, width, height; lowerable below water level, partly no height limitation for ro/ro |
| 1 man-B&W/alpha diesel, Type 8L 28/32-FVO / 1140 kw @ 775 min ⁻¹ | | |
| 1 decontrollable pitch propeller | | 2 removable cardecks, international traffic via ramps |
| 1 reduction gear | | 1 crane, 5 t/11 m |
| Auxiliary Engines | | internal means to lift up to 50 t from trailers "take home" installation |
| 3 KHD diesel, type BA6M-OLLK, each 184 kw @ 1500 min ⁻¹ | | |
| 3 generators, each 215 kVA, 380/220 V, 50 Hz | | 480 medium size cars on 5 decks, 214 20 ft containers |
| 1 shaft driven generator, 500kVA, 380/220 V, 50 Hz | | 18 reefer plugs |



Multi-Purpose INF-2 Ro/Lo/So Vessel.

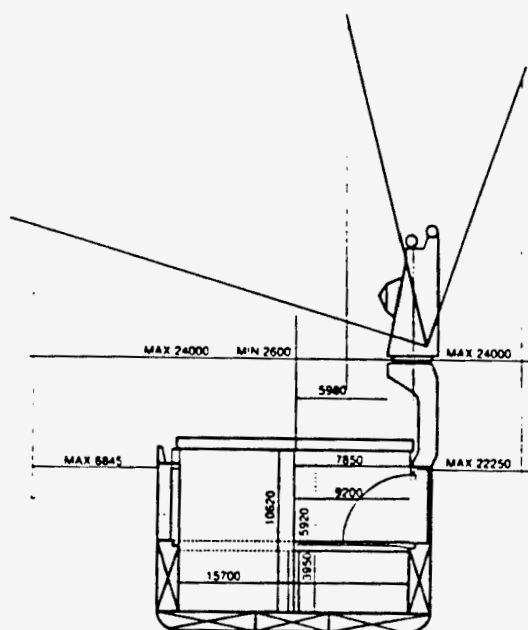
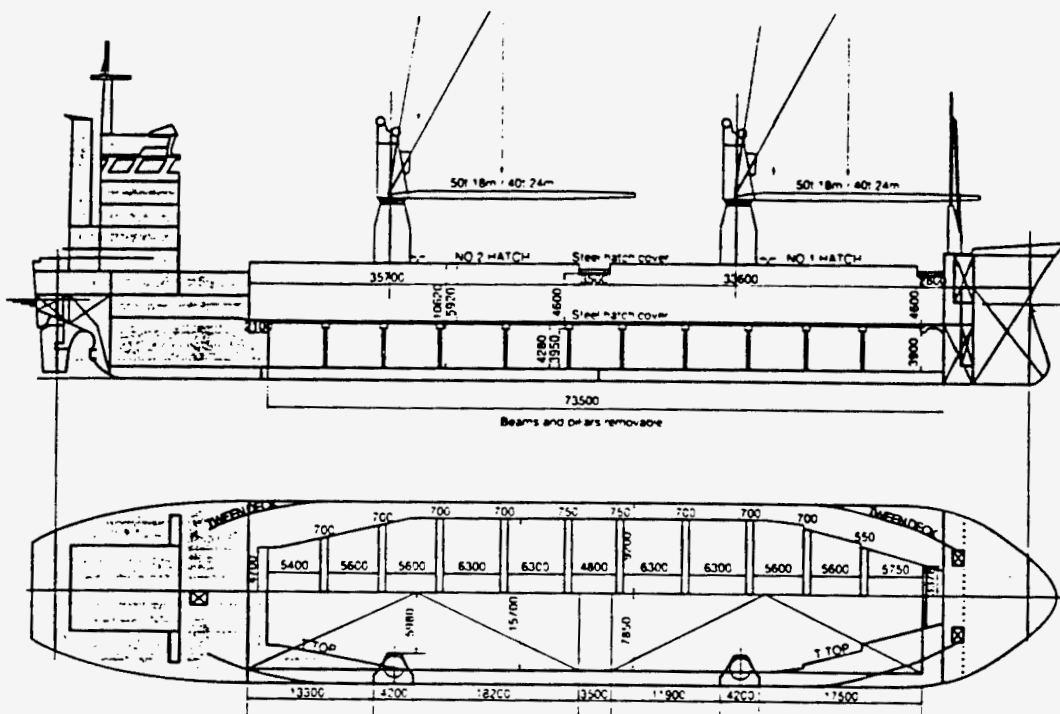


Vehicles in Hold of Multi-Purpose INF-2 Ro/Lo/So Vessel.

Part B. Break-Bulk Freighters

Radioactive materials are sometimes shipped on larger break-bulk freighters that carry other cargo besides the radioactive materials. Part B of this appendix presents a schematic and data for P2 and L type break-bulk freighters, some of which meet both INF-1 and INF-2 requirements and have been used to transport radioactive materials.

Sandia National Laboratories gratefully acknowledges permission from **Spliethoff's Bevrachtungskantoor B.V.** to reproduce the schematic and data for the P2 and L type break-bulk freighters.



P₂- AND L-TYPE

P₂-TYPE

1986 POOLGRACHT
1986 PARKGRACHT
1986 PIETERSGRACHT

L-TYPE

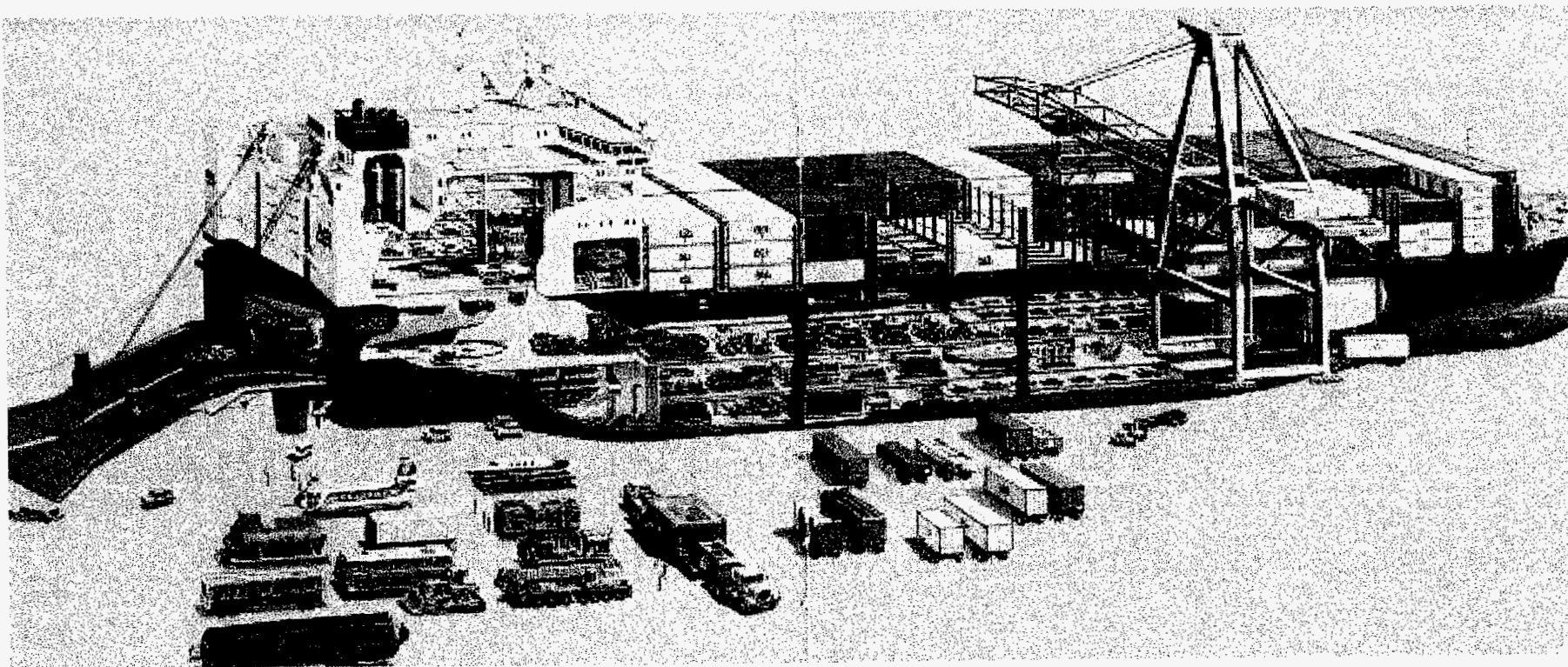
1987 LELIEGRACHT
1987 LODIERSGRACHT
1987 LUNBAANSGRACHT
1988 LAURIERGRACHT

1988 LEVANTGRACHT
1988 LEMMERGRACHT
1988 LINDENGRACHT
1989 LOOTSGRACHT

| | | P2-TYPE AND L-TYPE | | | | | |
|---|--------------|---|-----|-------|------------------|-----|-------|
| CLASS | | LLOYD'S * 100 A1 * LMC - UMS | | | | | |
| Ice Class Finnish/Swedish | | 1A | | | | | |
| | | strengthened for heavy cargoes: Great Lakes fitted optional | | | | | |
| PRINCIPAL DIMENSIONS | | | | | | | |
| Length over all | | 113.00 m | | | | | |
| Breadth moulded | | 18.90 m | | | | | |
| Height in hold as SID | | 10.62 m | | | | | |
| Height in lower hold as TWD | | 3.95 m | | | | | |
| Height in tween deck as TWD | | 5.92 m | | | | | |
| Summer draft | | 8.54 m | | | | | |
| Draft for timber | | 8.79 m | | | | | |
| GT | | 5.998 | | | | | |
| NT | | 3.607 | | | | | |
| DEADWEIGHT all told | | 9.653 mt | | | | | |
| | timber mark | 10.123 mt | | | | | |
| CAPACITY | grain | LH 161.000 + UH 283.000 = 444.000 cbft/12.750 m³ | | | | | |
| | bale | LH 161.000 + UH 257.000 = 418.000 cbft/11.840 m³ | | | | | |
| FLOOR SPACE | tank top | 1.012 m² | | | | | |
| | tween deck | 1.114/1.312 m² | | | | | |
| | weather deck | 1.090/1.170 m² | | | | | |
| AIR CHANGES (basis empty holds) | | abt 25 x per hour | | | | | |
| CONTAINER INTAKE | | P2-TYPE | | | L-TYPE | | |
| | | TEU | FEU | + TEU | TEU | FEU | + TEU |
| Hold | units | 234 | 96 | + 42 | 234 | 96 | + 42 |
| Deck | units | 253 | 115 | + 23 | 333 | 152 | + 30 |
| Total | units | 487 | 211 | + 65 | 567 | 248 | + 72 |
| Without pedestals | minus | 18 | 8 | 2 | 18 | 8 | 2 |
| Power available for reefer connections | | up to 360/450 kW | | | up to 360/540 kW | | |
| TIMBER INTAKE | | abt 14.000 m³ length packages | | | | | |
| HATCHES | weather deck | no 1: 33.60 x 15.70 m no 2: 35.70 x 15.70 m | | | | | |
| | | steel, end folding type | | | | | |
| | tween deck | 70.70 x 15.70 m | | | | | |
| | | steel, side folding type; beams and pillars removable | | | | | |
| Bulkheads/compartments | | 2 sets removable for up to 6 compartments | | | | | |
| MAXIMUM LOAD | | | | | | | |
| Weather deck hatch covers | | 1.75 t/m² | | | | | |
| Tween deck hatch covers | | 3.70 t/m² | | | | | |
| Tank top | | 20.00 t/m² | | | | | |
| DECK CRANES restricted combinable | | | | | | | |
| Situating on starboard side, tons/reach | | 2 of 50 mt SWL/18 m or 40 mt SWL/24 m | | | | | |
| MAIN ENGINE | | Hanshin 6.000 HP/4 410 kW | | | | | |
| Speed | ballast | abt 15 knots | | | | | |
| | laden | abt 14 knots | | | | | |
| Fuel consumption per day | | abt 16.5 mt IFO 380 cSt | | | | | |
| | | no MDO at sea, except when manoeuvring | | | | | |
| BUNKER CAPACITY | | | | | | | |
| Intermediate Fuel Oil | | 594 m³ | | | | | |
| Marine Diesel Oil | | 120 m³ | | | | | |
| BALLAST CAPACITY | | 2.200 m³ | | | | | |

These particulars are believed to be correct, but without guarantee, and they must not be used as basis for Charter Parties or contracts without Owners' explicit written authority.

Part C. Picture of Container Ship with Ro-Ro Ramp

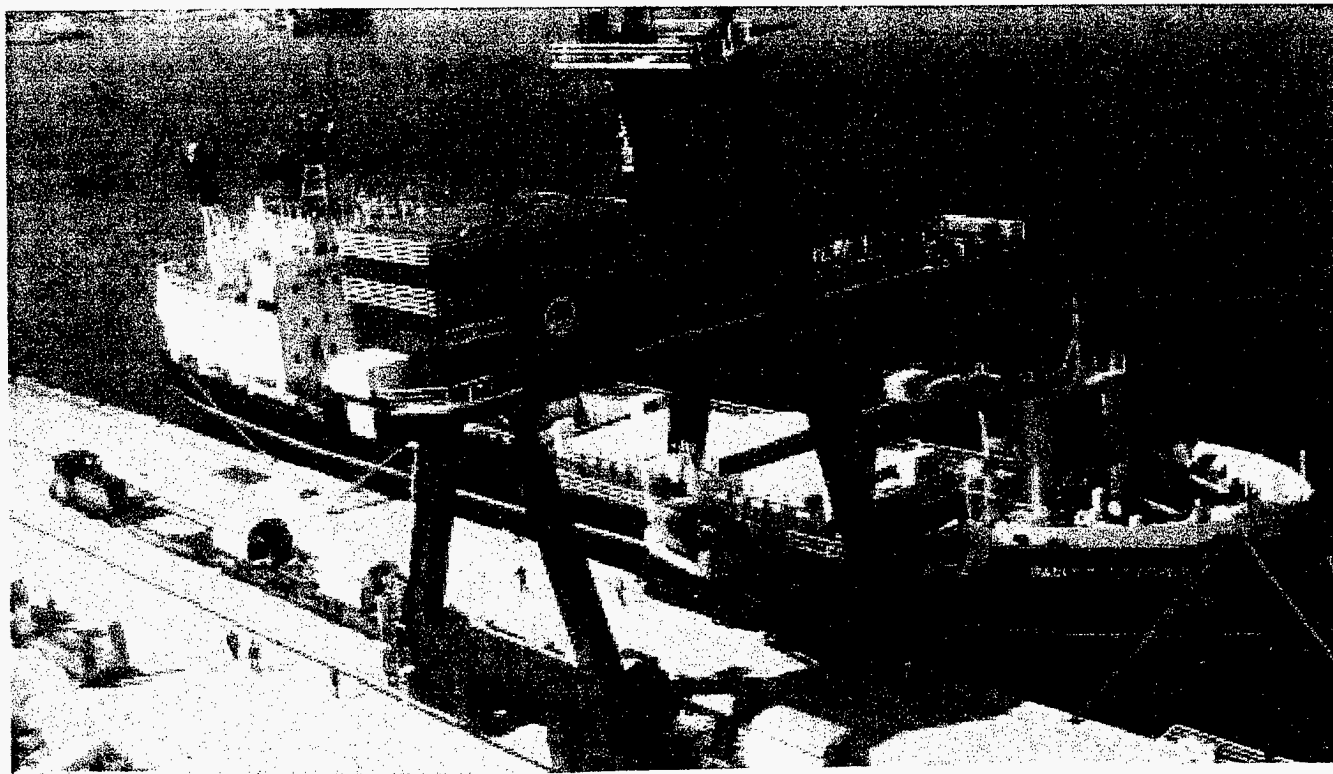


Container Ship with Ro-Ro Ramp.

Part D. Purpose-Built Ship

Highly radioactive materials are packaged in Type B casks and shipped in double-hulled ships specifically designed and built to transport these materials. Part D of this appendix reproduces an article that describes a “purpose-built” ship, which was originally published in *Transportation for the Nuclear Industry*, edited by D.G. Walton and S.M. Blackburn.

Sandia National Laboratories gratefully acknowledges permission from **British Nuclear Fuels Limited (BNFL)** to reproduce the journal article titled “Design of Ships for the Transport of Spent Nuclear Fuels” authored by H. E. Spink.



Purpose-Built Ship.

Part E. Transport Index and Segregation Requirements

Part E of this appendix reproduces portions of the International Maritime Dangerous Goods (IMDG) Code that describe the Transport Index (TI) and segregation requirements that guide the maritime shipment of radioactive materials.

CLASS 7 - Radioactive materials

4.4 TI limits for freight containers and conveyances

| Type of freight container or conveyance | Limit on total sum of transport indices in a single freight container or aboard a conveyance | | | |
|---|--|------------------|----------------------|-----------------------|
| | Not under exclusive use | | Under exclusive use | |
| | Non-fissile material | Fissile material | Non-fissile material | Fissile material |
| Freight container - small | 50 | 50 | not applicable | not applicable |
| Freight container - large | 50 | 50 | no limit | 100 |
| Road vehicle or railway wagon | 50 | 50 | no limit | 100 |
| Cargo space or defined deck area ¹ : | | | | |
| 1 Packages, overpacks, small freight containers | 50 | 50 | no limit | 100 |
| 2 Large freight containers | 200 ² | 50 | no limit | 100 |
| Whole ship ¹ : | | | | |
| 1 Packages, overpacks, small freight containers | 200 ² | 200 ² | no limit | 200 ³ |
| 2 Large freight containers | 200 ² | 200 ² | no limit | no limit ³ |

¹ Packages or overpacks carried in or on a road vehicle or railway wagon in exclusive use may be transported by ship provided that they are not removed from the road vehicle or railway wagon at any time while on the ship.

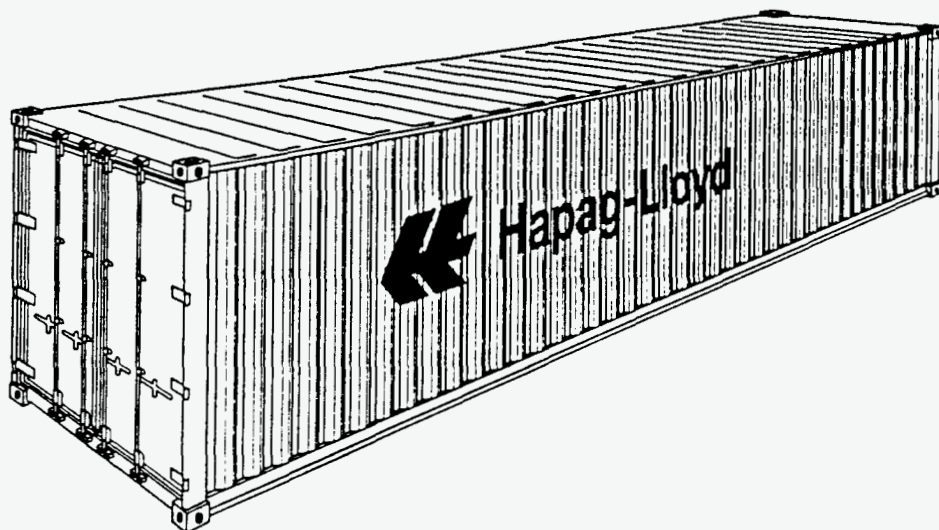
² The consignment shall be so handled and stowed that the total sum of TI's in any individual group does not exceed 50, and that each group is handled and stowed so that the groups are separated from each other by at least 6 metres.

³ The consignment shall be so handled and stowed that the total sum of TI's in any individual group does not exceed 100, and that each group is handled and stowed so that the groups are separated from each other by at least 6 metres. The intervening space between groups may be occupied by other cargo in accordance with IAEA paragraph 405.

Part F. Ocean Containers

When transported by ship, radioactive materials are transported inside of ocean containers. Part F of this appendix presents data sheets for several representative ocean containers.

Sandia National Laboratories gratefully acknowledges permission from **Hapag-Lloyd Container Linus GMBH** to reproduce representative ocean container data sheets from the *1996 Hapag-Lloyd Container Specification Booklet*.



Suitable for any general cargo.

Various lashing devices on the top and bottom longitudinal rails and the corner posts.
Lashing devices have a permissible load of 1 000 kg (2 205 lbs) each.

Note permissible weight limits for road and rail transport.

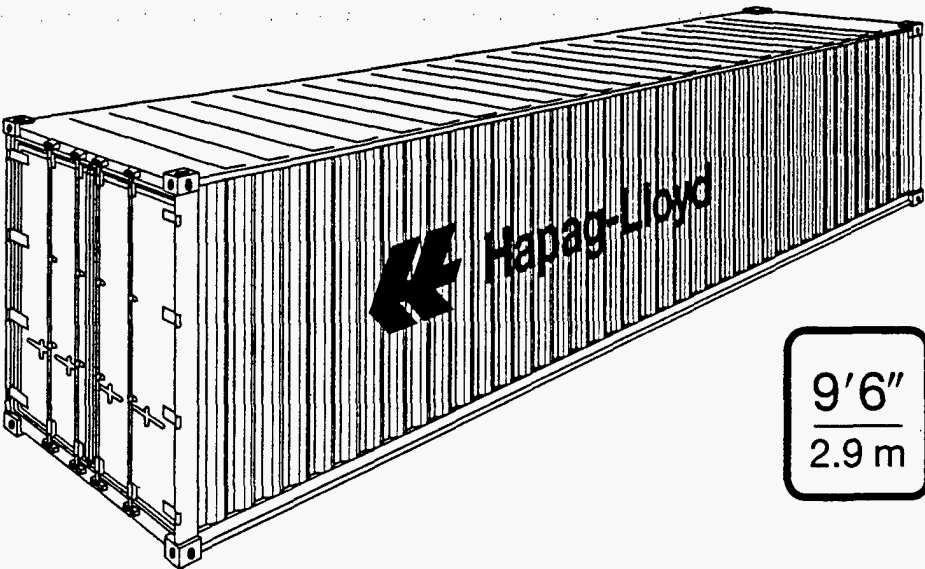
General Purpose Container

40'

| Construction | Inside Dimensions | | | Door Opening | | Weights | | | Capacity | Hapag-Lloyd Serial Number | Foot-note |
|--|-------------------|----------|-----------|--------------|----------|------------|-------|--------------|----------------|--|-------------------|
| | Length | Width | Height | Width | Height | Max. Gross | Tare | Max. Payload | | | |
| | mm | mm | mm | mm | mm | kg | kg | kg | m ³ | | |
| | ft | ft | ft | ft | ft | lbs | lbs | lbs | cu.ft | | |
| 8'6" high | | | | | | | | | | | |
| Steel container with corrugated walls and wooden floor | 12 029 | 2350 | 2392 | 2340 | 2292 | 30 480 | 3 780 | 26 700 | 67.7 | HLCU 400 000 – 428 599 HLCU 438 600 – 439 099 HLXU 400 000 – 408 999 | 1) 1) 1) 2) |
| | 39'5 1/2" | 7'8 1/2" | 7'10 1/8" | 7'8 1/2" | 7'6 1/4" | 67 200 | 8 330 | 58 870 | 2390 | | |
| | 12 024 | 2350 | 2387 | 2340 | 2292 | 30 480 | 3 810 | 26 670 | 67.7 | | |
| | 39'5 3/8" | 7'8 1/2" | 7'10" | 7'8 1/8" | 7'6 1/4" | 67 200 | 8 400 | 58 800 | 2390 | HLCU 437 100 – 438 599 | |
| | 12 033 | 2350 | 2394 | 2338 | 2280 | 30 480 | 3 800 | 26 680 | 67.7 | HLCU 435 000 – 437 099 | |
| | 39'5 3/4" | 7'8 1/2" | 7'10 1/4" | 7'8" | 7'5 3/4" | 67 200 | 8 377 | 58 823 | 2390 | | |

Remarks:

- 1) 21 lashing rings on each top longitudinal rail; particularly suitable for the transport of hanging garments.
2) Provided with passive vents.



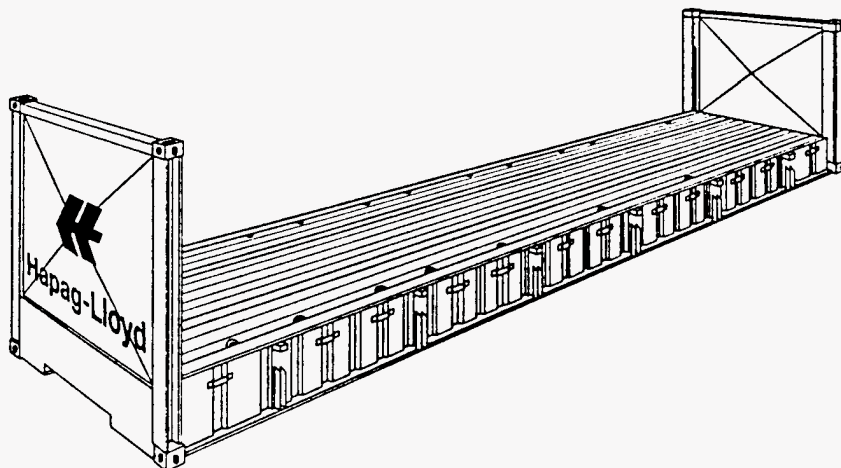
- Especially for light, voluminous cargo and overheight cargo up to max. 2.70 m (8' 10 1/4") (see table).
 - Numerous lashing devices on the top and bottom longitudinal rails and the corner posts.
- Lashing devices have a permissible load of 1 000 kg (2 205 lbs) each.
- Consider overheight for inland transportation.
 - Note permissible weight limits for road and rail transport.

High Cube General Purpose Container

40'

| Construction | Inside Dimensions | | | Door Opening | | Weights | | | Capacity | Hapag-Lloyd Serial Number | Foot- note |
|---|--------------------|-----------------|------------------|-----------------|-----------------|------------------|----------------|------------------|--------------|--|---------------|
| | Length | Width | Height | Width | Height | Max. Gross | Tare | Max. Payload | | | |
| | mm ft | mm ft | mm ft | mm ft | mm ft | kg lbs | kg lbs | kg lbs | | | |
| 9'6" high | | | | | | | | | | | |
| Steel container with corrugated walls and wooden floor | 12 024 39'53/8" | 2350 7'81/2" | 2697 8'101/8" | 2340 7'81/8" | 2597 8'61/4" | 30 480 67 200 | 4 020 8 860 | 26 460 58 340 | 76.3 2694 | HLCU 453 800 – 454 999 HLCU 455 700 – 459 799 | |
| | 12 024 39'53/8" | 2350 7'81/2" | 2697 8'101/8" | 2338 7'8" | 2585 8'53/4" | 30 480 67 200 | 4 020 8 860 | 26 460 58 340 | 76,3 2694 | HLCU 455 400 – 455 699 HLXU 450 000 – 452 999 | 1) |

Remarks:
1) Provided with passive vents.



Especially for heavy loads and overwidth cargo.

Higher loadings possible if required (please see footnote 2).

Strong bottom construction with fixed endwalls (which allow bracing and lashing of cargo as well as stacking).

Gooseneck tunnel on both ends of all 40' flats.

Numerous very strong lashing devices on the corner posts, longitudinal rails and on the floor. Lashing devices on the longitudinal rails and on the floor of 40' containers have a permissible load of 4 000 kg (8 820 lbs) each.

Maximum payload can only be used if distributed over the total floor area of the flat.

If concentration of heavy load on a small part of floor area is required please contact your Hapag-Lloyd partner office for stowage advice.

Flats are delivered without stanchions. If stanchions are required please inform us upon booking.

Note permissible weight limits for road and rail transport.

Flat

40'

| Construction | Inside Dimensions | | | | | | Weights | | | Hapag-Lloyd Serial Number | Foot- note |
|---|--------------------|-----------------------------------|-------------------|--------------------------------|---------------|---------------------|------------------|-----------------|------------------|--|----------------|
| | Length of floor | Length between Corner Posts | Width of floor | Width between Stanchions | Height | Height of Bottom | Max. Gross | Tare | Max. Payload | | |
| | mm ft | mm ft | mm ft | mm ft | mm ft | mm ft | kg lbs | kg lbs | kg lbs | | |
| 8' 6" high | | | | | | | | | | | |
| Steelframe with fixed endwalls and softwood floor | 12 008 39'4¾" | 11 712 38'5½" | 2318 7'7¼" | 2232 7'3⅞" | 1981 6'6" | 610 2' | 30 480 67 200 | 4 750 10 470 | 25 730 56 730 | HLCU 465 600 – 465 879 | 1) |
| | 11 990 39'4" | 11 722 38'5½" | 2400 7'10½" | 2202 7'2¾" | 1981 6'6" | 610 2' | 30 480 67 200 | 5 100 11 240 | 25 380 55 960 | HLCU 465 880 – 465 914 | 1) |
| | 11 990 39'4" | 11 758 38'6⅞" | 2338 7'8" | 2228 7'3¾" | 1981 6'6" | 610 2' | 30 480 67 200 | 4 200 9 265 | 26 280 57 935 | HLCU 466 000 – 466 299 | 1) |
| | 12 010 39'4⅞" | 11 832 38'9⅞" | 2228 7'3¾" | 2228 7'3¾" | 1981 6'6" | 610 2' | 30 480 67 200 | 4 200 9 265 | 26 280 57 935 | HLCU 466 300 – 466 549 | 1) |
| | 12 086 39'7⅞" | 11 826 38'9⅞" | 2224 7'3½" | 2224 7'3½" | 1981 6'6" | 610 2' | 30 480 67 200 | 4 200 9 265 | 26 280 57 935 | HLCU 466 550 – 466 899 | 1) |
| | 12 010 39'4⅞" | 11 826 38'9⅞" | 2244 7'4⅜" | 2204 7'2¾" | 1981 6'6" | 610 2' | 30 480 67 200 | 4 200 9 265 | 26 280 57 935 | HLCU 466 900 – 466 999 | 1) |
| 9' 6" high | | | | | | | | | | | |
| Steelframe with collapsible endwalls and softwood floor | 12 060 39'6¾" | 11 660 38'3½" | 2365 7'9⅞" | 2200 7'2⅝" | 2245 7'4⅜" | 648 2'1½" | 45 000 99 210 | 5 700 12 570 | 39 300 86 640 | HLCU 468 400 – 468 599 HLXU 468 000 – 468 849 | 2) 3) 2) 3) |

Remarks:

- 1) Higher loadings possible, if required up to max. gross weight 45 000 kg (99 210 lbs) according to CSC plate but please consider concentrated loads and change of weight markings of Flat.
 2) Height of bottom in folded condition 648 mm (2'1½").
 3) Timber treated according to Australian requirements.

Hardtop Container

20'

- This container type has been designed and developed by Hapag-Lloyd.
- It has especially been constructed for
 - heavy loads
 - high, and excessively high loads
 - loading, e.g. by crane, through roof opening and door side.
- The steel roof of some series (please see footnote) is fitted with fork-lift rings so that it can be removed by using a forklift. The weight of the steel roof is approx. 450 kg (990 lbs).
- With the roof removed and the door-header swung out, it is much easier to load cargo using a crane via the door side.

In case your cargo has overheight the roof sections can be lashed to a side-wall inside the container using only some 13 cm (5 1/8") of space.

If required, we can provide disposable tarpaulins for the transport which can be fastened to the walls on the outside using lashing devices.

The capacity of the container floor exceeds the ISO 1496/1 standard by 33 %, so that a fork-lift whose front axle weight does not exceed 7,280 kg (16,000 lbs) can be used inside.

The hardtop container provides many lashing devices to fasten your goods.

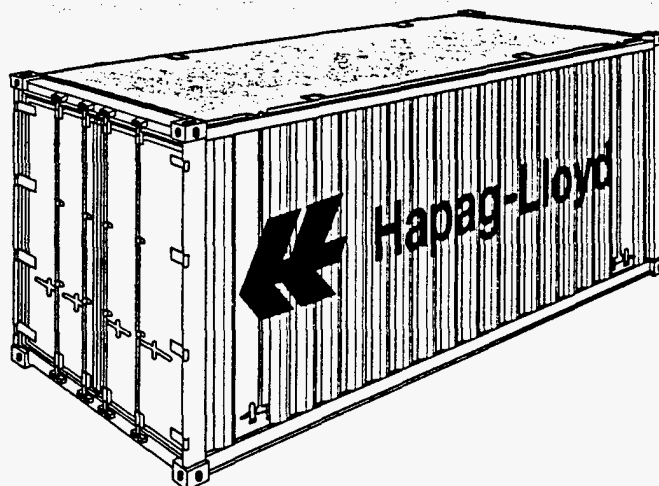
The lashing devices on the corner posts and on the longitudinal rails of the roof and floor are capable of bearing loads of up to 2,000 kg (4,410 lbs) each, and those in the middle of the side walls up to 500 kg (1,100 lbs) each. Lashing to the side walls can only be done after the roof has been closed.

This container type has been designed for heavy loads. Whilst considering the technical data (including the permissible

spreaded load limitations) please bear in mind the prevalent weight restrictions for land transport.

For further information please see page 15 and our brochure "The 20' Hardtop".

Note permissible weight limits for road and rail transport.



Hardtop Container

20'

| Construction | Inside Dimensions | | | | Weights | | | Capacity |
|--|-------------------|------------------|--------------------|------------------|------------------|----------------|------------------|-------------------------|
| | Length | Width | Height | | Max. Gross | Tare | Max. Payload | |
| | mm ft | mm ft | Middle mm ft | Side mm ft | kg lbs | kg lbs | kg lbs | m ³ cu.ft |
| 8'6" high | | | | | | | | |
| Steel container with corrugated walls and wooden floor | 5886 19'33/4" | 2342 7'8 1/8" | 2388 7'10" | 2313 7'7" | 30 480 67 200 | 2 700 5 950 | 27 780 61 250 | 32,8 1160 |
| | 5886 19'33/4" | 2342 7'8 1/8" | 2388 7'10" | 2313 7'7" | 30 480 67 200 | 2 700 5 950 | 27 780 61 250 | 32,8 1160 |
| | 5886 19'33/4" | 2342 7'8 1/8" | 2375 7'9 1/2" | 2330 7'7 3/4" | 30 480 67 200 | 2 590 5 710 | 27 890 61 490 | 32,8 1160 |
| | 5871 19'31/8" | 2338 7'8" | 2390 7'10" | 2335 7'8" | 24 000 52 910 | 2 580 5 690 | 21 420 47 220 | 32,8 1158 |

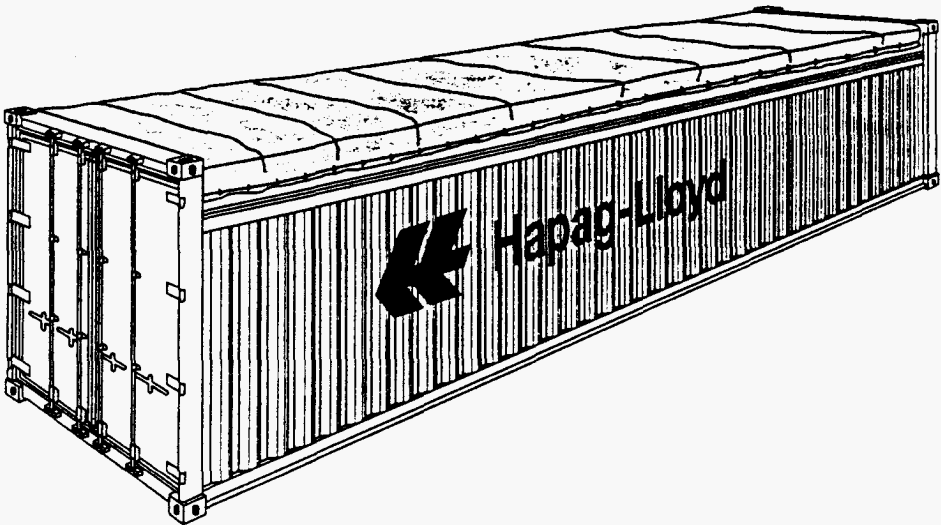
| Hapag-Lloyd Serial-Number | Footnote |
|---------------------------|----------|
| HLCU 260 200 – 261 399 | 1) 2) |
| HLXU 265 000 – 265 999 | 1) 2) |
| HLCU 261 400 – 261 799 | 1) 2) |
| HLCU 261 800 – 261 999 | 1) |
| HLCU 262 600 – 262 999 | 1) |
| HLCU 262 000 – 262 557 | |

Remarks:

1) Fork-lift pockets.

2) Roof with hinged rings for easy removal by fork lift truck.

Roof and door openings please see next page.



Especially for

- overheight cargo
- loading from top side, e.g. by crane
- loading from door side, e.g. with cargo hanging from overhead tackle.

Door header can be swung out on all open top containers.

If required, we can provide disposable tarpaulins. For fastening tarpaulins, lashing bars are available on the outside of the walls. Using one way tarpaulins requires the corner castings to be accessible.

The capacity of the floor for use of fork-lift trucks exceeds the ISO standard by 33 % on all 40' open top containers.

Numerous lashing devices on the top and bottom longitudinal rails and the corner posts.

Lashing devices have a permissible load of 1 000 kg (2 205 lbs) each.

Dimensions of roof and door openings please see page 25.
Note permissible weight limits for road and rail transport.

Open Top Container

40'

| Construction | Inside Dimensions | | | | Weights | | | Capacity | Hapag-Lloyd Serial-Number | Footnote |
|--|--------------------|-----------------|--------------------|------------------|------------------|----------------|------------------|--------------|--|----------|
| | Length | Width | Height | | Max. Gross | Tare | Max. Payload | | | |
| | mm ft | mm ft | Middle mm ft | Side mm ft | kg lbs | kg lbs | kg lbs | m³ cu.ft | | |
| 8'6" high | | | | | | | | | | |
| Steel container with corrugated walls and wooden floor | 12 023 39'53/8" | 2335 7'8" | 2378 7'95/8" | 2318 7'71/4" | 30 480 67 200 | 3 800 8 380 | 26 680 58 820 | 66,7 2354 | HLCU 460 200 – 460 289 HLCU 469 990 – 469 999 | |
| | 12 038 39'57/8" | 2338 7'8" | 2363 7'9" | 2313 7'71/8" | 30 480 67 200 | 3 650 8 050 | 26 830 59 150 | 66,7 2354 | HLCU 460 300 – 460 399 | |
| | 12 025 39'51/2" | 2330 7'73/4" | 2360 7'87/8" | 2325 7'71/2" | 30 480 67 200 | 3 890 8 580 | 26 590 58 620 | 66,0 2330 | HLCU 460 900 – 460 999 | |
| | 12 038 39'57/8" | 2336 7'8" | 2370 7'91/4" | 2320 7'71/4" | 30 480 67 197 | 3 700 8 157 | 26 780 59 040 | 65,3 2306 | HLCU 461 000 – 461 199 | |
| | 12 029 39'51/2" | 2342 7'81/8" | 2376 7'91/2" | 2326 7'71/2" | 30 480 67 200 | 3 810 8 400 | 26 670 58 800 | 65,5 2310 | HLCU 461 200 – 461 499 | |
| | 12 022 39'51/4" | 2346 7'83/8" | 2365 7'91/8" | 2315 7'71/8" | 30 480 67 200 | 3 740 8 250 | 26 740 58 950 | 65,3 2306 | HLCU 461 500 – 461 749 | |
| | 12 007 39'43/4" | 2315 7'71/8" | 2362 7'9" | 2317 7'71/4" | 30 480 67 200 | 3 950 8 710 | 26 530 58 490 | 65 2295 | HLCU 464 000 – 464 099 | |
| | 12 005 39'45/8" | 2330 7'73/4" | 2380 7'95/8" | 2340 7'81/8" | 30 480 67 200 | 4 350 9 590 | 26 130 57 610 | 65,5 2315 | HLCU 464 460 – 464 809 HLXU 460 000 – 461 549 | |

Roof and door openings please see next page.

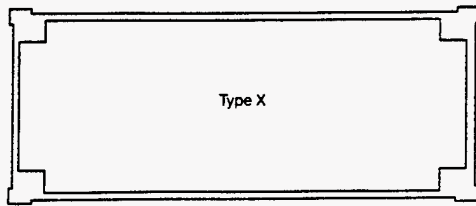
Roof and Door Openings of Open Top Containers

40'

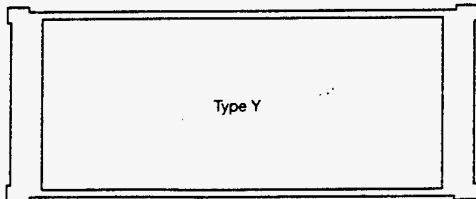
Types:

Roof Openings:

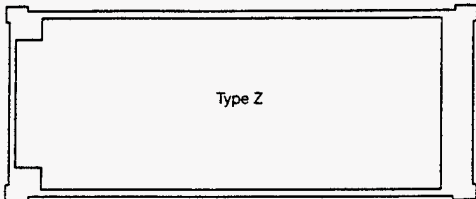
Door Openings:



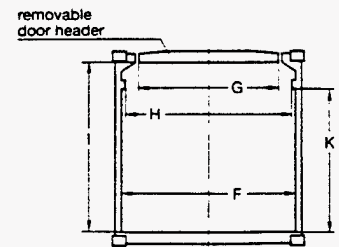
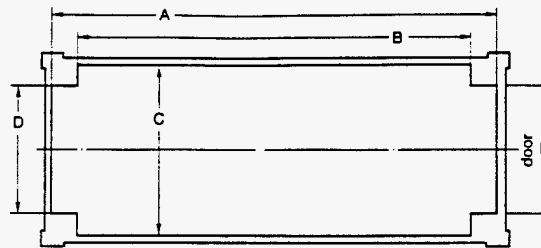
Type X



Type Y



Type Z



Roof and Door Openings of Open Top Containers

40'

Roof Openings

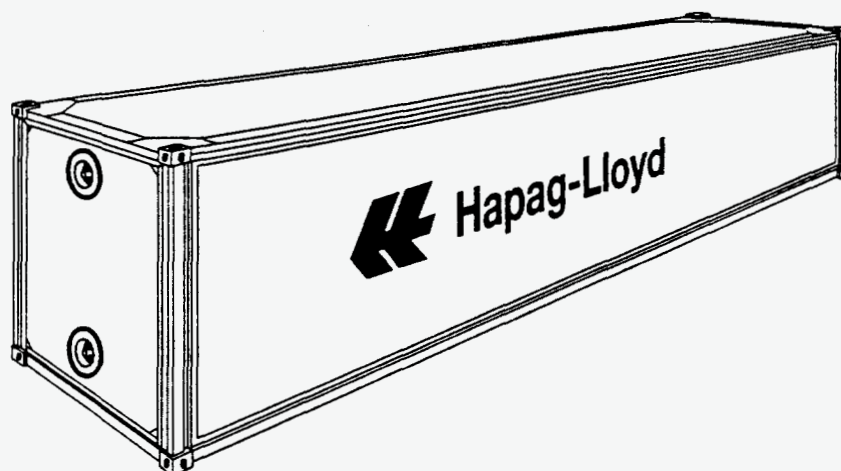
| Type | Length | | Width | | |
|------|-------------------------|---|------------------------|--|---|
| | A | B | C | D | E |
| | Max. Length mm ft | Between Gusset Plates mm ft | Max. Width mm ft | Front End, between Gusset Plates mm ft | Door End, between Gusset Plates mm ft |

Door Openings

| Width | | | Height | |
|------------------------|----------------------------------|--|-------------------------------------|---|
| F | G | H | I | K |
| Max. Width mm ft | At Door Header mm ft | Between Top Longi- tudinal Rails mm ft | Up to Door Header mm ft | Up to Top Longi- tudinal Rail mm ft |

Hapag-Lloyd
Serial No.

| | | | | | | | | | | | |
|---|---|---|--|---|--|---|--|--|---|--|--|
| Z | 11 800 38'8 ⁵ / ₈ " | 11 317 37'11 ¹ / ₂ " | 2205 7'2 ³ / ₄ " | 1728 5'8" | — | 2335 7'8" | 1840 6'1 ¹ / ₂ " | 2205 7'2 ³ / ₄ " | 2287 7'6" | 1889 6'2 ³ / ₈ " | HLCU 460 200 – 460 289 HLCU 469 990 – 469 999 |
| Z | 11 787 38'8" | 11 563 37'11 ¹ / ₄ " | 2208 7'2 ⁷ / ₈ " | 1850 6'7 ⁷ / ₈ " | — | 2335 7'8" | 1844 6'5 ⁵ / ₈ " | 2208 7'2 ⁷ / ₈ " | 2287 7'6" | 1896 6'2 ⁵ / ₈ " | HLCU 460 300 – 460 399 |
| X | 11 917 39'11 ¹ / ₈ " | 10 837 35'6 ⁵ / ₈ " | 2128 6'11 ³ / ₄ " | 1600 5'3" | 1816 5'11 ¹ / ₂ " | 2330 7'7 ³ / ₄ " | 1816 5'11 ¹ / ₂ " | 2128 6'11 ⁷ / ₈ " | 2201 7'2 ⁵ / ₈ " | 1957 6'5" | HLCU 460 900 – 460 999 |
| Y | — | 11 550 37'10 ⁵ / ₈ " | 2220 7'3 ³ / ₈ " | — | — | 2336 7'8" | 1845 6'5 ⁵ / ₈ " | 2220 7'3 ³ / ₈ " | 2292 7'6 ¹ / ₄ " | 2125 6'11 ⁵ / ₈ " | HLCU 461 000 – 461 199 |
| Z | 11 544 37'10 ¹ / ₂ " | 11 444 37'6 ¹ / ₂ " | 2230 7'3 ³ / ₄ " | — | 1885 6'2 ¹ / ₈ " | 2336 7'8" | 1885 6'2 ¹ / ₈ " | 2230 7'3 ³ / ₄ " | 2280 7'5 ³ / ₄ " | 2146 7'1 ¹ / ₂ " | HLCU 461 200 – 461 499 |
| Z | 11 550 37'10 ³ / ₄ " | 11 515 37'9 ³ / ₈ " | 2205 7'2 ³ / ₄ " | — | 1880 6'2" | 2335 7'8" | 1880 6'2" | 2205 7'2 ³ / ₄ " | 2280 7'5 ³ / ₄ " | 2125 6'11 ⁵ / ₈ " | HLCU 461 500 – 461 749 |
| Y | — | 11 379 37'4" | 2205 7'2 ³ / ₄ " | — | — | 2315 7'7 ¹ / ₈ " | 1855 6'1" | 2205 7'2 ³ / ₄ " | 2266 7'5 ¹ / ₄ " | 1957 6'5" | HLCU 464 000 – 464 099 |
| X | 11 825 38'9 ¹ / ₂ " | 11 496 37'8 ⁵ / ₈ " | 2100 6'10 ⁵ / ₈ " | 1774 5'9 ⁷ / ₈ " | 1774 5'9 ⁷ / ₈ " | 2335 7'8" | 1750 5'8 ⁷ / ₈ " | 2100 6'10 ⁵ / ₈ " | 2180 7'1 ³ / ₄ " | 2180 7'1 ³ / ₄ " | HLCU 464 460 – 464 809 HLXU 460 000 – 461 549 |



- Especially for cargo which needs constant temperatures above or below freezing point.
- Walls in "sandwich-construction", with Polyurethane foam to provide maximum insulation.
- Temperature is controlled by ship's/terminal's cooling plant or "clip-on-unit".
- The air, delivered at the correct temperature, is circulated in the container through two apertures in the front wall (supply air via the lower aperture, return air via the upper aperture).

• Possible temperatures inside the 20' containers, depending on specification of respective cooling device, from about +12 °C to -25 °C (+ 54 °F to -14 °F).

• Please note maximum stowage height in below table and as indicated by red line inside container in order to ensure proper ventilation.

• Possible temperatures inside the 40' containers, depending on specification of respective cooling device, from about +13 °C to -22 °C (+ 57 °F to -8 °F).

• Note permissible weight limits for road and rail transport.

Insulated Container

20'

| Construction | Inside Dimensions | | | Door Opening | | Weights | | | Capacity | Hapag-Lloyd Serial Number | Foot-note |
|---|-------------------|----------|---------------------|--------------|----------|------------|-----------|--------------|-------------|---------------------------|-----------|
| | Length | Width | Max. Stowage Height | Width | Height | Max. Gross | Tare | Max. Payload | | | |
| | mm ft | mm ft | mm ft | mm ft | mm ft | kg lbs | kg lbs | kg lbs | m³ cu.ft | | |
| 8' high | | | | | | | | | | | |
| Steelframe. Walls: outside plywood, coated with GRP, inside GRP shell | 5652 | 2235 | 2000 | 2235 | 2083 | 20 320 | 2 500 | 17 820 | 26,35 | HLCU 274 100 – 274 207 | 1) |
| | 18'6 1/2" | 7'4" | 6'6 3/4" | 7'4" | 6'10" | 44 800 | 5 510 | 39 290 | 930 | | |
| Steelframe. Walls outside and inside GRP | 5652 | 2235 | 2000 | 2235 | 2083 | 24 000 | 2 450 | 21 550 | 26,3 | HLCU 274 208 – 274 607 | 1) |
| | 18'6 1/2" | 7'4" | 6'6 3/4" | 7'4" | 6'10" | 52 910 | 5 400 | 47 510 | 930 | | |
| Steelframe. Walls outside and inside GRP | 5652 | 2235 | 2000 | 2218 | 2083 | 20 320 | 2 633 | 17 687 | 26,3 | HLCU 274 650 – 274 899 | 1) |
| | 18'6 1/2" | 7'8" | 6'6 3/4" | 7'3 1/4" | 6'10" | 44 800 | 5 800 | 39 000 | 930 | | |
| Steelframe. Walls outside and inside stainless steel | 5724 | 2286 | 2014 | 2286 | 2067 | 24 000 | 2 550 | 21 450 | 26,4 | HLCU 274 900 – 275 399 | 1) |
| | 18'9 3/8" | 7'6" | 6'7 1/4" | 7'6" | 6'9 3/8" | 52 910 | 5 620 | 47 290 | 933 | | |

Insulated Container

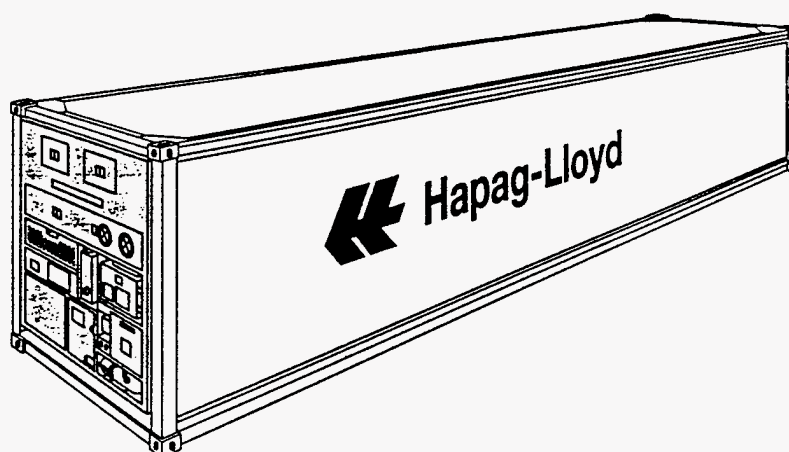
40'

| Construction | Inside Dimensions | | | Door Opening | | Weights | | | Capacity | Hapag-Lloyd Serial Number | Foot-note |
|--|-------------------|----------|---------------------|--------------|----------|------------|-----------|--------------|-------------|---------------------------|-----------|
| | Length | Width | Max. Stowage Height | Width | Height | Max. Gross | Tare | Max. Payload | | | |
| | mm ft | mm ft | mm ft | mm ft | mm ft | kg lbs | kg lbs | kg lbs | m³ cu.ft | | |
| 8'6" high | | | | | | | | | | | |
| Steelframe. Walls outside/inside: GRP coated plywood/stainless steel and aluminium/aluminium | 11 750 | 2250 | 2080 | 2250 | 2180 | 30 480 | 4 650 | 25 830 | 58,4 | HLCU 474 415 – 474 619 | 2) |
| | 38'6 5/8" | 7'4 1/2" | 6'9 7/8" | 7'4 1/2" | 7'1 7/8" | 67 200 | 10 250 | 56 950 | 2060 | | |
| Steelframe. Walls outside and inside stainless steel | 11 840 | 2286 | 2120 | 2286 | 2195 | 30 480 | 3 850 | 26 630 | 60,6 | HLCU 474 620 – 474 819 | 2) |
| | 38'10 1/8" | 7'6" | 6'11 1/2" | 7'6" | 7'2 3/8" | 67 200 | 8 490 | 58 710 | 2140 | | |
| Steelframe. Walls outside and inside stainless steel | 11 790 | 2290 | 2130 | 2286 | 2262 | 34 000 | 4 260 | 29 740 | 61,3 | HLXU 474 000 – 474 249 | 2) |
| | | | | | | | | | | | |

Remarks: 1) Used solely in the Australia/New Zealand Service. 2) Used solely in the Caribbean and South America West Coast Services.

Refrigerated Container (Temperature Controlled Container)

40'



- Especially for cargo which needs constant temperatures above or below freezing point.
- Controlled fresh-air supply is possible. Containers are ATO-approved (formerly SPRENGER).
- Walls in "sandwich-construction", with Polyurethane foam in order to provide maximum insulation.
- The reefer unit is a compact-design compressor unit with aircooled condenser. It switches automatically from cooling to heating operation (and vice versa), if a change of the outside temperatures makes it necessary.
- Please note maximum stowage height in below table and as indicated by red line inside the container in order to ensure proper ventilation.
- Possible voltages:
 - 380 V/50 Hz to 460 V/60 Hz (all refrigerated containers),
 - 200 V/50 Hz to 220 V/60 Hz (exceptions footnote 2)
- Technical specification and illustration of electric plugs see page 45.
- Note permissible weight limits for road and rail transport.

Refrigerated Container

40'

- Permissible temperature setting:
 - + 25 °C to - 25 °C
 - (+ 77 °F to - 13 °F).
- Diesel generators are installed on some 40' containers to provide a power supply (please see footnote).
- The set temperatures can be kept as long as the difference between the average outside temperature and cargo temperature does not exceed the following limits:
 - for heating 42 °C (76 °F),
 - for cooling 60 °C (108 °F).

| Construction | Inside Dimensions | | | | Door Opening | | Weights | | | Capacity | Hapag-Lloyd Serial Number | Foot note |
|---|----------------------|------------------|------------------|--------------------------|------------------|------------------|----------------------------|-------------------|------------------------------|---------------|---------------------------------|--------------|
| | Length | Width | Height | Max. Stow- age Height | Width | Height | Max. Gross kg lbs | Tare kg lbs | Max. Payload kg lbs | | | |
| | mm ft | mm ft | mm ft | mm ft | mm ft | mm ft | kg lbs | kg lbs | kg lbs | | | |
| 8'6" high | | | | | | | | | | | | |
| Steel frame. Walls: outside plywood coated with GRP, inside GRP shell | 11 141 36'4 5/8" | 2197 7'2 1/2" | 2216 7'3 1/4" | 2096 6'10 1/2" | 2197 7'2 1/2" | 2173 7'1 1/2" | 30 480 67 200 | 6 010 13 250 | 24 470 53 950 | 54,2 1920 | HLCU 370 000 – 370 199 | 1) 4) |
| | 11 141 36'4 5/8" | 2197 7'2 1/2" | 2216 7'3 1/4" | 2096 6'10 1/2" | 2197 7'2 1/2" | 2173 7'1 1/2" | 30 480 67 200 | 6 010 13 250 | 24 470 53 950 | 54,2 1920 | HLCU 470 390 – 471 089 | 1) |
| Steel frame. Walls: outside plywood coated with GRP, inside stainless steel | 11 141 36'4 5/8" | 2197 7'2 1/2" | 2216 7'3 1/4" | 2096 6'10 1/2" | 2197 7'2 1/2" | 2173 7'1 1/2" | 30 480 67 200 | 6 010 13 250 | 24 470 53 950 | 54,2 1920 | HLCU 471 090 – 471 239 | 1) |
| | 11 140 36'4 5/8" | 2226 7'3 5/8" | 2221 7'3 3/8" | 2101 6'10 5/8" | 2226 7'3 5/8" | 2173 7'1 1/2" | 30 480 67 200 | 6 010 13 250 | 24 470 53 950 | 55 1945 | HLCU 471 240 – 471 549 | 1) 2) |
| Steel frame. Walls: outside aluminium, inside stainless steel | 11 170 36'7 3/4" | 2286 7'6" | 2235 7'4" | 2115 6'11 1/4" | 2286 7'6" | 2200 7'2 5/8" | 30 480 67 200 | 5 200 11 460 | 25 280 55 740 | 57,3 2023 | HLCU 471 550 – 471 649 | 1) |
| | 11 192 36'8 5/8" | 2286 7'6" | 2240 7'5 1/4" | 2120 6'11 1/2" | 2286 7'6" | 2195 7'2 3/8" | 30 480 67 200 | 5 200 11 460 | 25 280 55 740 | 57,3 2023 | HLCU 571 650 – 572 099 | 1) |
| | 11 572 37'11 5/8" | 2286 7'6" | 2254 7'4 3/4" | 2134 7' | 2286 7'6" | 2207 7'2 7/8" | 30 480 67 200 | 4 400 9 700 | 26 080 57 500 | 59,64 2106 | HLCU 473 050 – 473 149 | 3) |
| Steel end frames. Rails aluminium. Walls: outside aluminium, inside stainless steel | 11 558 37'11" | 2286 7'6" | 2188 7'1 7/8" | 2068 6'9 3/8" | 2286 7'6" | 2161 7'1" | 30 480 67 200 | 4 140 9 130 | 26 340 58 070 | 57,8 2023 | HLCU 473 150 – 473 399 | 3) |

- Remarks:
- Equipped with diesel generator set.
 - Cannot be used with voltage 200 V/50 Hz. to 220 V/60 Hz.
 - Suitable for clip-on generator.

4) Not to be used for foodstuffs.

Part G. Secured Cell Slots

When a radioactive material transport cask is transported on a commercial container ship, the cask is placed inside an ocean container and the container is stowed in an appropriate location in accordance with the ship's container stowage/securing plan. Depending on the dimensions of the container and the structure of the stowage bay, each section of the container ship, whether on deck or below, can accommodate a specific number of a given type of container. In addition, each stowage bay is equipped with the securement tools and guides required for loading, safe storage, and discharging of each type of container. Container stowage plans must be carefully developed to ensure safe transport of cargo, optimal utilization of the ship's cargo capacity, and the shortest possible loading and discharge times. Hapag-Lloyd uses a Computer Aided Planning Stowage and Networking (CAPSTAN) software system to ensure that cargo is safely and efficiently stowed. Part G of this appendix describes the CAPSTAN system used by Hapag-Lloyd to develop container stowage plans. This description illustrates the level of detail used to construct the stowage plans for a typical container ship. Part G of this appendix also presents representative pages from a Hapag-Lloyd container securing manual that illustrate how containers are stowed on a typical container ship.

Sandia National Laboratories gratefully acknowledges permission from **Hapag-Lloyd Container Linus GMBH** to reproduce the description of their CAPSTAN system and representative pages from the *Hapag-Lloyd Container Securing Manual*.

CAPSTAN

Stowage planning on container ships capable of carrying up to 4,600 containers and a cargo weight of almost 50,000 tons on a round trip via 24 ports and three continents requires the highest precision. The safety of crew, ship and cargo is—as always—top priority. Other key aspects include:

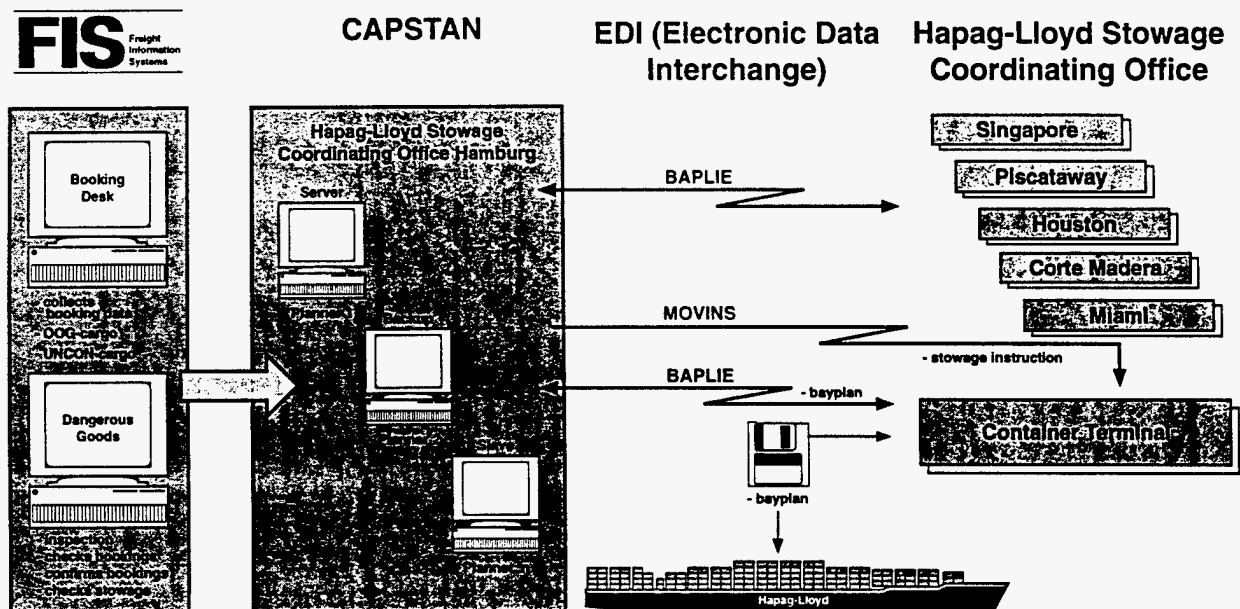
- Sound detailed planning
- Optimal capacity utilization of the container ships deployed
- Keeping to schedule and optimizing port lay days

At Hapag-Lloyd, this complex task is handled by ... stowage coordinators ... with the aid of modern computer systems. Hapag-Lloyd uses the planning system CAPSTAN. In the CAPSTAN planning module, the various bays of the respective Hapag-Lloyd container ships are represented on graphic user surfaces, [and] ports of loading and unloading [are] underlined in different colours.

The containers to be loaded are provided electronically from the Hapag-Lloyd Freight Information System (FIS) for the stowage system. This is called a "loading list" or "container announcement list" and contains all relevant data.

With a click of the mouse, the stowage coordinators take the containers from the loading list for stowing in the [container ship] bays. Symbols indicate containers with special types of cargo such as chilled or refrigerated ... At each planning phase, the stowage coordinator is given a precise overview of the ship's loading condition, i.e., capacity utilization, draught, trim, stability, bending and torsion moments, and sheer forces.

Hapag-Lloyd's CAPSTAN systems are currently installed in [Hapag-Lloyd] stowage headquarters in Hamburg, Piscataway (New York), Corte Madera (San Francisco), Houston, Miami, and Singapore. These are electronically linked with all container terminals served by Hapag-Lloyd.



From the final planning data, a stowage message is relayed electronically to these terminals (EDIFACT message MOVINS), which then serves as the basis for deployment of container cranes in the ports of call. After conclusion of loading/unloading operations in a port, the current status data from the terminal is transferred via an electronic message (EDIFACT BAPLOE) to CAPSTAN. The stowage plan thus decided on is passed on via CAPSTAN to the subsequent ports of call, [where] the [process] begins again together with the data of [any new] cargo that has to be transported. After the container ship has left the last port of loading on the continent, the message is electronically relayed to the CAPSTAN system of the overseas region and the data exchange continues.

CUSTOMER : HAPAG LLOYD

YARD / No. : HDW
NB.235

YEAR OF DELIVERY :

CLASSIFICATION SOCIETY
FOR THE SHIP : GL

CLASSIFICATION SOCIETY
FOR THE STOWAGE SYSTEM: GL

Ausfertigung
Genehmigt

Approved

Hamburg, den Tgb. Nr.

12.05.92 * 41925 / 92

Germanischer Lloyd

CONTAINER—SECURING MANUAL

DIMENSION OF THE SHIP

| | | |
|-------------------------------|------|----------|
| LENGTH OVER ALL | abt. | 235.64 r |
| LENGTH BETWEEN PP. | " | 222.49 r |
| MOULDED BREADTH | | 32.20 r |
| MOULDED DEPTH | | 18.80 r |
| DRAUGHT | | 11.02 r |
| MAX. ALLOWABLE GM VALUE | | r |
| SERVICE SPEED | | k |

12974-10-30 SHEET 1-47

CONVEI
CONVER-OSR
OCEAN-SERVICE-REPAIR-UND-
INGENIEURTECHNIK GMBH

29/2

n 2 11121 1007

[illegible]

| | | |
|------|----------|----------------|
| | 20 CONT. | 40/45/48 CONT. |
| DECK | • 60 l | 50 l |
| HOLD | 171.5 l | 213.5 l |

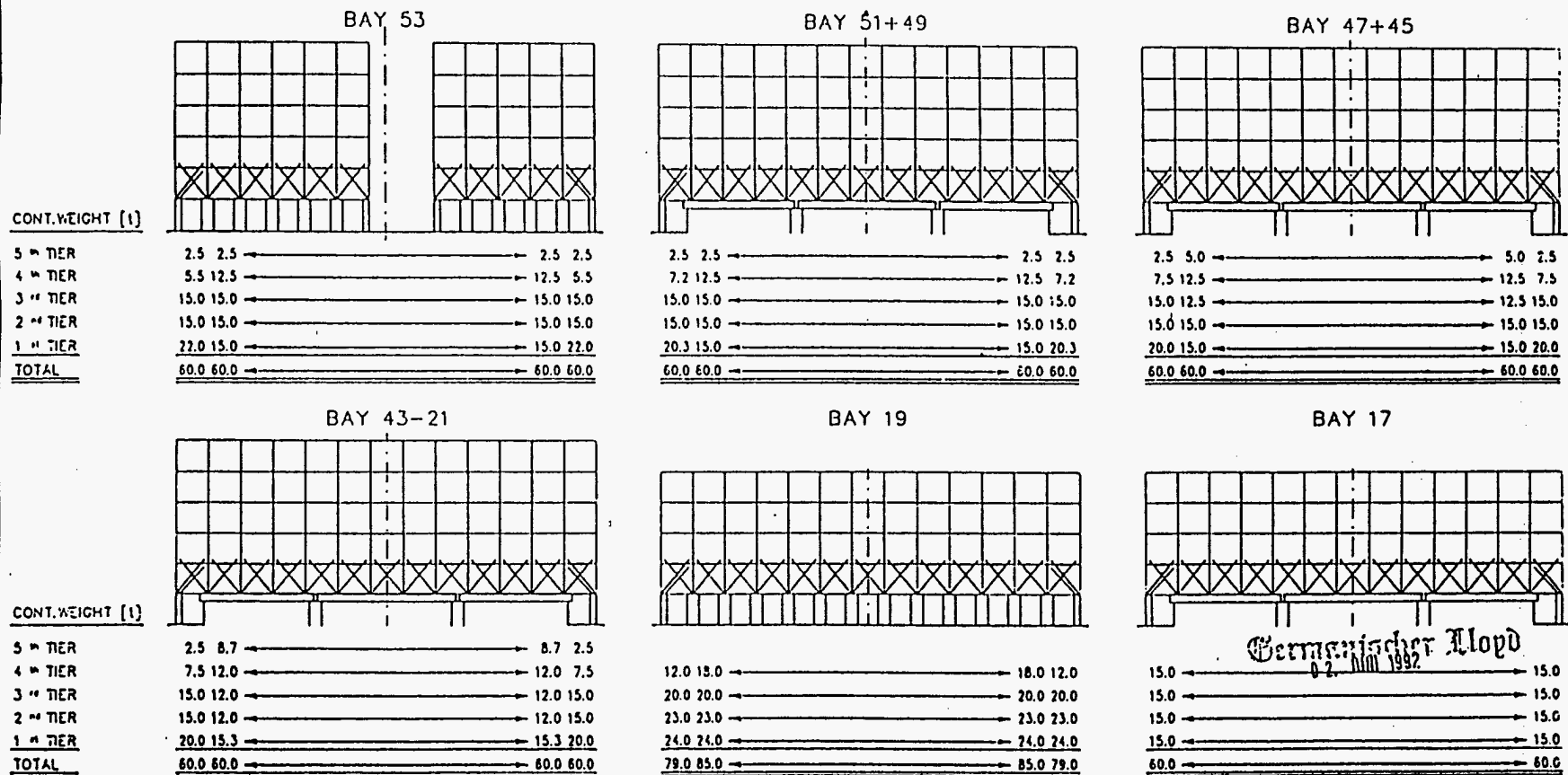
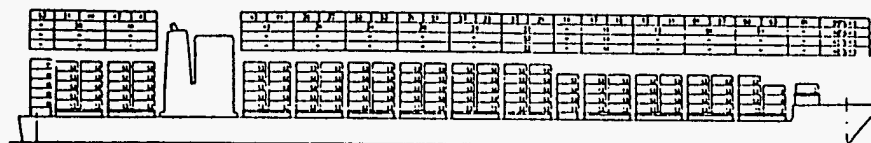
SPACES BETWEEN CONTAINERS

.9.6x.9.8x.87
 .9.6x.8x.57
 .9.8x.6x.07
 .9.8x.8x.02

CLASS OF VESSEL

ABT. 235.64 m
222.49 m
32.20 m
18.80 m
11.02 m

[illegible]

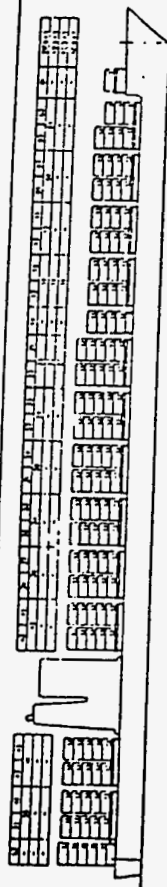


Copying of this document, and giving it to others and the use or communication of contents thereof, are forbidden without express authority. Offenders are liable to the payment of damages. All rights are reserved in the event of the grant of patent or registration of a utility model or design.

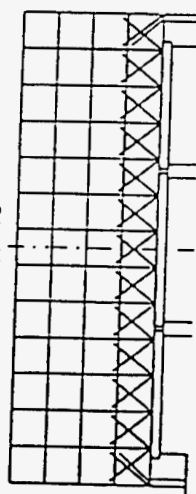
| | | | |
|--------------------|--|--------------------------|--|
| CONVER | | CONVER-OSR | |
| a Bay 03 (4.tier) | | 21.04.92 / H.H. | |
| Index Modification | | Date Name 2.04.92 / H.H. | |

20' CONTAINER STOWAGE
- DECK -

12974-10-30c
Sheet 2 /



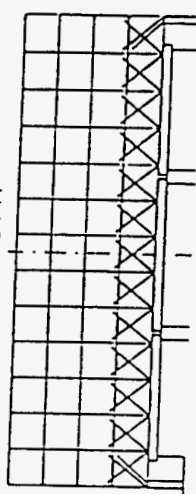
BAY 15



CONT. WEIGHT (1)

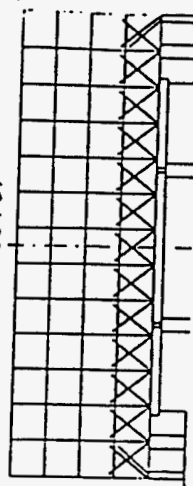
| | |
|----------------------|------|
| 5 th TIER | 15.0 |
| 4 th TIER | 15.0 |
| 3 rd TIER | 15.0 |
| 2 nd TIER | 15.0 |
| 1 st TIER | 15.0 |
| TOTAL | 60.0 |

BAY 13+11



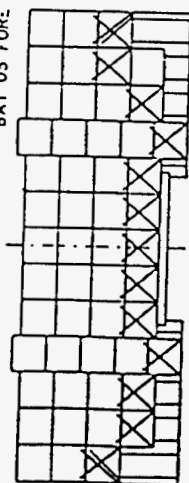
| | |
|------|------|
| 15.0 | 15.0 |
| 15.0 | 15.0 |
| 15.0 | 15.0 |
| 15.0 | 15.0 |
| 60.0 | 60.0 |

BAY 09+07



| | | | |
|------|------|------|------|
| 14.0 | 15.0 | 15.0 | 15.0 |
| 15.0 | 15.0 | 15.0 | 15.0 |
| 15.0 | 15.0 | 15.0 | 15.0 |
| 16.0 | 15.0 | 15.0 | 15.0 |
| 60.0 | 60.0 | 60.0 | 60.0 |

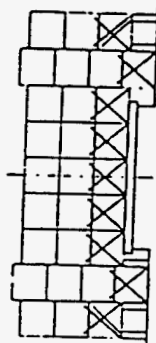
BAY 05 AFT



CONT. WEIGHT (1)

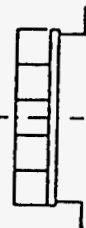
| | | | | | |
|----------------------|------|------|------|------|------|
| 5 th TIER | 15.0 | 15.0 | 8.0 | 15.0 | 15.0 |
| 4 th TIER | 15.0 | 15.0 | 8.0 | 15.0 | 15.0 |
| 3 rd TIER | 15.0 | 15.0 | 8.0 | 15.0 | 15.0 |
| 2 nd TIER | 15.0 | 15.0 | 8.0 | 15.0 | 15.0 |
| 1 st TIER | 15.0 | 15.0 | 8.0 | 15.0 | 15.0 |
| TOTAL | 60.0 | 60.0 | 60.0 | 60.0 | 60.0 |

BAY 03



| | |
|------|------|
| 15.0 | 15.0 |
| 20.0 | 15.0 |
| 20.0 | 15.0 |
| 20.0 | 15.0 |
| 60.0 | 60.0 |

BAY 01



Germanis A/C 11/11/83

24.0 24.0 24.0 24.0 24.0
24.0 24.0 24.0 24.0 24.0

Copying of this document, and giving it to others and the use or communication of contents thereof, are forbidden without express authority. Offenders are liable to the payment of damages. All rights are reserved in the event of the grant of patent or registration of a utility model or design.

CONVER 05R
CONVER-OSR
CONVER-OSR20' CONTAINER STORAGE
- DECK -

12974-10-30

Sheet 3 /

Copying of this document, and giving it to others and the use or communication of contents thereof, are forbidden without express authority. Clients are liable to the payment of damages. All rights are reserved in the event of the grant of patent or registration of a utility model or design.

| Index | Modification |
|-------|-----------------|
| 0 | Bay 03 (4.11er) |

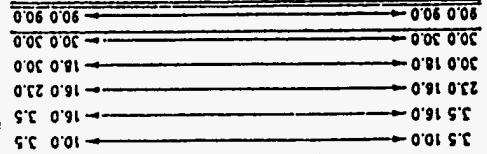
| Date | Name |
|----------|------|
| 21.01.97 | J.L. |

| Date | Name |
|---------|------|
| 2.04.92 | J.L. |

| Sheet | 12 / |
|-------------|------|
| 12974-10-30 | |

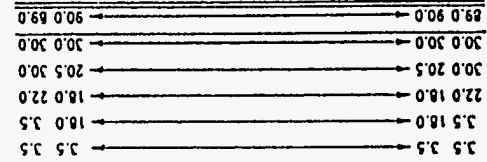
40' / 45' / 48' CONTAINER STOWAGE
- DECK -

| CONT. WEIGHT (t) |
|------------------|
| TOTAL |
| 1 " MER |
| 2 " MER |
| 3 " MER |
| 4 " MER |
| 5 " MER |

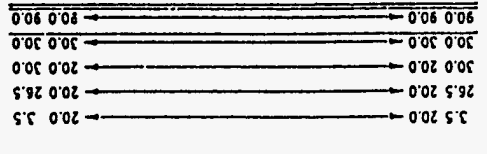


BAY 22

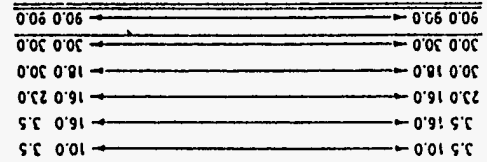
| CONT. WEIGHT (t) |
|------------------|
| TOTAL |
| 1 " MER |
| 2 " MER |
| 3 " MER |
| 4 " MER |
| 5 " MER |



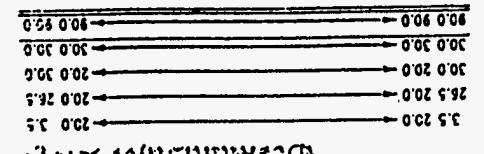
BAY 50



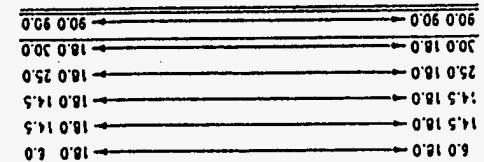
45' CONT. BAY 22+16



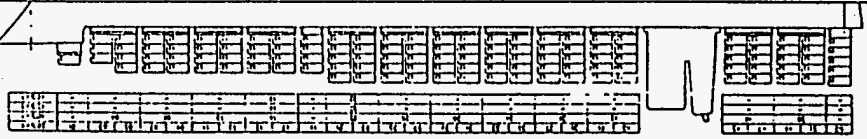
BAY 46

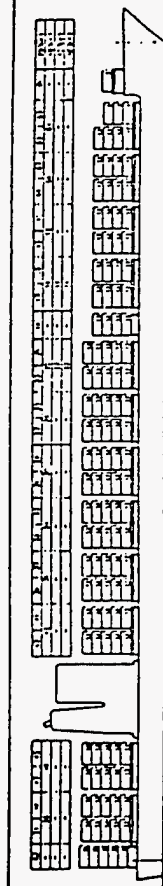


48' CONT. BAY 22+16

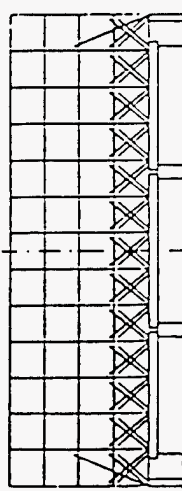


BAY 42, 38, 34, 30, 26





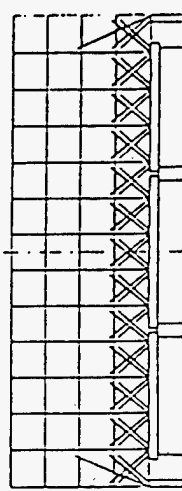
BAY 16



CONT. WEIGHT (t)

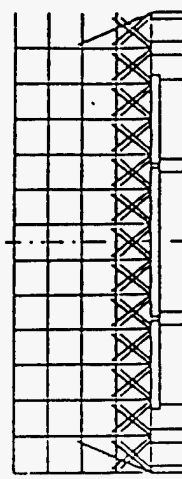
| | | | |
|----------------------|-------------|---|-----------|
| 5 th TIER | 13.5 20.0 | → | 20.0 13.5 |
| 4 th TIER | 25.0 20.0 | → | 20.0 25.0 |
| 3 rd TIER | 25.0 22.5 | → | 22.5 25.0 |
| 2 nd TIER | 26.5 27.5 | → | 27.5 26.5 |
| 1 st TIER | 90.0 90.0 | → | 90.0 90.0 |
| TOTAL | → 90.0 90.0 | | |

BAY 12



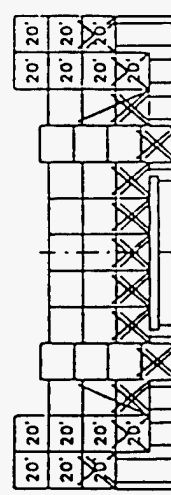
| | | | |
|----------------------|-------------|---|-----------|
| 5 th TIER | 13.5 20.0 | → | 20.0 13.5 |
| 4 th TIER | 25.0 20.0 | → | 20.0 25.0 |
| 3 rd TIER | 25.0 22.5 | → | 22.5 25.0 |
| 2 nd TIER | 26.5 27.5 | → | 27.5 26.5 |
| 1 st TIER | 90.0 90.0 | → | 90.0 90.0 |
| TOTAL | → 90.0 90.0 | | |

BAY 08



| | | | |
|----------------------|-------------|---|-----------|
| 5 th TIER | 11.5 19.0 | → | 19.0 11.5 |
| 4 th TIER | 25.0 20.0 | → | 20.0 25.0 |
| 3 rd TIER | 25.0 20.0 | → | 20.0 25.0 |
| 2 nd TIER | 27.5 30.0 | → | 30.0 27.5 |
| 1 st TIER | 29.0 89.0 | → | 89.0 29.0 |
| TOTAL | → 89.0 89.0 | | |

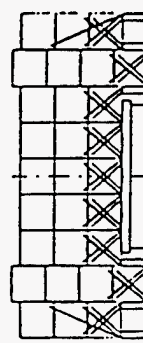
BAY 04 AFT



CONT. WEIGHT (t)

| | | | |
|----------------------|----------------------------|---|--------------------------|
| 5 th TIER | 15.0 10.0 | → | 10.0 15.0 |
| 4 th TIER | 20.0 15.0 30.0 20.0 30.0 | → | 30.0 20.0 30.0 15.0 20.0 |
| 3 rd TIER | 20.0 15.0 30.0 30.0 30.0 | → | 30.0 30.0 30.0 15.0 20.0 |
| 2 nd TIER | 20.0 15.0 30.0 30.0 30.0 | → | 30.0 30.0 30.0 15.0 20.0 |
| 1 st TIER | 60.0 60.0 90.0 90.0 90.0 | → | 90.0 90.0 90.0 60.0 60.0 |
| TOTAL | → 90.0 90.0 90.0 60.0 60.0 | | |

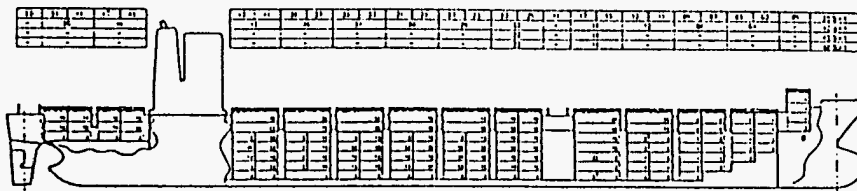
BAY 04 FORE



| | | | |
|----------------------|------------------|---|----------------|
| 5 th TIER | 10.0 10.0 | → | 10.0 10.0 |
| 4 th TIER | 30.0 20.0 30.0 | → | 30.0 20.0 30.0 |
| 3 rd TIER | 30.0 30.0 30.0 | → | 30.0 30.0 30.0 |
| 2 nd TIER | 30.0 30.0 30.0 | → | 30.0 30.0 30.0 |
| 1 st TIER | 90.0 90.0 90.0 | → | 90.0 90.0 90.0 |
| TOTAL | → 90.0 90.0 90.0 | | |

02. April 1992
Germanischer Lloyd

| | | | | | |
|--|--|---|--|-------------------------------------|---------------------------|
| Copying of this document, and giving it to others and the use or communication of contents thereof, are forbidden without express authority. Offenders are liable to the payment of damages. All rights are reserved in the event of the grant of patent or registration of a utility model or design. | | 5 Bay 03 (4 tier) Index Modification | 71013 / ALK Date Name 2.04.92 / ALK | 40' CONTAINER STOWAGE -- DECK -- | 12974-10-30 Sheet 13 / |
|--|--|---|--|-------------------------------------|---------------------------|

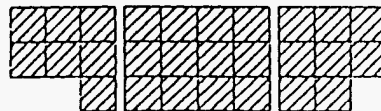


BAY 01,03,05,21,23 : 20' CELL GUIDE
 BAY 08-50 : 40' CELL GUIDE

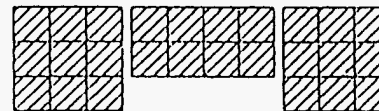
MAX. CONTAINER WEIGHTS

BAY 37,39,41,43
 4 TIERS = 20.3t/CONT.
 BAY 11,13,09,07
 4 TIERS = 18.38t/CONT.
 3 TIERS = 24.0t/CONT.
 2 TIERS = 24.0t/CONT.

BAY 51

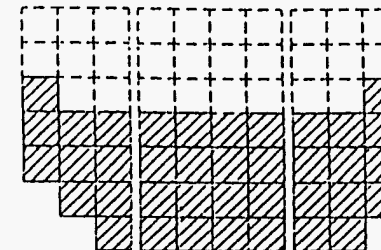


BAY 49

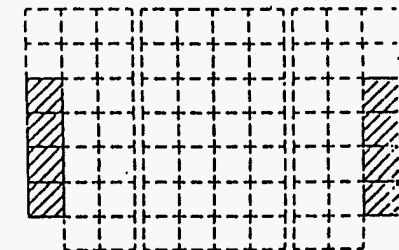


BAY 47+45

BAY 43

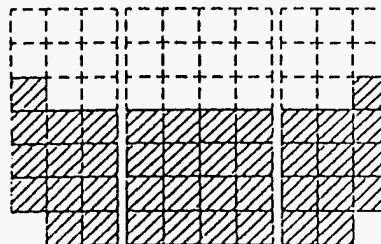


BAY 41

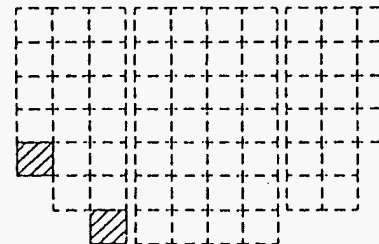


BAY 39+37

BAY 35-25

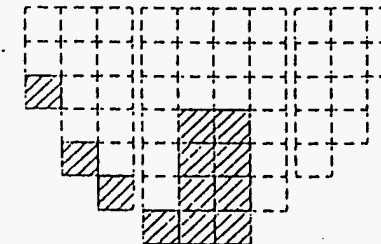


BAY 17



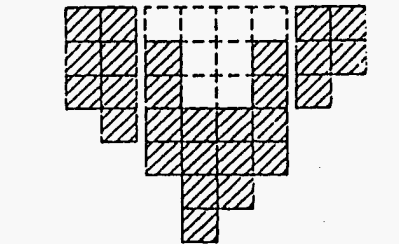
BAY 15

BAY 13



BAY 11

BAY 09



BAY 07

Germanischer Lloyd
 02. JUNI 1992

Copying of this document, and giving it to others and the use or communication of contents thereof, are forbidden without express authority. Offenders are liable to the payment of damages. All rights are reserved in the event of the grant of patent or registration of a utility model or design.

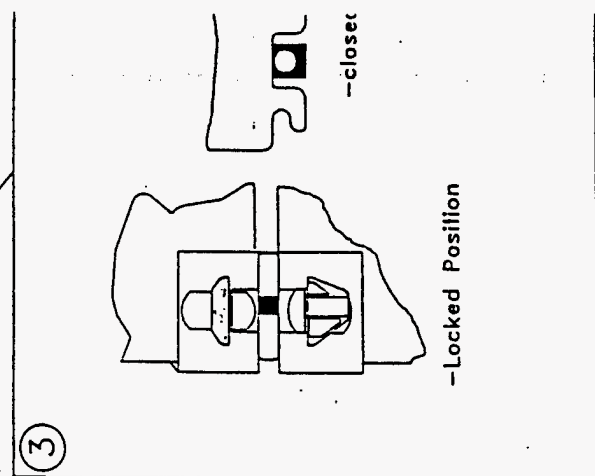
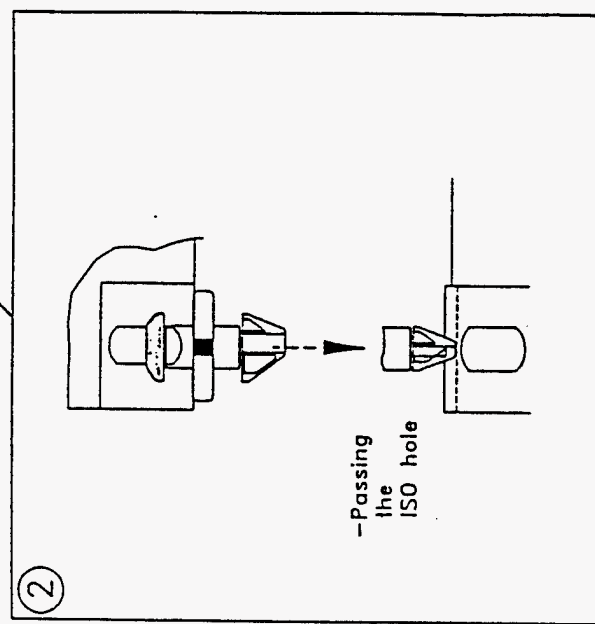
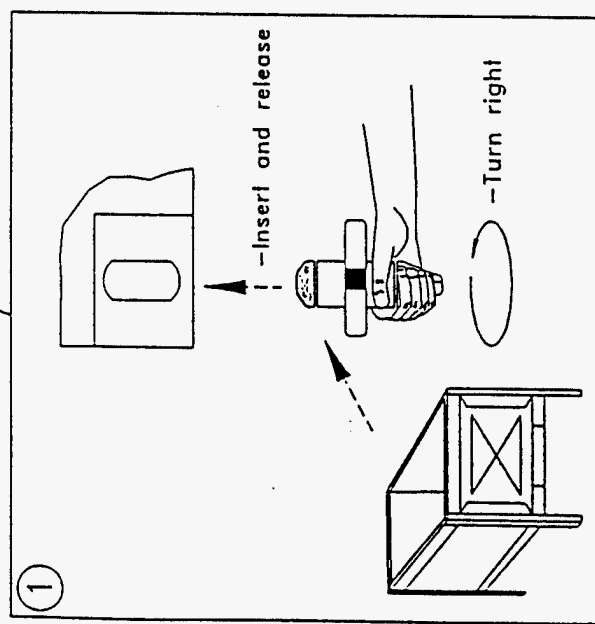
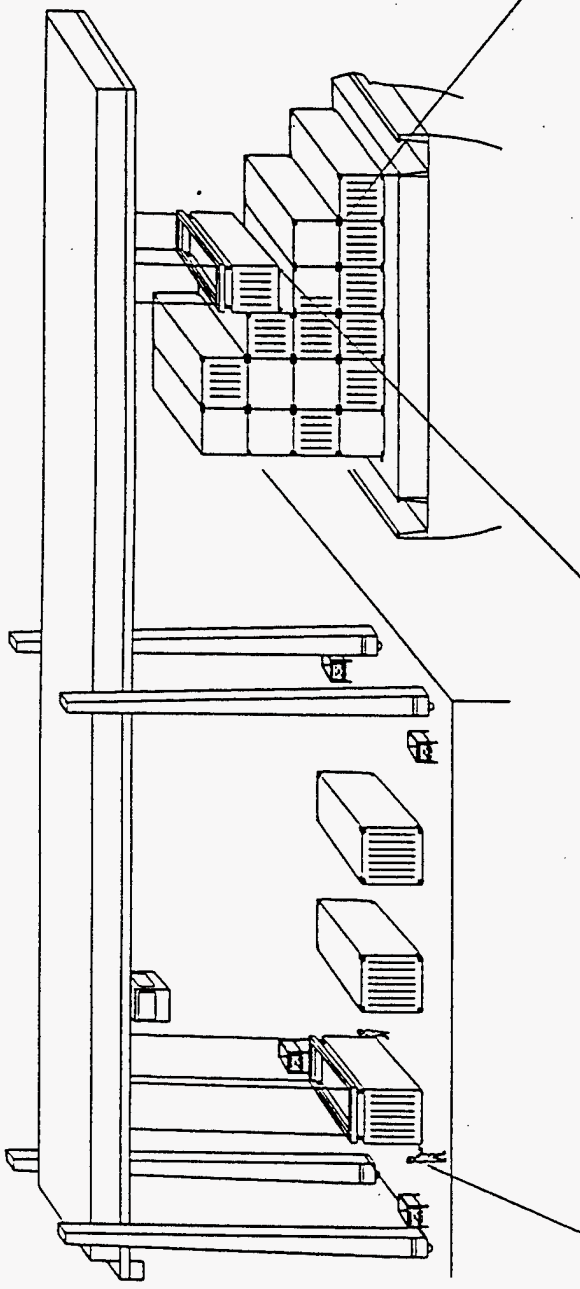
| | | | |
|-------|--------------|---------|--------|
| Index | Modification | Date | Name |
| | | 6.04.92 | / H.H. |



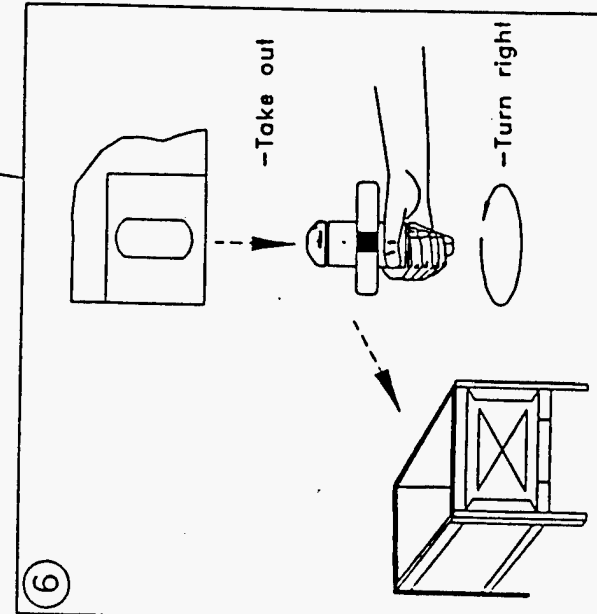
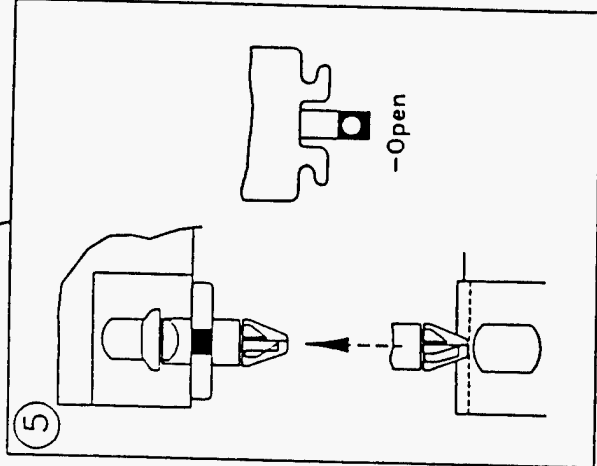
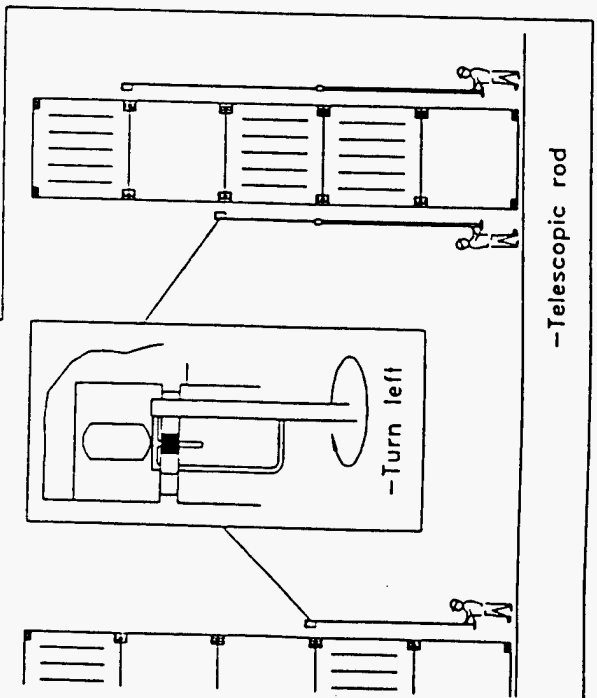
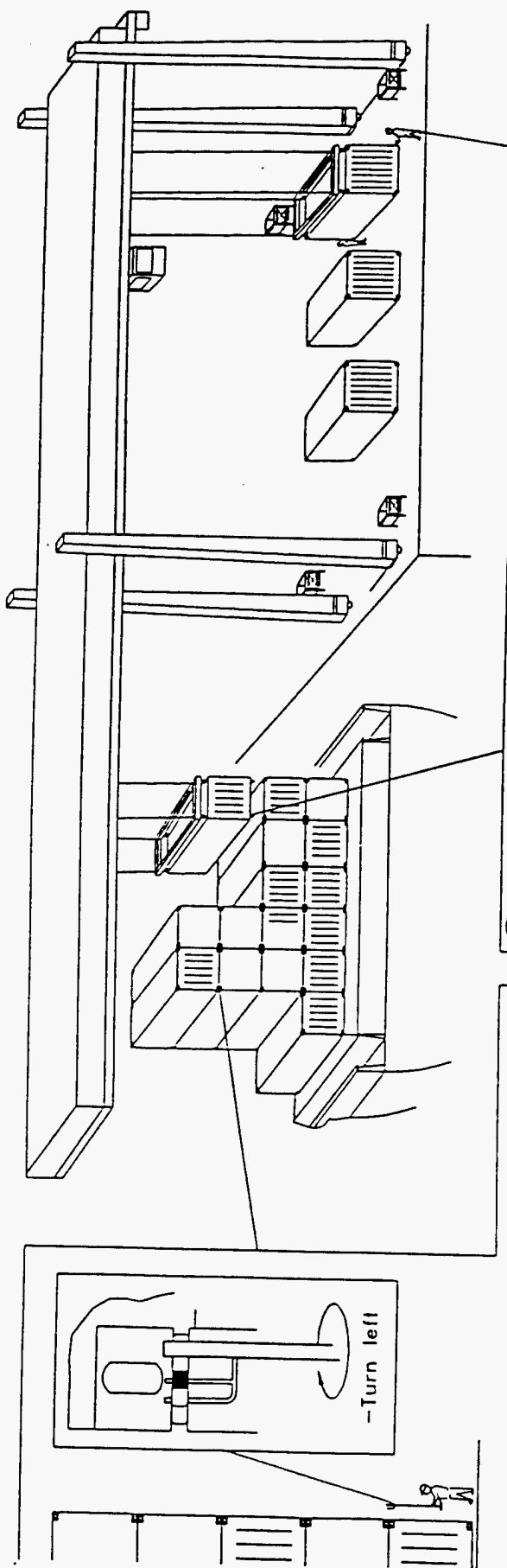
20' CONTAINER STOWAGE
 - HOLD -

12974-10-30
 Sheet 22 /

Loading Operation
for Semi Automatic Twistlock CV-14



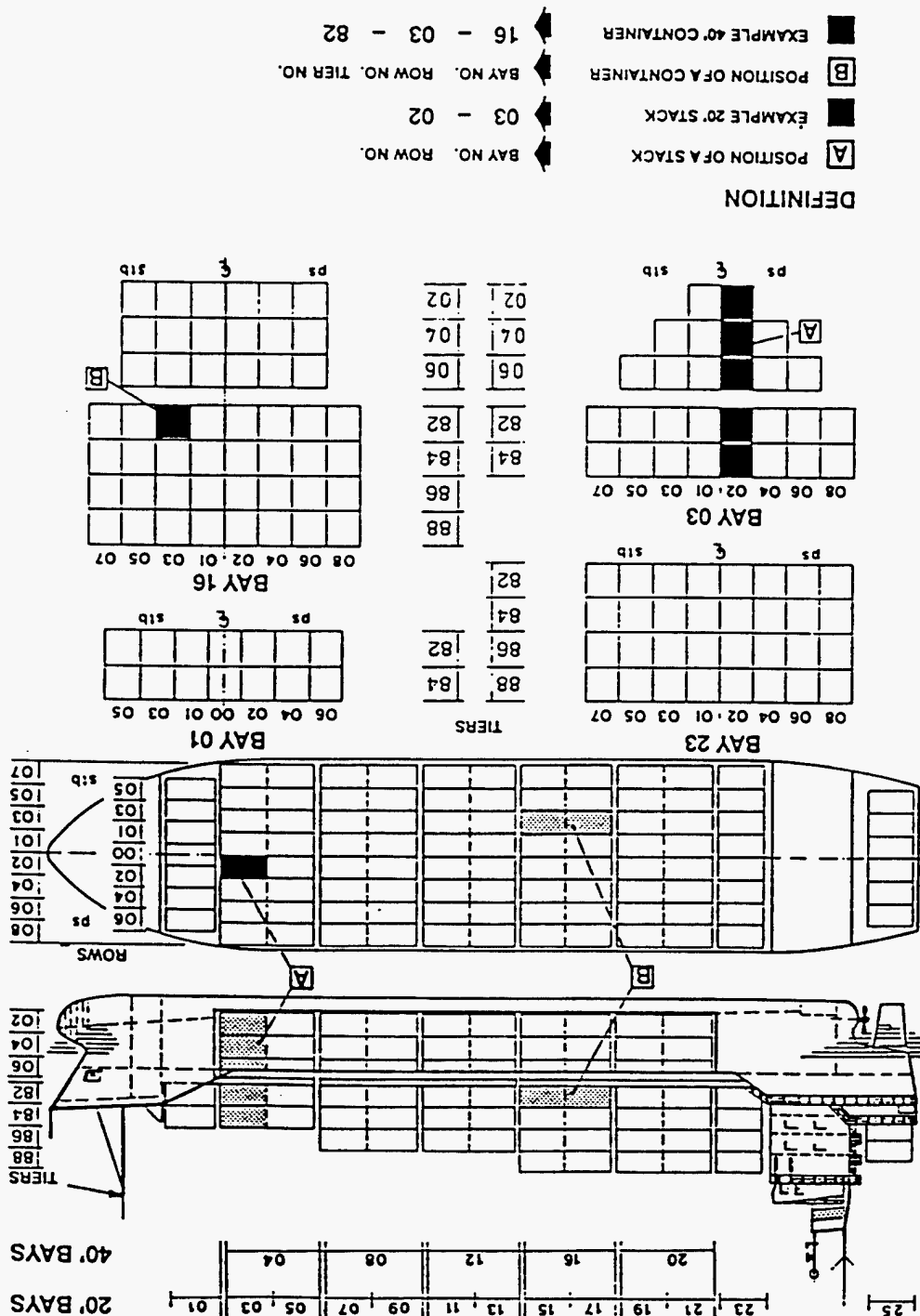
Discharging Operation for Semi Automatic Twistlock CV-14



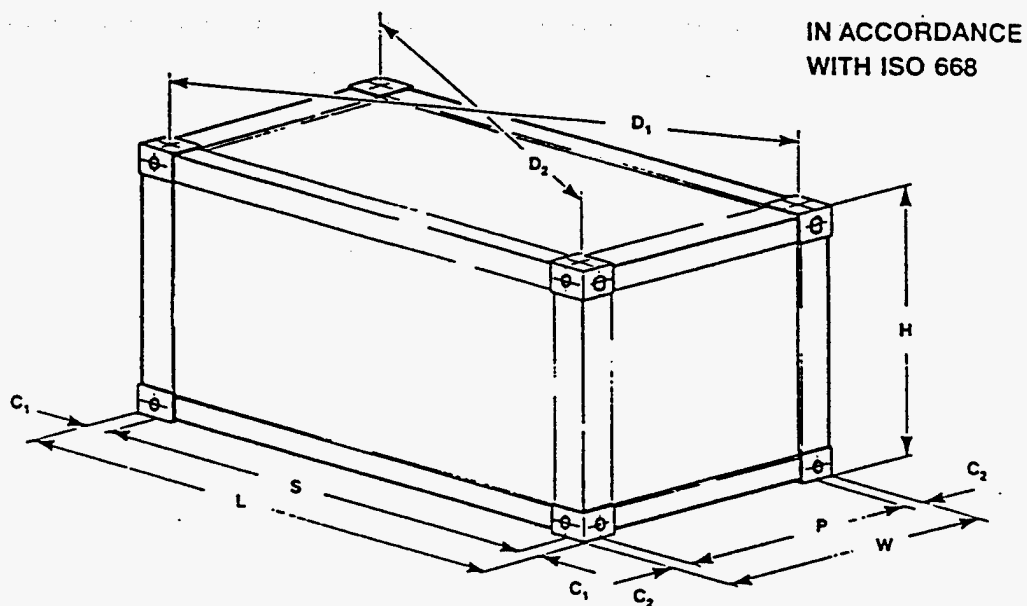
Part H. Lashings and Securements

Ocean containers are secured to a ship using a variety of securements and lashings. Part H of this appendix presents examples of the various types of securements and lashings used to hold casks to a ship.

Sandia National Laboratories gratefully acknowledges permission from **MacGregor-Conver GmbH** to reproduce representative pages from the *Conver-OSR Container Stowage and Lashing Systems Catalog*.



Copyright of this document, and giving it to others, and the use of its contents, without the express written authority of the Office, are hereby prohibited. All rights are reserved on the text of this document and the reproduction of its contents.



| DESIGNATION | | ISO 668 | | | | | | | | | | |
|--|-------------------|-------------------------|----------------------|----------------------|------|-----------------------|----------------------|----------------------|------|-----------------------|----------------------|------|
| | | 40' | | | | 30' | | | | 20' | | |
| | | 1A | 1AA | 1AAA | 1AX | 1B | 1BB | 1BBB | 1BX | 1C | 1CC | 1CX |
| HEIGHT | ft | 8' | 8'6" | 9'6" | < 8' | 8' | 8'6" | 9'6" | < 8' | 8' | 8'6" | < 8' |
| | H mm | 2430 ^{0/-5} | 2591 ^{0/-5} | 2896 ^{0/-5} | 2430 | 2430 ^{0/-5} | 2591 ^{0/-5} | 2896 ^{0/-5} | 2430 | 2430 ^{0/-5} | 2591 ^{0/-5} | 2430 |
| LENGTH | L ft | 40' | | | | 29'11 1/4" | | | | 19'10 1/2" | | |
| | mm | 12192 ^{0/-10} | | | | 9125 ^{0/-10} | | | | 6058 ^{0/-6} | | |
| | S mm | 11985 ^{-4/-6} | | | | 8918 ^{-4/-6} | | | | 5853 ^{-3/-5} | | |
| | C ₁ mm | 101,5 ^{0/-1.5} | | | | | | | | | | |
| WIDTH | W ft | 8' | | | | | | | | | | |
| | mm | 2438 ^{0/-5} | | | | | | | | | | |
| | P mm | 2259 ^{0/-5} | | | | | | | | | | |
| | C ₂ mm | 89 ^{0/-1.5} | | | | | | | | | | |
| DIFFERENCE D ₁ -D ₂ | | ≤ 19 mm | | | | ≤ 16 mm | | | | ≤ 13 mm | | |
| MAX. GROSS MASS, kg | | 30 480 | | | | 25 400 | | | | 24 000 | | |

Copying of this document, and giving it to others, and the use or communication of the contents thereof, are forbidden without express authority. Offenders are liable to the payment of damages. All rights are reserved in the event of the reprinting of a patent or the reproduction of a design. Modification of design is to be reserved.

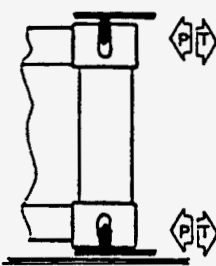
1.9

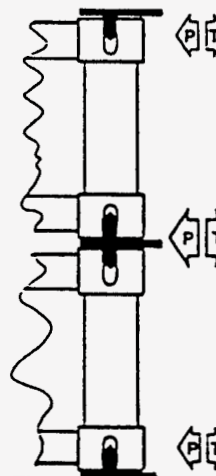
Consequently, the three interest groups, and therefore, the community, are not held together by a single, and spreading, of collective interests. However, each of the three institutional components, although different, are held together by a common goal: the achievement of the common good. This is the only way to ensure the sustainability of the community.

✳ TO "BELL LINES"
VIEW ON TOP

+0 - 6mm FOR 24' - 20' CONTAINERS

Copyright of this document, and power of its rights and their use or communication of the contents thereof, are reserved without express authority. Offenders are held to the payment of damages. All rights are reserved in the event of a patent or the registration of a utility model or design. Modification of this sign to the interest.

| SHORING FORCES IN LONGITUDINAL DIRECTION (kN) | | STANDARDIZATION/CLASSIFICATION SOCIETY | | | | | | | |
|---|--------|--|-----|-----|-----|-----|-----|-----|-----|
| | | STANDARD CONTAINER | | | | | | 1) | 2) |
| | | ISO | ABS | BV | DnV | GL | LR | LR | BV |
|  | TOP | TENSION | 20' | 75 | 100 | | | | |
| | | | 40' | | | | | | |
| | | COMPRESSION | 20' | | -/- | -/- | 125 | -/- | -/- |
| | | | 40' | | | | | | |
| | BOTTOM | TENSION | 20' | | | | | | |
| | | | 40' | | | | | | |
| | | COMPRESSION | 20' | -G- | | | | | |
| | | | 40' | | | | | | |


| SHORING FORCES IN TRANSVERSAL DIRECTION (kN) | | | | STANDARDIZATION/CLASSIFICATION SOCIETY | | | | | | | |
|---|---|-------------|-----|--|-----|-----|-----|-----|-----|-----|-----|
| | | | | STANDARD CONTAINER | | | | | 1) | 2) | |
| | | | | ISO | ABS | BV | DnV | GL | LR | LR | BV |
|  | TOP | TENSION | 20' | 150 | 200 | | | 250 | 225 | 270 | 200 |
| | | | 40' | | 250 | 300 | 250 | | 340 | -/- | 300 |
| | | COMPRESSION | 20' | 100 | 200 | | | 250 | 225 | 270 | 200 |
| | | | 40' | | 250 | 300 | 250 | | 340 | -/- | 300 |
| | SUPPORTING TENSION A STACK AT AN INTERMEDIATE LEVEL | TENSION | 20' | 300 | 500 | 520 | 400 | 650 | 575 | 620 | 520 |
| | | | 40' | | 600 | 700 | 500 | | 840 | -/- | 700 |
| | | COMPRESSION | 20' | 250 | 500 | 520 | 500 | 650 | 575 | 620 | 520 |
| | | | 40' | | 600 | 700 | 600 | | 840 | -/- | 700 |
| | BOTTOM | TENSION | 20' | 150 | 300 | 320 | 200 | 400 | 350 | 350 | 320 |
| | | | 40' | | 350 | 400 | 250 | | 500 | -/- | 400 |
| | | COMPRESSION | 20' | 150 | 300 | 320 | 300 | 400 | 350 | 350 | 320 |
| | | | 40' | | 350 | 400 | 350 | | 500 | -/- | 400 |

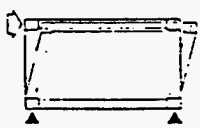
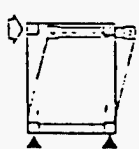
1) CONTAINER TESTED TO HIGHER STRENGTH STANDARDS

2) CLASS A CONTAINER

-G-: CONTAINER WEIGHT

1.12 PERMISSIBLE FORCES ON CONTAINERS

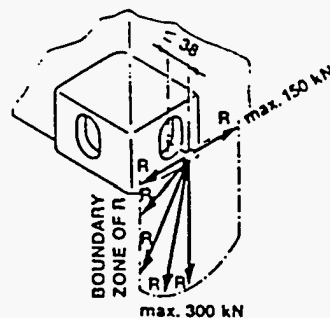
| FORCES IN VERTICAL DIRECTION (kN) | | | | STANDARDIZATION/CLASSIFICATION SOCIETY | | | | | | | |
|---|---------------|---------|-----|--|-----|-----|------|-----|-----|-----|-----|
| | | | | STANDARD CONTAINER | | | | | | 1) | 2) |
| | | | | ISO | ABS | BV | DnV | GL | LR | LR | BV |
|  | TENSION | TOP | 20' | 100 | 150 | 150 | 120 | 200 | 150 | 200 | 200 |
| | | 40' | 150 | 150 | | | 250 | | | 250 | |
| | | BOTTOM | 20' | 100 | 200 | | | | 250 | 250 | |
| | | | 40' | | -/- | | | | | | |
| | COM-PRES-SION | TOP AND | 20' | 450 | 550 | 450 | 864 | -/- | 450 | 550 | |
| | | BOTTOM | 40' | 675 | | | 1080 | | 675 | -/- | 750 |

| RACKING FORCES (kN) | | | STANDARDIZATION/CLASSIFICATION SOCIETY | | | | | | | |
|---|-----------|-----|--|-----|------|-----|-----|-----|-----|----|
| | | | STANDARD CONTAINER | | | | | | 1) | 2) |
| | | | ISO | ABS | BV | DnV | GL | LR | LR | BV |
|  | EACH SIDE | 20' | 75 | 100 | 75** | 75* | 125 | 100 | 200 | |
| | | 40' | | | | | | | | |
|  | EACH END | 20' | 150 | | | | | | 200 | |
| | | 40' | | | | | | | | |

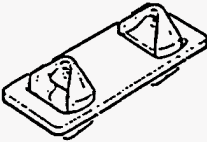
- 1) CONTAINER TESTED TO HIGHER STRENGTH STANDARDS
2) CLASS A CONTAINER

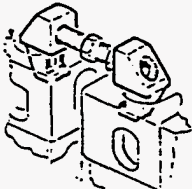
- * 150 kN FOR CLOSED BOX CONTAINERS
** 150 kN ON CLOSED SIDE WALL

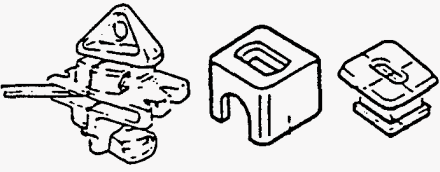
FORCES ACTING PARALLEL TO
FRONT AND SIDE FACE
AT TOP AND BOTTOM CORNER FITTING

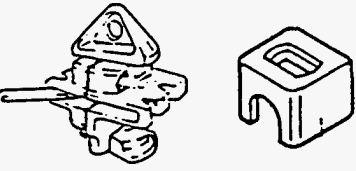


Copyright of this document, and opening of its contents, shall be a continuous action of the copyright holder. The copyright holder shall be responsible for the copyright of the document. All rights are reserved in the event of the copyright of the document. All rights are reserved in the event of the copyright of the document.

| STACKING-CONES | | CLASSIFICATION SOCIETY | | | | |
|---|----------|------------------------|-----|-----|------------------|-------------------|
| | | ABS | BV | DnV | GL ¹⁾ | LR |
|  | μ | 1,1 | 1,3 | 1,1 | D.1,25 H.1,1 | 1,5 ²⁾ |
| | γ | 1,67 ³⁾ | 2,0 | 2,0 | D.2,0 H.1,3 | 2,0 ²⁾ |
| | SWL | 450 | 400 | 400 | D.200 H.560 | 400 |
| | PL | 525 | 520 | 440 | D.250 H.620 | 600 |
| | BL | 750 | 800 | 800 | D.400 H.730 | 800 |
| | | | | | | |
| | | | | | | |
| | | | | | | |
| | | | | | | |
| | | | | | | |

| BRIDGE FITTINGS | | CLASSIFICATION SOCIETY | | | | |
|---|----------|------------------------|-----|-----|------|-----|
| | | ABS | BV | DnV | GL | LR |
|  | μ | 1,1 | 1,3 | 1,1 | 1,25 | 1,5 |
| | γ | 1,67 ³⁾ | 2,0 | 2,0 | — | 2,0 |
| | SWL | 50 | 50 | 50 | 50 | 50 |
| | PL | 55 | 65 | 55 | 62,5 | 75 |
| | BL | 85 | 100 | 100 | — | 100 |

| TWISTLOCKS AND DECK SOCKETS (TENSION LOAD) | | CLASSIFICATION SOCIETY | | | | |
|---|----------|------------------------|-----|-----|------|-----|
| | | ABS | BV | DnV | GL | LR |
|  | μ | 1,1 | 1,3 | 1,1 | 1,25 | 1,5 |
| | γ | 1,67 ³⁾ | 2,0 | 2,0 | 2,0 | 2,0 |
| | SWL | 200 | 200 | 200 | 200 | 200 |
| | PL | 220 | 260 | 220 | 250 | 300 |
| | BL | 335 | 400 | 400 | 400 | 400 |

| TWISTLOCK AND RAISED DECK SOCKETS (SHEAR LOAD) | | CLASSIFICATION SOCIETY | | | | |
|---|----------|------------------------|-----|-----|------|-----|
| | | ABS | BV | DnV | GL | LR |
|  | μ | 1,1 | 1,3 | 1,1 | 1,25 | 1,5 |
| | γ | 1,67 ³⁾ | 2,0 | 2,0 | 2,0 | 2,0 |
| | SWL | 150 | 150 | 150 | 210 | 150 |
| | PL | 165 | 195 | 165 | 263 | 225 |
| | BL | 250 | 300 | 300 | 420 | 300 |


1) Hold: $\mu = 1,1 / \gamma = 1,3$
Deck: $\mu = 1,25 / \gamma = 2,0$

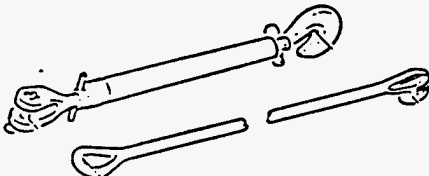
2) If SWL > 400 kN
then: PL = SWL + 200 kN
BL = SWL + 400 kN

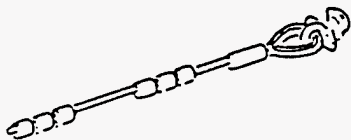
3) If $\delta\gamma < 315 \text{ N/mm}^2$
or nodular iron then $\gamma = 2$

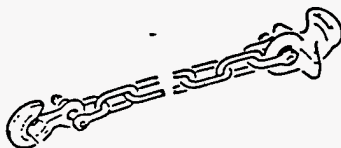
4) If $\delta\gamma < 315 \text{ N/mm}^2$ then $\gamma = 3$


1.14 ACTING FORCES ON FITTINGS

| LASHING EYES 50 t LASHING PLATES 50 t | | CLASSIFICATION SOCIETY | | | | |
|---|----------|------------------------|-----|-----|------|-----|
| | | ABS | BV | DnV | GL | LR |
|  | μ | 1,1 | 1,3 | 1,1 | 1,25 | 1,5 |
| | γ | 1,67 ²⁾ | 2,0 | 2,0 | 2,0 | 2,0 |
| | SWL | 293 | 245 | 245 | 245 | 245 |
| | PL | 322 | 319 | 270 | 306 | 367 |
| | BL | 490 | 490 | 490 | 490 | 490 |

| LASHING BARS 50 t TURNBUCKLES 50 t | | CLASSIFICATION SOCIETY | | | | |
|---|----------|------------------------|-----|-----|------|-----|
| | | ABS | BV | DnV | GL | LR |
|  | μ | 1,1 | 1,3 | 1,1 | 1,25 | 1,5 |
| | γ | 1,67 ²⁾ | 2,0 | 2,0 | 2,0 | 2,0 |
| | SWL | 293 | 245 | 245 | 245 | 245 |
| | PL | 322 | 319 | 270 | 306 | 367 |
| | BL | 490 | 490 | 490 | 490 | 490 |

| LASHING WIRES 36 t | | CLASSIFICATION SOCIETY | | | | |
|---|----------|------------------------|-----|-----|------|-----|
| | | ABS | BV | DnV | GL | LR |
|  | μ | — | — | — | — | — |
| | γ | 2,0 | 2,5 | 2,0 | 2,25 | 3,0 |
| | SWL | 180 | 145 | 180 | 160 | 120 |
| | PL | — | — | — | — | — |
| | BL | 360 | 360 | 360 | 360 | 360 |

| LASHING CHAINS 20 t | | CLASSIFICATION SOCIETY | | | | |
|---|----------|------------------------|------|-----|------|-------------------|
| | | ABS | BV | DnV | GL | LR |
|  | μ | 1,1 | 1,3 | 1,1 | 1,25 | — |
| | γ | 2,0 | 2,85 | 2,0 | 2,5 | 2,5 ⁴⁾ |
| | SWL | 100 | 70 | 100 | 80 | 80 |
| | PL | 110 | 90 | 110 | 100 | — |
| | BL | 200 | 200 | 200 | 200 | 200 |

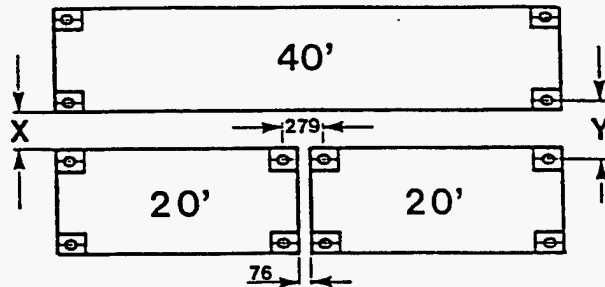
| TENSION/COMPRESSION ELEMENTS | | CLASSIFICATION SOCIETY | | | | |
|---|----------|------------------------|-----|-----|-----|-------------------|
| | | ABS | BV | DnV | GL | LR |
|  | μ | 1,1 | 1,3 | 1,1 | 1,1 | 1,5 ²⁾ |
| | γ | 1,67 ²⁾ | 2,0 | 2,0 | 1,3 | 2,0 ²⁾ |
| | SWL | 500 | 420 | 420 | 650 | 440 |
| | PL | 550 | 545 | 462 | 715 | 640 |
| | BL | 835 | 840 | 840 | 850 | 840 |

ANNOTATION SEE PAGE 1.13

Copying of this document, and issuing of its copies, and the use or dissemination of its contents, however, and in whatever way, without express written permission of the copyright holder, is prohibited. All rights are reserved in the event of the reprinting of this document. Modifications of this document are not allowed.

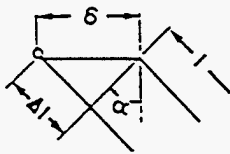
CONTAINER SPACES

THE FIGURES SHOWN ARE THE MOST COMMON ONES, BUT ALL OTHERS ARE ALSO POSSIBLE.



| CONTAINER SPACES X | CONTAINER CENTRE DISTANCES Y |
|--------------------|------------------------------|
| 25 | 203 |
| 38 | 216 |
| 80 | 258 |

DETERMINATION OF FORCES IN THE LASHING SYSTEM



RACKING FORCE 'T'

$$T_1 = \frac{1}{2} Fq_2 + \frac{1}{4} Fq_1 - H \text{ (kN)}$$

TOTAL LASHING FORCE 'Z'

$$Z = Z_0 + \Delta Z$$

$$H = Z \cdot \sin \alpha$$

$$Z_0 = \text{PRESTRESSING}$$

$$\Delta Z = \delta \cdot E_z \cdot \frac{A}{l} \cdot \sin \alpha$$

$$A = \text{EFF. CROSS-SECTION OF LASHING (cm}^2\text{)}$$

$$E_z = \text{OVERALL MODULUS OF ELASTICITY}$$

$$\delta = C_c \cdot T_1 + V = \text{TRANSVERSAL DISLOCATION AT UPPER EDGE}$$

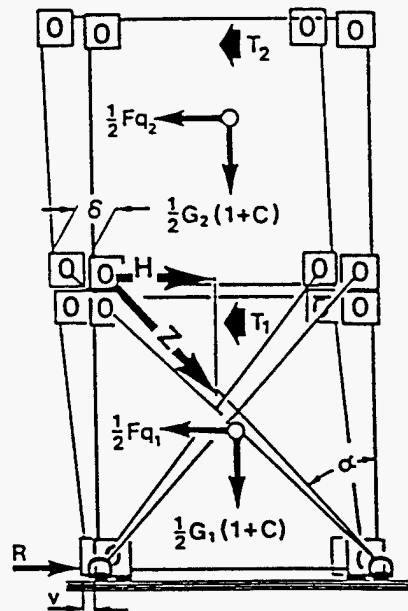
$$C_c = \text{RESILIENCE OF CONT TRANSV. FRAME}$$

$$V = \text{POSSIBLE DISLOCATION}$$

$$L = \text{LENGTH OF LASHING}$$

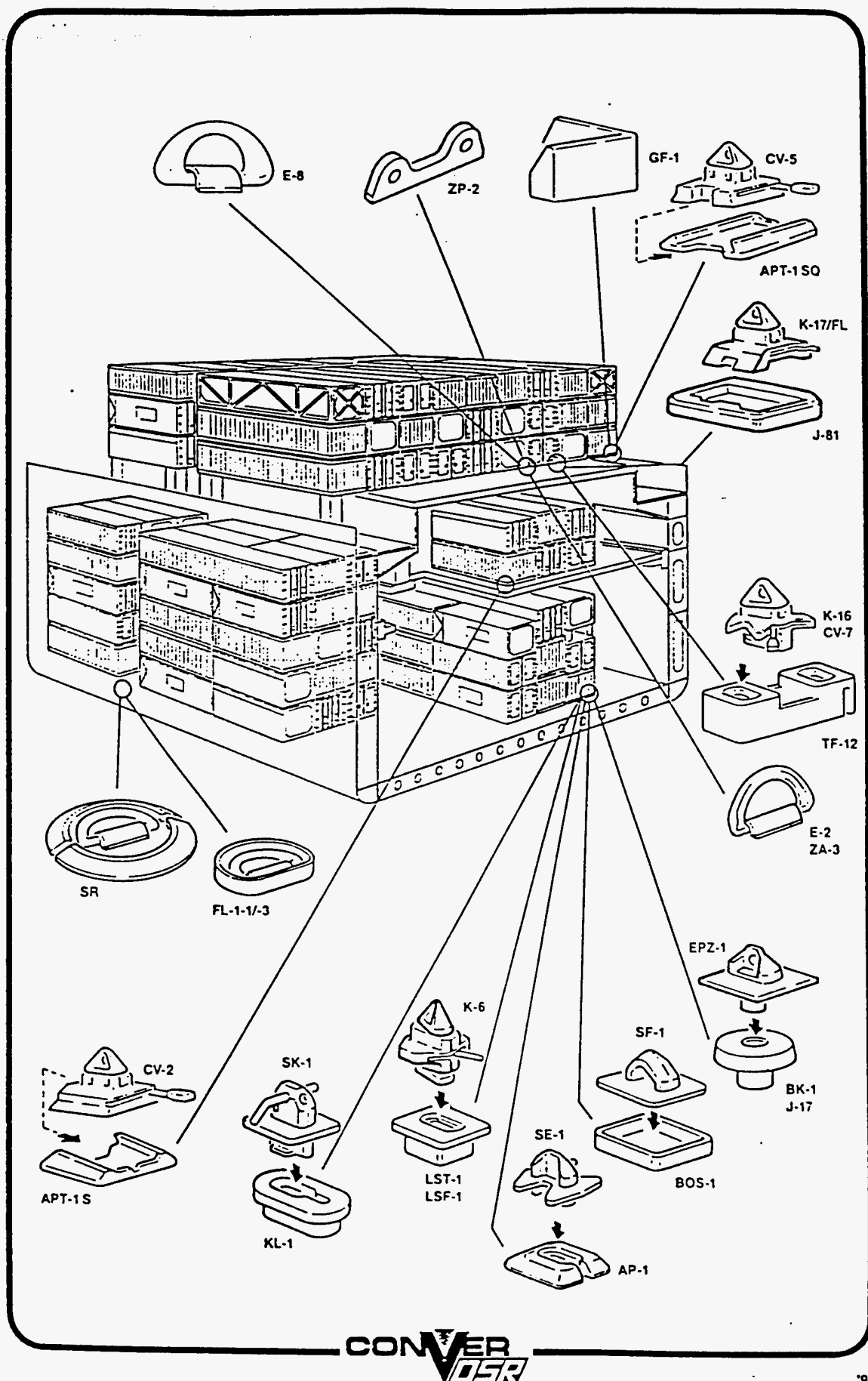
$$R = \text{FRICTIONAL LOAD}$$

$$C = P'_1 \text{ OR } P'_2$$



Copyright of this document, and giving it to others, and the use or reproduction of the contents thereof, are forbidden without express authority. Offenders are liable to the payment of damages. All rights are reserved in the event of a patent or the registration of a utility model or design. Modification of design to be reserved.

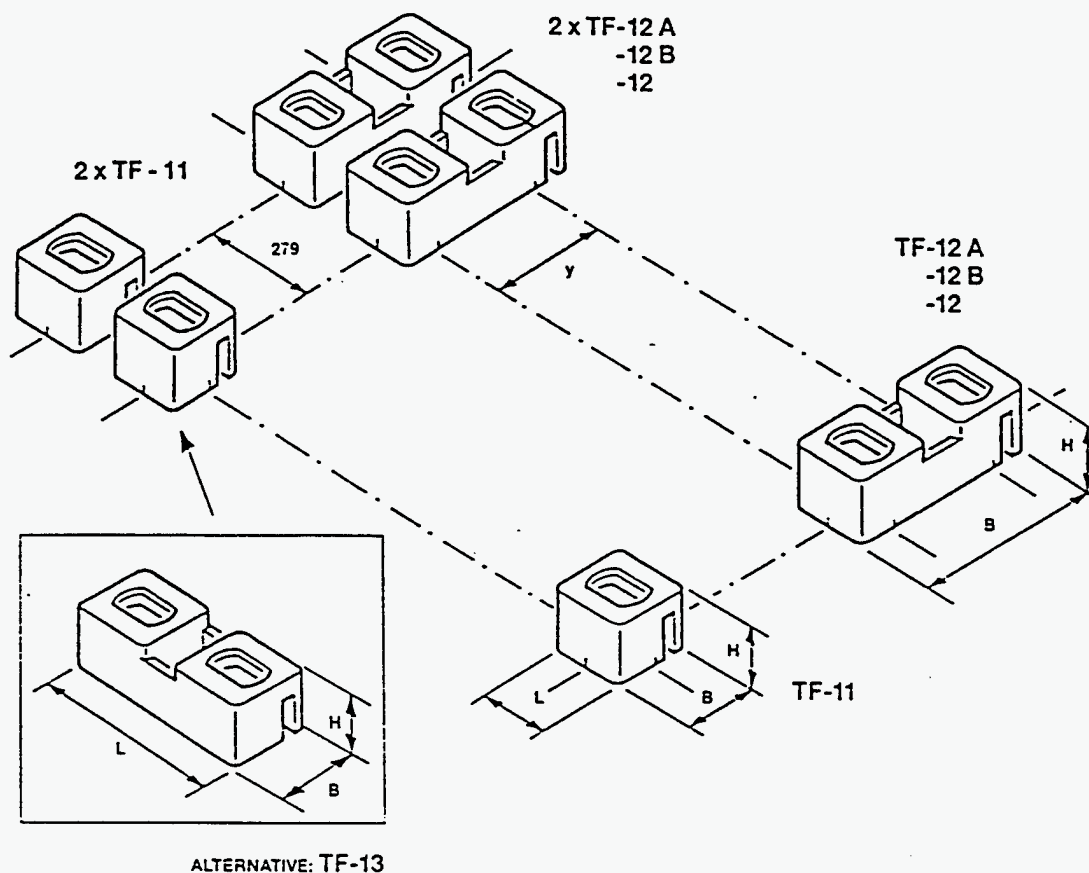
2 BOTTOM FOUNDATIONS AND LASHING POINTS



Copyright of this document, and every of its copies, and the use or reproduction of this document in any form or by any means, is prohibited without the express written permission of the copyright owner. All rights are reserved. No part of this document may be reproduced or transmitted in any form or by any means, electronic or mechanical, including photocopying, recording, or by any information storage and retrieval system, without the express written permission of the copyright owner.

CONVER
OSR

Copyright of this document, and passing it to others, and the use or communication of the contents thereof, are forbidden without express authority. Clients are liable to the payment of damages. All rights are reserved in the event of the total or partial reproduction of this document or the use of its contents for any purpose.



| CODE | TYPE | L - (mm) | B - (mm) | H - (mm) | Y - (mm) | WGT. (~ kg) |
|-----------|---------|-------------|-------------|-------------|-------------|----------------|
| 1300.5100 | TF-11 | 160 | 160 | 110 | / | 8.1 |
| 1300.5200 | TF-12 A | | 363 | | 203 | 16.1 |
| 1300.5210 | TF-12 B | | 376 | | 216 | 16.1 |
| 1300.5220 | TF-12 | | 418 | | 258 | 16.9 |
| 1300.5300 | TF-13 | 439 | 160 | | / | 17.3 |

COUNTER PARTS:

TWISTLOCKS : CV-1, CV-1A, CV-7, K-16
CV-9, CV-9G, K-6, K-6GS
CV-12, CV-14

LOCKING STACKER: SL-1

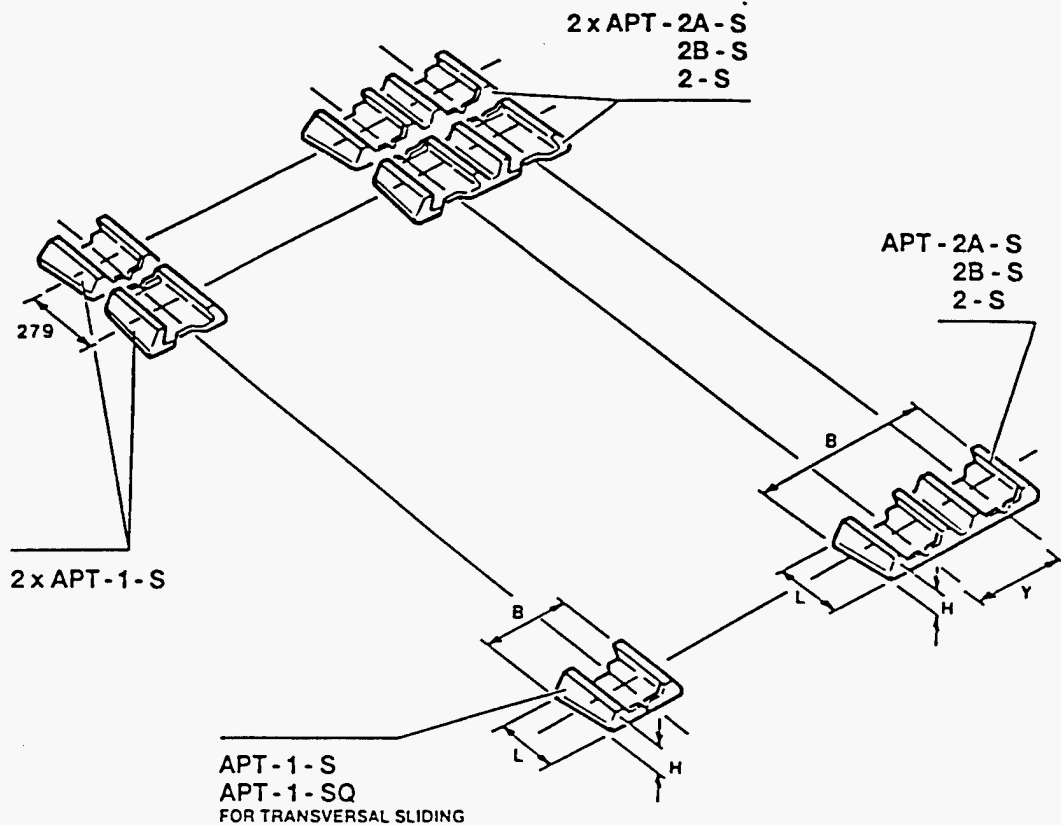
POSITION:

PREFERABLY LOCATED ON DECKS AND
HATCH COVERS

SPECIFICATION:

MATERIAL : STRUCTURAL STEEL
FINISH : NON-TREATED

CLASS. APPROVAL: ALL ITEMS CAN BE SUPPLIED
WITH THE APPROVAL OF ANY
CLASSIFICATION SOCIETY UPON
CLIENT'S REQUEST.



| CODE | TYPE | L ~ (mm) | B ~ (mm) | H ~ (mm) | Y ~ (mm) | WGT. (~ kg) |
|-----------|----------|-------------|-------------|-------------|-------------|----------------|
| 1800.3100 | APT-1-S | 190 | 240 | 38 | — | 5,5 |
| 1800.3200 | APT-2A-S | | 443 | | 203 | 9,5 |
| 1800.3210 | APT-2B-S | | 456 | | 216 | 9,9 |
| 1800.3220 | APT-2-S | | 498 | | 258 | 11,5 |
| 1800.3110 | APT-1SQ | 240 | 240 | — | — | 6,7 |

COUNTER PARTS:

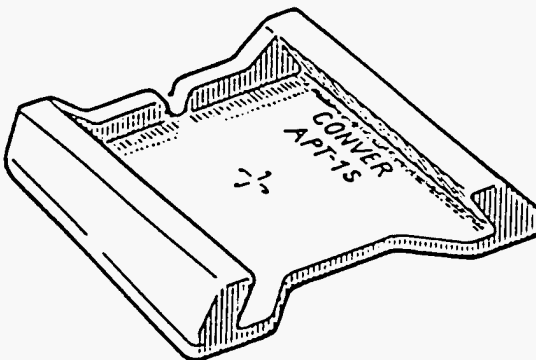
TWISTLOCKS : K-17FL, K-17FL-V, CV-2, CV-5
 SLIDING CONES : SC-1P, SC-1L
 'SLIDE' LOCK : AC-1
 SLIDING LASHING EYES: ZA-1E, ZA-E

POSITION:

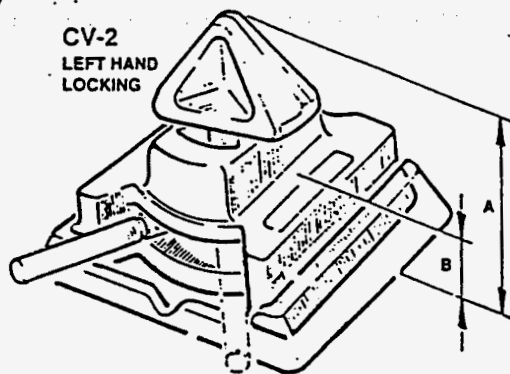
PREFERABLY LOCATED ON HATCH COVERS

SPECIFICATION:

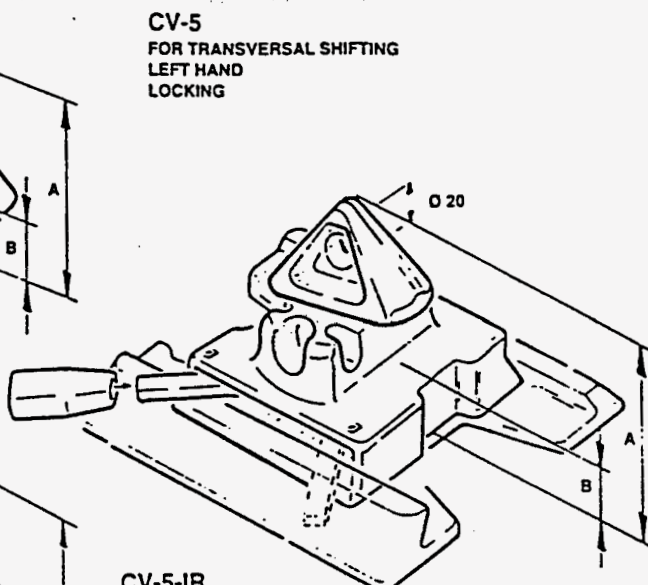
MATERIAL : CAST STEEL
 FINISH : NON-TREATED
 CLASS. APPROVAL: ALL ITEMS CAN BE SUPPLIED
 WITH THE APPROVAL OF ANY
 CLASSIFICATION SOCIETY UPON
 CLIENT'S REQUEST.



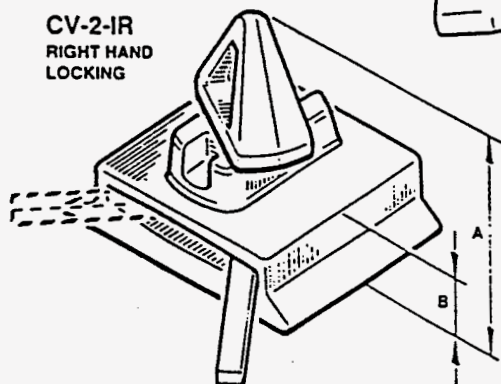
CONVER
OSR



CV-2
LEFT HAND
LOCKING

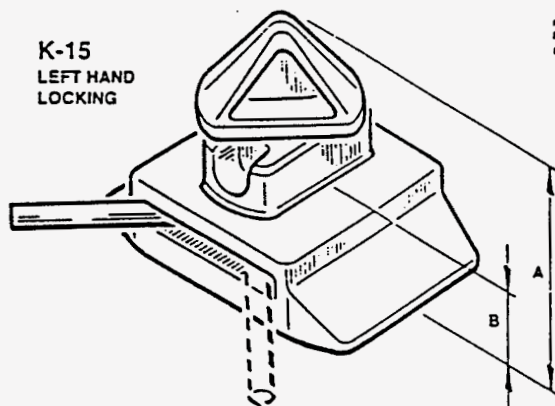
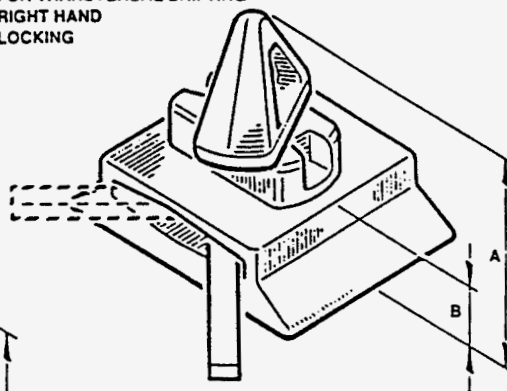


CV-5
FOR TRANSVERSAL SHIFTING
LEFT HAND
LOCKING



CV-2-IR
RIGHT HAND
LOCKING

CV-5-IR
FOR TRANSVERSAL SHIFTING
RIGHT HAND
LOCKING



K-15
LEFT HAND
LOCKING

| CODE | TYPE | A- (mm) | B- (mm) | WGT- (kg) | COUNTER PARTS |
|-----------|--------|------------|------------|--------------|---------------|
| 0600.2101 | CV-2 | 140 | 45 | 7.2 | DOVETAIL 55° |
| 0600.5101 | CV-5 | 140 | 47 | 6.7 | |
| 0600.3101 | CV-2IR | 135 | 42 | 6.8 | DOVETAIL 45° |
| 0600.3102 | K-15 | 143 | 50 | 7.2 | |
| 0600.3151 | CV-5IR | 135 | 42 | 7.1 | |

SPARE PARTS ON REQUEST

SPECIFICATION:

MATERIAL: NODULAR CAST IRON
DROP FORGED
CONES

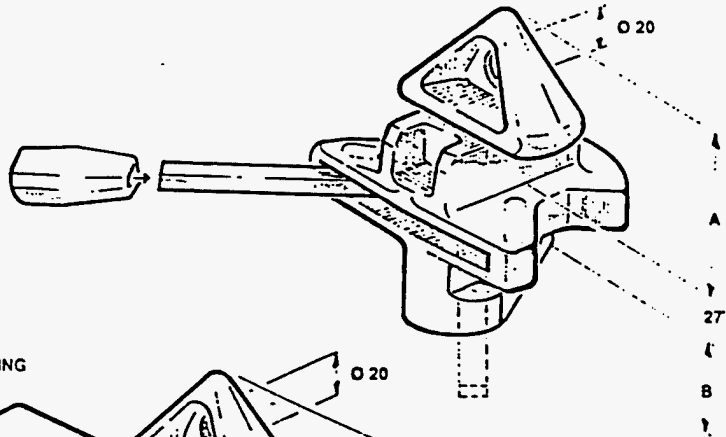
FINISH: ZINCED

CLASS. APPROVAL: ALL ITEMS CAN BE
SUPPLIED WITH THE
APPROVAL OF ANY
CLASSIFICATION
SOCIETY UPON
CLIENT'S REQUEST.

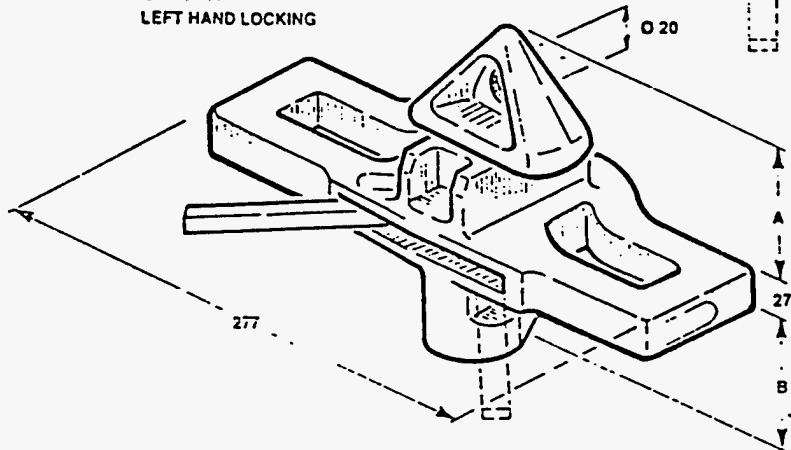
Copyright of this document and its contents, and the right to use the same, are reserved by the company. All rights are reserved in the event of a patent or the registration of a design. Modification of design is to be reserved.

3.30 FIXED BASE TWISTLOCK

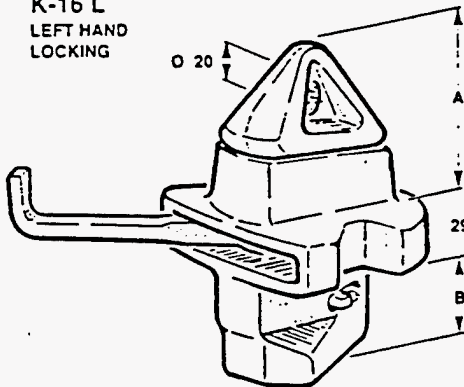
CV-7
LEFT HAND
LOCKING
CV-7R
(RIGHT HAND
LOCKING ON
REQUEST)



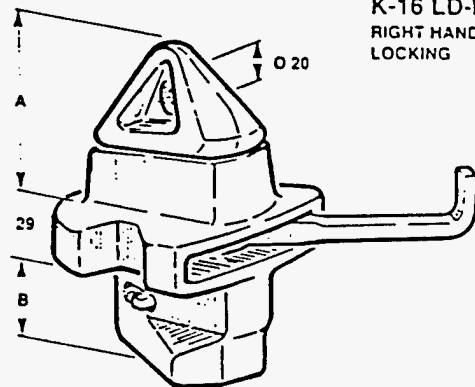
CV-7-W
LEFT HAND
LOCKING



K-16 L
LEFT HAND
LOCKING



K-16 LD-IV
RIGHT HAND
LOCKING



| CODE | TYPE | A- (mm) | B- (mm) | WGT- (kg) |
|-----------|-----------|------------|------------|--------------|
| 0600.7101 | CV-7 | 90 | 50 | 6.0 |
| 0600.7201 | CV-7R | 90 | 50 | 6.0 |
| 0600.7102 | CV-7W | 90 | 50 | 7.5 |
| 0600.7303 | K-16L | 92 | 54 | 6.7 |
| 0600.7402 | K-16LD-IV | 92 | 56 | 8.0 |

SPARE PARTS ON REQUEST

SPECIFICATION:

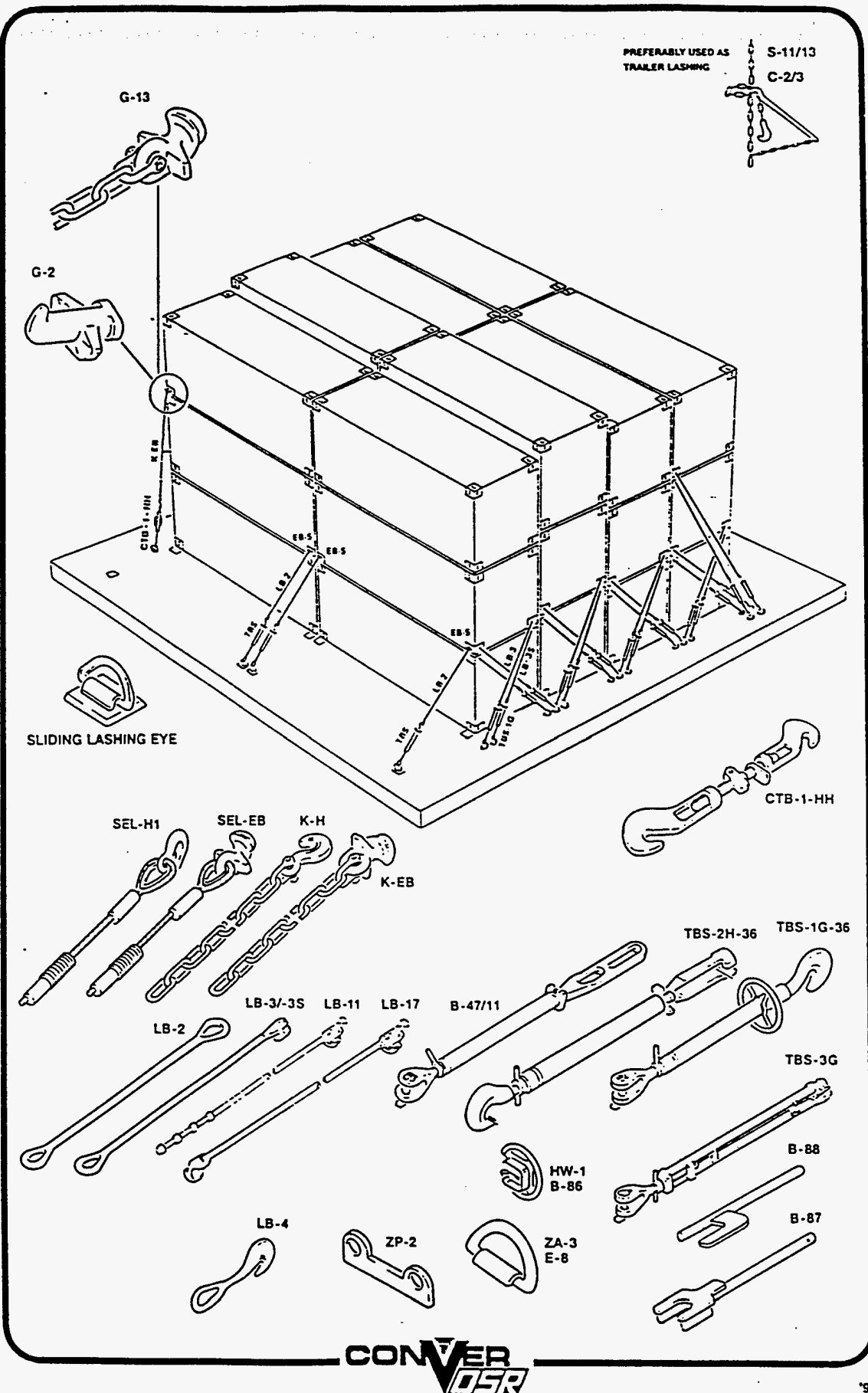
MATERIAL: NODULAR CAST IRON
DROP FORGED STEEL

FINISH: ZINCD

CLASS. APPROVAL: ALL ITEMS CAN BE
SUPPLIED WITH THE
APPROVAL OF ANY
CLASSIFICATION
SOCIETY UPON
CLIENT'S REQUEST.

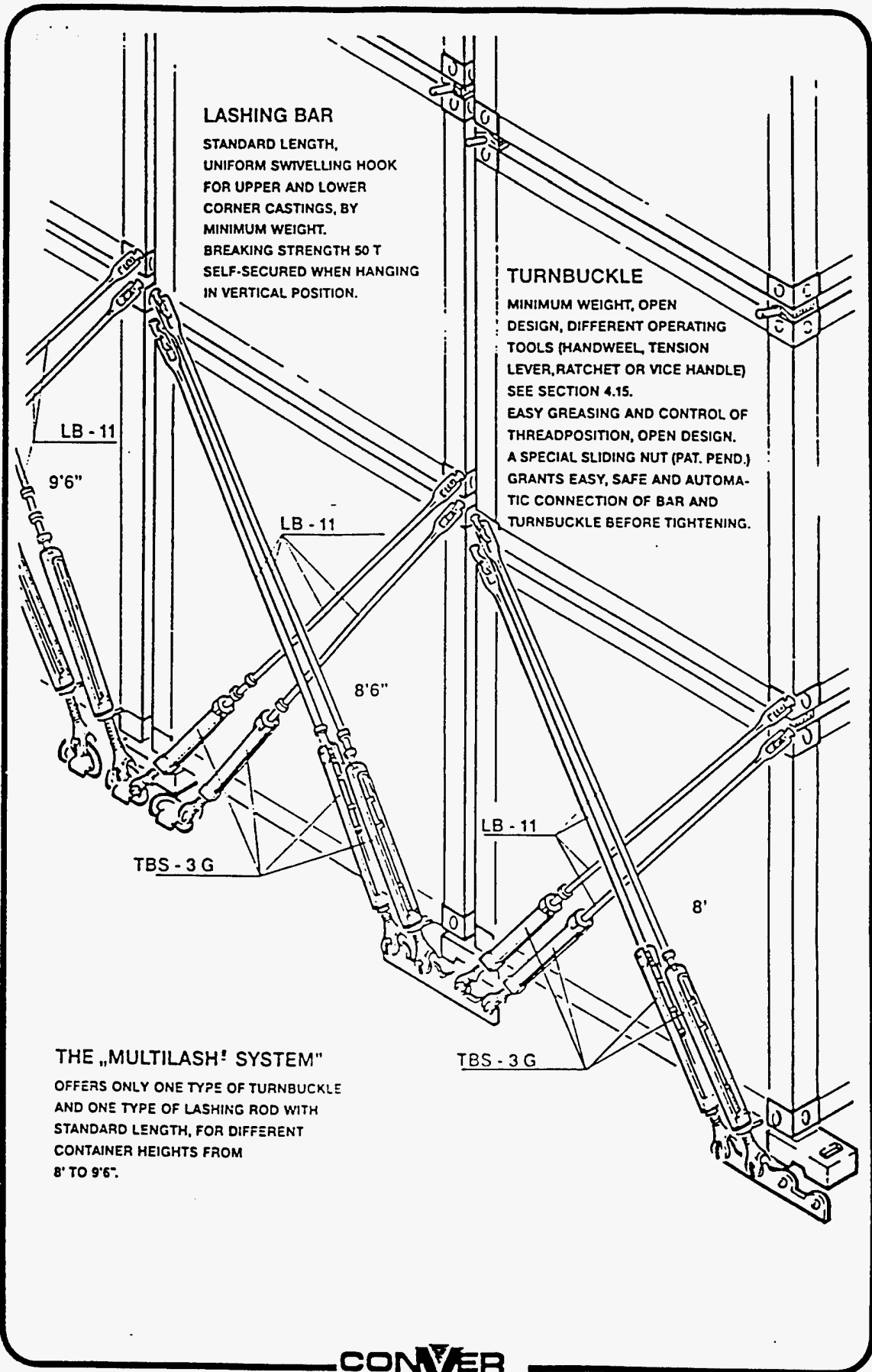
Copyright of this document, and issuing of its copies, and the use or communication of the contents thereof, are forbidden without express authority. Offenders are held to the payment of damages. All rights are reserved in the event of the publication of a printed or electronic copy of this document.

4 LASHING UNITS AND FITTINGS

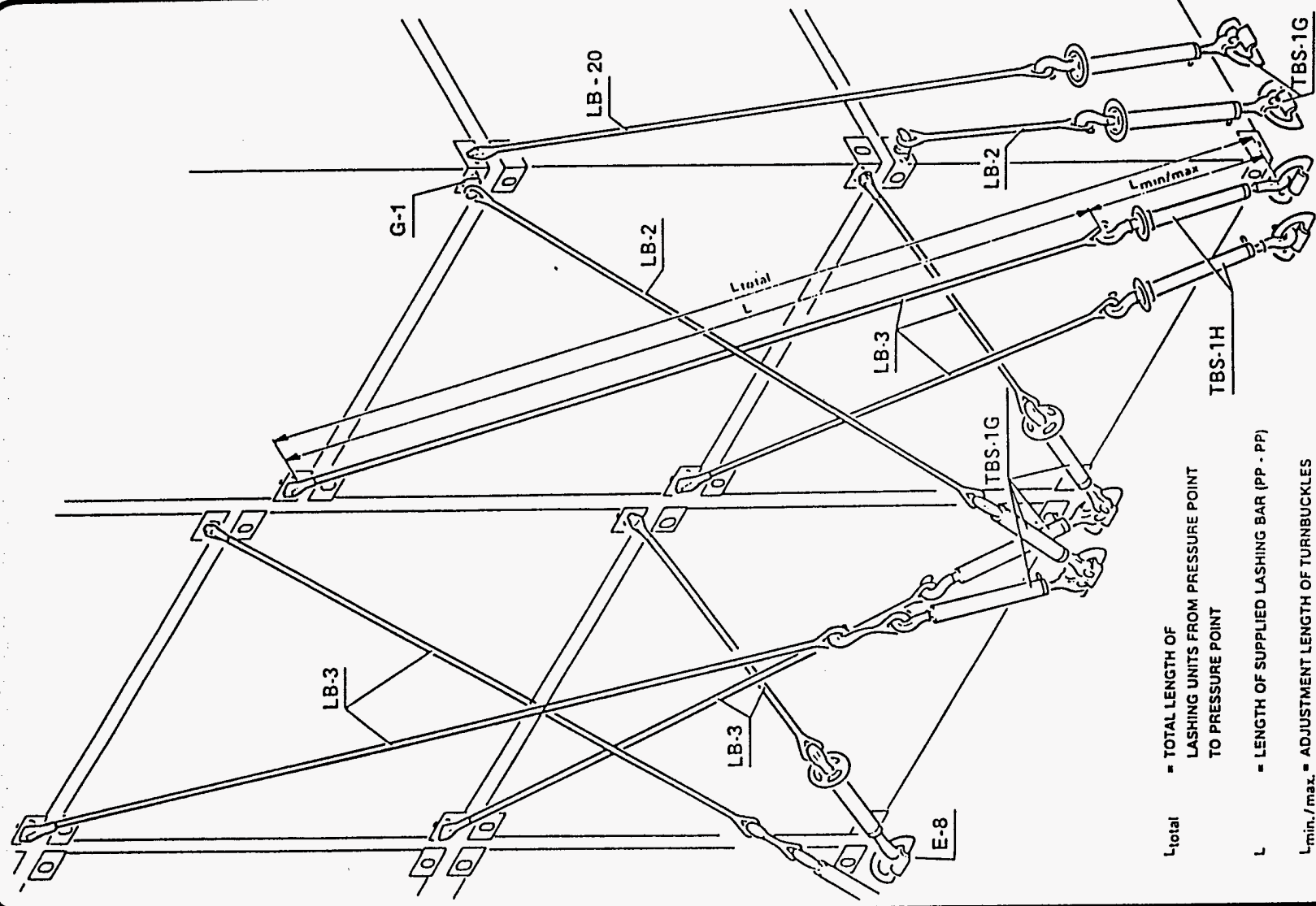


Copyright of this document, and queries if to others and the use or communication of the contents thereof, are the property of the originator. Offenders are liable to the payment of damages. All rights are reserved in the event of the grant of a patent or the registration of a utility model or design. Modification of design to be reserved.

Copying of this document, and giving it to others and the use or communication of the contents thereof, are forbidden without express authority. Offenders are liable to the payment of damages. All rights are reserved in the event of the grant of a patent or the registration of a utility model or design. Modification of design to be restored.

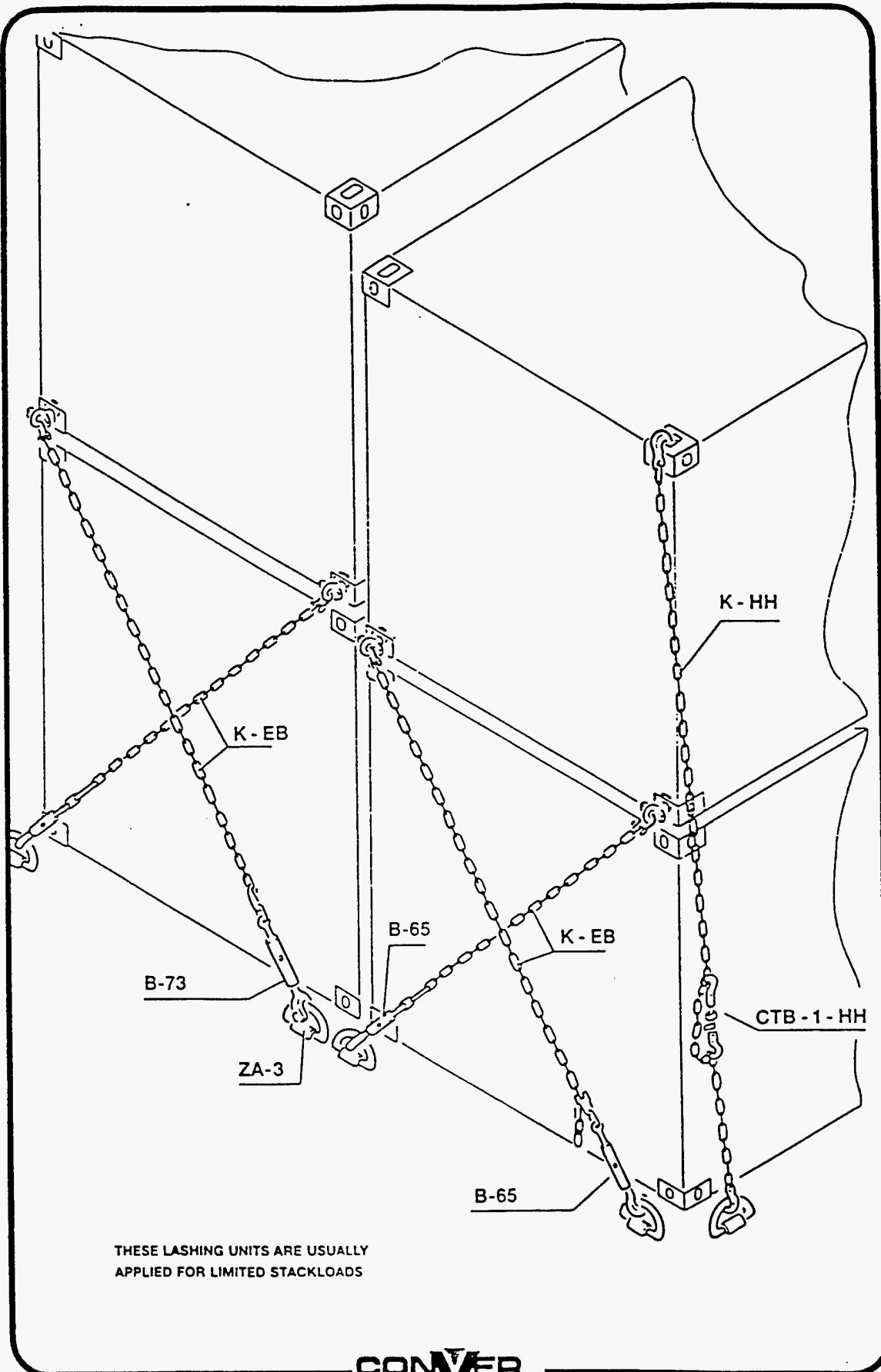


4.4 CONVENTIONAL LASHING SYSTEM

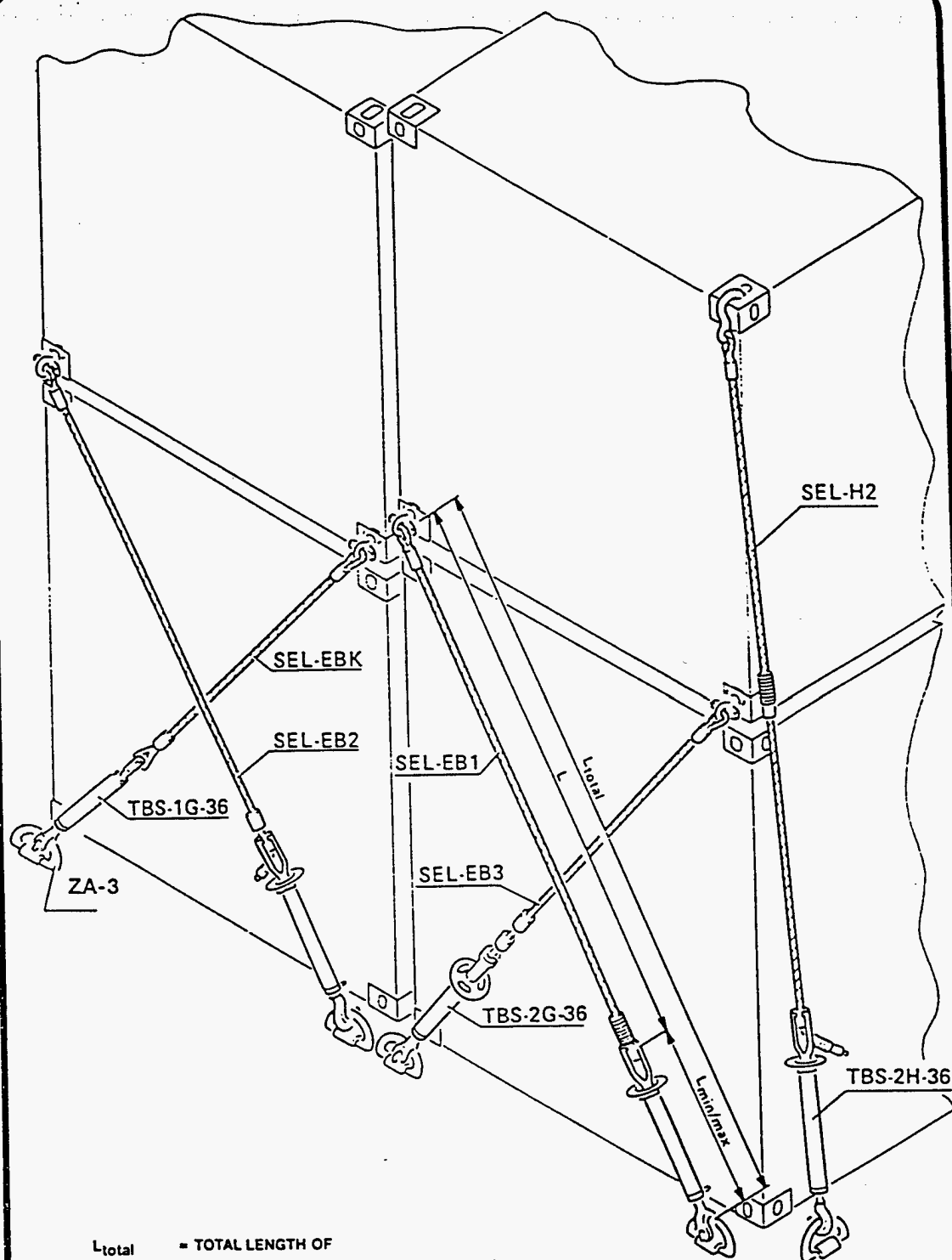


Copy of this document, and giving it to others and the use or communication of its contents (however, a violation will not expose author(s) or institution of design to the reward, the payment of damages, or rights reserved in the event of the grant of a patent) or the registration of a utility model or design, shall not be liable to

Copying of this document, and giving it in whole or in part, is prohibited without express written permission. Offenders, as well as the originator of the design, are liable for the payment of damages. All rights are reserved in the event of the patent or the registration of the design to be reserved.



CONVER
OSR



L_{total} = TOTAL LENGTH OF
LASHING UNITS FROM PRESSURE POINT
TO PRESSURE POINT

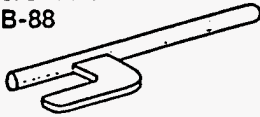
L = LENGTH OF SUPPLIED LASHING BAR (PP - PP)

$L_{min./max.}$ = ADJUSTMENT LENGTH OF TURNBUCKLES

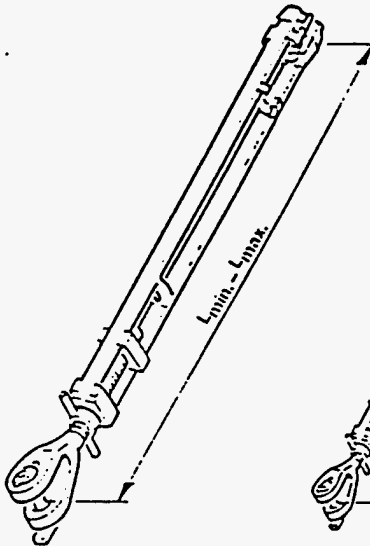
CONVER
OSR

Copying of this document, and giving it to others and the use or communication of its contents thereof, are forbidden without express authority. Offenders are liable to the payment of damages. All rights are reserved in the event of the grant of a patent or the registration of a utility model or design. Modification of design to be reserved.

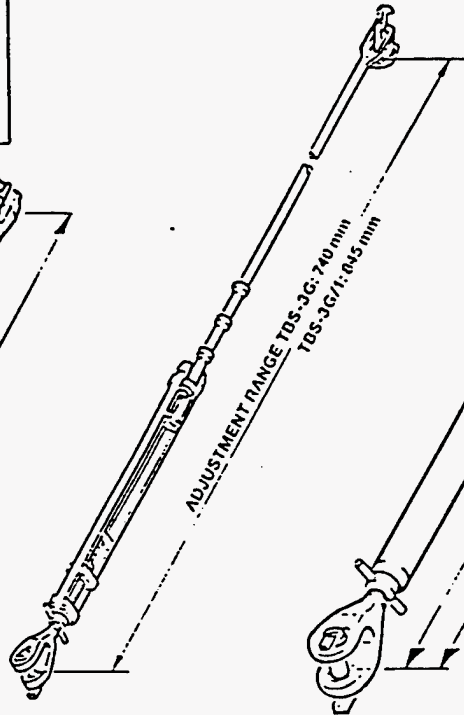
OPERATING TOOL
B-88



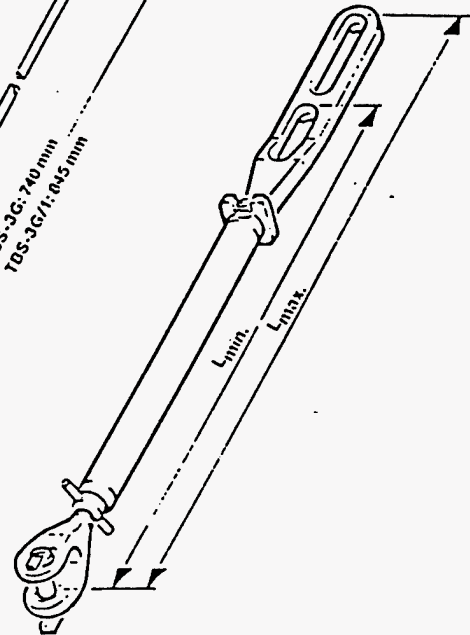
OTHER OPERATING TOOLS
SEE PAGE 4.15



TBS - 3 G...



TBS-3G...
IN CONNECTION WITH
THE LASHING BAR
LB-11

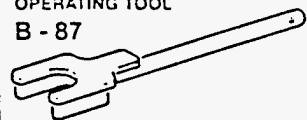


B - 47 / 11

SECURING BOLT



OPERATING TOOL
B - 87



OTHER OPERATING TOOLS
SEE PAGE 4.15

| CODE | TYPE | $L_{min} - L_{max}$ (mm) (PRESSURE POINT TO PRESSURE POINT) | BREAKING LOAD (kN) | WEIGHT (~ kg) | COUNTER PARTS |
|-----------|-------------|---|-----------------------|------------------|--|
| 0100.5010 | TBS - 3 G | 975 ÷ 1280 | 490 | 16,2 | LASHING PLATES LASHING EYES LASHING BARS LB - 11 |
| 0100.5011 | TBS - 3 G/1 | 1080 ÷ 1490 | 490 | 17,6 | |
| 0100.5310 | B - 47 / 11 | 958 ÷ 1580 | 490 | 23,3 | LASHING PLATES LASHING EYES LASHING BARS LB - 17/19 |

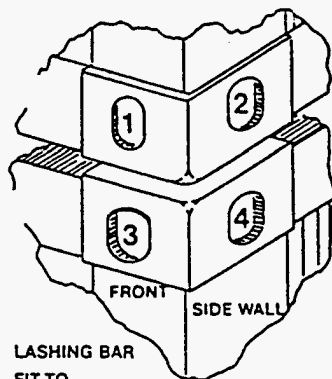
SPECIFICATION:

MATERIAL : HIGH TENSILE STEEL
FINISH : ZINCED
CLASS. APPROVAL : ALL ITEMS CAN BE SUPPLIED
WITH THE APPROVAL OF ANY
CLASSIFICATION SOCIETY UPON
CLIENT'S REQUEST

REMARK:

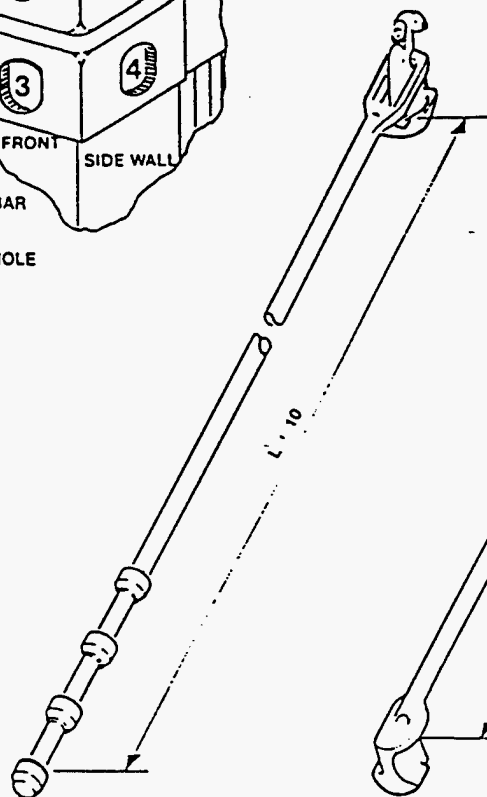
OTHER TURNBUCKLES
SEE PAGE
4.7, 4.18, 4.21

4.10 LASHING BARS

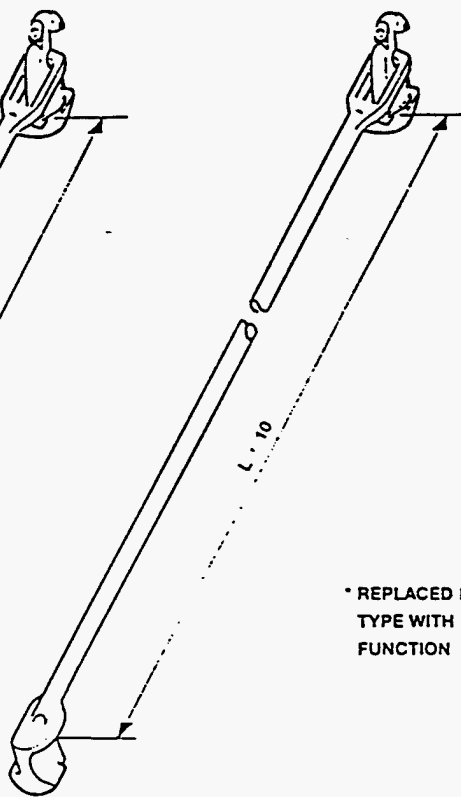


LASHING BAR
FIT TO
CORNER HOLE

LB - 11*



LB - 17



* REPLACED PREVIOUS
TYPE WITH SAME
FUNCTION

WHEN ORDERING LASHING BARS, PLEASE
STATE TYPE AND LENGTH L (FROM PRESSURE
POINT TO PRESSURE POINT).

| CODE | TYPE | BREAKING LOAD (kN) | WEIGHT (~ kg) L = 2 m | COUNTER PARTS | | |
|-----------|---------|-----------------------|-----------------------------|-----------------|-------------|-------------|
| | | | | CORNER HOLES | TURNBUCKLES | LASHING BAR |
| 0400.1110 | LB - 11 | 490 | 11,6 | No.: 1, 2, 3, 4 | TBS - 3 G | LB - 14 |
| 0400.1710 | LB - 17 | 490 | 12,5 | No.: 1, 2, 3, 4 | B - 47 / 11 | LB - 19 |

SPECIFICATION:

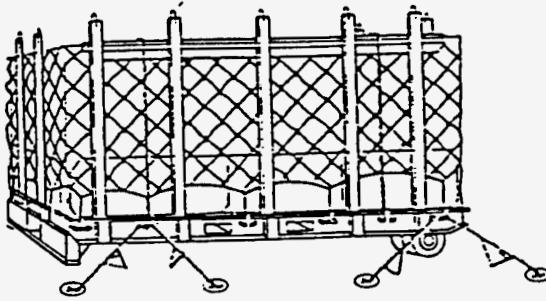
MATERIAL : HEAT-TREATED STEEL
FINISH : ZINCD
CLASS. APPROVAL : ALL ITEMS CAN BE SUPPLIED
WITH THE APPROVAL OF ANY
CLASSIFICATION SOCIETY UPON
CLIENT'S REQUEST

REMARK:

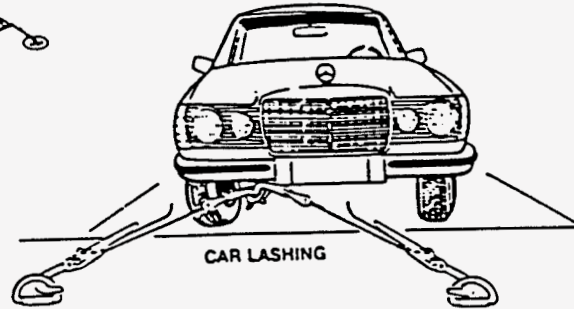
OTHER LASHING BARS
SEE PAGE 4.20

Copyright of this document, and every right in it, are reserved for the publisher. All rights are reserved in the event of a reprint or translation. Modifications of design to the extent of the publisher's discretion are reserved.

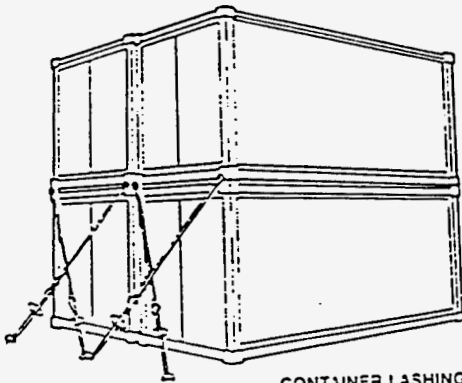
6 RO-RO/LO-LO EQUIPMENT



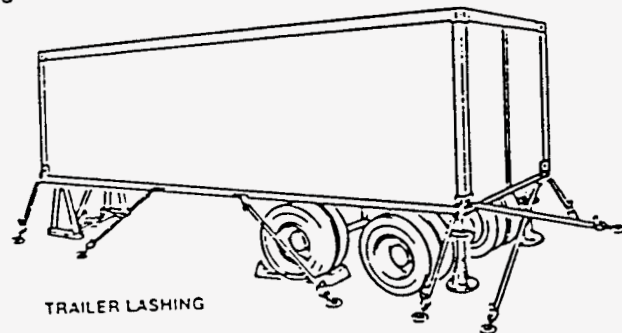
CARGO LASHING
ROLLTRAILER LASHING



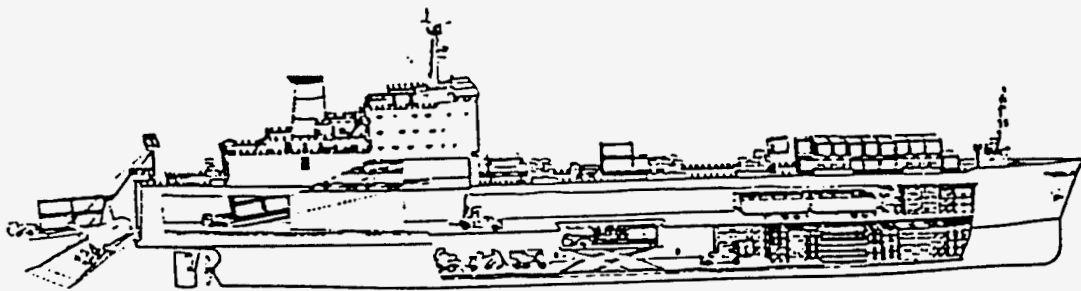
CAR LASHING



CONTAINER LASHING



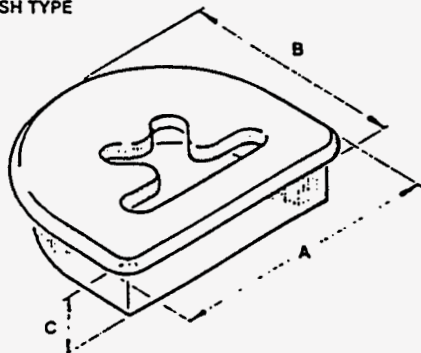
TRAILER LASHING



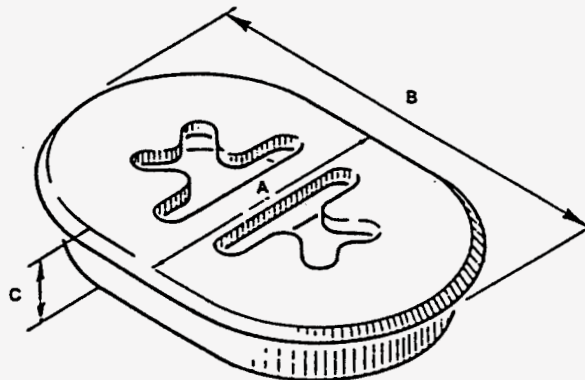
CONVER
OSR

Copyright of this document, and (pending if in others) and this use or reproduction of the contents, items, or features without express authority of the copyright owner are strictly prohibited. All rights are reserved in the event of the grant of a patent or the registration of a design. Modifications of design to be reserved for the payment of royalties. All rights are reserved in the event of the grant of a patent or the registration of a design. Modifications of design to be reserved for the payment of royalties.

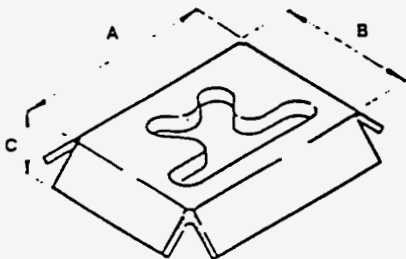
ZU-3
FLUSH TYPE



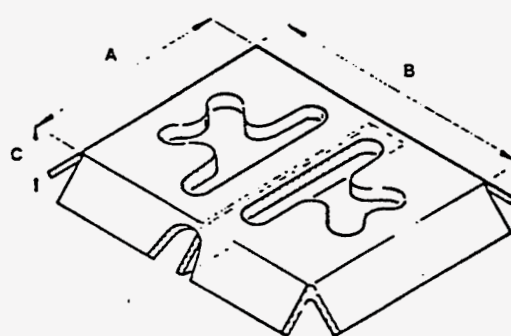
ZU-5
FLUSH TYPE



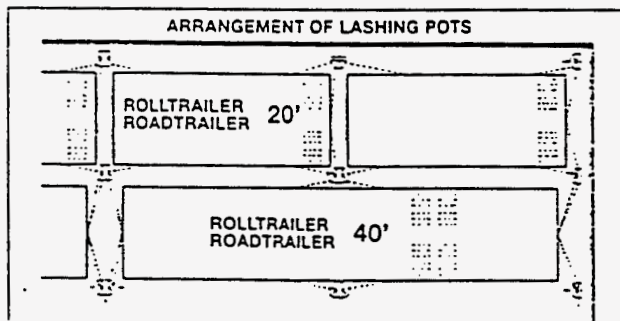
ZU-4
RAISED TYPE



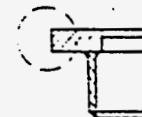
ZU-6
RAISED TYPE



ARRANGEMENT OF LASHING POTS



WELDING FORM
NO. SEE PAGE
6.28



COUNTER PARTS:

LASHING UNITS WHICH ARE FITTED WITH
ELEPHANT-FOOTS G-9, G-9/50, G-21

REMARK:

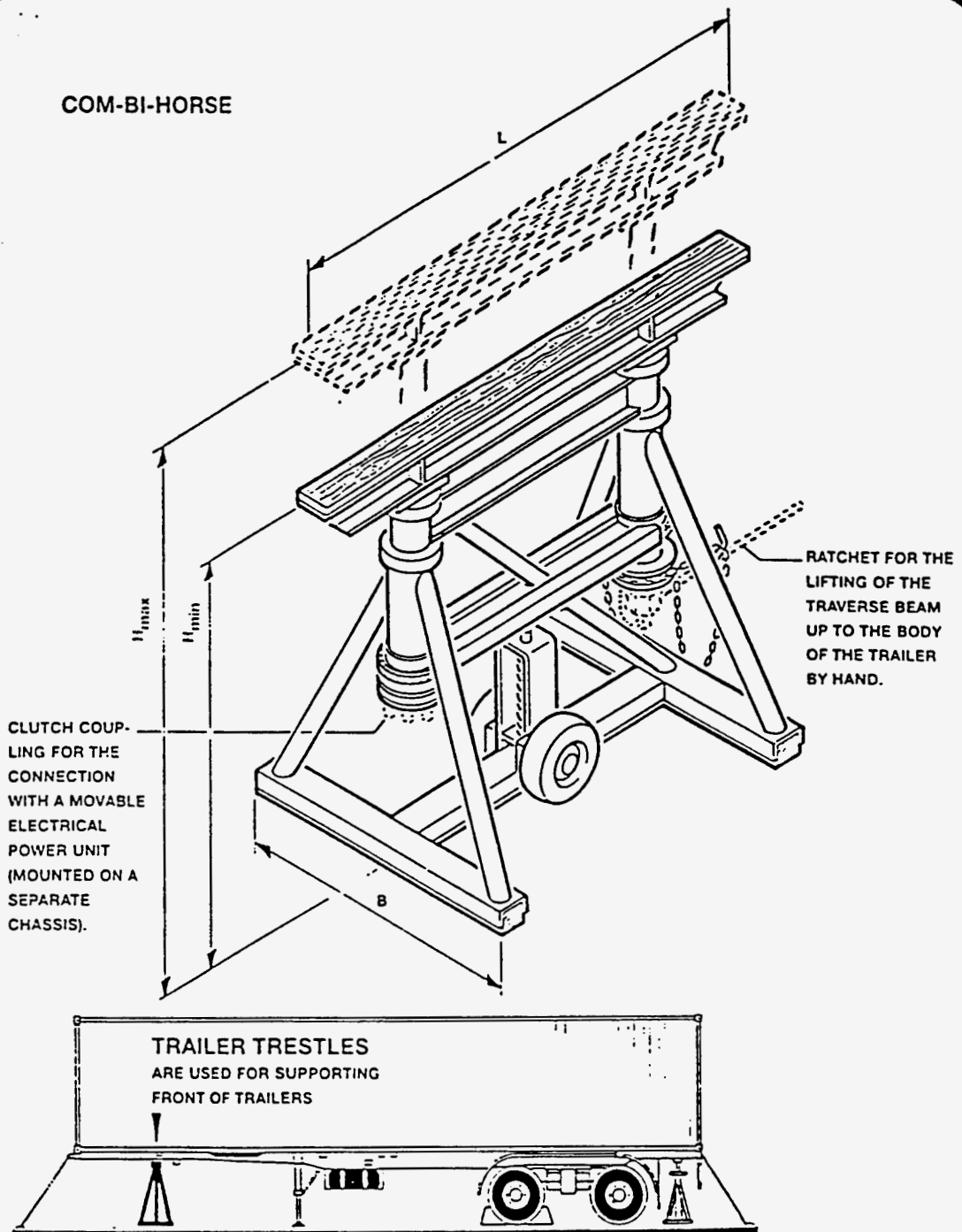
THE LASHING POTS ZU-3 AND ZU-5 CAN BE
DELIVERED WITH FOAM PLASTIC PLUGS
(PP-ZU 3/5) ON REQUEST.

SPECIFICATION:

MATERIAL : STRUCTURAL STEEL
FINISH : NON-TREATED
CLASS. APPROVAL: ALL ITEMS CAN BE
SUPPLIED WITH THE
APPROVAL OF ANY
CLASSIFICATION SOCIETY
UPON CLIENT'S REQUEST.

| CODE | TYPE | A (mm) | B (mm) | C (mm) | WEIGHT (kg) |
|-----------|-------------|--------|--------|--------|-------------|
| 2202.0110 | ZU-3 FLUSH | 300 | 260 | 79 | 17,00 |
| 2202.0120 | ZU-5 FLUSH | 300 | 450 | 79 | 27,00 |
| 2209.0212 | PP-ZU 3/5 | | | | |
| 2202.0710 | ZU-4 RAISED | 215 | 170 | 45 | 6,3 |
| 2202.0720 | ZU-6 RAISED | 215 | 340 | 45 | 11,5 |

COM-BI-HORSE



| CODE | TYPE | H _{min} (mm) | H _{max} (mm) | L (mm) | B (mm) | WEIGHT (kg) |
|-----------|--------------|--------------------------|--------------------------|-----------|-----------|----------------|
| 2801.0201 | COM-BI-HORSE | 1220 | 1420 | 1500 | 850 | 190,9 |

SPECIFICATION:

MATERIAL : STRUCTURAL STEEL
HARD WOOD (TOP) AND
SOFT WOOD (BOTTOM)

FINISH : PAINTED

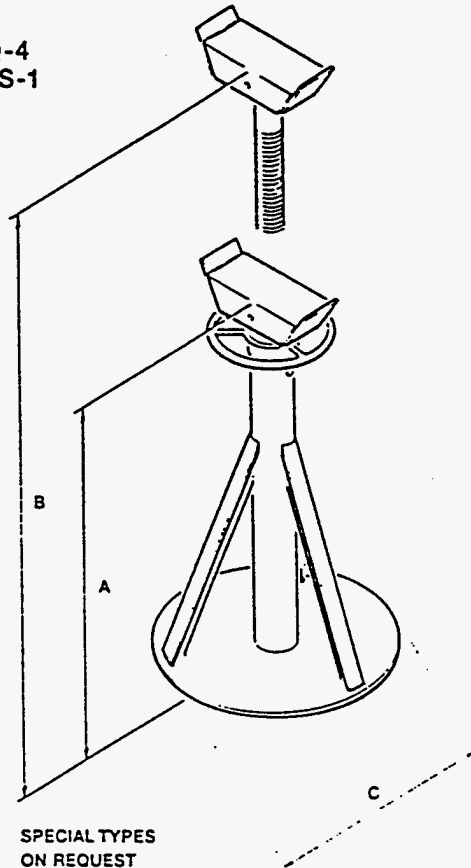
CLASS. APPROVAL: ALL ITEMS CAN BE
SUPPLIED WITH THE
APPROVAL OF ANY
CLASSIFICATION SOCIETY
UPON CLIENT'S REQUEST.

TRAILER SUPPORT JACKS AND WHEEL CHOCKS FOR TRAILER LASHING

6.5

TRAILER SUPPORT JACKS

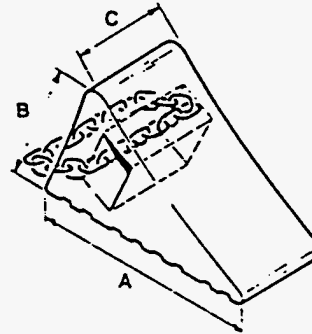
Q-4
TS-1



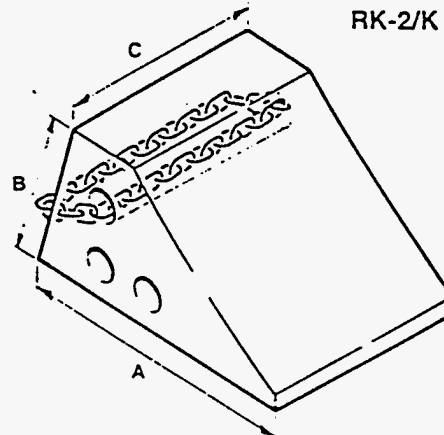
SPECIAL TYPES
ON REQUEST

WHEEL CHOCKS

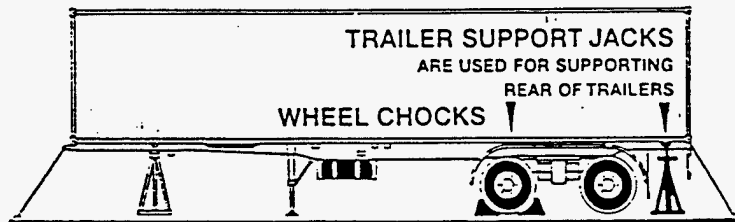
RK-3/K



RK-2/K



WHEEL CHOCKS CAN BE MADE
FROM HARD WOOD ON REQUEST

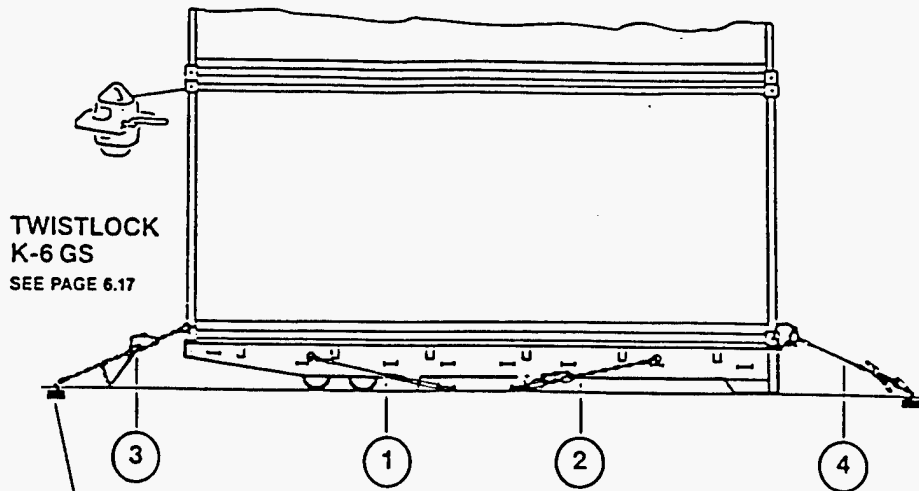


| CODE | TYPE | A (mm) | B (mm) | C (mm) | WEIGHT (kg) | MATERIAL | FINISH | SPECIFICATION |
|------------|--------|-----------|-----------|-----------|----------------|--------------------------------|--------------|------------------------|
| 2802.0100 | Q-4 | 915 | 1270 | 450 | 31,5 | STEEL TUBES, | PAIN- TED | |
| 2802.0200 | TS-1 | 750 | 1250 | 450 | 35,0 | ROLLED STEEL | | |
| 2803.0102 | RK-2 | 300 | 160 | 220 | 8,30 | NEOPRENE | BLACK | WITHOUT HANDLING-CHAIN |
| 2803.01021 | RK-2/K | — | — | — | — | RUBBER-QUALITY | | WITH HANDLING-CHAIN |
| 2803.0103 | RK-3 | 250 | 170 | 100 | 3,0 | (OIL AND SEA WATER RESIST.) | | WITHOUT HANDLING-CHAIN |
| 2803.01031 | RK-3/K | — | — | — | — | | | WITH HANDLING-CHAIN |

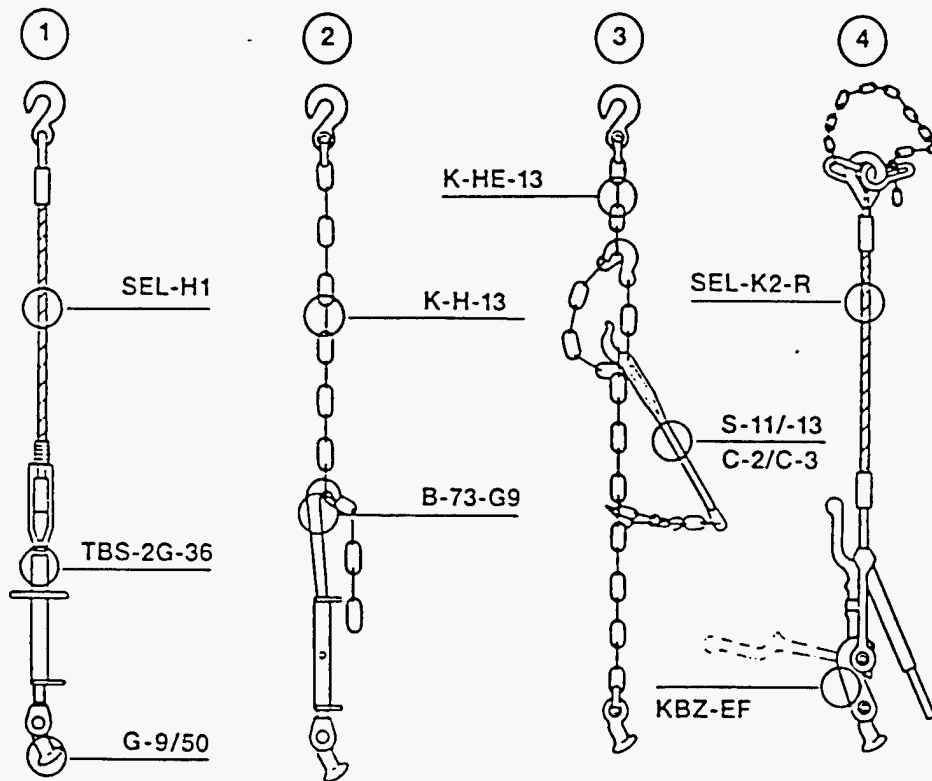
CLASS. APPROVAL: ALL ITEMS CAN BE SUPPLIED WITH THE APPROVAL OF ANY CLASSIFICATION SOCIETY UPON
CLIENT'S REQUEST.

CONVER
OSR

6.6 ROLLTRAILER LASHINGS



LASHING POT ZU-1/-2 SEE PAGE 6.2



| CODE | TYPE |
|-----------|-----------|
| — | SEL-H1 |
| 0100.4020 | TBS-2G-36 |
| 0591.3111 | G-9/50 |

| CODE | TYPE |
|-----------|---------|
| 0500.1033 | K-H-13 |
| 0110.3020 | B-73-G9 |

| CODE | TYPE |
|-----------|---------|
| 0500.3033 | K-HE-13 |
| 0120.1020 | S-11 |
| 0120.1030 | S-13 |
| 0120.1021 | C-2 |
| 0120.1031 | C-3 |

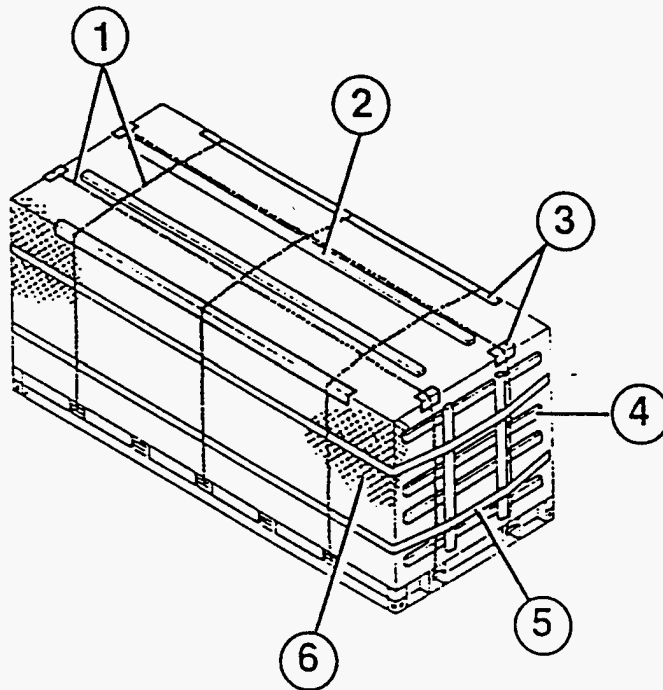
| CODE | TYPE |
|-----------|----------|
| — | SEL-K2-R |
| 0120.2012 | KBZ-EF |

CONVER
OSR

Copyrighted by, checked, and approved by the manufacturer, and the user is responsible for the correct use of the equipment. All rights are reserved in the event of the reproduction of this document without the written permission of the manufacturer.

CARGO-LASHING ON FLATS

- 1 CHAINS WITH HOOKS AND TENSION-LEVER
- 2 SQUARE TIMBERS
- 3 CORNER PROTECTORS
- 4 FLOOR GRIDS
- 5 BELTS (50 mm)
- 6 NETS

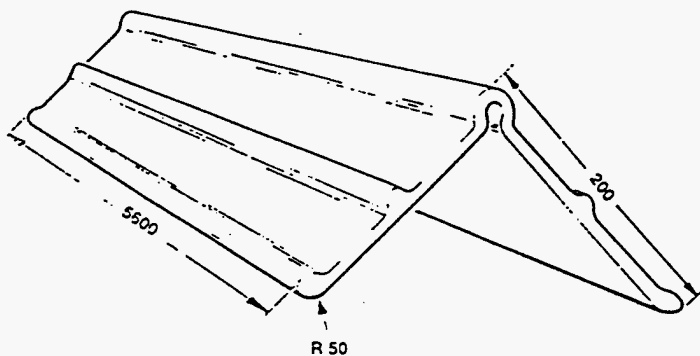


CORNER PROTECTOR

ALUMINIUM

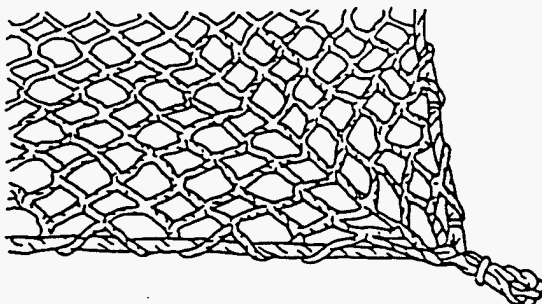
STANDARD LENGTH 5600 mm

OTHER LENGTHS ON REQUEST



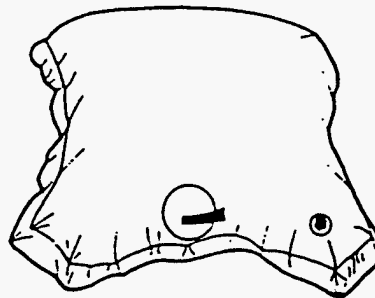
NET

FOR CARGO LASHING AND AS SAFETY NET
DIMENSIONS ON CLIENT'S REQUEST












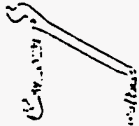
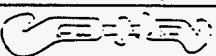
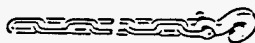
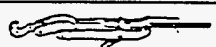
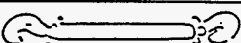
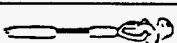


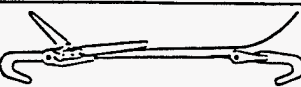


AIR BAG

DIMENSIONS: ~ 1200 mm x 1200 mm
VULCANIZED JOINT AND
REINFORCEMENT INSIDE



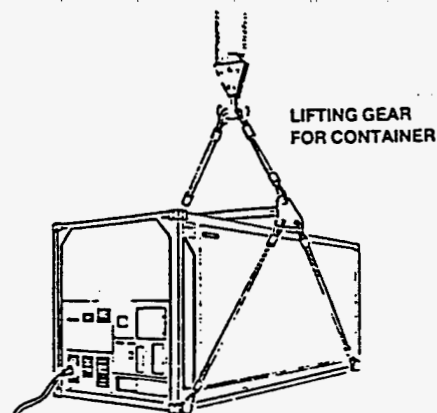
Copyright of this document and its contents are the property of the company. All rights are reserved. No part of this document may be reproduced or transmitted in any form or by any means electronic or mechanical, including photocopying and recording, or by any information storage or retrieval system, without permission in writing from the company.

| SYMBOL | DESCRIPTION | TYPE | PURPOSE |
|--|---------------------------------------|-------------------------------------|--|
| FIXED PARTS | | | |
|   | TWISTLOCK POCKET | LSF-..., LF-... LT-..., LS-ZU... | CONTAINER STOWAGE |
| | DOVETAIL FOUNDATION | APT-...L | |
| | CONIC GUIDE UNIT | J-81 R SERIES | |
|   | LASHING POT | ZU-1, F-4 ZU-2, F-3 | CONTAINER LASHING TRAILER LASHING CARGO LASHING CAR LASHING |
|   | FLUSH LASHING EYES | FL-... | |
| | LASHING EYES WITH PROTECTION RINGS | | |
| CONTAINER SECURING FITTINGS | | | |
|   | BOTTOM TWISTLOCK | K-17 FL, K-17 FL-V | ONLY CONTAINER LASHING |
| | TWISTLOCK | CV-9, K-6 GS | |
| TRAILER SUPPORTS | | | |
|    | TRAILER TRESTLES | TT-1/-2/-3 | ONLY ROAD-TRAILER LASHING |
| | TRAILER SUPPORT JACKS | TS-1 | |
| | WHEEL CHOCKS | RK-1/-2/-3 | |
| LASHING UNITS | | | |
|  | TENSION LEVER | C-2, C-3 S-9, S-11, S-13 | CONTAINER LASHING ROAD-TRAILER LASHING ROLL-TRAILER LASHING CARGO LASHING FLAT LASHING |
|  | CHAIN TURNBUCKLE | CTB-... | |
|  | LASHING CHAIN | K-... | |
|  | QUICK RELEASE LASHING | KBZ-... | |
|  | TURNBUCKLES | TBS-..., B-... | |
|  | LASHING WIRES | SEL-... | |
|  | CORNER PROTECTOR | | CARGO LASHING |
|  | NET | | |
|  | CAR LASHING | | CAR LASHING |

CONVER

Copyright of the U.S. Government and its successors, and the U.S. Government is authorized to reproduce and distribute reprints for government purposes, not withstanding any copyright notation that may appear hereon. All rights reserved in the event of the republication of this work. Modification of this work is prohibited.

7 LIFTING GEAR AND OTHER SHIP SUPPLIES

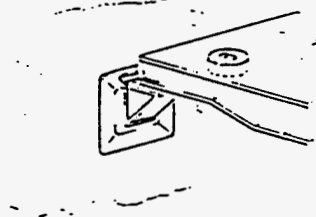


LIFTING GEAR
FOR CONTAINER

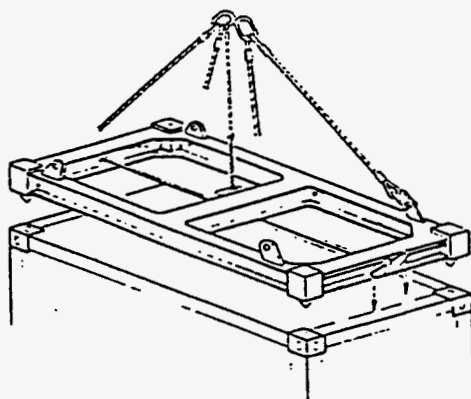
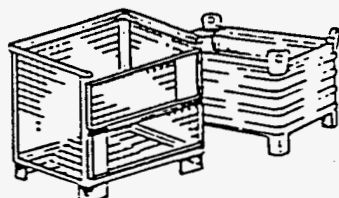


ELECTRICAL COMPONENTS
FOR REEFER CONTAINERS
IN ACCORDANCE WITH: DIN 4962/53
CEE 1772
IEC 309

SUPPORTS FOR TWEEDECK HATCH COVERS
ESPECIALLY FOR RO/RO SHIPS

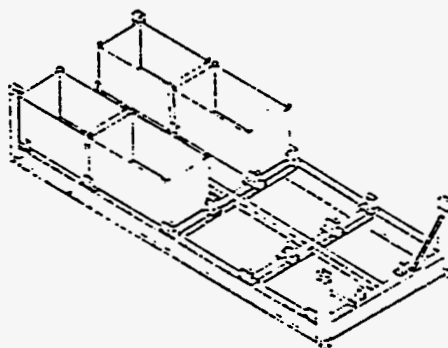
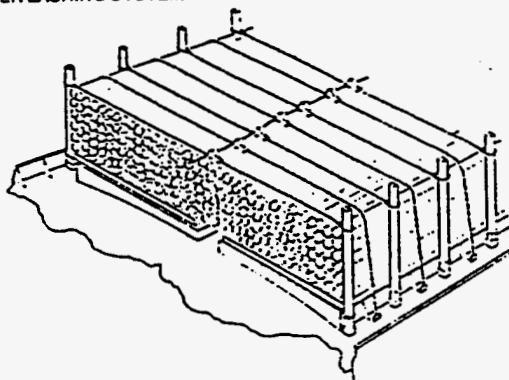


CONTAINERS FOR LOOSE MATERIAL



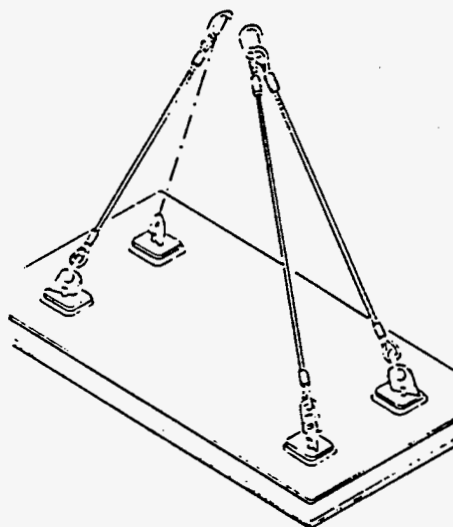
FRAME AND H-SPREADERS
FOR CONTAINERS
AND HATCH COVERS

TIMBER LASHING SYSTEM



FLAT WITH STORAGE BINS

LIFTING GEAR
FOR HATCH COVERS



Copying of this document, and giving it to others, and the use or communication of the contents thereof, are forbidden without express authority. Offenders are liable to the payment of damages. All rights are reserved in the event of the grant of a patent or the registration of a design. Modification of design to be reserved.

Part I. IMDG Segregation Requirements

CLASS 7 - Radioactive materials

4.5 Segregation requirements

- 4.5.1 Category I - WHITE or category II or III - YELLOW labelled packages, overpacks, freight containers and tanks shall be segregated from living quarters and from regularly occupied working spaces and from spaces that may be continually occupied by persons, except those exclusively reserved for couriers specially authorized to accompany such shipments, with due attention paid to radiation protection.
- 4.5.2 Category II or III - YELLOW labelled packages, overpacks, freight containers and tanks shall be segregated from persons and undeveloped photographic film and plates in accordance with 4.6.
- 4.5.3 Mail bags, whether loose or packed in freight containers, shall be assumed to contain undeveloped photographic film and plates and, therefore, be segregated from radioactive materials in the same way as undeveloped photographic film and plates.
- 4.5.4 Low specific activity materials and surface contaminated objects carried as unpackaged material shall be segregated in accordance with the transport index (see schedules 5 and 8).
- 4.5.5 As separation distances are based upon the sum of the transport indices of packages, overpacks, tanks and freight containers to be carried, carriers shall make due allowance in this respect in their initial stowage if they intend to load additional radioactive materials *en route*.
- 4.5.6 The appropriate segregation may be established by demonstrating that, for exposure times up to 700 hours in a year, the direct measurement of the radiation level at regularly occupied spaces and living quarters is less than 0.0075 mSv/h (0.75 mrem/h), taking into account any relocation of cargo during the voyage. If the exposure time of any individual whilst on board the vessel is likely to exceed 700 hours a year, then the measured radiation level at regularly occupied spaces and living quarters should be less than 0.0018 mSv/h (0.18 mrem/h). In all cases the measurements of the radiation level must be made and documented by a suitably qualified person.
- 4.5.7 On board a ship which is in special use for the carriage of radioactive materials in accordance with 4.3.1, the control of the separation distances and/or measured radiation levels, as appropriate, should be governed by the radiation protection programme as approved according to 4.3.1.4.

4.6 Separation distances

- 4.6.1 The nature and frequency of consignments of radioactive materials carried on board ships, other than ships specially used for the purpose of carrying radioactive materials, is such that exposure is low. Consequently, provided that the segregation provisions specified in this section are applied, individual radiation monitoring is not necessary for members of the crew. Moreover, there is neither a need for any crew member to systematically wear a personal dose meter nor need a ship routinely carry any instrument for measuring radiation.
- 4.6.2 The separation distances specified in this Code to control radiation exposure of passengers and crew are based upon the limiting values of dose recommended by the IAEA for the determination of separation distances for transport workers and members of the public of 5 mSv (500 mrem) per year and 1 mSv (100 mrem) per year, respectively (see IAEA paragraph 205).
- 4.6.3 One of the segregation tables (I, III and IV hereafter) shall be followed in respect to living quarters or spaces regularly occupied by persons. Table III and table IV include comprehensive provisions which are of general applicability. Table I provides simplified information which is applicable to certain ship sizes only.

CLASS 7 – Radioactive materials

- 4.6.4 The radiation exposure of undeveloped photographic film and plates shall be based upon a single-voyage exposure of 0.1 mSv (10 mrem). One of the segregation tables (II, III and IV hereafter) shall be followed. Tables III and IV include comprehensive provisions which are of general applicability. Table II provides simplified information which is applicable to certain ship sizes and voyage durations only.
- 4.6.5 As an alternative to the use of tables III and IV, separation distances may be estimated by the use of the nomographs in 4.8. These nomographs will be particularly useful in cases where stowage factors (cargo density or thickness of cargo) are significantly different from the figures given in tables III and IV.
- 4.6.6 The competent authority concerned shall arrange, as necessary, for periodic assessments of annual radiation doses received by passengers and crew.

4.7 Competent authority approvals

Any departure from the segregation requirements in 4.5 and 4.6 must be approved by the competent authority of the flag State of the ship and, when requested, by the competent authority at each port of call.

CLASS 7 – Radioactive materials

TABLE I

Simplified segregation table for persons

| Sum of transport indices (TI) | Segregation distance of radioactive materials from passengers and crew | | | |
|-------------------------------------|--|--------------------------------|--|---------------------------------------|
| | General cargo ship ¹ | | Ferry etc. ² | Offshore support vessel ³ |
| | Break-bulk (metres) | Containers (TEUs) ⁴ | | |
| Up to 10 | 6 | 1 | Stow at bow or stern furthest from living quarters and regularly occupied work areas | Stow at stern or at platform midpoint |
| More than 10 but not more than 20 | 8 | 1 | as above | as above |
| More than 20 but not more than 50 | 13 | 2 | as above | not applicable |
| More than 50 but not more than 100 | 18 | 3 | as above | not applicable |
| More than 100 but not more than 200 | 26 | 4 | as above | not applicable |
| More than 200 but not more than 400 | 36 | 6 | as above | not applicable |

¹ General cargo, break-bulk or lo-lo container ship of 150 metres minimum length.

² Ferry or cross-channel, coastal and inter-island ship of 100 metres minimum length.

³ Offshore support vessel of 50 metres minimum length. (In this case the practical maximum sum of TIs carried is 20.)

⁴ TEU means "20 ft Equivalent Unit" (this is equivalent to a standard freight container of 6 metres nominal length).

CLASS 7 – Radioactive materials

TABLE II

Simplified segregation table for photographic films and plates

| Sum of transport indices (TI) | Duration of voyage in days | | | | |
|------------------------------------|--|--|---|--|--|
| | Not more than 1 ^{1,2} | More than 1 but not more than 4 ^{1,2} | More than 4 but not more than 10 ² | More than 10 but not more than 30 ² | More than 30 but not more than 50 ² |
| Not more than 10 | <div style="display: flex; justify-content: space-around; align-items: center; height: 150px;"> <div style="border: 1px solid black; padding: 10px; margin: 5px;"> $\frac{1}{3}$ ship length </div> <div style="border: 1px solid black; padding: 10px; margin: 5px;"> $\frac{1}{2}$ ship length </div> </div> | | | | |
| More than 10 but not more than 20 | | | | | |
| More than 20 but not more than 50 | | | | | |
| More than 50 but not more than 400 | | | | | |

¹ Ferry or cross-channel, coastal and inter-island ship of 100 metres minimum length.

² General cargo, break-bulk or lo-to container ship of 150 metres minimum length.

³ Shielding required in the form of intervening cargo, either as a complete layer of filled containers or as a cargo space with 6 metres (minimum) carried between the film and class 7 packages.

TABLE III
Segregation table in metres
Safe distances for persons and undeveloped photographic films and plates

| <div>Sum of transport indices (Note (7))</div> <div>Cargo thick-ness, metres (unit density)</div> | | Minimum distance in metres from living quarters or spaces regularly occupied by persons | | Minimum distance in metres from undeveloped films and plates | | | | | | | | | | | | | | | | | | | | | | | |
|---|----|---|----|--|---|----|--------------|---|----|--------------|---|-----|---------------|---|-----|---------------|----|-----|---------------|----|-----|---------------|----|-----|---------------|----|---|
| | | | | 1 day voyage | | | 2 day voyage | | | 4 day voyage | | | 10 day voyage | | | 20 day voyage | | | 30 day voyage | | | 40 day voyage | | | 50 day voyage | | |
| | | | | Nil | 1 | 2 | Nil | 1 | 2 | Nil | 1 | 2 | Nil | 1 | 2 | Nil | 1 | 2 | Nil | 1 | 2 | Nil | 1 | 2 | Nil | 1 | 2 |
| 0.5 | 2 | X | 2 | X | X | 3 | X | X | 4 | X | X | 6 | 2 | X | 8 | 2 | X | 10 | 3 | X | 11 | 3 | X | 12 | 3 | X | |
| 1 | 2 | X | 3 | X | X | 4 | X | X | 5 | 2 | X | 8 | 2 | X | 11 | 3 | X | 13 | 4 | X | 15 | 4 | X | 17 | 4 | X | |
| 2 | 3 | X | 4 | X | X | 5 | 2 | X | 7 | 2 | X | 11 | 3 | X | 15 | 4 | X | 19 | 5 | X | 22 | 5 | X | 24 | 6 | X | |
| 3 | 4 | X | 5 | X | X | 6 | 2 | X | 9 | 2 | X | 13 | 4 | X | 19 | 5 | X | 23 | 6 | X | 27 | 7 | X | 30 | 7 | X | |
| 5 | 4 | X | 6 | 2 | X | 8 | 2 | X | 11 | 3 | X | 17 | 4 | X | 24 | 6 | X | 30 | 7 | X | 34 | 8 | X | 38 | 9 | X | |
| 10 | 6 | 2 | 8 | 2 | X | 11 | 3 | X | 15 | 4 | X | 24 | 6 | X | 34 | 8 | X | 42 | 10 | 3 | 48 | 12 | 3 | 54 | 13 | 3 | |
| 20 | 8 | 2 | 11 | 3 | X | 15 | 4 | X | 22 | 5 | X | 34 | 8 | X | 48 | 12 | 3 | 59 | 14 | 4 | 68 | 16 | 4 | 76 | 18 | 5 | |
| 30 | 10 | 3 | 13 | 4 | X | 19 | 5 | X | 26 | 7 | X | 42 | 10 | 3 | 59 | 14 | 4 | 72 | 17 | 4 | 83 | 20 | 5 | 93 | 22 | 6 | |
| 50 | 13 | 3 | 17 | 4 | X | 24 | 6 | X | 34 | 8 | X | 54 | 13 | 3 | 76 | 18 | 5 | 92 | 23 | 6 | 110 | 26 | 7 | 120 | 29 | 7 | |
| 100 | 18 | 5 | 24 | 6 | X | 34 | 8 | X | 48 | 12 | 3 | 76 | 18 | 5 | 110 | 25 | 8 | 130 | 32 | 8 | 150 | 36 | 9 | 170 | 40 | 10 | |
| 150 | 22 | 6 | 30 | 7 | X | 42 | 10 | 3 | 59 | 14 | 4 | 93 | 22 | 6 | 130 | 31 | 8 | 160 | 39 | 10 | 185 | 45 | 11 | * | 50 | 12 | |
| 200 | 26 | 6 | 34 | 8 | X | 48 | 12 | 3 | 68 | 16 | 4 | 110 | 26 | 7 | 150 | 36 | 9 | 185 | 43 | 11 | * | 51 | 13 | * | 58 | 14 | |
| 300 | 32 | 8 | 42 | 10 | 3 | 59 | 14 | 4 | 83 | 20 | 5 | 130 | 32 | 8 | 185 | 44 | 11 | * | 55 | 13 | * | 63 | 15 | * | 70 | 17 | |
| 400 | 36 | 9 | 48 | 12 | 3 | 68 | 16 | 4 | 95 | 23 | 6 | 150 | 36 | 9 | * | 50 | 13 | * | 63 | 15 | * | 73 | 18 | * | 81 | 20 | |

- NOTE: (1) X - indicates that thickness of screening cargo is sufficient without any additional segregation distance.
(2) By using 2 metres of intervening unit density cargo for persons, and 3 metres for films and plates, no distance shielding is necessary for any length of voyage specified.
(3) Using 1 steel bulkhead or steel deck - multiply segregation distance by 0.8.
Using 2 steel bulkheads or steel decks - multiply segregation distance by 0.64.
(4) "Cargo of unit density" means cargo stowed at a density of 1 tonne per m³, where the density is less than this the depth of cargo specified must be increased in proportion.
(5) "Minimum distance" means the least distance in any direction, whether vertical or horizontal, from the outer surface of the nearest package.
(6) The figures below the double line of the table should be used in those cases where the appropriate provisions of this class permit the total transport index to exceed 200.
(7) Transport indices of packages, overpacks, freight containers and tanks, as appropriate.

* Not to be carried unless screening by other cargo and bulkheads can be arranged in accordance with the other columns.

CLASS 7 - Radioactive materials

TABLE IV
Segregation table in feet

Safe distances for persons and undeveloped photographic films and plates

| <div>Sum of transport indices (Note (7))</div> <div>Cargo thick-ness, feet (unit density)</div> | | Minimum distance in feet from living quarters or spaces regularly occupied by persons | | Minimum distance in feet from undeveloped films and plates | | | | | | | | | | | | | | | | | | | | | | | |
|---|-----|---|-----|--|---|-----|--------------|----|-----|--------------|----|-----|---------------|----|-----|---------------|----|-----|---------------|----|-----|---------------|----|-----|---------------|----|---|
| | | | | 1 day voyage | | | 2 day voyage | | | 4 day voyage | | | 10 day voyage | | | 20 day voyage | | | 30 day voyage | | | 40 day voyage | | | 50 day voyage | | |
| | | | | Nil | 3 | 6 | Nil | 3 | 6 | Nil | 3 | 6 | Nil | 3 | 6 | Nil | 3 | 6 | Nil | 3 | 6 | Nil | 3 | 6 | Nil | 3 | 6 |
| 0.5 | 5 | X | 6 | X | X | 8 | X | X | 11 | X | X | 17 | 4 | X | 25 | 6 | X | 30 | 7 | X | 35 | 8 | X | 39 | 9 | X | |
| 1 | 6 | X | 8 | X | X | 11 | X | X | 16 | 4 | X | 25 | 6 | X | 35 | 8 | X | 42 | 10 | X | 50 | 12 | X | 55 | 13 | X | |
| 2 | 9 | X | 11 | X | X | 16 | 4 | X | 22 | 5 | X | 35 | 8 | X | 50 | 12 | X | 61 | 14 | X | 70 | 17 | X | 78 | 19 | X | |
| 3 | 10 | X | 14 | X | X | 19 | 5 | X | 27 | 6 | X | 42 | 10 | X | 61 | 14 | X | 74 | 18 | X | 86 | 20 | X | 96 | 23 | X | |
| 5 | 13 | X | 17 | 4 | X | 25 | 6 | X | 35 | 8 | X | 55 | 13 | X | 78 | 19 | X | 96 | 23 | X | 110 | 26 | X | 124 | 29 | 7 | |
| 10 | 19 | 4 | 25 | 6 | X | 35 | 8 | X | 50 | 12 | X | 78 | 19 | X | 110 | 26 | X | 135 | 33 | 8 | 155 | 37 | 9 | 175 | 42 | 10 | |
| 20 | 26 | 6 | 35 | 8 | X | 50 | 12 | X | 69 | 17 | X | 110 | 26 | X | 155 | 37 | 9 | 190 | 46 | 11 | 220 | 53 | 13 | 250 | 59 | 14 | |
| 30 | 32 | 8 | 43 | 10 | X | 61 | 14 | X | 85 | 20 | X | 135 | 32 | 8 | 190 | 45 | 11 | 235 | 56 | 13 | 270 | 65 | 16 | 305 | 72 | 17 | |
| 50 | 42 | 10 | 55 | 13 | X | 78 | 19 | X | 110 | 26 | X | 175 | 42 | 10 | 245 | 58 | 14 | 300 | 73 | 17 | 350 | 84 | 20 | 390 | 94 | 22 | |
| 100 | 59 | 14 | 78 | 19 | X | 110 | 26 | X | 155 | 37 | 9 | 245 | 59 | 14 | 350 | 82 | 20 | 430 | 105 | 24 | 515 | 118 | 28 | 550 | 130 | 32 | |
| 150 | 72 | 17 | 96 | 23 | X | 135 | 32 | 8 | 190 | 46 | 11 | 300 | 72 | 17 | 425 | 100 | 24 | 525 | 125 | 30 | 600 | 145 | 35 | * | 165 | 39 | |
| 200 | 84 | 20 | 110 | 26 | X | 155 | 37 | 9 | 220 | 53 | 13 | 350 | 84 | 20 | 490 | 115 | 28 | 600 | 140 | 35 | * | 165 | 40 | * | 190 | 45 | |
| 300 | 105 | 24 | 135 | 32 | 8 | 190 | 46 | 11 | 270 | 64 | 15 | 425 | 105 | 25 | 600 | 145 | 35 | * | 180 | 42 | * | 205 | 49 | * | 230 | 55 | |
| 400 | 120 | 28 | 160 | 37 | 9 | 220 | 53 | 13 | 310 | 75 | 18 | 500 | 120 | 28 | * | 165 | 40 | * | 205 | 49 | * | 235 | 57 | * | 265 | 63 | |

CLASS 7 - Radioactive materials

- NOTE: (1) X - indicates that thickness of screening cargo is sufficient without any additional segregation distance.
 (2) By using 6 feet of intervening unit density cargo for persons, and 10 feet for films and plates, no distance shielding is necessary for any length of voyage specified.
 (3) Using 1 steel bulkhead or steel deck - multiply segregation distance by 0.8.
 Using 2 steel bulkheads or steel decks - multiply segregation distance by 0.64.
 (4) "Cargo of unit density" means cargo stowed at a density of 1 ton (long) per 36 cubic feet; where the density is less than this the depth of cargo specified must be increased in proportion.
 (5) "Minimum distance" means the least distance in any direction, whether vertical or horizontal, from the outer surface of the nearest package.
 (6) The figures below the double line of the table should be used in those cases where the appropriate provisions of this class permit the total transport index to exceed 200.
 (7) Transport indices of packages, overpacks, freight containers and tanks, as appropriate.

* Not to be carried unless screening by other cargo and bulkheads can be arranged in accordance with the other columns.

CLASS 7 – Radioactive materials

4.8 Rules for the use of the nomographs

4.8.1 When there is no intervening cargo between the radioactive materials and the persons or the undeveloped photographic film or plates, calculate the safe distance as follows:

- .1 for persons – use the FG scales, read off the safe separation distance in metres or feet (D_p) on the G scale adjacent to the sum of the transport indices (N) on the F scale; and
- .2 for film and plates – draw a straight line between the length of the voyage (t), I scale, and the sum of the transport indices (N), F scale; separation distance in metres or feet (D_t) will be the intersection on the H scale.

4.8.2 When there is intervening cargo between the radioactive materials and the persons or undeveloped photographic film or plates, calculate the safe distance as follows:

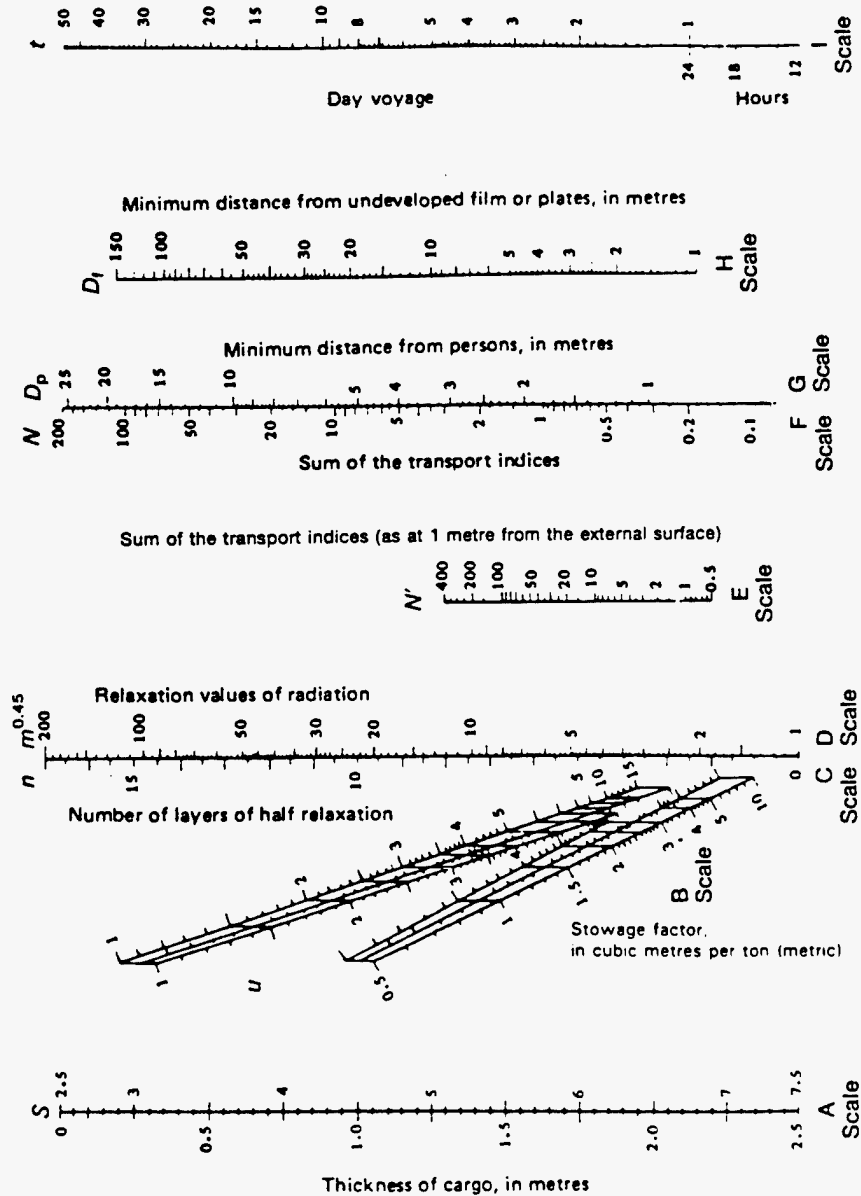
- .1 for persons – draw a straight line through the thickness of cargo (S) in metres or feet, A scale, and the stowage factor (u), B scale, which is the cargo density, intersecting the CD scales. From this intersection draw another straight line through the value of the sum of the transport indices (as at 1 metre/3 feet from the external surface), E scale, cutting the G scale at the safe separation distance figure (D_p); and
- .2 for film and plates – as for persons, but from intersection on FG scales draw a straight line to the I scale; this line will cut the H scale at the separation distance for film and plates in metres or feet (D_t).

Note: For thickness of cargo (S) up to 2.5 metres (10 feet), use the left of A scale and the left (lower) of B scale. For S between 2.5 metres (10 feet) and 7.5 metres (30 feet) use the right of A scale and the right (or upper) of B scale. For S in excess of 7.5 metres (30 feet) divide both S and u by 10 and use the corresponding parts of A and B scales. When there is no intervening bulkhead use the lower lines of B scale, for one bulkhead the middle lines, and for two bulkheads the top lines.

4.8.3 Other problems, such as estimating the minimum thickness of cargo or determining the stowage factor of intervening cargo when the thickness of the cargo is known, can also be solved by means of the nomographs.

CLASS 7 - Radioactive materials

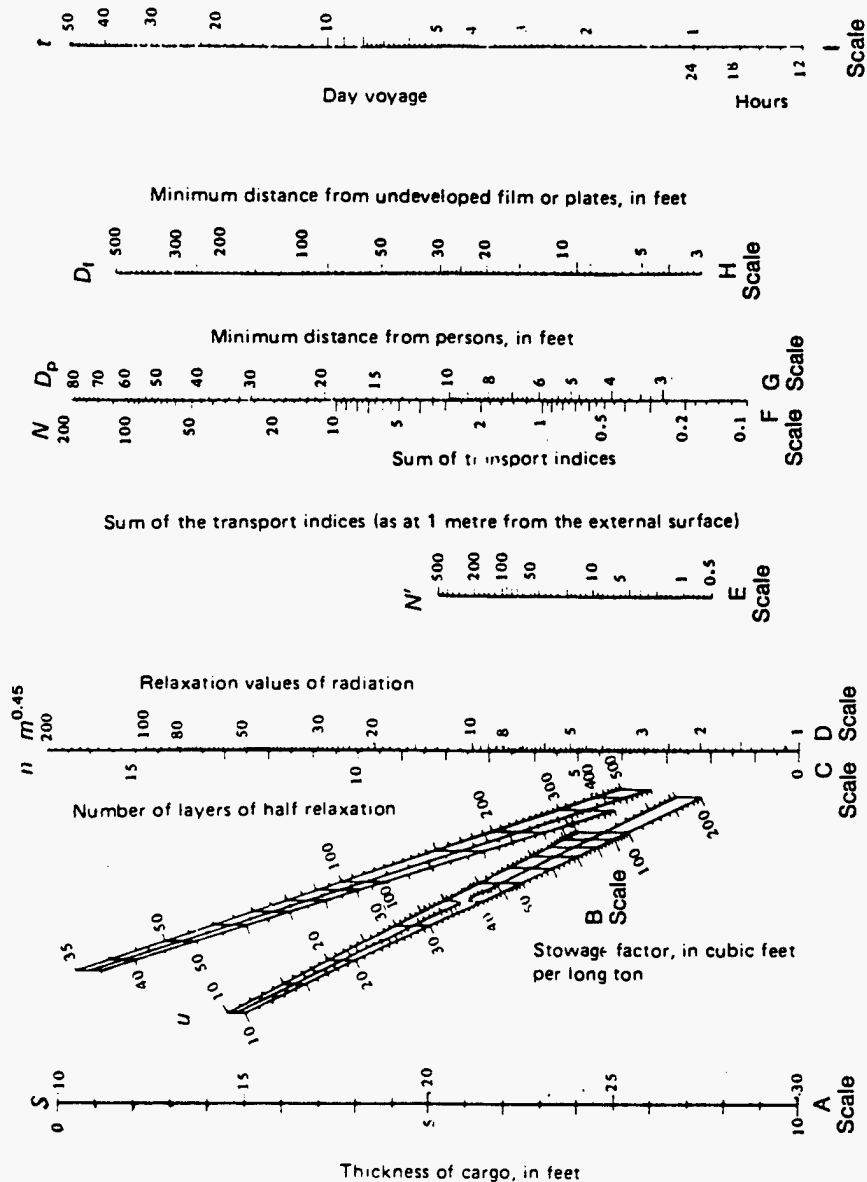
NOMOGRAPH FOR THE SAFE DISTANCE
(METRES)



IMDG CODE - PAGE 7026
Amdt. 27-94

CLASS 7 - Radioactive materials

NOMOGRAPH FOR THE SAFE DISTANCE
(FEET)



IMDG CODE - PAGE 7027
Amdt. 27-94

CLASS 7 - Radioactive materials

5 CONTAMINATION/DECONTAMINATION

5.1 Contamination on packages, overpacks, freight containers, tanks and in conveyances

5.1.1 The non-fixed contamination on the external surfaces of a package shall be kept as low as practicable.

5.1.2 Except as provided for in 5.2.2, under conditions likely to be encountered in routine transport, the non-fixed contamination of the external surfaces of packages and tanks, of external and internal surfaces of overpacks and freight containers, and of the surfaces of conveyances and their equipment shall not exceed the levels specified in the table hereunder.

Limits of non-fixed contamination on surfaces

| Type of package, overpack, freight container, tank or conveyance and its equipment | Contaminant | | | |
|---|--|------------------------|---|------------------------|
| | Limit ¹⁾ of beta and gamma emitters and the low-toxicity alpha emitters ²⁾ | | Limit ¹⁾ of all other alpha emitters | |
| | Bq/cm ² | (μCi/cm ²) | Bq/cm ² | (μCi/cm ²) |
| External surfaces of: | | | | |
| 1. Excepted packages of radioactive material | 0.4 | (10 ⁻⁵) | 0.04 | (10 ⁻⁶) |
| 2. All other packages of radioactive material | 4 | (10 ⁻⁴) | 0.4 | (10 ⁻⁵) |
| External and internal surfaces of overpacks, freight containers and conveyances and their equipment when carrying or being prepared to carry: | | | | |
| 1. Loads consisting only of radioactive material in packages other than excepted packages | 4 | (10 ⁻⁴) | 0.4 | (10 ⁻⁵) |
| 2. Loads including excepted packages of radioactive material and/or non-radioactive consignments | 0.4 | (10 ⁻⁵) | 0.04 | (10 ⁻⁶) |
| External surfaces of freight containers, tanks, and conveyances and their equipment, used in the carriage of unpackaged radioactive material | 4 | (10 ⁻⁴) | 0.4 | (10 ⁻⁵) |

¹⁾ The limits are applicable when averaged over any area of 300 cm² of any part of the surface.

²⁾ See subsection 2.8.

Part J. DOT Segregation Requirements

Subpart D—General Segregation Requirements**§176.80 Application.**

(a) This subpart sets forth segregation requirements in addition to any segregation requirements set forth elsewhere in this subchapter.

(b) Hazardous materials in limited quantities when loaded in transport vehicles and freight containers, are excepted from the segregation requirements of this subpart and any additional segregation specified in this subchapter for transportation by vessel.

§176.83 Segregation.

(a) *General.* (1) This section applies to all cargo spaces on deck and under deck on all types of vessels.

(2) Segregation is obtained by maintaining certain distances between incompatible hazardous materials or by requiring the presence of one or more steel bulkheads or decks between them or a combination thereof. Intervening spaces between such hazardous materials may be filled with other cargo which is not incompatible with the hazardous materials.

(3) In addition to general segregation between classes of hazardous materials, there may be a need to segregate a particular material from other materials which would contribute to its hazard. Such segregation requirements are indicated by code numbers in Column 10B of the §172.101 Table.

(4) Segregation is not required between hazardous materials of different classes which comprise the same substance but vary only in their water content (e.g., sodium sulphide in Division 4.2 or Class 8).

(5) Whenever hazardous materials are stowed together, whether or not in a transport unit, the segregation of such hazardous materials from others must always be in accordance with the most restrictive requirements for any of the hazardous materials concerned.

(6) When the §172.101 Table or §172.402 requires packages to bear a subsidiary hazard label or labels, the segregation appropriate to the subsidiary hazards must be applied when that segregation is more restrictive than that required by the primary hazard. For the purposes of this paragraph, the segregation requirements corresponding to an explosive subsidiary hazard are—except for organic peroxides which are those corresponding to Division 1.3—those for Division 1.4 (Class C explosive) materials.

(7) Where, for the purposes of segregation, terms such as "away from" a particular hazard class are used in the §172.101 Table, the segregation requirement applies to:

(i) All hazardous materials within the hazard class; and

(ii) All hazardous materials for which a secondary hazard label of that class is required.

(8) Notwithstanding paragraphs (a)(6) and (a)(7) of this section, hazardous materials of the same class may be stowed together without regard to segregation required by secondary hazards if the materials are not incompatible.

(9) Stowage in a shelter-tween deck cargo space is not considered to be "on deck" stowage.

(b) *General Segregation Table.* The following table sets forth the general requirements for segregation between the various classes of hazardous materials. The properties of materials within each class may vary greatly and may require greater segregation than is reflected in this table. If the §172.101 Table sets forth particular requirements for segregation, they take precedence over these general requirements.

Table §176.83(b)—General Segregation Requirements for Hazardous Materials

[Segregation must also take account of a single secondary hazard label, as required by paragraph (a)(6) of this section.]

| Class | 1.1 1.2 1.5 | 1.3 | 1.4 1.6 | 2.1 | 2.2 | 2.3 | 3 | 4.1 | 4.2 | 4.3 | 5.1 | 5.2 | 6.1 | 6.2 | 7 | 8 | 9 |
|---|-------------------|-----|------------|-----|-----|-----|---|-----|-----|-----|-----|-----|-----|-----|---|---|---|
| Explosives, 1.1, 1.2, 1.5 | (*) | (*) | (*) | 4 | 2 | 2 | 4 | 4 | 4 | 4 | 4 | 4 | 2 | 4 | 2 | 4 | X |
| Explosives, 1.3..... | (*) | (*) | (*) | 4 | 2 | 2 | 4 | 3 | 3 | 4 | 4 | 4 | 2 | 4 | 2 | 2 | X |
| Explosives, 1.4, 1.6 | (*) | (*) | (*) | 2 | 1 | 1 | 2 | 2 | 2 | 2 | 2 | 2 | X | 4 | 2 | 2 | X |
| Flammable gases 2.1 | 4 | 4 | 2 | X | X | X | 2 | 1 | 2 | X | 2 | 2 | X | 4 | 2 | 1 | X |
| Non-toxic, nonflammable gases 2.2 | 2 | 2 | 1 | X | X | X | 1 | X | 1 | X | X | 1 | X | 2 | 1 | X | X |
| Poisonous gases 2.3 | 2 | 2 | 1 | X | X | X | 2 | X | 2 | X | X | 2 | X | 2 | 1 | X | X |
| Flammable liquids 3 | 4 | 4 | 2 | 2 | 1 | 2 | X | X | 2 | 1 | 2 | 2 | X | 3 | 2 | X | X |
| Flammable solids 4.1 | 4 | 3 | 2 | 1 | X | X | X | X | 1 | X | 1 | 2 | X | 3 | 2 | 1 | X |
| Spontaneously combustible substances 4.2 | 4 | 3 | 2 | 2 | 1 | 2 | 2 | 1 | X | 1 | 2 | 2 | 1 | 3 | 2 | 1 | X |
| Substances which are dangerous when wet 4.3 | 4 | 4 | 2 | X | X | X | 1 | X | 1 | X | 2 | 2 | X | 2 | 2 | 1 | X |
| Oxidizing substances 5.1 | 4 | 4 | 2 | 2 | X | X | 2 | 1 | 2 | 2 | X | 2 | 1 | 3 | 1 | 2 | X |
| Organic peroxides 5.2 | 4 | 4 | 2 | 2 | 1 | 2 | 2 | 2 | 2 | 2 | 2 | X | 1 | 3 | 2 | 2 | X |
| Poisons 6.1..... | 2 | 2 | X | X | X | X | X | X | 1 | X | 1 | 1 | X | 1 | X | X | X |
| Infectious substances 6.2 | 4 | 4 | 4 | 4 | 2 | 2 | 3 | 3 | 3 | 2 | 3 | 3 | 1 | X | 3 | 3 | X |
| Radioactive materials 7 | 2 | 2 | 2 | 2 | 1 | 1 | 2 | 2 | 2 | 2 | 1 | 2 | X | 3 | X | 2 | X |
| Corrosives 8..... | 4 | 2 | 2 | 1 | X | X | X | 1 | 1 | 1 | 2 | 2 | X | 3 | 2 | X | X |
| Miscellaneous dangerous substances 9 | X | X | X | X | X | X | X | X | X | X | X | X | X | X | X | X | X |

Numbers and symbols relate to the following terms as defined in this section:

1—"Away from."

2—"Separated from."

3—"Separated by a complete compartment or hold from."

4—"Separated longitudinally by an intervening complete compartment or hold from."

X—The segregation, if any, is shown in the §172.101 Table.

*—See §176.144 of this Part for segregation within Class 1.

(c) *Segregation requirements for breakbulk cargo.* (1) The requirements of this paragraph apply to the segregation of packages containing hazardous materials and stowed as breakbulk cargo;

(2) Definition of the segregation terms:

(i) Legend:

Part K. Presentations from the IMO Special Consultative Meeting, March 4-6, 1996

Addressing Safety Issues in the Sea Transport of Radioactive Materials

Presentation by the Solomon Islands

Presentation by Argentina

Presentation by Ireland

Ecological and Public Health Implications from Flasks Lost at Sea

Applying the Precautionary Principle to Ocean Shipments of Radioactive Material

*Environmental Impact Assessment of Radioactive Materials During Sea Transportation: Case of
Plutonium Released in the Ocean*

Sandia National Laboratories gratefully acknowledges permission from the **International Maritime Organization** to reproduce these seven presentations from the IMO report titled *Draft Proceedings of the Special Consultative Meeting of Entities Involved in the Maritime Transport of Materials Covered by the INF Code* (4-6 March 1996).

Addressing Safety Issues in the Sea Transport of Radioactive Materials

Edwin S. Lyman, PhD
Scientific Director
Nuclear Control Institute

Presentation to the
IMO Special Consultative Meeting
4-6 March 1996
London

Introduction

Institution of the INF ("Irradiated Nuclear Fuel") Code was originally inspired by a drive in 1985 by some IMO member states to correct an inconsistency in the rules regulating the transport of dangerous goods by sea, which neglect to impose any specific requirements on the transport system when the goods in question are radioactive materials (RAM). The IAEA disputed the need for such requirements, arguing that safety is assured through its regulatory philosophy that the primary responsibility for transport safety should lie not in the details of the transport system, but in the design of the shipping package. The IAEA has the authority to regulate packages for the shipment of RAM through the specification of performance criteria in IAEA Safety Series No. 6 (SS6), "Regulations for the Safe Transport of Radioactive Material." In spite of the initial objections of the IAEA, the INF Code was ultimately recommended by a joint IMO/IAEA working group and subsequently adopted in 1993 as a standard for ships carrying INF, plutonium, and high-level reprocessing wastes (HLW), albeit only as a voluntary Code of Practice.

Whether the INF Code is necessary (or sufficient) therefore depends on the extent to which the standards for Type B package design laid out in SS6 are stringent enough to guarantee safety with respect to a broad range of sea accident environments. Many observers have pointed out that the mechanical and thermal stresses that may occur during marine accidents can far exceed those imposed by the Type B test series. Also, studies by this author have identified numerous technical uncertainties associated with the sea shipment of vitrified high-level reprocessing wastes (VHLW) that at best reduce confidence in the accuracy of risk assessments, and at worst could have serious implications for safety.

The IAEA has consistently dismissed the possibility that Type B casks may not be robust enough to be safely used for marine transport. However, because the information and analysis necessary for a definitive resolution of this issue is not now available, this position is largely based on speculation. In response to public concerns, the IAEA initiated the Coordinated Research Program (CRP) in 1994 in an attempt to establish a more rigorous quantitative basis for evaluating the risks involved in transport of RAM by sea.

The joint IMO/IAEA working group stipulated that, should new evidence

demonstrate that the severity of sea accidents is indeed greater than that of the Type B test, upgrading of the package standards through the established SS6 revision process, rather than a strengthening of requirements for the other elements of the marine transport system, should be undertaken. However, the IAEA strategy appears to be designed to guarantee that neither of these measures will ever be enacted, no matter what the outcome of assessments like the CRP. The IMO must take a harder look at the IAEA approach and evaluate whether it is adequate for resolution of the legitimate safety concerns of States which are at risk today from sea shipments of RAM.

The "Type B" Package Controversy

As defined in the 1985 version of IAEA SS6, "Type B" is the designation given to packages which are designed to be partially "accident-resistant" and are permitted to carry radioactive materials in unrestricted quantities in any transport mode. (In the 1996 revision, a new, more durable package, designated Type C, will be introduced to replace Type B casks in some air transport applications, although serious questions remain, both as to the adequacy of the Type C cask and the safety of the special exemption for so-called "low dispersible materials, including fresh MOX fuel.¹)

In order for a shipping cask to qualify as a Type B package, one must demonstrate (by testing actual specimens, using computer simulations, or some combination thereof) that the cask will be able to maintain significant containment function following a series of tests intended to simulate the conditions of a transport accident. The required tests include a drop test from a height of 9 m (corresponding to an impact velocity of 13.3 m/s) onto an essentially unyielding surface, a thermal test involving exposure for 30 minutes to conditions equivalent to a fire with a flame temperature of 800°C, and a water immersion test (200 m depth for 1 hour for large inventory packages).

Many observers have pointed out, in submissions to the IMO, to the joint IMO/IAEA Working Group, and in the public record, that historical marine accidents have often been of a duration which greatly exceeds that of the Type B test sequence. For example, the U.S. delegation to the IMO noted in 1990 that "fires on board ships, which can burn for days, certainly have the potential to exceed the testing parameters of IAEA, and further strengthen the need for special requirements."² There are also several examples

¹ P. Leventhal and E. Lyman, Nuclear Control Institute, letter to Hans Blix, Director General, IAEA, February 26, 1996.

² "Requirements for Purpose-Built and Non-Purpose-Built Ships Intended for the Carriage of Irradiated Nuclear Fuel." Submission of the United States Delegation to the IMO Sub-Committee on Ship Design and Equipment," DE 34/8, 6 December 1990.

of fires at sea that have burned for weeks.³

Another well-known fact is that typical hydrocarbon fuels can burn at temperatures several hundred degrees higher than that specified by the Type B thermal test. This discrepancy has led to unease among governments as well as environmentalists. For example, in the course of a joint U.S.-Russian development program for a container to transport plutonium weapon components, the Russians expressed concern that the IAEA thermal test was inadequate and requested that the container be tested at 1000°C.⁴

The joint IAEA/IMO working group, which met only twice, asserted that "there was no information or data in the papers submitted to the first and second sessions that would cast doubt on the adequacy of the IAEA Regulations." Does the IAEA have the information available, however, to demonstrate the adequacy of the regulations? The answer is, quite unambiguously, no. Proposals before the IMO to study this issue quantitatively were made as far back as 1990; now, over five years later, the effort has only just begun (see the section on the Coordinated Research Program, below). The burden of proof clearly must lie with the IAEA to demonstrate why historically severe marine accidents can be safely excluded from consideration.

Regulatory Inertia and IAEA Safety Series No.6

Why is the IAEA so reluctant to reconsider its packaging standards for marine transport? A fundamental principle applied in the ongoing SS6 revision process is "the need to maintain regulatory stability."⁵ The Agency is under tremendous pressure from the nuclear industry to refrain from introducing more stringent transport standards which could increase costs, even if they are clearly warranted from a safety perspective. On the other hand, it has shown little reluctance to make changes that lighten the regulatory burden. This is seen in a number of different areas.

One example is IAEA's selective incorporation of new radiological protection information into the 1996 revision of the SS6. Since the 1985 edition was published, new data from the ongoing study of Japanese atomic bomb survivors has demonstrated that the carcinogenic potential of ionizing radiation is more than four times greater than was

³ Eco Engineering, Inc., "A Review of the Proposed Marine Transportation System of Reprocessed Plutonium from Europe to Japan," paper prepared for the Nuclear Control Institute and Greenpeace International, March 1992.

⁴ R. Glass *et al.* (Sandia National Laboratories), "The Development of the Russian Fissile Material Container," presentation to the PATRAM '95 Conference, Las Vegas, Nevada, 3-8 December 1995.

⁵ R. Rawl and J. Mairs (IAEA), "The 1996 Revision of the International Atomic Energy Agency's Regulations for the Safe Transport of Radioactive Materials," presentation to the PATRAM '95 Conference, Las Vegas, Nevada, 3-8 December 1995.

previously thought, a conclusion which has led to reductions in the international recommendations for occupational and public exposures to radiation.⁶ However, in spite of a professed commitment to "keeping abreast of the latest radiation protection practices,"⁷ the IAEA refused to reduce the coefficients in SS6 describing permissible radiation releases accordingly. This means that the revised SS6 will permit, by default, a fourfold increase in the health consequences of a transport accident.

On the other hand, SS6 does incorporate a new dosimetric model which permits *increases* in the permissible releases of a significant fraction of radionuclides (only "very few" of the changes are more restrictive). For example, permissible releases of plutonium and higher actinides are increased by a factor of five in the 1996 revision. This inconsistency is a prime example of the fundamentally political nature of the SS6 revision process.

Another blatant example is the development of standards for air transport casks. After years of wrangling, the IAEA finally produced a standard which has been judged to be inadequate by a number of international associations of air transport professionals.⁸ To add insult to injury, it recently voted to exempt plutonium from the new standard if it is in the form of MOX fuel, on the basis of flimsy technical arguments.

This discussion makes apparent that in its quest for "regulatory stability," the IAEA is providing a level of safety through its recommendations which is increasingly divergent from that of other international organizations.

Type B Package Vulnerabilities: An Example

It is useful to examine some of the implications of the possibility that the IAEA is overestimating the safety of marine transport of RAM in Type B casks.

The following discussion of safety issues is based largely on an analysis, conducted by this author in 1994, of the transport of vitrified high-level radioactive wastes (VHLW), the first shipment of which took place from France to Japan in early 1995.⁹ It should be

⁶ International Commission for Radiological Protection. *ICRP Publication 60 (1990 Recommendations)*, Pergamon Press, Oxford. 1991.

⁷ R. Rawl and J. Mairs, *op. cit.*

⁸ S. Tanzer. "Updated Status Report on Plutonium Air Shipments," Nuclear Control Institute, Washington, D.C., September 20, 1995.

⁹ E. Lyman. "Safety Issues in the Sea Transport of Vitrified High-Level Radioactive Wastes to Japan," Center for Energy and Environmental Studies, Princeton University, Princeton, New Jersey, December 1994, prepared for the Nuclear Control Institute, Greenpeace International and the Citizens' Nuclear Information

noted that, while the companies involved in the transport issued blanket condemnations of the report, they have never responded to it in a substantive way, despite repeated attempts to engage them in a dialogue. On the other hand, private conversations with experts in government and industry over the last year have confirmed the validity of many of the technical issues raised in the report; furthermore, the paper has been accepted for publication in a peer-reviewed journal. This episode is in itself an indication of the fundamental unresponsiveness of the IAEA regulatory process to external criticism.

a) Elastomer cask seals

The weaknesses of the Type B standards are exemplified by the fact that they have not prevented the widespread use of elastomeric materials to seal the lids on RAM shipping casks. The lid seals play an essential role in preventing the escape of radioactive gases and fine particulates from the cask following an accident. However, elastomeric materials have poor heat resistance and will fail after exposure for a couple of hours to temperatures in the vicinity of 250°-300°C; above this range, they will fail in under one hour. Furthermore, elastomers are damaged by exposure to high radiation fields. For these reasons, elastomer seals do not appear to be the best choice for casks transporting heat-generating, highly gamma-emitting materials like spent fuel or VHLW, especially when compared to costlier metallic seals, which offer superior heat and radiation resistance.¹⁰

Transport casks with elastomer seals are able to be qualified as Type B packages because the heat input generated by the Type B thermal test is low enough so that the seal temperature remains below the failure threshold (provided the cover protecting the seal remains intact following the impact tests). But the current regulations do not require the cask designer to determine the conditions which *would* cause the seal to fail and ensure that a large safety margin is present.

For instance, when a prototype VHLW transport cask was tested by Japanese authorities, the seal temperature reached 178°C following exposure to Type B thermal conditions, an increase of 30°C.¹¹ While this result was judged to provide a "sufficient safety margin" of around 70°-100°C below the failure threshold, this conclusion is open to argument. Extrapolating from this result and assuming a linear average seal heating rate, an 800°C fire would cause the seal to fail after approximately 2.5 hours. Exposure to higher temperatures would obviously reduce the time to seal failure. Seal failure could also be

Center Tokyo, to appear in the journal *Science and Global Security*.

¹⁰ The industry has denied that elastomer seals are a bad choice. However, they do not refute the argument that metallic seals would be far more likely to survive a severe fire.

¹¹ H. Yamakawa *et al.* (CRIEPI), "Demonstration Test for Transporting Vitrified High-Level Radioactive Waste: Thermal Test," presentation to the PATRAM '95 Conference, Las Vegas, Nevada, 3-8 December 1995.

induced by fires of lower temperature and longer duration. Furthermore, the synergistic effect of gamma radiation damage may lower the temperature threshold or reduce the time to failure at elevated temperature, a point which the Japanese did not consider when assessing the safety margin.¹² Without an understanding of the probabilities with which different fire scenarios may be encountered during marine transport, it is impossible to judge whether a particular "safety margin" is sufficiently conservative.

b) Barriers internal to the package: the stainless steel VHLW canister

Should the seals of a shipping cask fail in the event of a severe marine accident, the burden of radionuclide containment would then shift to the barriers internal to the cask; e.g. the inner packaging and the robustness of the RAM itself to resist dispersal. SS6 does not have any control over the form of the contents of a Type B cask transported via land- or sea-based modes. However, as the following example shows, clearly it should.

Current industry practice is to solidify liquid high-level radioactive wastes (HLW) from spent fuel reprocessing by using a process known as vitrification, in which they are blended with glass-forming materials and melted at a temperature of about 1150°C. The melt is then poured into stainless steel canisters and cooled to below 500°C to form glass blocks. The canisters are then placed in a storage facility until they are ready to be transported. Each vitrified HLW (VHLW) canister contains tens of thousands of terabecquerels (TBq) of radioactivity.

The integrity of the stainless steel canister is crucial for the effective containment of radioactive particles and vapor during storage and transport of VHLW. However, it can be shown that under the thermal conditions to which it is exposed during VHLW production, the type of stainless steel utilized by Cogema (austenitic Type 309) undergoes a process known as *sensitization*, which dramatically reduces its resistance both to fracture and to localized corrosion mechanisms such as intergranular corrosion and stress-corrosion cracking.¹³ This raises the possibility that the canisters will corrode at an accelerated rate in storage, due to the presence of corrosive contaminants either in the atmosphere of the storage facility or in the VHLW itself. Corrosion in turn increases the risk that the canister will leak during normal transport conditions, or fail catastrophically in the event of a transport accident.

Sensitization is a well-known problem, and there are many commercially available grades of stainless steel which are resistant to it. In fact, a grade of this type (304L) was

¹² M. Warrant and C. Ottinger, "Compilation of Current Literature on Seals, Closures and Leakage for Radioactive Material Packagings," SAND88-1015, Sandia National Laboratories, January 1989, p.4-10.

¹³ E. Lyman, "Sensitization of Stainless Steel Vitrified High-Level Waste Canisters During Production," Center for Energy and Environmental Studies, School of Engineering and Applied Science, Princeton University, February 1995.

chosen to be used at the vitrification plant for U.S. defense HLW partly to avoid sensitization during VHLW production. In view of this, it is not clear why Type 309 was chosen by Cogema.

The nuclear industry throughout its history has demonstrated a lack of understanding of the behavior of materials under the conditions to which they are exposed in nuclear applications. Steam generator tube cracking and pressure vessel embrittlement are two principal examples. In transport, the use of chloride-containing insulation in 21PF overpacks for uranium hexafluoride containers caused extensive pitting of the stainless steel shell with which they were in contact.

The issue of VHLW canister sensitization took on greater urgency when it was revealed in August 1995 that one of the 28 canisters sent from France to Japan had failed one of the inspection tests performed by Japanese authorities.¹⁴ In this incident, an unusually high emission rate of a fission product, cesium-137 (Cs-137), was observed for a number of days during a confinement test, in which the canister was placed in a vacuum chamber and the radioactivity deposited on the outlet filters of the chamber was measured. This raised the possibility that the canister indeed had developed a leak.

The contention that this event could be the signature of a leaky canister was quickly denied by Japanese authorities, who claimed instead that it was due to "loose contamination" on the surface which was somehow dislodged during the test procedure. However, the arguments they offered to support their position have been shown to be faulty.

For instance, Japanese authorities claimed that if Cs-137 were leaking from within the canister, then another volatile fission product, ruthenium-106, would have been observed as well, but was not. However, the ratio of Ru-106 to Cs-137 is very low in the VHLW (0.002), and one can show from the published radionuclide inventories that the amount of Ru-106 that one would expect to observe would be very close to or even below the detection limit of the equipment. Thus the fact that Ru-106 was not detected does not mean that a leak can be excluded as the source.

The Japanese also maintained that their observation that the Cs-137 emission eventually decreased to "normal levels" implies that the emission did not originate from a leak. This conclusion is inaccurate. Repeated application of the vacuum test could have caused a leak to become plugged with small glass particles.

Instead of denying the problem, the Japanese authorities should request that a broader investigation be launched into whether the cesium contamination incident is an ominous signal that accelerated corrosion of the VHLW canisters, as a result of

¹⁴ N. Usui and A. MacLachlan, "Cesium Contamination on HLW Canister Fuels Debate in Japan," *Nucleonics Week*, August 24, 1995, p.1.

sensitization, is occurring. Otherwise, one cannot exclude the possibility that more serious leaks, or the complete failure of a VHLW canister during a transport accident, will occur in the future.

The IAEA Coordinated Research Program (CRP)

To address concerns that marine accidents may be more severe than those represented by the Type B regulatory test, the IAEA decided in 1994 to undertake a Coordinated Research Program (CRP) on the subject of "Accident Severity at Sea During Transport of Radioactive Material." This endeavor has two principal goals: the first is to collect and analyze marine casualty data to provide a more quantitative understanding of the severity and frequency of sea accidents, and the second is to evaluate the impacts of such accidents on the integrity of RAM packages.¹⁵

The scope of the CRP is commendable and is the direct outgrowth of a research program proposed by independent observers, including members of the United States Congress.¹⁶ However, the prospect that it will result in an objective, relevant study credible to all stakeholders is clouded by the appearance of conflict of interest among its participants, as well as by inconsistencies in its approach.

Nations participating in the administration of the CRP are France, Germany, Sweden, UK, the US and perhaps Japan. One should note that most members of this group have a strong commercial or political interest in a favorable outcome and have already gone on the record with affirmations of the safety of marine transport of RAM. Also notable is the complete absence of coastal en-route states which derive no benefit from such transports but must bear the risks.

Although the CRP is ostensibly technical in nature, non-technical factors can shape the way problems are posed, statistics are manipulated and data are presented. The following quote from the introduction of a paper describing the *SeaRAM* program, a project conducted by Sandia National Laboratories in the United States in support of the CRP, provides a worrisome indication that the directors of the study have a predisposition towards its outcome: "The premise of this project is not that these regulations are inadequate to ensure the safety of RAM transport by sea. Rather, the aim of *SeaRAM* is to substantiate the regulations and hence confirm the safety of RAM sea transport."¹⁷ Such a

¹⁵ H. Selling, "Marine Transport of Irradiated Nuclear Fuel, Plutonium and High Level Wastes," *RAMTRANS* 5 (1994) p.139.

¹⁶ U.S. Representative Neil Abercrombie *et al.*, letter to T. Grumbly, Assistant Secretary for Environmental Restoration and Waste Management, U.S. Department of Energy, May 20, 1994; T. Grumbly, letter to N. Abercrombie, Oct. 3, 1994.

¹⁷ P. McConnell *et al.* (Sandia National Laboratories). "SeaRAM: An Evaluation of the Safety of RAM Transport by Sea," presentation to the PATRAM '95 Conference. Las Vegas, Nevada, 3-8 December 1995.

blatant expression of bias casts doubts over the objectivity of the whole exercise.

The IMO should conduct vigilant oversight of the CRP to ensure that it is conducted in a manner suitable for addressing the concerns of en-route states. If this is resisted by IAEA, then the IMO should consider initiating a study independent of IAEA control that will have input from en-route States.

There also appears to be confusion with regard to the objectives and approach of the CRP. According to one observer, "the prime objective ... is to ensure the continuing validity of the principle of providing safety 'designed into' packages."¹⁸ Presumably, this implies that if the CRP eventually finds that the severity of a significant proportion of accidents at sea exceeds that of the Type B test, then the package standard will be made more stringent through a revision to IAEA SS6.

However, in apparent contradiction to this objective, the stated approach of the CRP is to explicitly take ship design and modes of fire propagation into account when determining the accident environment experienced by a RAM package.¹⁹ This is reflected in preliminary results from the *SeaRAM* program, which argue that although collision and fire environments may be more severe in marine accidents than those simulated by the Type B tests, the actual environment encountered by the RAM package will be less severe because of the protection provided by bulkheads and ship geometry.²⁰ For instance, one calculation obtains the trivial result that a RAM package protected from a Type B regulatory fire from an intact bulkhead experiences a lower heating rate than if it were fully immersed in the fire.²¹ Even more peculiar, however, is that this result is presented as a "reinforcement" of the "basic regulatory concept...that the shipping cask, not the ship, is the primary protection barrier to consider,"²² whereas it is apparent that this result is a reinforcement of exactly the opposite conclusion.

There is nothing wrong in principle with giving credit to the transport system for safety, provided it is accompanied by an acknowledgment that that the principle of

¹⁸ H. Hesse (IMO) and C. Young (U.K. Dept. of Transport), "Code for the Safe Carriage of Irradiated Nuclear Fuel, Plutonium and High-Level Radioactive Wastes in Flasks on Board Ships (INF Code)," presentation at PATRAM '95, Las Vegas, Nevada, 3-8 December 1995.

¹⁹ R. Rawl and H. Selling (IAEA), "Marine Transport of Irradiated Nuclear Fuel, Plutonium and High Level Wastes," presentation to PATRAM '95, Las Vegas, Nevada, 3-8 December 1995.

²⁰ P. McConnell *et al.*, *op. cit.*

²¹ J. Koski *et al.* (Sandia National Laboratories), "Estimates of Fire Environments in Ship Holds Containing Radioactive Material Packages," presentation to the PATRAM '95 Conference, Las Vegas, Nevada, 3-8 December 1995.

²² J. Koski *et al.*, *op. cit.*

fundamental package safety has been abandoned, and the adoption of a regulatory structure which is capable of verifying that the protection provided by the entire system is adequate. IAEA, however, is pursuing an internally inconsistent strategy of assigning a central role to the marine transport system, while continuing to oppose any international measures to regulate the quality of such systems.

Conclusions and Recommendations

The IAEA cannot have it both ways. Should further independent investigations confirm that Type B casks are not robust enough to withstand the conditions that may be encountered in accidents at sea, *without giving credit to the rest of the transport system*, the situation can be rectified only in one of two ways. Either the package used for marine transport must be upgraded or the other elements of the transport system (such as the robustness of the ship and the reliability and effectiveness of its safety systems) must formally become part of the containment system and be placed under binding regulatory scrutiny.

Rather than see the INF code strengthened, the IAEA prefers that the standards for marine transport packages be upgraded through the ongoing SS6 revision process. However, institutional inertia at the IAEA makes it extremely difficult for that body to address urgent safety issues in a timely way. It is too late for changes in the upcoming revision of SS6, scheduled to be issued in 1996; a new marine transport standard would have to await the next planned revision in 2005. This approach would lead to a decade-long window in which large quantities of highly radioactive materials would continue to be transported by sea in casks that could well be inadequate for the purpose.

For this reason, the IMO should err on the side of caution and recommend that the INF Code be strengthened to provide adequate compensation for RAM package vulnerabilities that have not yet been thoroughly evaluated. Approaches for doing this include:

1. the exploration of legal mechanisms that would enable the Code to be instituted as a binding rule, e.g. by including it as an amendment to the Safety of Life at Sea Convention (SOLAS), which does not contain any requirements for ships carrying RAM;
2. the development of a protocol for inspection and certification, including mandatory evaluations of the transport system to verify that it meets safety goals, as well as provisions for full-scale system testing as necessary. Attention in particular should be paid to scenarios which may cause "common mode" failures of redundant safety systems;
3. the revision of excessively liberal language which currently permits large quantities of RAM, e.g. approximately 1 tonne of reactor-grade plutonium or 4 fully loaded casks of vitrified HLW, to be carried on non-purpose-built passenger ships.

SPECIAL CONSULTATIVE MEETING
MARITIME TRANSPORT OF NUCLEAR MATERIALS
SUBJECT TO THE INF CODE

Presentation by Solomon Islands

Solomon Islands welcomes the initiative of this Special Consultative Meeting (SCM). We see it as a constructive means to advance the debate, and clarify questions on the issues involved, without prejudice or delay to the ongoing work in IMO Committees and Sub-Committees on the complementary requirements for the Code and related matters.

2. Solomon Islands' objective is the creation of a consolidated and comprehensive code for the safe carriage of radioactive materials which will provide for a safe ship, safe containers (flasks), credible voyage planning and consultation with coastal states, a safe voyage, effective emergency response and retrieval arrangements and a realistic liability regime. It is not Solomon Islands' aim to interfere with legitimate safe transport activities or the energy policies of other States.

3. Resolution A 748(18) requires that the INF Code should be kept under review, and to consider urgently inclusion of matters complementary to the carriage in the Code. These matters were identified as:

- 1) a credible and effective liability regime to compensate damage and take effective measures to avoid damage to the environment, human life, property and the economy ;
- 2) credible route planning and notification and consultation with coastal states;
- 3) restrictions and exclusion of certain routes;
- 4) a credible emergency response plan, included in the voyage plan, in respect of the ship and cargo;
- 5) sufficient information on the material and packaging included in the voyage plan;
- 6) equipment and devices which will facilitate the location and salvage of the ship and/or cargo; and,
- 7) a [compulsory] requirement to salvage radioactive material and the pre-determination of the responsibility for this in the voyage plan.

Current action in the IMO Committees and Sub-Committees and IAEA aims at addressing these proposed requirements.

4. Solomon Islands notes that much of what is asked is currently being done by existing ship operators. What is notably missing is transparency and the inclusion of the arrangements in a binding comprehensive and consolidated code of conduct.

5. We also recognise some major obstacles to agreement, but do not see them as insurmountable. We see as difficulties:

- 1) The prior consultation process - because of the physical security aspect. This may have relevance to the plutonium cargo, but not to the waste, or the INF and other radioactive materials.
- 2) An 'absolute' retrieval requirement. We accept that this must take into account practicability in the light of prevailing technology. We have strong reservations on the 'cost v. benefit' considerations.
- 3) the liability regime. We recognise that current and draft Conventions touching on this do not and may not be able to accommodate what we seek. We expect liability not only for actual damage, but also for action to prevent future damage which may arise from an incident.

6. Solomon Islands accepts that the present INF Code, adopted by Resolution A748(18), provides for a safe ship to carry radioactive materials. Yet, a continuing review is necessary. We have doubts about the safety of carrying INF Code materials on passenger ships.

7. Solomon Islands does not accept that the lasting protection of people, the environment and economies is ensured by the integrity of the existing containers (flasks) in which the materials are packed. This needs further study. The unqualified concept of leaving lost containers, materials or contaminated ships in the sea is not acceptable.

8. Existing and planned liability regimes for the transportation of radioactive materials are not adequate. This type of trade is limited in volume and to a few operators at present. For this reason it may not be necessary to provide a liability regime through a global Convention. It could be met by specific undertakings of liability by ship operators or owners. Such an arrangement should be enshrined in the Code.

9. Coastal states along the route of a ship are entitled to be advised and consulted about the voyage in advance. The concerns arising from the need for physical protection of certain materials is recognised and must be taken into account when formulating procedures. A voyage plan must set out not only the routine route arrangements, but also the agreed emergency response arrangement and plans. Responsibility for actions must be pre-determined and stated in the plan.

10. Coastal states must have an input in the course of voyage planning, in the context of safe routing, en-route facilities and routine and emergency support available in their territories. The risks in the case of an incident or accident must be known, so that appropriate preparations can be made.

11. Crew training on ships carrying radioactive material needs special attention. All crew likely to come into contact with or work near such cargo should have basic training in awareness and precautionary action. There should be a sufficient number of crew on board with training to take immediate initial precautionary and remedial actions in case of an incident or accident involving or likely to involve radioactive materials.

12. Because at present the carriage of irradiated nuclear fuel, plutonium and high level radioactive wastes is a specialised and limited trade, some of the detailed stringent requirements sought for this type of carriage are probably inappropriate for inclusion in global Conventions or Codes of general application.

13. Solomon Islands takes the view that radioactive materials, particularly those addressed by the INF Code, are inherently dangerous, and that the risks are of such magnitude, that special precautions are justified. For this reason, the precautions and guarantees asked for should be included in a consolidated and comprehensive dedicated Code of practice.

14. Furthermore, in considering the responsibilities and liabilities which rest on the owners of dangerous cargoes, and the operators of ships which carry them, the principles of the 'precautionary approach' and the 'polluter pays' must be applied as the guiding philosophy.

15. A particular duty to 'hold harmless' is owed to the people, environments and economies of the 'innocent bystanders'. Countries, such as Solomon Islands, which neither directly benefit from nor invite such activities in their vicinity, will wish to be assured that the risks to their people, environment and economic well being are minimised to the utmost and that no financial or other burden will fall on them in the event of an accident or incident to the ship or cargo.

16. Solomon Islands's considers that its well being, environment and economy would be jeopardised if such dangerous cargoes or contaminated ships remain unretrieved in its sea or EEZ. Solomon Islands also has concern for other environments, outside its own area, having regard to the fact that marine and atmospheric pollution cannot normally be contained in or restricted to any particular location or area.

/4

17. It has been argued that the carriage of radioactive materials should be treated on the same basis as the carriage of other dangerous goods, and that existing provisions in IMO Conventions and Codes, including the existing INF Code, provide adequate safeguards. While not minimising the risks from other categories of dangerous goods, and hazardous and noxious substances, Solomon Islands takes the view, set out in paragraph 13, that radioactive materials create a particular risk which justifies the special measures proposed.

18. Unfortunately, Solomon Islands does not have the expertise to offer solutions to these problems, but is willing to participate and assist in finding ways to meet the concerns regarding the carriage of radioactive materials in ships. It looks to the expertise available among member States of the IMO, particularly those with experience in this field, to help in this endeavour. Far better to take precautions now, than to agonise over an accident later !

19. This Special Consultative Meeting offers the opportunity for open and constructive exchange of views on the several problems, with the aim of resolving disagreement. Solomon Islands looks to this Meeting to give impetus to the ongoing work at the IMO and IAEA on these matters, and to propose ways to overcome any difficulties - such as are mentioned in paragraph 5 of this document.

Document presented by ARGENTINA

TOWARDS AN ADEQUATE REGULATION OF THE MARITIME TRANSPORT OF
IRRADIATED NUCLEAR FUEL, PLUTONIUM AND HIGH-LEVEL
RADIOACTIVE WASTES

When evaluating at its 64th meeting (December 1994) the "Code for the safe carriage of irradiated nuclear fuel, plutonium and high-level radioactive wastes in flasks on board ships" (INF Code) -approved by IMO Assembly Resolution A.748 (18)-, the Maritime Safety Committee (MSC) consulted the Legal Committee (LEG) on the possibility that States adopt, within the Code, measures of restriction to the maritime traffic of ships transporting such kind of materials. At its 72nd meeting (April 1995), the LEG concluded that this question should be first analysed from a technical point of view by the MSC and the Sub-committee on Safety of Navigation (NAV), taking into account the relevant provisions of the United Nations Convention on the Law of the Sea, 1982 (UNCLOS).

At its 65th meeting (may 1995), the MSC approved an amendment to the Rule 8 (Routeing) of Part V (Safety of Navigation) of the International Convention for the Safety of Life at the Sea, 1974 (SOLAS). By such amendment, it is now established that ships routeing systems are not only important for the safety of life at sea and the safety and efficiency of navigation, but also for the protection of the marine environment, and therefore are recommended for use by, and may be mandatory for, all ships, certain categories of ships or ships carrying certain cargoes. Rule V/8-1 of the SOLAS Convention, approved in 1994, -which makes possible to State Parties to implement, with IMO authorization, a system of notification of the ships transporting certain cargoes- is thus complemented.

Both the 37th meeting of the Marine Environmental Protection Committee (MEPC) and the 41st meeting of the NAV (September 1995), insisted on the need to further regulate this matter, with particular reference to complementing the INF Code with provisions related to the previous knowledge, planning and routeing of the transport, and the adoption of emergency measures in the case of an accident. Fundamentally as a result of such insistence, the IMO Secretary General, with the support of the 19th Assembly

(November 1995), fostered the organization of the present Meeting.

The brief review presented in the preceding paragraphs shows that in the last three years the issue of the maritime transport of irradiated nuclear fuel, plutonium and high-level radioactive wastes in flasks on board ships (hereinafter, "INF materials") was dealt with intensively in the principal organs -with different competencies- of IMO, as the international organization with primary responsibility on the regulation of international maritime transport. Such concern is an evidence, in turn, of a growing concern, in the international public opinion, for the risks derived from this kind of transport.

Due to its geographic characteristics and location, Argentina is particularly interested on the consequences of the traffic of ships carrying INF materials. In fact, endowed with a long maritime coastline -on which a great part of its population is settled- and a wide continental shelf -home to valuable fishing resources-, an accident suffered by any of such ships during its passage along the Argentine coasts could result in highly detrimental consequences of an environmental and economic nature. Even if the real risks were low, the very possibility of such consequences generates a public opinion strongly adverse to such kind of traffic. As was demonstrated by the recent passage of the "Pacific Pintail", such reaction tends to reinforce itself in the southern Atlantic maritime spaces -including the Magellan Straits and Drake Passage- where the marine currents, the heavy seas and the strong storms naturally increase the probability of a maritime accident.

Although at the birth of UNCLOS, activities such as the maritime transport of INF materials were not a major cause of concern, the negotiators of the Convention wisely left open for States the possibility of introducing the necessary regulation to protect the marine environment from the risks that the said activities could generate. In fact, several UNCLOS provisions allow for such regulation as a natural counterpart of the freedom of navigation that the Convention codifies. In particular, Part XII enables States to adopt, individually or jointly, as appropriate, measures consistent with the Convention which are necessary to prevent, reduce and control the pollution of the marine environment from any source. The rationale for such provisions was confirmed by the normative plexus developed as from United Nations Conference on Environment and

Development, 1992 (UNCED) -in particular, Chapter 17 of Agenda 21.

The limit of this regulation is provided by the need to ensure that it does not annul the principle of freedom of navigation -legal basis of the international free maritime trade, and of particular importance to Argentina. However, as long as such limit is respect, no technical or legal consideration can prevail over the objective of ensuring that the transport of INF materials is done in such a way as to cause the lowest achievable risk to the marine environment. In this sense, for instance, the existence of detailed safety requirements demanded both for the flasks in which this type of cargo is transported and for the ship transporting it -undoubtedly, indispensable from the point of view of the safety of the transported cargo- cannot prevent to analyse, from the perspective of the global regulation of this kind of traffic, the need and convenience of adopting complementary measures to such requirements.

Taking into account the aforementioned, Argentina purports that it is necessary that the international community, through the competent international organizations, proceed, as rapidly as possible, to adequately revise the existing regulation of the maritime transport of INF materials -in particular, to complement and systematise such regulation. Any unjustified delay on his matter may only induce states to adopt unilateral measures to protect the marine environment adjacent to their coasts, such as happened when, also by virtue of an absolute interpretation of the principle of freedoms of the high seas, it was attempted to justify the depletion of marine natural resources in maritime areas immediately adjacent to the Exclusive Economic Zone.

In this sense, the presence of the coastal States in any planning or enforcement activity related to the maritime transport of INF materials should be indispensable. In fact, such presence constitutes a specific corollary to the general premise -derived from the UNCLOS substantive provisions- according to which the consent of the coastal State presides over the carrying out of activities in the maritime spaces in which such States exercise different aspects of their sovereignty.

In order to achieve a regulation reflecting an adequate balance between the general obligation to protect the

marine environment and the specific rights which arise from the principle of freedom of navigation, some areas can be identified on which the international community could initially concentrate its efforts. Such areas, in respect of which Argentina will foster specific proposals at the competent IMO organs, are the following:"

1. SAFETY OF THE CARGO AND CONTAINERS.

This seems to be the area in which the efforts in favour of an international regulation have been most successful, both within the International Atomic Energy Agency (IAEA) and IMO. The "Regulations for the Safe Transport of Radioactive Material" -periodically revised and updated by IAEA-, the Convention on Physical Protection of Nuclear Materials, 1989 and the International Maritime Code of Dangerous Goods (IMDG) evidence such efforts.

Notwithstanding these important precedents, the **specific** regulation of the conditions in which materials such as plutonium, irradiated nuclear fuel and high-level radioactive wastes are transported, arises only from the creation of the INF Code in 1993. However, the INF Code is not mandatory, is not generally recognised as the IAEA Regulations, and probably needs a formal mechanism of review and updating.

Within this framework, the international community should consider setting up a formal mechanism to periodically improve the INF Code, as well as a normative implementation to increase its observance and application. It is hoped, for instance, that the Joint IMO-IAEA-UNEP Working Group increases its efforts in this regard.

2. SHIPS ROUTEING

Any effective regulation in this area should be oriented according to the following criteria:

a) ensure that any ship transporting INF materials only enters the jurisdictional or territorial waters of a third State -in exercise of freedom of navigation, innocent or transit passage, as recognised by UNCLOS- when there is no a high-seas route of similar convenience with respect to navigational and hydrographical characteristics.

b) ensure that the ships of this kind that, absent an adequate high-seas route, have to enter the jurisdictional or territorial waters of another State, comply with the routing systems set up by such States in the maritime spaces subject to their jurisdiction -assuming that such systems do not annul free navigation or innocent or transit passage. In order to achieve this aim, both the actual wording of Rule V-8 of the SOLAS Convention and the IMO General Provisions on Ship Routing provide an important point of departure.

3. COMPLEMENTARY MEASURES OF PREVENTION.

The need to establish a permanent mechanism of co-operation and information between the Flag State of the ship transporting INF materials and the States along whose coasts the ship navigates should be highlighted. The modern technology of satellite communications and tracking of vessels provide States nowadays with the necessary instruments to ensure such co-operation. The eventual need to preserve confidentiality, in accordance with the principles arising from the Convention on physical protection of nuclear materials (1989), can be efficiently met employing the proper instruments. This fact should allay the fears provoked by a possible action of terrorist groups.

The implementation of such a mechanism, complemented by a specific mandatory reporting system, is particularly important in the cases in which the ship in question has to enter -in exercise of free navigation or innocent or transit passage- the jurisdictional or territorial waters of a third State. Again, a good starting point on this matter is the reporting system provided in present text of Rule V-8-1 of the SOLAS Convention.

4. REPARATION

Taking into account its wide continental shelf, in which valuable fishing resources develop, Argentina finds it would be more convenient for the protection of its marine environment that the ships transporting INF materials navigate as far as possible from its coastline. However, this could contribute little to mitigate the reluctance towards this kind of traffic if, as a consequence of a maritime accident, the INF materials sink at depths from

which they are hardly recoverable with conventional salvage technology. This highlights the importance of having a mechanism to ensure that all States -including those lacking the appropriate technologies- can rapidly adopt the necessary salvage measures and contingency plans to ensure the control and possible elimination of the pollution eventually resulting from an accident -including the recovery of the containers of such materials, eventually falling into the sea due to the accident. Such measures and plans should be consistent with the widely accepted intervention criteria in cases of radiological emergencies.

Finally, the international community should examine the possibility of having an independent legal scheme to compensate those States or individuals specifically affected by a maritime accident occurring during a transportation of this kind. Such scheme, which could be negotiated within the framework of a joint IMO-IAEA-UNEP working group, could provide, for instance, a legal mechanism to extend the responsibility of the operator of a nuclear installation -recognised in the multilateral conventions in force on this matter- to the maritime carrier of INF materials."

Special Consultative Meeting (SCM) of entities involved with the maritime transport of material covered by the Code for the Safe Carriage of Irradiated Nuclear Fuel, Plutonium and High-level Radioactive Waste in Flasks On-board Ships (INF Code)

Submitted by Ireland

Ireland recognises that the International Maritime Organisation (IMO) is the global body with the responsibility for regulating the safe transportation of all materials carried by sea to ensure the fullest possible protection of the marine environment. Accordingly, Ireland expects that this meeting will address what we consider to be an issue of major relevance to the protection of the marine environment and we are proud to play an active part in this work.

Throughout the world, there has been an increasing awareness of the need to protect the marine environment and this has received added relevance since the outcome of Agenda 21 of the United Nations Conference on Environment and Development (UNCED). These concerns are shared by the Irish Government and the people of Ireland who are particularly concerned about the dangers to the marine environment, to coastal communities, to fishing and to human life and health, from the transportation by sea of various nuclear materials.

We consider that irradiated nuclear fuels, plutonium and high level radioactive wastes pose the greatest threat of longterm pollution to the marine environment. We consider that these materials are unique in their danger and potential for catastrophe. Leakage of radioactivity from these materials would pose an uncontrollable risk for human life and health, far beyond the immediate vicinity of any accident or incident. The slow rate of decay of nuclear materials poses a threat to the marine environment which is less reversible than any other known source of pollution. The possible uses of these materials raises issues of security which do not arise in the case of other substances being transported on our seas.

Ireland, therefore, considers that it is essential that the IMO should ensure that we have in place a code for the transportation of these materials which adequately reflects the unique pollution potential of these cargoes.

In 1993, the IMO adopted the Code for the Safe Carriage of Irradiated Nuclear Fuel, Plutonium and High-Level Radioactive Wastes in Flasks on Board Ships (INF Code).

Ireland welcomes the establishment of the INF Code and the commitment to continue to review it. We appreciate the considerable work which has been done to date by the IMO and its associated bodies and committees. However, we consider the INF Code to be deficient in a number of very important respects and we have consistently expressed this view at the appropriate IMO fora. In general, our concerns in relation to the inadequacies of the INF Code are contained in our paper to the 19th Assembly (A 19/10/9) and further reflected in Assembly Resolution A.790(19).

Therefore, we especially welcome the initiative of the Secretary General to convene this special meeting. We note that the objective of this meeting is "as a matter of priority, to encourage a thorough examination of all aspects of the carriage by sea of materials falling under the purview of the INF Code".

Ireland is particularly concerned about the deficiencies in the INF Code because these materials are being transported past our coast on a frequent and increasing basis. We are very vulnerable to the possible catastrophic consequences of an accident involving these materials. If such an accident were to occur, then international opinion would likely wonder why the IMO had not a stricter regulatory regime for the transportation of such materials.

We feel that the need to strengthen the INF Code is an urgent one and we hope that this special meeting will help to expedite improvements to the Code.

In particular, Ireland recommends the following:

1. We would like to see the same method of hazard evaluation, as is used for all other potential marine pollutants applied to INF materials. There should be a requirement to mark the flasks externally reflecting that hazard evaluation in the same way as all other packages are required to be marked.
2. The design and construction of the cargo flasks should be considered taking into account the specific hazards associated with marine transportation. Such evaluation should include the consequences of catastrophic accident scenarios which can arise in shipping accidents and include fire, explosion, sinking in deep water, etc. Ship design and securing of the flasks within the vessels must be considered taking into account different accident scenarios including capsizing of the vessel.
3. We are concerned about the difficulty of locating packages which may have been lost as a result of an accident, especially where such loss occurs in deep water. Consideration must be given to the availability and adequacy of existing salvage equipment and expertise relevant to the recovery of these materials.
4. Because of the unique pollution threat being posed by INF materials, Ireland feels that there is a need to monitor the progress of a vessel throughout its voyage. Coastal states should be notified in advance of the passage of INF cargoes past their coastlines. There must be a clear reporting requirement to ensure that coastal states are notified immediately in the event of any accident or event which could endanger the safety of the vessel or result in the loss of these materials into the marine environment. We consider that there is a need for bi-lateral or multi-lateral agreements between concerned states regarding response arrangements in the event of an accident.

5. Ireland considers that the particular pollution potential of these materials warrants the exclusion of vessels carrying such cargoes from particularly sensitive areas.
6. Ireland notes that mandatory liability regimes exist for other materials and we feel a similar mandatory regime must be established to cover the costs of salvage measures and compensation for any damage caused by the loss of INF materials into the marine environment.

PAPER PRESENTED AT A SPECIAL CONSULTATIVE MEETING (SCM) OF ENTITIES INVOLVED IN THE MARINE TRANSPORT OF NUCLEAR MATERIALS COVERED BY THE INF CODE, 4-6 MARCH 1996, INTERNATIONAL MARITIME ORGANIZATION, LONDON, UK

ECOLOGICAL AND PUBLIC HEALTH IMPLICATIONS FROM FLASKS LOST AT SEA

Sven P. Nielsen

Risø National Laboratory
Denmark

1. INTRODUCTION

Forecasting of environmental consequences of hypothetical accidents at sea involving releases of radionuclides may be carried out by the use of modelling to predict the dispersion of radioactivity in the marine environment and the subsequent transfer to man and marine fauna. Modelling the dispersion of contaminants in a marine environment is a complex process. Many factors can affect the dispersion of radionuclides including the physical and chemical form of the contamination, the mode and location of release, the physical energy of the receiving environment, sedimentary processes and marine biological productivity. For a particular assessment it is clearly inadvisable to use a generic description of the discharge of a large-scale release of radioactivity to the marine environment. But for the purpose of providing data that illustrate the potential risks to man and the environment from flasks containing irradiated nuclear fuel lost at sea, a small set of generic scenarios is used. The scenarios are constructed with assumptions that are likely to lead to pessimistic estimates between the introduction of radionuclides to the sea and their dose consequences. The results are based on work done for the International Atomic Energy Agency (IAEA) in connection with application of radiological exemption principles to sea disposal.

2. EXPOSURE PATHWAYS

In order to calculate collective intakes of radioactivity resulting from discharges to the sea it is necessary to model the dispersion of radionuclides in marine waters, their possible reconcentration in environmental materials and their pathways to man. Of the various pathways by which man might be exposed, the ingestion of marine foodstuffs is the most important in terms of collective intake, the most significant foods being fish, crustacea and molluscs. Other pathways could be important in the context of maximum individual doses, notably external doses from contaminated sediments and the resuspension and subsequent inhalation of seaspray and contaminated sediments.

A comprehensive list of exposure pathways was included in the study carried out by the IAEA in their Definition and Recommendations for the Convention on the Prevention of Marine Pollution by dumping of Wastes and Other Matter (IAEA 1986). The exposure pathways from this study are listed in Table 1.

A range of these exposure pathways were included in the CEC Marina Study that dealt with the radiological exposure of the population of the European Community from radioactivity in North European marine waters (CEC 1990). This study examined the collective doses from radioactive liquid effluents discharged from civil nuclear sites. The following contributions to the collective dose were found: fish consumption (40%), mollusc consumption (34%), beach exposure (15%), crustacea consumption (7%), seaweed consumption (3%), and inhalation of contaminated beach sediment and seaspray (0.0004%).

Table 1. Exposure pathways covered in the IAEA Safety Series No. 78 (IAEA 1986).

| <i>Pathway</i> | <i>Intake rate or occupancy time</i> |
|-------------------------------|---|
| Fish consumption | 300 g d ⁻¹ |
| Crustacea consumption | 100 g d ⁻¹ |
| Mollusc consumption | 100 g d ⁻¹ |
| Seaweed consumption | 100 g d ⁻¹ |
| Salt consumption | 3 g d ⁻¹ |
| Desalinated water consumption | 2000 g d ⁻¹ |
| Suspended airborne sediment | 23 m ³ d ⁻¹ (10 µg m ⁻³ water and particles) |
| Marine aerosols | 23 m ³ d ⁻¹ (10 g m ⁻³ vapour) |
| Boating | 5000 h a ⁻¹ |
| Swimming | 300 h a ⁻¹ |
| Beach sediments | 2000 h a ⁻¹ |
| Deep sea mining | 500 h a ⁻¹ |

It must be noted, however, that the dominating exposure pathway to man from a given radioactive contamination of the marine environment depends on the elemental and isotopic composition of the contamination as well as the geographical location of the release. Transfer through the marine ecosystems and foodchains vary considerably for the different radionuclides for geochemical and biological reasons.

Compared to the existing knowledge of doses to man from radioactive contamination of the marine environment, much less is known of doses to marine organisms. The reason for this is the general assumption that the standards adopted for the protection of man will result in sufficiently low concentrations of radionuclides in the environment that the environment itself will be adequately protected. However, there is information available on doses to marine fauna in the deep sea (IAEA 1988a) and in coastal waters (Pentreath and Woodhead 1988). The dosimetric approach used involves calculations of exposures of gamma, beta and alpha radiation from radionuclides in the seawater, in the surface sediments and in the organisms themselves. The organisms have been classified in different groups, e.g. small crustacea, small molluscs, larger molluscs and fish.

3. RELEASE OF RADIOACTIVITY IN DEEP WATERS

The calculation of individual doses to members of the public from a release of radioactivity in deep ocean waters are based on data from the Definition and Recommendations for the Convention on the Prevention of Marine Pollution by dumping of Wastes and Other Matter, 1972 (IAEA 1986). The models are described in the GESAMP Report No. 19 (IAEA 1983) and summarised in the IAEA Safety Series report No. 66 (IAEA 1984).

Different models were used for different regions of the ocean: the near field and the far field. The near field was defined as the region in the vicinity of the release in which the concentration is significantly greater than the ocean basin average (usually less than

10% of the volume of the ocean basin), and the far field was defined as the rest of the ocean.

The near-field model was developed primarily to predict the extent of the region of elevated contaminant concentrations around a source. In the model it was assumed that the ocean is purely diffusive, which can have the effect of underestimating the extent to which radionuclides are dispersed by physical processes unless sufficiently large eddy diffusion coefficients are chosen. Both interior scavenging (i.e. removal of radionuclides from the water column by sorption to falling particulates) and boundary scavenging (i.e. burial by accumulating sediments, diffusion in sediment pore water and mixing within the bioturbated layer) were included.

In addition to diffusion, boundary scavenging and interior scavenging the far-field model included upwelling of water, together with a corresponding downward movement. This additional feature enabled the model to reproduce the fluxes of substances that are recycled between the surface and the deep ocean. It was therefore particularly valuable for predicting concentrations of long-lived radionuclides which are not very strongly adsorbed on particulates and bottom sediments (e.g. I-129). Although this model is only one-dimensional, calculations have shown that it provides adequate estimates of laterally averaged concentrations and therefore has wide applications.

The calculation of collective doses to members of the public from release of radioactivity in deep ocean waters are based on data from a study on the radiological impact of selected radionuclides (Smith et al. 1986; Mobbs 1994). The model used for the dispersion of activity in the ocean was essentially the same as that developed for the 1984/85 NEA dump-site suitability review (NEA 1985). This model was of the compartment type consisting of a model to predict rates and patterns of dispersion by physical processes (advection and diffusion) and, overlaid on this, a model to represent sediment interactions. The model contained 92 water compartments in total, of which 68 represent the Atlantic Ocean and 24 represent the Pacific, Antarctic, Indian and Arctic Oceans and the Mediterranean Sea. Collective doses were calculated making suitable allowance for coastal sedimentation.

Doses rates to marine organisms from releases of radioactivity in the deep sea were calculated in three different areas as indicated in Figure 1 (IAEA 1988a). The first area was the release site itself, including water to a height of 75 m above the sea bed and assuming contact of the benthic organisms with the top layer of the sediment. The second area was a square of 250 km centred on the site of release, and the third was that of the bottom waters of the European Basin. The most limiting data were selected for relating dose rates to marine organisms to release rates.

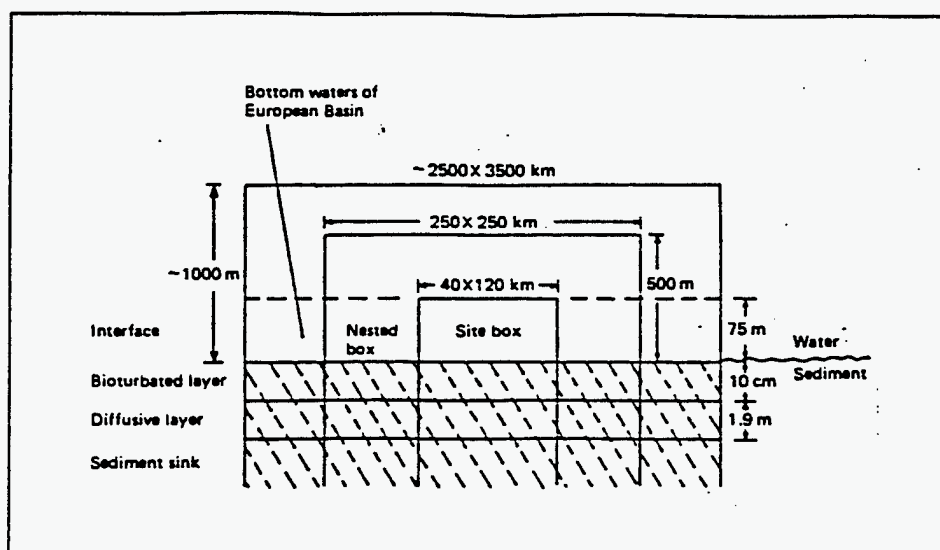


Fig. 1. Nested boxes around the dump site (IAEA 1988a).

The relationships between releases of radionuclides at the bottom of the deep sea and doses to man (individual and collective doses) and doses to marine organisms are shown in Table 2 for selected radionuclides. These radionuclides were chosen because they cover physical and chemical properties that represent different classes of nuclides with respect to physical half life, sediment distribution coefficient, biological concentration factor and radiation type and energy and because experience has shown that they tend to be dominating for the dose consequences.

Table 2. Individual and collective doses to man and doses to marine organisms from unit releases of selected radionuclides in the deep sea (terabecquerels = 10^{12} Bq).

| Nuclide | Individual dose (Sv TBq ⁻¹) | Collective dose (manSv TBq ⁻¹) | Fauna dose (Sv TBq ⁻¹) |
|---------|--|---|---------------------------------------|
| Co-60 | $4 \cdot 10^{-13}$ | $2 \cdot 10^{-10}$ | $2 \cdot 10^{-4}$ |
| Sr-90 | $3 \cdot 10^{-11}$ | $2 \cdot 10^{-7}$ | $1 \cdot 10^{-7}$ |
| Cs-137 | $6 \cdot 10^{-10}$ | $3 \cdot 10^{-6}$ | $1 \cdot 10^{-6}$ |
| Pu-239 | $4 \cdot 10^{-6}$ | $5 \cdot 10^0$ | $1 \cdot 10^{-3}$ |
| Am-241 | $1 \cdot 10^{-9}$ | $2 \cdot 10^{-3}$ | $3 \cdot 10^{-3}$ |

4. RELEASE OF RADIOACTIVITY IN SHALLOW WATERS

For the calculation of collective doses to members of the public from releases in shallow waters, an existing compartment model (NRPB et al. 1995) was used which was updated with more recent data (Nielsen 1995). Figure 2 shows the European coastal areas covered by the model. The model includes transfers of radioactivity between adjacent boxes due to mean advective water flow and mixing due to winds and tides. Furthermore, the model includes transfer of radioactivity associated with suspended sediment particles and their transfer to the top sediments (interior scavenging), ex-

changes of radioactivity between surface sediments and water due to diffusion and bioturbation as well as removal of activity from the top sediment layer due to burial (boundary scavenging). The data for the model (parameter values, marine produce, nuclide-specific values) are taken from the existing model (NRPB et al. 1995). The calculations of collective dose commitments were truncated at 1,000 a. Calculations of collective doses were made from inputs of activity into water regions covered by the box model ranging from the Barents Sea to the Bay of Biscay, and the collective doses from the upper end of the range were selected (inputs into the English Channel and Cumbrian Waters).

For the calculation of individual doses to members of the public from releases in shallow waters, a simple box model was used. The model is depicted in diagrammatic form in Figure 3 which shows the water box and the top sediment box in addition to the associated transfers of radioactivity. The model includes the same processes as the model described above. The rate of dispersion is determined by the flux of water out of the water box and indicated by k_{out} , the rates of sedimentation and sediment/water exchange are indicated by k_1 and k_2 , and the rate of burial is indicated by k_3 . Doses to individuals were calculated from ingestion, inhalation and external exposure with the values assigned to these pathways corresponding to those used for dumping practices (Section 2).

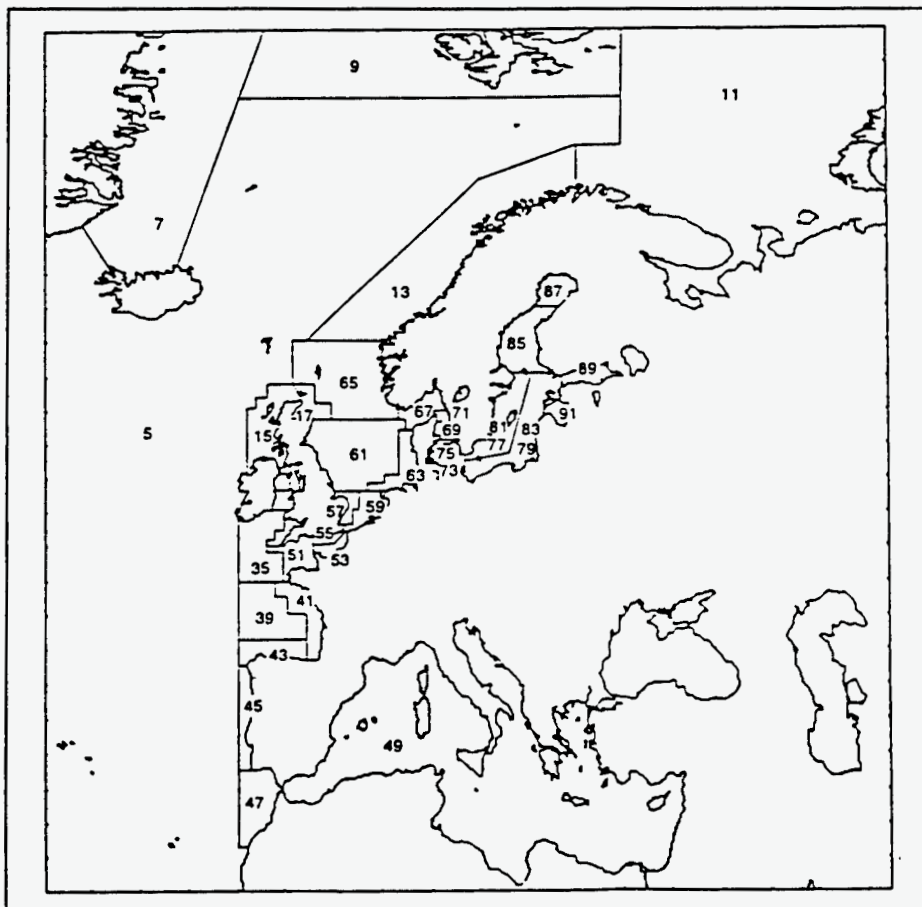


Fig. 2. European coastal waters covered by the box model (Nielsen 1995)

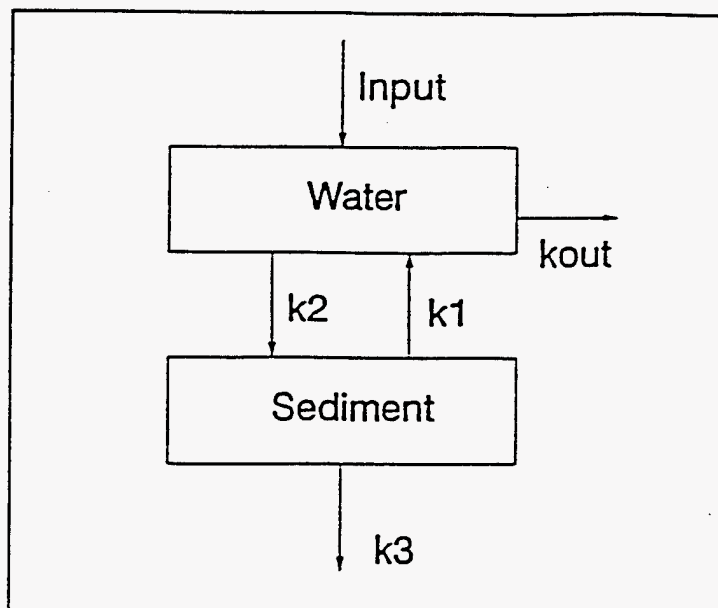


Fig. 3. Diagrammatic representation of the box model used for calculation of doses to individuals from releases in shallow waters.

Doses to marine organisms from releases of radionuclides in shallow waters were calculated by Pentreath and Woodhead (1988). They compared their generalised modelling approach with more direct measurements using data near the point of discharge of the Sellafield plant and found that the modelling approach tended to give higher values.

The relationships between releases of radionuclides in shallow waters and doses to man (individual and collective doses) and doses to marine organisms are shown in Table 3 for the same radionuclides as above.

Table 3. Individual and collective doses to man and doses to marine organisms from unit releases of selected radionuclides in shallow waters.

| Nuclide | Individual dose (Sv TBq ⁻¹) | Collective dose (manSv TBq ⁻¹) | Fauna dose (Sv TBq ⁻¹) |
|---------|--|---|---------------------------------------|
| Co-60 | 7 10 ⁻⁴ | 2 10 ⁻¹ | 6 10 ⁻³ |
| Sr-90 | 8 10 ⁻⁷ | 2 10 ⁻³ | 3 10 ⁻⁵ |
| Cs-137 | 2 10 ⁻⁵ | 4 10 ⁻² | 6 10 ⁻⁵ |
| Pu-239 | 8 10 ⁻⁴ | 3 10 ⁰ | 2 10 ⁻² |
| Am-241 | 4 10 ⁻⁴ | 2 10 ⁰ | 6 10 ⁻² |

5. IMPLICATIONS OF ACCIDENT SCENARIOS

A range of accidents may be envisaged for the transport of radioactive materials involving the loss of the materials to the sea as discussed at the Technical Committee Meeting of the Second Joint IAEA/IMO Working Group on the Safe Carriage of Irradiated Nuclear Fuel (INF) by Sea, held in Vienna, 26-30 April 1993. Several papers

from this meeting deal with consequences of such accidents where various assumptions have been made on releases to the sea of radioactive material.

The flasks used to transport spent nuclear fuel have been designed to withstand any impact likely to be suffered in a transport accident. Furthermore, other barriers such as sealed containers and fuel cladding provide additional containment between the radioactive material and the transport flask. Therefore, most probably no immediate release of radioactivity to the environment would occur if a flask was lost at sea; and if a flask was lost in shallow waters, a salvage operation might retrieve the flask before leakage would occur. However, releases to the environment might take place due to failure of the protective barriers, e.g. because of long-term exposure to seawater and subsequent corrosion or failure due to hydrostatic pressure in deep waters.

For the purpose of the present paper, assumptions are made of releases to sea of radionuclides in amounts corresponding to assumptions made in the papers from the above mentioned IAEA/IMO meeting. The release is assumed to comprise the radionuclides mentioned in amounts of the same order of magnitude as the inventory of one fuel assembly of 180-day cooled PWR fuel. The releases are shown in Table 4.

Table 4. List of radionuclides included in the present calculations showing physical half lives of radionuclides and amounts of activity released.

| <i>Nuclide</i> | <i>Half life (y)</i> | <i>Quantity released (TBq)</i> |
|----------------|--------------------------|------------------------------------|
| Co-60 | 5.3 | 100 |
| Sr-90 | 29 | 1000 |
| Cs-137 | 30 | 1000 |
| Pu-239 | 24,000 | 10 |
| Am-241 | 430 | 10 |

The public-health implications of the present release in terms of individual doses are shown in Table 5 for a release to deep waters as well as to shallow waters. For the deep-sea release the doses are dominated by the long-lived nuclide Pu-239 at a value of 0.04 milli-sieverts (mSv) with contributions from the other radionuclides orders of magnitude lower. For the shallow-water release the doses are dominated by Co-60 and Cs-137 at a total value of about 100 mSv. The difference between the consequences of the two release scenarios is primarily due the fact that the shallow waters considered are close to human populations while the deep waters are far from human populations. The individual doses may be compared with the world-wide annual average dose to man from natural background radiation which is about 2 mSv (UNSCEAR 1993). The individual doses from both scenarios are below the level of a few sieverts at which deterministic effects of ionising radiation (acute radiation symptoms) are observed, even if the dose was delivered over a short time. Taking a rounded value of 10^{-2} Sv^{-1} for the risk factor for stochastic effects (IAEA 1988b), the individual doses mean increased risks of fatal cancers of $4 \cdot 10^{-7}$ and $1 \cdot 10^{-3}$ for the deep-sea and the shallow-water scenario, respectively. These risks may be compared with the average individual risk of fatal cancer over a lifetime in the industrialised countries of about 0.2.

Table 5. Individual doses to critical-group members of the public (millisieverts, rounded numbers) from the release occurring in deep waters and in shallow waters.

| <i>Nuclide</i> | <i>Deep waters (mSv)</i> | <i>Shallow waters (mSv)</i> |
|----------------|------------------------------|---------------------------------|
| Co-60 | $4 \cdot 10^{-8}$ | $7 \cdot 10^1$ |
| Sr-90 | $3 \cdot 10^{-5}$ | $8 \cdot 10^{-1}$ |
| Cs-137 | $6 \cdot 10^{-4}$ | $2 \cdot 10^1$ |
| Pu-239 | $4 \cdot 10^{-2}$ | $8 \cdot 10^0$ |
| Am-241 | $1 \cdot 10^{-5}$ | $4 \cdot 10^0$ |
| Total | $4 \cdot 10^{-2}$ | $1 \cdot 10^2$ |

The public-health implications of the present release in terms of collective doses are shown in Table 6 for the two release scenarios. For the deep-sea release the collective dose is dominated by the long-lived nuclide Pu-239 at a rounded value of 50 man-sieverts (manSv) with contributions from the other radionuclides orders of magnitude lower. For the shallow-water release the total collective dose of about 100 manSv is almost equally divided between Co-60, Cs-137, Pu-239 and Am-241 while the contribution from Sr-90 is much lower. The difference between the collective doses for the two release scenarios is much less significant than for the individual doses which is due to the contribution to the collective dose from long-range dispersion of Pu-239 for the deep-sea release. These collective doses are assumed to be received by large populations which also receive doses from natural background radiation. It may be noted for comparison, that the UK population annually receives a collective dose of about 100,000 manSv. The collective doses from the two release scenarios may also be interpreted in terms of stochastic risks using the same risk factor as above, which gives estimates of 0.5 and 1 fatal cancers from the deep-water and shallow-water release, respectively.

Table 6. Collective doses to members of the public (mansieverts, rounded numbers) from the release occurring in deep waters and in shallow waters.

| <i>Nuclide</i> | <i>Deep waters (manSv)</i> | <i>Shallow waters (manSv)</i> |
|----------------|--------------------------------|-----------------------------------|
| Co-60 | $2 \cdot 10^{-8}$ | $2 \cdot 10^1$ |
| Sr-90 | $2 \cdot 10^{-4}$ | $2 \cdot 10^0$ |
| Cs-137 | $3 \cdot 10^{-3}$ | $4 \cdot 10^1$ |
| Pu-239 | $5 \cdot 10^1$ | $3 \cdot 10^1$ |
| Am-241 | $2 \cdot 10^{-2}$ | $2 \cdot 10^1$ |
| Total | $5 \cdot 10^1$ | $1 \cdot 10^2$ |

The doses to marine organisms from the two release scenarios are shown in Table 7. The doses have not been added up across nuclides because the doses are generally delivered to different marine organisms. Doses from the nuclides Sr-90 and Cs-137 which tend to remain soluble in seawater are mainly delivered to fish, while doses from the nuclides Co-60, Pu-239 and Am-241 which tend to be associated with sediments are mainly delivered to benthic organisms like crustacea and molluscs. The differences between the doses from the two release scenarios are due to the different physical sizes of the receiving environments and their sedimentation regimes. Sedimentation rates

are much higher in shallow waters than in deep waters causing higher radionuclide concentrations in coastal surface sediments for the same water concentrations.

On the basis of a review of fauna dose/effect relationships, the IAEA has concluded that populations of non-human organisms in the aquatic environment would be protected provided that chronic exposures were received at rates of less than 0.01 Sv d^{-1} (IAEA 1992). The doses from Table 7 fall well below this criterion considering release times of the order of years.

Table 7. Doses to marine organisms (sieverts, rounded numbers) from the release occurring in deep waters and in shallow waters.

| <i>Nuclide</i> | <i>Deep waters (Sv)</i> | <i>Shallow waters (Sv)</i> |
|----------------|-----------------------------|--------------------------------|
| Co-60 | $2 \cdot 10^{-2}$ | $6 \cdot 10^{-1}$ |
| Sr-90 | $1 \cdot 10^{-4}$ | $3 \cdot 10^{-2}$ |
| Cs-137 | $1 \cdot 10^{-3}$ | $6 \cdot 10^{-2}$ |
| Pu-239 | $1 \cdot 10^{-2}$ | $2 \cdot 10^{-1}$ |
| Am-241 | $3 \cdot 10^{-2}$ | $6 \cdot 10^{-1}$ |

6. CONCLUSIONS

This paper has reviewed pathways by which man and marine fauna would be exposed from releases of radioactive material to the sea. Consequences of unit releases of radionuclides to the deep sea and to shallow waters have been presented based on existing studies. As an illustrative example of the implications of a flask lost at sea, a release scenario comprising the radionuclides Co-60, Sr-90, Cs-137, Pu-239 and Am-241 in amounts of the same order of magnitude as those of a 180-day cooled PWR fuel assembly has been selected.

The public-health implications of the accident scenario in terms of doses to individuals of critical groups give values of 0.04 mSv and 100 mSv for releases in deep waters and in shallow waters, respectively. These doses are below the level of deterministic effects of ionising radiation. Taking a rounded value of 10^{-2} Sv^{-1} for the risk factor for stochastic effects, these doses mean increased individual risks of fatal cancers of $4 \cdot 10^{-7}$ and $1 \cdot 10^{-3}$, respectively.

The public-health implications of the accident scenario in terms of doses to populations give collective doses of 50 manSv and 100 manSv for releases in deep waters and in shallow waters, respectively. Using the same risk factor as above these doses may be interpreted to correspond to 0.5 and 1 fatal cancers, respectively.

The ecological implications of the accident scenarios have been investigated in terms of risk to populations of non-human organisms in the marine environment. The doses to the marine organisms indicate that any risk at the population level to marine organisms is very unlikely.

REFERENCES

- CEC, 1990. The radiological exposure of the population of the European Community from radioactivity in North Marine waters, Project 'Marina', Commission of the European Communities, EUR 12483 EN.
- IAEA, 1983. GESAMP-IMO/FAO/UNESCO/WMO/WHO/IAEA/UN/UNEP Joint Group of Experts on the Scientific Aspects of Marine Pollution, An Oceanographic Model for the Dispersion of Wastes Disposed of in the Deep Sea, Reports and Studies No. 19, International Atomic Energy Agency, Vienna.
- IAEA, 1984. The Oceanographic and Radiological Basis for the Definition of High-Level Wastes Unsuitable for Dumping at Sea, Safety Series No. 66, International Atomic Energy Agency, Vienna.
- IAEA, 1986. Definition and Recommendations for the Convention on the Prevention of Marine Pollution by Dumping of Wastes and Other Matter, 1972, Safety Series No. 78, International Atomic Energy Agency, Vienna.
- IAEA, 1988a. Assessing the Impact of Deep Sea disposal of Low Level Radioactive Waste on Living Marine Resources. Technical Reports Series No. 288, International Atomic Energy Agency.
- IAEA, 1988b. Principles for the Exemption of Radiation Sources and Practices from Regulatory Control. Safety Series No. 89, International Atomic energy Agency, Vienna.
- IAEA, 1992. Effects of Ionizing Radiation on Plants and Animals at Levels Implied at Current Radiation Protection Standards. Technical Report Series No. 332, International Atomic Energy Agency.
- Nielsen, S.P. A box model for North-East Atlantic coastal waters compared with radioactive tracers. *J. Marine Systems* 6; 1995.
- NRPB, IPSN, CIEMAT, CSN and CEEOP, 1995. Simmonds, J.R., Lawson, G. and Mayall, A. Methodology for assessing the radiological consequences of routine releases of radionuclides to the environment, Commission of the European communities, Luxembourg, EUR Report 15760.
- Mobbs, S., 1994. Personal communication.
- NEA 1985. Review of the continued suitability of the dumping site for radioactive waste in the North-East Atlantic. Nuclear Energy Agency, OECD-NEA, Paris.
- Pentreath, R.J. and Woodhead, D.S., 1988. Towards the development of criteria for the protection of marine fauna in relation to the disposal of radioactive wastes into the sea; IAEA-CN-51/83. In: Proc. of an International Conference on Radiation Protection in Nuclear Energy Organised by the International Atomic Energy Agency, Sydney, 18-22 April 1988.
- Smith, G.M., Fearn, H.S., Delow, C.E., Lawson, G. and Davis, J.P., 1986. Calculations of the radiological impact of disposal of unit activity of selected radionuclides. DOE Report No. DOE/RW/86-136, Department of the Environment, UK.
- UNSCEAR, 1993. Sources and Effects of Ionizing Radiation. United Nations Scientific Committee on the Effects of Atomic Radiation, United Nations, New York.

QUESTIONS, ANSWERS AND COMMENTS FOLLOWING:

PRESENTATION IV

- Ecological and public health implications from flasks lost at sea
Sven Nielsen
Danish Dept of Environmental Science and Technology

Ireland:

Mr. Chairman I would like to ask Mr. Nielsen about the risk factor which he mentioned in his conclusions. He said taking a rounded value of ten to the 10^{-2} per mSv for the risk factor etc. Now we were told earlier this morning by Mr. Webb that the risk factor is 0.005 per mSv. I believe Mr. Webb is correct, that Mr. Nielsen is in error. Would you like to comment Mr. Nielsen?

Mr. Nielsen:

There is some ambiguity on the risk perceived. As it is now, the International Commission on Radiation Protection (ICRP) is recommending a risk factor .005 as Mr. Webb cited. However, that risk factor, well I was looking more in terms of orders of magnitude, so I do not see any big difference between 0.01 and 0.005, but I agree that the internationally agreed risk factor is .005, but for the purpose of this presentation here, where we are dealing with orders of magnitude, I do not see the importance to stress this factor.

Ireland:

I would suggest that there is a very large difference and I would also suggest that 100 mSv, as reported in your paper in the conclusion, to individuals of critical groups is a very, very significant dose. Its a hundred times the recommended limit for a member of the public and this would be a dose to a member of a critical group arising from one accident, so that is an extremely high dose in my view and it would cause an awful lot of upset in the state that would be effected.

Japan:

Thank you Mr. Nielsen for your interesting presentation. If I may, I would like to make the following two comments on your findings. Firstly, irradiated fuel is in the form of ceramics type and it is hard to be dissolved in the sea water, therefore, in order to be more realistic, a leakage rate of spent irradiated fuel into the sea water should have been taken into account. According to my estimations, the annual dose will be reduced by approximately 10^{-3} by this consideration, and secondly, if the flask sank in shallow sea, the flask can be a barrier to contain the nucleus inside the flask. The leakage rate of the nucleus into the sea water would become small. According to our estimations, if the barrier effect is taken into account, the annual dose will be further reduced by approximately 1/10, so considering these two effects, the annual dose will be reduced by approximately 10^{-4} .

Solomon Islands:

Regarding containment of the flasks, you mentioned that the flasks should provide containment, particularly in the case of deep sea where they cannot be retrieved, but the question is for how long, particularly with regard to the fact that deep waters in the Pacific are not necessarily remote for people. We can go down to 100 fathoms or more just off the reef.

APPLYING THE PRECAUTIONARY PRINCIPLE
TO OCEAN SHIPMENTS OF RADIOACTIVE MATERIALS

by Jon M. Van Dyke¹
William S. Richardson School of Law
University of Hawaii at Manoa
Honolulu, Hawaii

The transport of unusually hazardous radioactive materials by sea may become more common now that Japan appears to have committed itself to reprocessing its nuclear wastes and acquiring a stockpile of plutonium.² These shipments from France to Japan (and back) present hazards that are of a different dimension than those presented by other dangerous cargoes. Many countries along the route of these shipments have protested vigorously against them, and some have explicitly cited the "precautionary principle" as the norm of international law that provides a framework to regulate such transports.³

The "precautionary principle" has gained almost universal acceptance during the past decade as the basic rule that should govern activities that affect the ocean environment.⁴ This principle requires users of the ocean to exercise caution by undertaking relevant research, developing nonpolluting technologies, and avoiding activities that present uncertain risks to the marine ecosystem. The precautionary principle lays down a set of specific responsibilities that must be met before shipments of unusually hazardous materials may be undertaken. This paper will outline these responsibilities and will demonstrate that they have not been complied with by the Japanese agencies in charge of the shipments.

The Shipments. The controversial Japanese plutonium shipment began in November 1992, when a refitted freighter called the Akatsuki Maru carried 2200 pounds (one metric ton) of weapons-usable plutonium from France to Japan, traveling around the Cape of Good Hope at the tip of Africa, and then going eastward south of Australia and New Zealand, and finally

¹ The author would like to acknowledge the assistance of the Nuclear Control Institute in supporting the research for this paper and the assistance of Karl Espaldon, University of Hawaii Law School Class of 1996, in organizing sources and research materials.

² See generally Jon M. Van Dyke, Sea Shipment of Japanese Plutonium under International Law, 24 Ocean Dev. & Int'l L. 399 (1993) [hereafter cited as Van Dyke, Japanese Plutonium]; Andrew Pollack, Japan Throws the Switch on Reactor, N.Y. Times, Aug. 30, 1995, at A6, col. 6 (nat'l ed.).

³ See infra notes 79-106 and accompanying text. When a Chilean naval vessel protested the transit of the Pacific Pintail through Chile's exclusive economic zone, it said: "I inform you that the carrying of your radioactive material is a violation of the precaution[ary] principle ... stated in the Rio de Janeiro declaration" Transcript of a radio conversation between the Pacific Pintail and the Chilean navy, March 20, 1995.

⁴ See infra notes 8-16 and accompanying text.

turning north through the Pacific Islands to Japan. More recently, a vessel registered in the United Kingdom called the Pacific Pintail left La Hague, France on February 23, 1995, carrying 28 logs of high-level vitrified nuclear waste in glass blocks each weighing 1,000 pounds. These solidified liquid residues are extremely hot, even in normal conditions. This ship traveled in the opposite direction, going southwest across the Atlantic to Cape Horn at the tip of South America and then northwest across the Pacific, passing close to Hawaii, and finally reaching Rokkasho, Aomori Prefecture, Japan on April 25, 1995.⁵ Then, on May 25, 1995, the Pacific Sandpiper left Omaezaki Port in Shizuoka Prefecture, carrying spent nuclear fuel to France, presumably through the Panama Canal. Despite the many protests that have been raised,⁶ Japan has announced that these shipments will continue in increasing numbers over the coming decades.⁷

The Precautionary Principle. Although this principle has been phrased in many ways in recent agreements and commentaries,⁸ perhaps the phrasing in Principle 15 of the 1992 Rio Declaration on Environment and Development⁹ best reflects the international community's views on this principle:

In order to protect the environment, the precautionary approach shall be widely applied by States according to their capabilities. Where there are threats of serious or irreversible damage, lack of full scientific certainty shall not be used

⁵ The vessel had to drift offshore for 24 hours because Governor Morio Kimura of Aomori Prefecture refused entry to the port until the central government and the electric utilities promised that the waste would be removed from Aomori after an intermediate storage of 30-50 years. The Governor finally allowed the ship to land after an ambiguous "assurance" from Japan's Science and Technology Agency, because he concluded that letting the deadly waste drift offshore was too dangerous. Citizen's Nuclear Information Center (Tokyo, Japan), Press Release, June 16, 1995.

⁶ See *infra* notes 79-106 and accompanying text.

⁷ It has been estimated that 44,500 cubic meters of nuclear wastes are to be returned to Japan according to present reprocessing contracts during the next 15-20 years. This transport would require between 120 and 1,200 shipments, depending on how many logs are loaded onto a single ship. Citizens Nuclear Information Center, Tokyo, Japan, Press Release, April 17, 1995.

⁸ The precautionary principle is a logical corollary from the established international-law norm that no state has the right to engage in activities within its borders that cause harm to other states. See, e.g., Trail Smelter Arbitration (U.S. v. Can.), 3 R. Int'l Arb. Awards 1905 (1941). In the Trail Smelter Arbitration, the arbitrators required Canada to pay damages even though the causal link between the emissions in Canada and the damages remained somewhat uncertain. See Bernard A. Weintraub, Science, International Environmental Regulation, and the Precautionary Principle: Setting Standards and Defining Terms, 1 N.Y.U. Envtl. L. J. 173, 182-82 (1992)(citing 3 R. Int'l Arb. Awards at 1912, 1921, 1922).

⁹ A/CONF.151/5/Rev.1 (June 13, 1992).

as a reason for postponing cost-effective measures to prevent environmental degradation.¹⁰

What specific burdens does this principle impose users of the ocean?"¹¹ It requires policy

¹⁰ See also Agenda 21, Chapter 17, 17.22, in Report of the United Nations Conference on Environment and Development (Rio de Janeiro, June 3-14, 1992), A/CONF.151/26 (Vol.II)(Aug. 13, 1992):

States, in accordance with the provisions of the United Nations Convention on the Law of the Sea on protection and preservation of the marine environment, commit themselves, in accordance with their policies, priorities and resources, to prevent, reduce and control degradation of the marine environment so as to maintain and improve its life-support and productive capacities. To this end, it is necessary to:

(a) Apply preventive, precautionary and anticipatory approaches so as to avoid degradation of the marine environment, as well as to reduce the risk of long-term or irreversible adverse effects upon it ...

¹¹ Commentators have discussed whether the precautionary principle has been officially accepted as a norm of customary international law that is formally binding on all nations. The principle has been so universally included in recent treaties that it appears now to have that status. One commentator has stated that the Organization of Economic Cooperation and Development (OECD) (of which Japan is a member) adopted the precautionary principle as early as 1979, and that today "modern international environmental law is largely precautionary." Harold Hohmann, Precautionary Legal Duties and Principles of Modern International Environmental Law 141, 203, 341-45 (1979)(citing the Declaration of Anticipatory Environmental Policies, adopted by the OECD environment ministers on May 8, 1979). See also Daniel Bodansky, Remarks: New Developments in International Environmental Law, 85 Am. Soc'y Int'l L. Proc. 401, 413 (1991)("Indeed, so frequent is its invocation that some commentators are even beginning to suggest that the precautionary principle is ripening into a norm of customary international law"); David Freestone, The Precautionary Principle, in International Law and Global Climate Change 21, 36 (Robin Churchill and David Freestone eds. 1991):

The speed with which the precautionary principle has been brought on to the international agenda, and the range and variety of international forums which have explicitly accepted it within the recent past, are quite staggering The significance of the repeated public acceptance and endorsement of principles by government representatives should not be underrated, particularly if, as is increasingly the case, this is supported by binding measures explicitly implementing the principle [citing to the 1989 action under the Oslo Convention to ban dumping of industrial wastes and the Bamako Convention on the Ban of the Import into Africa and the Control of Transboundary Movement and Management of Hazardous Wastes within Africa, Jan. 29, 1991, 30 I.L.M. 773 (1991)].

Also relevant to its acceptance is fact that it is impossible to find examples of nations rejecting the precautionary principle or citing scientific uncertainty as a legitimate basis for action or inaction.

makers to be alert to risks of environmental damage, and the "greater the possible harm, the more rigorous the requirements of alertness, precaution and effort."¹² It rejects the notion that the oceans have an infinite or even a measurable ability to assimilate wastes, and it instead recognizes that our knowledge about the ocean's ecosystems may remain incomplete and that policy makers must err on the side of protecting the environment.¹³ It certainly means at a minimum that a thorough evaluation of the environmental impacts must precede actions that may affect the marine environment. All agree that it requires a vigorous pursuit of a research agenda in order to overcome the uncertainties that exist.¹⁴

Some commentators have explained the precautionary principle by emphasizing that it shifts the burden of proof: "[W]hen scientific information is in doubt, the party that wishes to develop a new project or change the existing system has the burden of demonstrating that the proposed changes will not produce unacceptable adverse impacts on existing resources and

The specific content of the precautionary principle is, however, still controversial. For a summary of the recent treaties and documents using the term and an analysis of some of the unresolved issues, see James E. Hickey, Jr., and Vern R. Walker, Refining the Precautionary Principle in International Environmental Law, 14 Va. Env't'l L.J. 423 (1995). See also Gregory D. Fullem, Comment, The Precautionary Principle: Environmental Protection in the Face of Scientific Uncertainty, 31 Willamette L. Rev. 495 (1995); John M. Macdonald, Appreciating the Precautionary Principle as an Ethical Evolution in Ocean Management, 26 Ocean Dev. & Int'l L. 255 (1995).

¹² Freestone, supra note 11, at 31.

¹³ Ellen Hey, The Precautionary Concept in Environmental Policy and Law: Institutionalizing Caution, 4 Geo. Int'l Env'tl. L. Rev. 303, 305 (1992). Some observers believe the precautionary principle to be essential because no amount of advanced research can predict the impact of significant polluting events. See, e.g., William H. Rodgers, Environmental Law 35-39 (2d ed. 1994) (discussing "chaos theory").

Examples of application of the precautionary principle include the decisions of the contracting parties to the London Dumping Convention, 26 U.S.T. 2403, 11 I.L.M. 1294 (1972), to phase out all dumping of industrial wastes and prohibit dumping of low-level radioactive wastes; the 1982 decision of the International Whaling Commission to impose a moratorium on commercial whaling; the protection of endangered species under the Convention on International Trade in Endangered Species of Wild Fauna and Flora (CITES), 12 I.L.M. 1085 (1973); the U.N. General Assembly's ban on driftnet fishing, Resolutions 44/225 (1989) and 45/197 (1990); and the 1987 Montreal Protocol on Substances that Deplete the Ozone Layer. See Freestone, supra note 11, at 35-36; Robert Jay Wilder, The Precautionary Principle and the Law of the Sea Convention, in Implications of Entry into Force of the Law of the Sea Convention 50 (Ocean Governance Study Group, 1995).

¹⁴ OECD Secretariat, The Role of Uncertainty in Decision-Making in the Area of Environmental Protection, ENV/EC/ECO(91)12; Hey, supra note 13, at 311.

species."¹⁵ Others have suggested that the principle has an even more dynamic element, namely that it requires all users of the ocean commons to develop alternative nonpolluting technologies.¹⁶ These requirements are explained in detail in the sections that follow.

The Duty to Prepare an Environmental Impact Assessment. This duty has been recognized in numerous recent treaties,¹⁷ and a treaty has been drafted that spells out the procedures to be used in drafting such an assessment in the international context.¹⁸ The Organization of Economic Cooperation and Development (OECD) (of which Japan is a member) issued a document in 1985 "requiring that developmental assistance projects and programs which could significantly affect the environment be comprehensively assessed from an environmental

¹⁵ Freedom for the Seas in the 21st Century 477 (Jon M. Van Dyke, Durwood Zaelke, and Grant Hewison eds. 1993). This view is also found in the World Charter for Nature, Art. 11(b), Oct. 28, 1982, G.A. Res. 37/7, 37 U.N.G.A.O.R. Supp. (No. 51) 17, U.N. Doc. A/37/51, 22 I.L.M. 455 (1983):

Activities which are likely to pose a significant risk to nature shall be preceded by an exhaustive examination; their proponents shall demonstrate that expected benefits outweigh potential damage to nature, and where potential adverse effects are not fully understood, the activities should not proceed.

See also P.W. Birnie and Alan E. Boyle, International Law and the Environment 98 (1992)(concurring with this view in the context of the London Dumping Convention, supra note 13; Weintraub, supra note 8, at 204-07 (justifying the shifting of the burden of proof to the polluter as the "more efficient" approach); Macdonald, supra note 11, at 263-64 (discussing the burden of proof issue). Another commentator has written that "[t]here is some evidence to suggest that this interpretation [that the precautionary principle shifts the burden of proof to those who are carrying out the activities] is gaining acceptance, even if it cannot yet be considered to be a rule of general application." Philippe Sands, The "Greening" of International Law: Emerging Principles and Rules, 1 Ind. J. Global Legal Stud. 293, 301 (1994) (citing recent examples).

¹⁶ Hey, supra note 13, at 308 n.22 and 309-11.

¹⁷ See generally Van Dyke, Japanese Plutonium, supra note 2, at 402-03; World Charter of Nature, supra note 15, Principle 11(c). One European commentator explained that an environmental impact assessment is "an almost indispensable means of realizing Stockholm Principle 21 [requiring countries to avoid causing transboundary pollution to other countries], so that the legal significance of the EIA can be compared to that of the information and notification duty." Hohmann, supra note 11, at 201. The Stockholm Principles were promulgated by the United Nations Conference on the Human Environment on June 16, 1972, and are reprinted in 11 I.L.M. 1416, 1420 (1972).

¹⁸ Convention on Environmental Impact Assessment in a Transboundary Context, Feb. 25, 1991, 30 I.L.M. 800 (1991). This Convention does not explicitly refer to shipments of ultrahazardous cargoes, but its descriptions of the appropriate procedures to follow in preparing an assessment are universally applicable.

standpoint by Member States at the earliest possible stage."¹⁹ With regard to the 1992 plutonium shipment, some limited testing and evaluation was undertaken by Japanese and U.S. agencies, but nothing like a formal environmental assessment was prepared.²⁰ The Abercrombie Amendment to the Energy Policy Act of 1992 required the Department of Energy to conduct a safety analysis of plutonium shipments by sea, and a safety analysis was transmitted to Congress in February 1994, but it was characterized by members of the House of Representatives from Hawaii, Guam, American Samoa, Puerto Rico, and the U.S. Virgin Islands as "wholly inadequate."²¹

Japan has not had extensive experience in conducting environmental impact assessments, and its efforts in undertaking such efforts have not always been successful.²² For its shipment of vitrified nuclear wastes, Japan's Science and Technology Agency released on February 13, 1995 a very short summary of a report entitled "Environmental Impact Assessment of High Level Radioactive Waste Cask Sinking in the Sea" in response to demands that it conduct a full

¹⁹ Hohmann, supra note 11, at 146 (citing Rec. C(85) 104 of 20 June 1985). OECD recommendations require unanimity for adoption. According to Rule 19(b) of the OECD Rules of Procedure, "Recommendations shall be submitted to the Members for consideration, in order that they may, if they consider it opportune, provide for their implementation." In practice, even though a recommendation may not be legally enforceable in a tribunal, "each of the Member States can remind the deviant member of this recommendation, which was supported by all members after lengthy negotiations, and can insist upon appropriate conduct." Hohmann at 181.

²⁰ See Van Dyke, Japanese Plutonium, supra note 2, at 404-07.

²¹ Letter to President William Clinton signed by Representatives Neil Abercrombie (Hawaii), Patsy T. Mink (Hawaii), Victor O. Frazer (U.S. Virgin Islands), Robert A. Underwood (Guam), Carlos A. Romero-Barcelo (Puerto Rico), and Eni F.H. Faleomavaega (American Samoa), Jan. 10, 1995; Pete Pichaske, Lawmakers Want Waste Transit Delayed, Honolulu Star-Bulletin, Jan. 13, 1995, at A-7, col. 2.

The Energy Policy Act of 1992 called for a safety analysis of the sea shipments of plutonium. The Nuclear Regulatory Commission released a draft report in December 1992 which was criticized as inadequate. In a letter dated September 24, 1993, Thomas P. Grumbly, Assistant Secretary for Environmental Restoration and Waste Management, Department of Energy, agreed to expand the scope of the study to include an evaluation of glassified high-level waste. Two months later, however, because of objections from the State Department, the Energy Department withdrew this commitment and in February 1994, more than a year late, it released the original report to Congress. Letter from Thomas P. Grumbly, Assistant Secretary for Environmental Restoration and Waste Management, Department of Energy, to Representative Neil Abercrombie, Feb. 8, 1994.

²² For an analysis of the Japan's efforts to assess its proposed dumping of low-level nuclear wastes in the ocean, see Jon M. Van Dyke, Ocean Disposal of Nuclear Wastes, 12 Marine Policy 82 (1988).

environmental assessment of the shipment.²³ This report was commissioned by the Central Research Institute of Electric Power Industry in 1990 and consisted of a four-page summary of the industry's findings.²⁴ The Science and Technology Agency stated that it did not believe that a formal environmental impact assessment was required, because in its view its transport is legitimate if it complies with the standards of the International Atomic Energy Agency (IAEA), but that it commissioned a study on this one issue nonetheless to "promote further understanding."²⁵ The conclusion of the study is that "even in the event of the worst accident scenario--the sinking of all 28 canisters under the sea--the effect to human health would be negligible."²⁶ The report presents no detailed description of its methodology or assumptions.²⁷ Nor does it analyze the accident that could present a much greater danger--a collision followed by an intense fire on the vessel.

A U.S. scientist, Dr. Edwin S. Lyman, at the Center for Energy and Environmental Studies at Princeton University's School of Engineering and Applied Science, issued an analysis of the shipment in which he concluded that the stainless steel used in the casks can weaken at extremely high temperatures and could rupture in an accident at sea.²⁸ The alloy used by France is susceptible to "sensitization" or weakening, and had previously been found by U.S. experts to be unsafe for such high-temperature applications. Dr. Lyman characterized the decision to

²³ Japan's Arrogance and Irresponsibility Harshly Criticized, Nuke Info Tokyo (Citizens' Nuclear Information Center), March/April 1995, at 3.

²⁴ This assessment has not been widely disseminated, and is titled simply "Summary of environmental impact assessment (Draft)" and marked "Confidential." It reports a measurement of the dose exposure to individuals and groups from two hypothetical sinkings, and concludes that they are less than the exposure from natural radiation and hence are insignificant. This assessment has been described in one publication of the Japan Atomic Industrial Forum, the March 1995 issue of the English-language periodical "Atoms in Japan," which contains a four-paragraph summary stating that the tests performed "proved that exposure dose equivalents to the public would be significantly less than the effective dose equivalent limits recommended by the ICRP." This short summary contains a typographical error regarding the "calculated exposure dose equivalent to the public" that makes it impossible to evaluate even the limited information provided. Representatives of Japan's Science and Technology Agency held a briefing on February 13, 1995 on this "assessment," but those conducting the briefing for the Agency acknowledged that they did not know the assumptions on which the calculations were based. Citizens Nuclear Information Center, Brief Record of Meeting with STA on February 13, 1995.

²⁵ Japan's Arrogance, *supra* note 23, at 4.

²⁶ *Id.*

²⁷ *Id.*

²⁸ Edwin S. Lyman, Sensitization of Stainless Steel Vitrified High-Level Waste Canisters during Production (Feb. 14, 1995); Edwin S. Lyman, Safety Issues in the Sea Transport of Vitrified High-Level Radioactive Wastes to Japan (Dec. 12, 1994).

use this alloy as "a bad engineering decision ... at best imprudent, and at worst irresponsible."²⁹ The weakness in the cask "would increase the probability of a canister breach and radionuclide release in the event of mechanical or thermal shocks, such as a collision during sea transport, a hoist failure during loading or unloading of transport cases, or the rapid quenching of a hot fire."³⁰ Dr. Lyman also concluded that the IAEA standards do not appear to provide an adequate measure of safety and he recommended that a series of tests be undertaken to measure the ability of the casks to withstand a shipboard fire following a collision.³¹

Four months after the Pacific Pintail arrived in Japan, the government-owned company Japan Nuclear Fuel Ltd. acknowledged that a small amount of cesium-137 had been detected on the surface of one of the 28 transported canisters of vitrified radioactive waste.³² This announcement reinforces the view that the packaging procedures may not have been properly evaluated and gives credence to the perspective that no further shipments should occur until a thorough and independent environmental assessment has been completed.³³

The Duty to Conduct Research. Everyone agrees that research efforts to overcome uncertainties are essential.³⁴ Commentators disagree on what type of research is required, with environmentalists emphasizing that the research should focus on developing nonpolluting alternative technologies rather than on measuring the assimilative capacity of the oceans.³⁵

The Duty to Notify. The duty to notify other countries of risks in order to enable them to prepare contingency plans to deal with accidents and emergencies "is almost a fundamental principle of the international law of the environment, which is quite distinct from the duty of

²⁹ Lyman, Feb. 14, 1995, supra note 28, at 1.

³⁰ Id. at 3.

³¹ Lyman, Dec. 12, 1994, supra note 28. Dr. Lyman also questioned the use of elastomer for the O-ring seals, which "are the most vulnerable sites on the cask." Id. at x-xi. Elastomer seals are prone to failure at temperatures above 230 degrees Centigrade and can be damaged by high radiation fields.

³² Cesium Contamination on HLW Canister Fuels Debate in Japan, Nucleonics Week, Aug. 24, 1995. The cesium could have contaminated the canister at the vitrification plant at La Hague, France, or could possibly have emerged "from 'sweating' of the canister during transport, meaning that one or more pinholes in it provided a channel for cesium inside to leak out." Id. The Japanese have rejected the latter possibility, arguing that ruthenium would also have been detected if any leaks had occurred. Id.

³³ Letter from Paul Leventhal, President, Nuclear Control Institute, to Kiyoshi Nozawa, President, Japan Nuclear Fuel Ltd., Aug. 30, 1995.

³⁴ OECD Secretariat, supra note 14; Hey, supra note 13, at 311.

³⁵ Hey, supra note 13, at 311.

'prompt notification' in case of emergency."³⁶ This duty is explicitly recognized and given content by OECD documents³⁷ and in the Basel Convention on the Control of Transboundary Movement of Hazardous Wastes and their Disposal.³⁸

The Duty to Consult. This duty is now universally recognized as a requirement when one nation plans an activity that creates risks for other nations.³⁹ The OECD explained these obligations in some detail in two documents that were issued in 1978, in response to the Sandoz and Chernobyl accidents.⁴⁰ The 1982 United Nations Law of the Sea Convention gives this duty particular teeth by requiring--in cases where nations can anticipate the possibility of marine pollution--that they "jointly develop and promote contingency plans for responding to pollution incidents in the marine environment."⁴¹

The Duty to Develop Alternative Techniques. The precautionary principle requires decisionmakers to move away from polluting activities even if the scientific data remain cloudy regarding the specific damage imposed upon the environment. The contracting parties to the

³⁶ Laura Pineschi, The Transit of Ships Carrying Hazardous Wastes through Foreign Coastal Zones, in International Responsibility for Environmental Harm 299, 314 (F. Francioni and Tullio Scovazzi eds. 1991)(citing sources in support in her note 55). This duty (and the duty to consult) can also be seen as deriving from Stockholm Principle 21 (1972)(requiring countries to avoid causing transfrontier pollution to other countries and to areas beyond national jurisdiction). See Hohmann, supra note 11, at 197.

³⁷ This duty was recognized as early as 1974 in the OECD Principles Concerning Transfrontier Pollution, Rec. C(74)224 of 14 November 1974, discussed in Hohmann, supra note 11, at 148-49.

³⁸ Basel Convention on the Control of Transboundary Movements of Hazardous Wastes and their Disposal, art. 4(2)(f), UNEP Doc. T/BSL/OOO, March 22, 1989, reprinted in 28 I.L.M. 652 (1989) [hereafter cited as Basel Convention].

³⁹ See Van Dyke, Japanese Plutonium, supra note 2, at 400-02.

⁴⁰ Rec. C(88)84 of 8 July 1988, 28 I.L.M. 247 (1989), requires countries to exchange information on planned hazardous installations that could cause transfrontier damage in the event of an accident.

Rec. C(88)85 of 8 July 1988, 28 I.L.M. 277 (1989), entitled "Provision of Information to the Public and Public Participation in Decision-Making Processes Related to the Prevention of, and Response to, Accidents Involving Hazardous Substances," assumes that persons potentially affected by transfrontier accidents have a right to know of the risks they are being subjected to, and to participate in the development of emergency measures to be taken in the event of such an accident. Nuclear installations are, however, excluded from these specific requirements. See generally Hohmann, supra note 11, at 149-50.

⁴¹ United Nations Convention on the Law of the Sea, art. 199, second sentence, Dec. 10, 1982, U.N.Doc. A/CONF.62/122 (1982), 21 I.L.M. 1261 (1982) [hereafter cited as Law of the Sea Convention].

Oslo Convention and the London Dumping Convention, for instance, both agreed to phase out ocean incineration of wastes—even though the specific harm to the marine environment had not been established—because alternative technologies such as recycling and land-based treatments were available.⁴² One commentator has summarized this requirement as follows:

The precautionary concept does not insist that all risk of harm be avoided at all cost. Rather, it requires that society be willing to accept higher costs now in order to avoid the possibility of environmental degradation in the future.⁴³

The Duty to Mitigate All Reasonably Foreseeable Damage. This obligation follows directly from the precautionary principle and from the core notions developed at Stockholm in 1972 and Rio de Janeiro in 1992. The shipping nation must act systematically to reduce all foreseeable damages. This responsibility requires it to explore all alternative nonpolluting technologies, alternatives to nuclear power, alternatives to using plutonium in commercial nuclear plants, and—in particular—alternatives to reprocessing spent nuclear fuel. Better encasements for the transported radioactive materials must also be developed and used.

In the context of sea shipments of ultrahazardous cargoes, the important question is whether this duty to mitigate is inconsistent with the freedom of navigation, which is a cornerstone of the modern law of the sea. The apparent conflict can be resolved by understanding that the freedom of navigation is not an absolute freedom and is subject to qualifications in all international agreements.

Traditional Navigational Freedoms Do Not Apply to Ultrahazardous Cargoes. The 1982 Law of the Sea Convention guarantees freedom of navigation through the high seas,⁴⁴ exclusive economic zones,⁴⁵ straits used for international navigation,⁴⁶ and archipelagic sea lanes,⁴⁷ and it permits the exercise of "innocent passage" through territorial seas⁴⁸ and archipelagic waters.⁴⁹ But it also imposes an obligation on all states to protect and preserve the marine environment,⁵⁰ and to take measures to prevent pollution from vessels by "preventing accidents and dealing with

⁴² Hey, *supra* note 13, at 309 n.25.

⁴³ *Id.* at 310.

⁴⁴ Law of the Sea Convention, *supra* note 41, art. 87.

⁴⁵ *Id.*, art. 58(1).

⁴⁶ *Id.*, arts. 34-44.

⁴⁷ *Id.*, art. 53.

⁴⁸ *Id.* arts. 17-19.

⁴⁹ *Id.*, art. 52.

⁵⁰ *Id.*, art 192.

emergencies, ensuring the safety of operations at sea, preventing intentional and unintentional discharges, and regulating the design, construction, equipment, operation and manning of vessels."³¹ The Convention recognizes specific powers of coastal nations to regulate "ships carrying nuclear or other inherently dangerous or noxious substances or materials"³² and ships transiting through ice-covered areas.³³ It recognizes a duty to notify other affected nations immediately in cases where "the marine environment is in imminent danger of being damaged or has been damaged by pollution."³⁴ The balance between these conflicting rights and duties has been given greater precision in more recent agreements.

The 1989 Basel Convention on the Control of Transboundary Movements of Hazardous Wastes and their Disposal does not govern the movement of radioactive wastes if other international arrangements governing movements of these wastes are in place,³⁵ but its approach to protecting the environment provides guidance on this topic. The Basel Convention requires states transporting hazardous wastes to notify states through which the waste is traveling, and appears to allow the transit states to object to such transport.³⁶ The Japanese government, however, filed a declaration to the Basel Convention stating that it "understands" that the convention does not "require notice to or consent of any state for the mere passage of hazardous

³¹ *Id.*, art 194(3)(b).

³² *Id.*, art. 22(2); see also art. 23.

³³ *Id.*, art. 234.

³⁴ *Id.* art. 198. One commentator has observed that "[t]his rule might be applicable even when a State becomes aware that a ship flying its flag and carrying harmful wastes is not complying with the safety regulations prescribed by Article 194. Pineschi, supra note 36, at 306.

³⁵ Basel Convention, supra note 38, art. 1(3):

"Wastes which, as a result of being radioactive, are subject to other international control systems, including international instruments, applying specifically to radioactive materials, are excluded from the scope of this convention."

This language would appear to mean that the Basel Convention would apply to radioactive wastes if no international arrangements covering these wastes were in place. The report on the Basel Convention issued by U.S. Deputy Secretary of State Lawrence Eagleburger on May 13, 1991 contains the interesting comment that "[t]he Convention does not regulate movements of low-level radioactive wastes that are covered by other international control systems, such as the Code of Practice of the International Atomic Energy Agency (IAEA), to which the U.S. adheres" Reprinted in Marian Nash Leich, Contemporary Practice of the United States Relating to International Law, 85 Am. J. Int'l L. 674, 675 (1991) (emphasis added). See generally Barbara Kwiatkowska and Alfred Soons, Plutonium Shipments--A Supplement, 25 Ocean Dev. & Int'l L. 419 (1994) [hereafter cited as Kwiatkowska and Soons, Plutonium Shipments].

³⁶ Basel Convention, supra note 38, art. 6(1), (4). Article 4(2)(i) and (h) also require dissemination of information regarding proposed transboundary movement of hazardous wastes to "the States concerned." See generally Pineschi, supra note 36, at 300-01.

wastes on a vessel of a Party exercising its navigation rights under international law."⁷ The Japanese declaration appears to be directly in conflict with the convention itself. One commentator has said that "Article 6.4 of the [Basel] Convention does not allow the exporting State to authorize a transfrontier movement of hazardous waste without the previous written consent of every transit State party to the Convention."⁸ Article 4(12) does interject some ambiguity on this matter by reaffirming the "navigational rights and freedoms as provided for in international law,"⁹ but the specific requirements in Article 6(4) would normally be thought to prevail over the general language in Article 4(12) according to normal methods of interpretation.¹⁰ The Basel Convention also requires parties to take appropriate measures to reduce the movement of wastes "to the minimum consistent with the environmentally sound and efficient management of such wastes" and to conduct such transportation that is necessary "in a manner which will protect human health and the environment against the adverse effects which may result from such movement."¹¹

⁷ Final Act of the 1989 Convention, UNEP T/BSL/000, at 19, reprinted in Transboundary Movements and Disposal of Hazardous Wastes in International Law 32 (Barbara Kwiatkowska and Alfred H.A. Soons eds. 1993) [hereafter cited as Kwiatkowska and Soons, Transboundary Movements]. The Federal Republic of Germany issued a similar "understanding" stating that "nothing in this Convention shall be deemed to require the giving of notice to or the consent of any State for the passage of hazardous wastes on a vessel under the flag of a party exercising its right of innocent passage through the territorial sea or the freedom of navigation in an exclusive economic zone under international law." Multilateral Treaties Deposited with the Secretary General, Status as of 31 December 1989 (1990) at 857. The United Kingdom and Italy filed "declarations" using similar language. See Pineschi, supra note 36, at 303-04.

Other nations noted a contrary interpretation. Portugal stated that it "requires notification of any transboundary movement of hazardous wastes effected across the area under its national jurisdiction ..." Final Act, supra, at 31; Kwiatkowska and Soons, Transboundary Movements, at 37. And Mexico, Uruguay, and Venezuela indicated in their declarations that they approved the protection the convention provided to their coastal areas. Pineschi at 304; Kwiatkowska and Soons, Transboundary Movements, at 37-38.

⁸ Pineschi, supra note 36, at 301.

⁹ Basel Convention, supra note 38, art. 4(12).

¹⁰ The debate has focused on what it means to be a "transit state." Article 2(12) of the Basel Convention, supra note 38, defines "State of transit" as "any State, other than the State of export or import, through which a movement of hazardous wastes or other wastes is planned or takes place." The United States has taken the position that this term refers only to situations where transport goes over the land territory or internal waters of another country. See Leich, supra note 55, at 676. The territorial sea of a nation is, however, part of its sovereign territory under Article 2(1) of the Law of the Sea Convention, supra note 41. It would be logical, therefore, to view passage through the territorial sea as passage through a "transit state."

¹¹ Basel Convention, supra note 38, art. 4(2)(d).

Another important recent agreement on this topic is the "Code of Practice on the International Transboundary Movement of Radioactive Waste," adopted by resolution in 1990 by the General Conference of the International Atomic Energy Agency (IAEA).⁴² Again, some tension is found between the specific provisions and the general language. Principle 3 states that "It is the sovereign right of every State to prohibit the movement of radioactive waste into, from or through its territory." Principle 5 builds on this by saying that:

Every State should take the appropriate steps necessary to ensure that, subject to the relevant norms of international law, the international transboundary movement of radioactive waste takes place only with the prior notification and consent of the sending, receiving and transit States in accordance with their respective laws and regulations.⁴³

These explicit prohibitions are softened by earlier language that states that the Code is "advisory"⁴⁴ and a footnote that states that:

Nothing in this Code prejudices or affects in any way the exercise by ships and aircraft of all States of maritime and air navigation rights and freedoms under customary international law, as reflected in the 1982 United Nations Convention on the Law of the Sea, and under other relevant international legal instruments.⁴⁵

⁴² International Atomic Energy Agency, General Conference Resolution on Code of Practice on the International Transboundary Movement of Radioactive Waste, Sept. 21, 1990, 30 I.L.M. 556 (1991) [hereafter cited as IAEA Code of Practice]. This Code applies to "any material that contains or is contaminated with radionuclides at concentrations or radioactivity levels greater than the 'exempt quantities' established by the competent authorities and for which no use is foreseen." "Spent fuel which is not intended for disposal is not considered to be radioactive waste. Annex I, Section II, 30 I.L.M. at 562. Kwiatkowska and Soons, Plutonium Shipments, *supra* note 55, at 421, point out that because of this language the 1992 plutonium shipment and the shipment of spent nuclear fuel from Japan to Europe for reprocessing do not fall directly under the IAEA Code of Conduct. The Pacific Pintail's shipment of vitrified glass blocks of high level wastes back to Japan would be covered by this Code of Conduct because these wastes are "intended for disposal."

⁴³ Kwiatkowska and Soons, Plutonium Shipments, *supra* note 55, at 420, have summarized the rules governing shipments of radioactive wastes as follows:

The IAEA code of practice and the respective regional instruments affirm, with respect to [transboundary movements of radioactive wastes], the general principles of the Basel Convention, including the critical regime of prior notification and prior informed consent (PIC) that extend the scope of duties of notification, environmental impact assessment, and consultation with respect to transboundary interference (or its risk) as the duties have evolved under existing customary law.

⁴⁴ IAEA Code of Practice, *supra* note 62, Annex I, Section I, 30 I.L.M. at 562.

⁴⁵ *Id.*, 30 I.L.M. at 562 n.2.

These provisions obviously can create some confusion in interpretation and application. Does the freedom of navigation have a superior status as compared to the duty to protect the environment, or vice versa? Because both the Basel Convention and the Radioactive Waste Code of Practice refer to the Law of the Sea Convention, it is important to examine its Article 19 on the "Meaning of innocent practice" and note that it includes in its list of noninnocent activities subparagraph (h) "any act of wilful and serious pollution contrary to this Convention." As evidenced by their reactions discussed in the next section, it is obvious that many coastal nations view the consequences of an accident involving a shipment of radioactive materials to be so catastrophic that such shipments constitute wilful acts of serious pollution even though the likelihood of an accident that would actually cause such pollution may be small.⁶⁶ Because of the risks created by such shipments, and because of the need to prepare contingency plans to deal with accidents and emergencies, a coastal nation would appear to be justified to require notification prior to such shipments passing through their territorial seas and exclusive economic zones or following a route that might result in the ship entering these waters to make an emergency port call.⁶⁷

Another useful source to examine in trying to resolve the apparent ambiguities in the Basel Convention and IMO Code of Practice is the 1991 Bamako Convention on the Ban of the Import into Africa and the Control of Transboundary Movement and Management of Hazardous Wastes within Africa.⁶⁸ This treaty explicitly applies to radioactive wastes (Article 2(2)), it calls upon parties "to adopt and implement the preventive, precautionary approach to pollution problems" (Article 4(3)(f)), and it requires exporting states to "receive the written consent of the State of transit" before commencing a shipment (Article 6(4)). The Bamako treaty specifically recognizes "the sovereignty of States over their territorial sea" and their jurisdiction over their exclusive economic zones and continental shelves (Article 4(4)(c)), thus implying that permission must be obtained at least for passage through the territorial sea.⁶⁹

⁶⁶ Pineschi, supra note 36, at 308 suggests that passage by ships carrying radioactive materials would not be innocent if such passage did not comply with the "special precautionary measures established for such ships by international agreements," as required by Article 23 of the Law of the Sea Convention, supra note 41.

⁶⁷ Pineschi, supra note 36, at 309 supports this conclusion, with respect to foreign territorial seas. She finds it harder to support this conclusion for foreign exclusive economic zones because the Law of the Sea Convention, supra note 41, does not have provisions comparable to Articles 22(2) and 23 that apply to the exclusive economic zones.

⁶⁸ Bamako Convention on the Ban of the Import into Africa and the Control of Transboundary Movement and Management of Hazardous Wastes Within Africa, Jan. 29, 1991, reprinted in 30 I.L.M. 773 (1991), and Kwiatkowska and Soons, Transboundary Movement, supra note 57, at 912.

⁶⁹ Article 4(4)(c) also, however, recognizes "navigational rights and freedoms as provided for international law," thus retaining some uncertainty in meaning.

In any event, the recent state practice⁷⁰ of coastal nations has been to protest against these shipments of ultrahazardous cargoes and to do everything possible to keep them away from their coasts, in order to protect their environmental interests and coastal populations and resources.

State Practice Requires Notification and Consultation Regarding Shipments of Ultrahazardous Cargoes. Even before the recent Japanese shipments, a number of countries had imposed restrictions on the movement of ultrahazardous cargoes through their waters. Pineschi⁷¹ identifies legislation from Egypt⁷² and Oman⁷³ that requires prior permission before such shipments can pass through their waters. She also quotes legislation from Haiti that prohibits from its territorial sea and exclusive economic zone "any vessel transporting wastes, refuse, residues or any other materials likely to endanger the health of the country's population and to pollute the marine, air and land environment,"⁷⁴ and states that Venezuela, the Ivory Coast, and Canada also have legislation that restricts free movement of hazardous wastes through their waters.⁷⁵ In 1992, the Philippines restricted entry "of substances and mixtures that present unreasonable risks or injury to health or to the environment and to prohibit the entry, even in transit, of hazardous nuclear wastes into Philippine territory."⁷⁶ At meetings of the International Maritime Organization's Marine Environment Protection Committee, Argentina, Brazil, and Chile have "reiterated their concern with the transport of nuclear substances through their territorial seas and 200-mile exclusive economic zones (EEZs)."⁷⁷ Similarly, the South Pacific Forum (consisting of all the independent island nations of the Pacific) issued a communiqué at its July 1992 meeting reaffirming "the importance of Japan consulting fully with Forum nations regarding its future shipments."⁷⁸ Although other countries--notably the United States, the

⁷⁰ Subsequent state practice should be examined to interpret treaty provisions, according to article 31 of the Vienna Convention on the Law of Treaties, May 23, 1969, 8 I.L.M. 679 (1969).

⁷¹ Pineschi, supra note 36, at 311-13.

⁷² Law of the Sea Bulletin, Special Issue (1987), at 3.

⁷³ Law of the Sea Bulletin, No. 14 (Dec. 1989), at 8.

⁷⁴ Law of the Sea Bulletin, No. 11 (July 1988), at 13.

⁷⁵ Pineschi, supra note 36, at 312-13.

⁷⁶ From Statement of H.E. President Fidel V. Ramos on the Reported Plan to Transport Plutonium Between France and Japan (citing Philippine Republic Act No. 6969 of 1990, otherwise known as the Toxic Substances and Hazardous and Nuclear Wastes Act).

⁷⁷ Kwiatkowska and Soons, Plutonium Shipments, supra note 55, at 423.

⁷⁸ Id. (citing UN Doc. A/48/359 (1993) at 12 and UN Doc. A/47/391 (1992) at 9, reprinted in 8 Int'l Organizations and the Law of the Sea: Documentary Handbook 74 (1994)).

Soviet Union, and Italy--have protested against such restrictions,⁷⁹ these constraints do mark a trend, and are consistent with the Basel Convention and the IAEA Code of Practice, which emphasize transparency and require that the transfer of hazardous wastes should not remain a secret.

Coastal nations have vigorously protested the Japanese transport of radioactive materials, and the Japanese have responded by modifying the routing of their ships. The efforts by the coastal nations to protect their populations and resources from a nuclear accident, and Japan's willingness to acquiesce to these protective claims, contributes to the development of customary international law. These claims and responses appear to establish a recognition that the normal rights of unimpeded navigational transit do not apply in cases of ultrahazardous cargoes.

When the 1992 plutonium shipment was in transit, South Africa⁸⁰ and Portugal⁸¹ explicitly requested Japan to stay out of their exclusive economic zones,⁸² and in response to an inquiry from Australia, Japan stated that "in principle" its plutonium vessel would stay outside the 200-nautical mile zone of all nations.⁸³ A few days later, Japan modified this statement to say that "the ship could enter the 200-nautical-mile zone of some country under unavoidable circumstances or under conditions where avoiding to enter the zone is considered impractical."⁸⁴ The plutonium ship did try to avoid exclusive economic zones by traveling far from the South African coast and staying south of the exclusive economic zones of Australia and New Zealand.⁸⁵ Finally, however, it did head north through the Pacific, and apparently traveled through the exclusive economic zones of some of the Pacific island nations.⁸⁶

⁷⁹ Pineschi, supra note 36, at 313.

⁸⁰ Ruth Youngblood, Japanese Secrecy over Plutonium Shipment Sparks Outcry, United Press International, Sept. 27, 1992.

⁸¹ Lisbon Asks Tokyo to Keep Akatsuki Maru Away, Kyodo News Agency, Nov. 10, 1992.

⁸² Similarly, just before the plutonium ship set sail, the heads of governments of the Caribbean Island nations adopted a Declaration on Shipments of Plutonium saying that "no such shipments should traverse the Caribbean and that the Caribbean should be declared a nuclear-free zone for purposes of shipment, storing, or dumping of not only toxic wastes but also any radioactive or hazardous substances." Kwiatkowska and Soons, Plutonium Shipments, supra note 55, at 424-25 (citing CARICOM Press Release No. 89/1992).

⁸³ Statement of Toichi Sakata, Director of the Japanese Science and Technology Agency's Nuclear Fuel Division, to participants in the Asia-Pacific Forum on Sea Shipments of Japanese Plutonium, Tokyo, Oct. 6, 1992.

⁸⁴ Id.

⁸⁵ Plutonium Ship to Pass West of Hawaii, Honolulu Star-Bulletin, Dec. 7, 1992, at 1, col. 1.

⁸⁶ Id.

Similar and more dramatic protests were issued prior to and during the 1995 shipment of glassified nuclear wastes, and again the Japanese acquiesced to the protests. A number of the nations along the route--Brazil, Argentina,⁸⁷ Chile, South Africa,⁸⁸ Nauru,⁸⁹ and Kiribati⁹⁰--expressly banned the Pacific Pintail from their 200-nautical-mile exclusive economic zones. On March 8, 1995, the Brazilian air force closely monitored the vessel and demanded all navigational details to ensure that the ship did not enter Brazil's exclusive economic zone.⁹¹ The bad weather encountered as the vessel approached Cape Horn apparently forced it to enter Argentina's exclusive economic zone, despite Argentina's strong protest.⁹² After Chile demanded that the ship leave Chile's EEZ and sent its ships and aircraft to enforce the ban, the

⁸⁷ Vice Foreign Minister Fernando Petrella stated to Greenpeace representatives on March 1, 1995, that Argentina had formally notified Japan that the Pacific Pintail would not be allowed entry into Argentina's 200-nautical-mile exclusive economic zone. On March 15, 1995, Argentina's Chamber of Deputies passed a declaration charging the government with ensuring that the Japanese cargo be prohibited from crossing Argentina's exclusive economic zone and the waters above its continental shelf, even where it extends beyond 200 nautical miles.

⁸⁸ Statement of South African Department of Environmental Affairs and Tourism, March 10, 1995 (statement prepared after an interagency meeting involving five ministries).

⁸⁹ Republic of Nauru Dept. of External Affairs, Note No. 9/1995, Jan. 17, 1995.

⁹⁰ Reuters, March 22, 1995.

⁹¹ Report from Greenpeace tracking vessel, Captain Ulf Birgander and Campaigner Bas Bruyne, March 9, 1995. The Brazilian Foreign Ministry issued a statement on February 24, 1995, saying that it would not allow the Pacific Pintail within Brazilian waters "under any circumstances." Agence France Presse, Ship with Nuclear Waste Headed to Japan Enters Brazilian Waters: Greenpeace, March 6, 1995. In a March 10, 1995 letter sent to Paul Leventhal at the Nuclear Control Institute, in Washington, D.C., the Brazilian Ambassador to the United States (Pauolo-Tarso Flecha de Lima) quoted a statement sent from Brazil to Japan as follows:

In reaffirming that no maritime coast or other areas under the Brazilian jurisdiction can be exposed to the risk of possible accidents with a cargo vessel of this nature, the Brazilian Government considers that the entrance of that cargo vessel into the above-mentioned regions of Brazilian jurisdiction is undesirable, under any circumstances.

The Pacific Pintail did pass within 45 miles of St. Peter and St. Paul Rocks, which are Brazilian possessions 450 miles off the Brazilian coasts. Reuters, Atomic Ship Breaks Ban, Enters Brazil Waters--Greenpeace, March 6, 1995. Although Brazil has declared an exclusive economic zone around these features, it is unclear whether such a claim is justified under Article 121 of the Law of the Sea Convention, supra note 41.

⁹² Deutsche Presse-Agentur, Chile to Protest Against British Nuclear Freighter, March 20, 1995.

ship did modify its route and left the area.⁹³ A resolution issued by the Chilean Maritime Authority⁹⁴ cited the precautionary principle and declared that the duty to protect the marine environment took precedence over the right to free navigation. The resolution also noted the severe weather conditions that exist at Cape Horn and stated that the means to address the unforeseeable consequences of a radioactive catastrophe did not exist. When the vessel was rounding Cape Horn it faced 30-foot waves and 60-mile-an-hour winds.⁹⁵

A number of Caribbean countries also issued statements insisting that the radioactive materials not be transported at all through the Caribbean Sea.⁹⁶ Another significant group of countries have prohibited the Pacific Pintail from passing through its territorial sea and archipelagic waters. These countries include Antigua and Barbuda,⁹⁷ Colombia,⁹⁸ the

⁹³ Transcript of a radio conversation between Pacific Pintail and Chilean Navy, March 20, 1995.

A few days earlier, Chile's Acting Foreign Minister Mariano Fernandez said: "We've got enough legal arguments to protect human health, ecology and the environment in the area to demand that this boat not pass through Chilean territorial waters." See generally Chile Threatens Force Against Nuke Freighter, Honolulu Star-Bulletin, March 21, 1995, at A-8, col. 1.

⁹⁴ Resolution 12600/67, issued March 16, 1995, by the Chilean Maritime Authority, General Directory for the Maritime Territory and Merchant Marine, DIRECTEMAR.

⁹⁵ Reuters, Nuclear Ship Braves Stormy Seas, Defies Chile Ban, March 20, 1995. Chilean Navy Commander-in-Chief Admiral Jorge Martinez Busch said: "These waters are not to be navigated. I know of big-tonnage ships that have been damaged by the extraordinarily rough sea in the area. Wind conditions are extraordinarily negative." Id. Chilean Foreign Minister Miguel Insulza said, "That is the worst route" for a ship with such a dangerous cargo, and that the Chilean government would issue a "very stern protest" to prevent any repetition of this shipment. Deutsche Presse-Agentur, Chile to Protest Against British Nuclear Freighter, March 20, 1995.

⁹⁶ News release issued by Owen S. Arthur, Chair of CARICOM and Prime Minister of Barbados, Dec. 23, 1994; statement issued by Brian Alleyne, Minister for External Affairs, Commonwealth of Dominica, Jan. 19, 1995; statements issued by the Conseil General of Martinique and the Conseil Municipal of Fort de France (capital of Martinique), Jan. 24, 1995; statement of Dr. Carlos A. Medina, Secretary for the Environment, Government of Honduras, Feb. 6, 1995; press release issued by Jamaica Ministry of Environment and Housing, Feb. 13, 1995; letter from G.F. Croes, Minister-President of Aruba, to the Dutch Minister of Foreign Affairs, Mr. H. Van Mierlo, Jan. 27, 1995.

⁹⁷ Press release issued by the Ministry of Foreign Affairs, Government of Antigua and Barbuda, Dec. 22, 1994.

⁹⁸ Statement issued by Colombian Ministry of Foreign Affairs, March 2, 1995 (stating that the "introduction into the national territory of nuclear waste and toxic wastes" is prohibited under the terms of the national constitution).

Dominican Republic,⁹⁹ the Federated States of Micronesia,¹⁰⁰ Fiji,¹⁰¹ Indonesia,¹⁰² the Philippines,¹⁰³ Puerto Rico,¹⁰⁴ and Uruguay.¹⁰⁵ The protests of the Caribbean nations apparently forced the vessel to abandon its preferred route, which was to go through the Panama Canal.¹⁰⁶ The route ultimately traveled by the Pacific Pintail apparently avoided all exclusive economic zones of coastal countries--except those of Argentina and Chile, which it was forced to leave, and that of French Polynesia in the Pacific which is governed by France.¹⁰⁷

Because of the number and range of these protests--and in particular because the vessels carrying Japanese radioactive materials responded by changing course both in their 1992 and 1995 shipments--it must be recognized that the shipments of ultrahazardous cargoes cannot proceed under the normal regime of navigational freedoms and are instead governed by a much more restrictive regime. Notice and consultation must precede such shipments, environmental assessments must be conducted and disseminated, and the routes to be used must be accepted by all affected parties as the least dangerous of all the possible routes.

Summary and Conclusions. The precautionary principle has been explicitly included in numerous recent treaties, has been invoked repeatedly as an authoritative norm, and is now seen

⁹⁹ Statement of Dominican Republic Vice President, Jacinto Paynando, head of government's Environmental Commission, Jan. 20, 1995; statement of Dominican Republic President Joaquin Balaguer, Feb. 10, 1995.

¹⁰⁰ Kyodo News International, Fiji Opposes Shipment of Radioactive Waste to Japan, Feb. 22, 1995.

¹⁰¹ Id.

¹⁰² Irawan Abidan of the Indonesian Foreign Ministry informed the press on Feb. 28, 1995, that the Japanese Embassy had guaranteed that the Pacific Pintail would not enter Indonesian or surrounding waters.

¹⁰³ Statement of H.E. President Fidel V. Ramos on the Reported Plan to Transport Plutonium Between France and Japan, Dec. 21, 1994. This statement noted that the Philippines had previously "refused to allow the Akatsuki Maru from entering and passing through Philippine territory based on information that the ship was carrying highly radioactive processed plutonium from France to Japan. We see no reason to change this policy."

¹⁰⁴ Statement issued by Puerto Rico's Secretary of Natural and Environmental Resources, Dec. 28, 1994.

¹⁰⁵ Statement issued by Uruguay's Vice-Minister of Foreign Affairs, Carlos Perez del Castillo, March 13, 1995.

¹⁰⁶ Reuters, Atomic Ship Breaks Ban, Enters Brazil Waters--Greenpeace, March 6, 1995; Deutsche Presse-Agentur, Plutonium Ship Will Not Go Through Panama Canal, March 6, 1995.

¹⁰⁷ Agence France Presse, Nuclear Waste Ship Near French Polynesia, April 3, 1995.

as a central guiding principle of environmental decisionmaking. It requires states and others whose actions may cause significant disruption to the marine environment to take a series of steps. As applied to the Japanese transport of radioactive materials, these steps include:

1. A thorough environmental impact assessment must be prepared. This task requires opportunities for input from the affected coastal states and the public, and should involve an interdisciplinary analysis of the situation. The assessment should be disseminated to all concerned parties.

2. The shipping nation must notify and consult with all concerned coastal countries. This process requires revealing the route a ship carrying an ultrahazardous cargo is going to follow to all affected countries and working with them to develop contingency plans for emergencies.

3. The shipping nation must develop a research program to discover as much information as possible regarding the consequences of an accident involving the proposed shipments, and must disseminate the results of such research.

4. The shipping nation must act systematically to mitigate damages. This duty requires the nation to explore all alternative nonpolluting technologies. Alternatives to nuclear power--and the use of plutonium in commercial reactors--must be examined in more detail. Alternatives to reprocessing spent nuclear fuel must be examined further. Better encasements for transporting the radioactive materials must be developed and used.

5. If shipments of ultrahazardous radioactive cargoes do continue, routings that minimize the threats to populated areas and fragile ecosystems must be chosen. The navigational freedoms that normally govern commercial shipping do not apply to ultrahazardous cargoes. This result has become clear in the language of the 1989 Basel Convention¹⁰⁸ and the 1990 IAEA Code of Practice on the Transboundary Movement of Radioactive Waste.¹⁰⁹ Affected coastal nations must be notified and consultations must be conducted to determine the least dangerous routing. The territorial seas and exclusive economic zones of coastal nations must be avoided unless no acceptable alternative routes are possible.

¹⁰⁸ Basel Convention, supra note 38.

¹⁰⁹ IAEA Code of Practice, supra note 62.

ENVIRONMENTAL IMPACT ASSESSMENT OF RADIOACTIVE MATERIALS DURING SEA TRANSPORTATION: ---CASE STUDY OF PLUTONIUM RELEASED IN THE OCEAN ---

Jean Christophe Niel

Institut de Protection et de Sûreté Nucléaire

1 - OBJECTIVES OF THE ENVIRONMENTAL IMPACT ASSESSMENT.

The safety of transports between France and Japan of radioactive materials is based on the packages, according to IAEA rules, and on the application of the INF code concerning the ships which carry these materials. Nevertheless, the environmental assessment of the release of such radioactive materials into the sea, during the years following the release, is valuable. The Science and Technology Agency (STA, Japan) and the Institut de Protection et de Sûreté Nucléaire (IPSN, France) are jointly involved in these assessments. Currently, STA is studying the case of vitrified waste release and IPSN the case of plutonium release.

The summary of the study [1] coordinated by IPSN is the object of the present paper

Indeed, to perform this assessment, the marine environment has to be modelled on a large scale and the exposure path to be calculated. Hypothesis has been made on the release phenomena as well

2 - MODELLING OF THE MARINE ENVIRONMENT.

The modelling of the marine environment has to cover a very large region from the Arctic sea to the Mediterranean and the Atlantic Ocean. It has to take into account the water streams and the sedimentation processes.

The model is based on a division of the European seas in 44 compartments (annex 1)

In each compartment, global parameters such as volume, depth, suspended sediment load and sediment rate, are defined (annex 3). Such parameters are supposed to be homogeneous inside the compartment. Moreover, above modelling approach imposes the radioactivity to be homogeneously distributed within each

compartment. Dispersion is evaluated using water exchange rate between compartments (annex 1).

These data were adapted from the Marina project about the radiological exposure of the population of the European Countries from radioactivity in North European marine waters performed by the European Commission[2].

3 - ORIGIN OF CONTAMINATION.

Two locations for the instantaneous release of 1 kg of plutonium were chosen, one in the North East part of the Atlantic Ocean and the other in the west part of the Channel

The composition of the plutonium is that issued from the reprocessing of PWR spent fuel irradiated at 33000 Mw/t and stored for 3 years, that is (annex 2) mainly.

Plutonium 239 (60 %)

Plutonium 240 (20%)

Plutonium 241 (10%)

4 - HYPOTHESES FOR THE CALCULATION.

Various hypotheses were made to perform the calculations. Indeed, it is supposed that :

- the physical parameters inside a compartment are uniform (suspended sediment load between 0.1 and 10g/m³, sediment rate between 10g and 5kg/m²/year, volume, volume exchange rate, depth)

- the above physical parameters are constant in time.

- the radionuclides are uniformly distributed in the volume of a compartment.

- the radioactive decay of radionuclides is taken in account.

5- THE EXPOSURE PATHWAY.

The exposure paths are calculated from the consumption of sea products (fish, shellfish, molluscs and seaweeds) using European fishing statistics. As a consequence, knowledge of the following data is needed (examples are given in annex 3).

- quantity of sea products in each compartment every year,

- concentration factor for each radionuclide expressing the relation between the radioactivity of the sea water and that of the sea products,

- edible fraction of the sea products.

All the sea products are supposed to be eaten within the European countries. The equivalent dose is then calculated from the activity ingested for each radionuclide using conversion factor from the ICRP 61.

6 - RESULT

The results are the following

| | Cumulated collective dose for European countries after 50 years | Average cumulated individual dose in European countries after 50 years |
|---|---|---|
| Western part of the Channel | 160 man Sv | 0.45 μ Sv |
| North Eastern part of the Atlantic Ocean | 4.47 man Sv | 0.013 μ Sv |

7 - FURTHER DEVELOPMENTS

IPSN, in collaboration with IFREMER, is elaborating a refined modelling of sea water currents to evaluate short time effects more precisely.

Moreover, the study mentioned above analyses the effects of the release collectively but not on individuals. IPSN is presently defining so called "reference groups" whose habits can vary according to their cultural, social, or economic environment. It will then be possible to detail this evaluation of the impact on individuals.

References:

[1] Raffestin D.: *Evaluation des conséquences radiologiques associées à un rejet de poudre d'oxyde de plutonium: application du code Poseidon*, CEPN, NTE 95/16

Raffestin D., Lopicard S.: *Poseidon: Un modèle de dispersion de matières radioactives en milieu maritime*, CEPN, Report 236, February 1995

Raffestin D., Lopicard S.: *Poseidon: a dispersion computer code for assessing radiological impacts in marine environment*, paper presented at the PATRAM'95 meeting, Las Vegas, 3-8 december 1995

[2] European Commission: *The radiation exposure of the population of the European community from radioactivity in North European Marine Waters Project 'Marina'*, RP 47, EUR 12483, 1990

Annex I

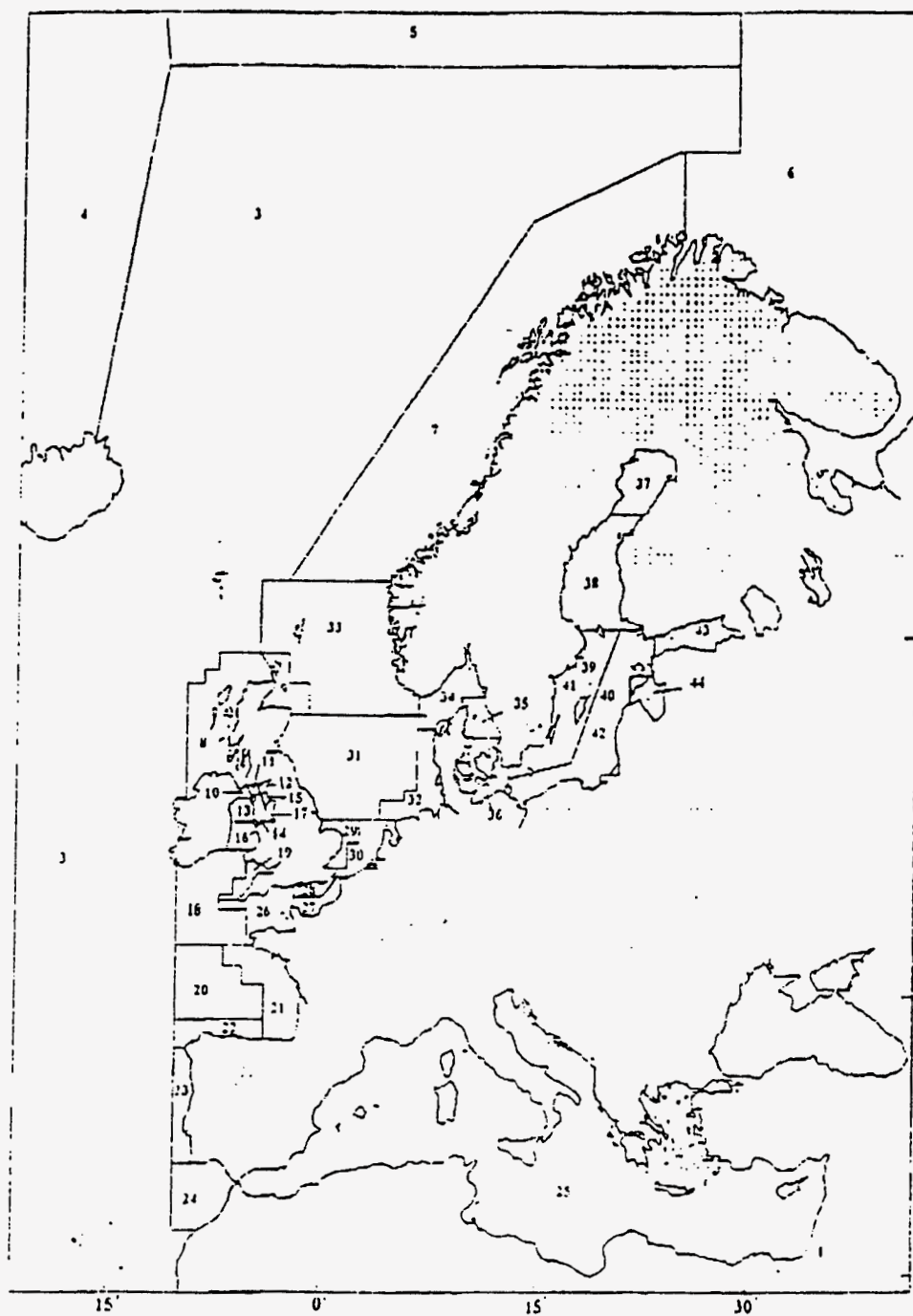


Figure 1. Carte des compartiments du modèle

Annex 1

Dénomination des compartiments régionaux

| n° | Nom des compartiments Régionaux |
|----|---------------------------------|
| 1 | Other Oceans |
| 2 | Atlantic Ocean |
| 3 | Atlantic North East |
| 4 | Arctic Ocean |
| 5 | Spitzbergen |
| 6 | Barents Sea |
| 7 | Norwegian Waters |
| 8 | Scottish Waters West |
| 9 | Scottish Waters East |
| 10 | Irish Sea North West |
| 11 | Irish Sea North |
| 12 | Irish Sea North East |
| 13 | Irish Sea West |
| 14 | Irish Sea South East |
| 15 | Cumbrian Waters |
| 16 | Irish Sea South |
| 17 | Liverpool & Morecambe Bays |
| 18 | Celtic Sea |
| 19 | Bristol Channel |
| 20 | Bay of Biscay |
| 21 | French Continental Shelf |
| 22 | Cantabrian Sea |
| 23 | Portuguese Continental Shelf |
| 24 | Gulf of Cadiz |
| 25 | Mediterranean Sea |
| 26 | English Channel West |
| 27 | English Channel South East |
| 28 | English Channel North East |
| 29 | North Sea South West |
| 30 | North Sea South East |
| 31 | North Sea Central |
| 32 | North Sea East |
| 33 | North Sea North |
| 34 | Skagerrak |
| 35 | Kattegat |
| 36 | Belt Sea |
| 37 | Bothnian Bay |
| 38 | Bothnian Sea |
| 39 | Baltic Sea West (Surface) |
| 40 | Baltic Sea East (Surface) |
| 41 | Baltic Sea West (Deep Waters) |
| 42 | Baltic Sea East (Deep Waters) |
| 43 | Gulf of Finland |
| 44 | Gulf of Riga |

Annex 2

Caractéristiques de la poudre de PuO₂

| Element | Période (années) | Fc ingestion ¹ (Sv/Bq) | Poids relatif (%) | Activité (Bq/kg de PuO ₂) | Filiation |
|---------|---------------------|--------------------------------------|----------------------|--|-----------|
| Pu-238 | 3.74E+01 | 5.1E-07 | 1.60 | 1.01E+10 | U-234 |
| Pu-239 | 2.41E+04 | 5.6E-07 | 53.49 | 1.23E+12 | U-235 |
| Pu-240 | 6.56E+03 | 5.6E-07 | 21.14 | 1.78E+12 | U-236 |
| Pu-241 | 1.44E+01 | 1.1E-08 | 8.96 | 3.41E+14 | Am-241 |
| Pu-242 | 3.73E+05 | 5.3E-07 | 0.33 | 4.78E+08 | U-238 |
| Am-241 | 4.32E+02 | 5.7E-07 | 2.69 | 3.41E+12 | Np-237 |

Annex 3

Caractéristiques des compartiments du modèle

| n° | Volume m3 | Qté poissons /an | Qté crustacés /an | Qté mollusques /an | Qté algues /an | Sédimen- tation t/m2.an | Profon- deur m | Mat. en Suspens. t/m3 | Nom des compartiments Régionaux |
|----|--------------|------------------------|-------------------------|--------------------------|----------------------|-------------------------------|----------------------|-----------------------------|------------------------------------|
| 1 | 1.00E18 | 0 | 0 | 0 | 0 | 5.20E-5 | 4000 | 1.00E-7 | Other Oceans |
| 2 | 3.00E17 | 0 | 0 | 0 | 0 | 1.00E-4 | 3500 | 1.00E-7 | Atlantic Ocean |
| 3 | 5.00E16 | 3.50E3 | 1.10E4 | 4.20E3 | 0 | 1.00E-5 | 3500 | 1.00E-7 | Atlantic North East |
| 4 | 1.70E16 | 0 | 0 | 0 | 0 | 1.00E-5 | 1200 | 1.00E-7 | Arctic Ocean |
| 5 | 1.00E14 | 1.50E4 | 7.60E3 | 0 | 0 | 1.00E-5 | 1200 | 1.00E-7 | Spitzbergen |
| 6 | 3.00E14 | 2.20E4 | 3.00E3 | 7.00E1 | 0 | 1.00E-5 | 200 | 1.00E-7 | Barents Sea |
| 7 | 1.00E15 | 1.20E5 | 6.70E2 | 6.20E2 | 0 | 1.00E-5 | 1200 | 1.00E-7 | Norwegian Waters |
| 8 | 1.00E13 | 3.10E5 | 6.90E3 | 4.80E3 | 1.40E4 | 1.00E-4 | 110 | 1.00E-6 | Scotish Waters West |
| 9 | 3.00E12 | 9.40E4 | 1.90E3 | 1.30E3 | 4.30E3 | 1.00E-4 | 110 | 1.00E-6 | Scotish Waters East |
| 10 | 4.08E11 | 6.80E3 | 1.10E3 | 1.70E3 | 0 | 3.00E-3 | 93 | 3.00E-6 | Irish Sea North West |
| 11 | 6.10E10 | 1.00E3 | 3.70E2 | 5.80E2 | 0 | 5.10E-3 | 34 | 3.00E-6 | Irish Sea North |
| 12 | 5.20E10 | 8.70E2 | 8.40E2 | 1.30E3 | 0 | 3.60E-3 | 24 | 3.00E-6 | Irish Sea North East |
| 13 | 6.62E11 | 1.10E4 | 1.60E2 | 2.30E3 | 0 | 2.00E-3 | 63 | 3.00E-6 | Irish Sea West |
| 14 | 1.62E11 | 2.70E3 | 4.50E2 | 6.90E2 | 0 | 4.70E-3 | 31 | 3.00E-6 | Irish Sea South East |
| 15 | 3.80E10 | 6.30E2 | 2.80E2 | 4.40E2 | 0 | 4.20E-3 | 28 | 3.00E-6 | Cumbrian Waters |
| 16 | 1.10E12 | 1.80E4 | 2.60E3 | 3.80E3 | 0 | 1.00E-4 | 57 | 1.00E-6 | Irish Sea South |
| 17 | 3.20E10 | 5.30E2 | 7.80E2 | 1.20E3 | 0 | 2.00E-3 | 13 | 3.00E-6 | Liverpool & Morecambe Bays |
| 18 | 2.00E13 | 9.40E4 | 5.40E3 | 4.20E3 | 0 | 1.00E-4 | 150 | 1.00E-6 | Celvic Sea |
| 19 | 1.00E12 | 2.60E4 | 5.40E2 | 3.40E3 | 0 | 1.00E-4 | 50 | 1.00E-6 | Bristol Channel |
| 20 | 6.50E14 | 0 | 0 | 0 | 0 | 1.00E-5 | 3990 | 1.00E-7 | Bay of Biscay |
| 21 | 3.50E13 | 5.20E4 | 1.70E4 | 1.20E5 | 3.60E1 | 1.00E-4 | 350 | 5.00E-7 | French Continental Shelf |
| 22 | 3.00E13 | 3.90E5 | 5.40E3 | 2.60E4 | 1.40E3 | 2.00E-4 | 760 | 1.00E-6 | Cantabrian Sea |
| 23 | 1.50E13 | 2.20E5 | 5.10E3 | 1.70E4 | 7.40E1 | 2.00E-4 | 490 | 1.00E-6 | Portuguese Continental Shelf |
| 24 | 2.30E14 | 6.40E4 | 5.20E3 | 1.20E4 | 0 | 5.00E-5 | 1870 | 2.00E-7 | Gulf of Cadiz |
| 25 | 3.57E15 | 4.80E5 | 4.40E4 | 2.50E5 | 0 | 7.50E-5 | 1400 | 1.00E-6 | Mediterranean Sea |
| 26 | 3.20E12 | 9.70E4 | 1.10E4 | 4.20E4 | 0 | 1.00E-4 | 60 | 1.00E-6 | English Channel West |
| 27 | 6.50E11 | 3.20E4 | 1.60E3 | 3.80E4 | 2.40E4 | 1.00E-4 | 40 | 1.00E-6 | English Channel South East |
| 28 | 6.50E11 | 3.20E4 | 3.80E2 | 1.50E3 | 0 | 1.00E-4 | 40 | 1.00E-6 | English Channel North East |
| 29 | 4.50E11 | 2.80E4 | 8.00E2 | 1.50E4 | 0 | 1.00E-4 | 31 | 6.00E-6 | North Sea South West |
| 30 | 9.50E11 | 5.90E4 | 5.90E3 | 7.90E4 | 0 | 1.90E-4 | 37 | 6.00E-6 | North Sea South East |
| 31 | 1.28E13 | 2.70E5 | 5.90E3 | 1.30E3 | 0 | 1.00E-4 | 50 | 6.00E-6 | North Sea Central |
| 32 | 1.20E12 | 2.50E4 | 2.40E4 | 4.40E4 | 0 | 4.40E-5 | 22 | 6.00E-6 | North Sea East |
| 33 | 5.60E13 | 3.60E5 | 4.50E1 | 1.50E3 | 0 | 1.00E-4 | 240 | 6.00E-6 | North Sea North |
| 34 | 6.78E12 | 1.20E5 | 1.80E3 | 6.70E2 | 0 | 5.00E-3 | 210 | 1.00E-6 | Skagerrak |
| 35 | 5.15E11 | 8.80E3 | 2.30E3 | 1.40E3 | 0 | 5.00E-4 | 23 | 1.00E-6 | Kattegat |
| 36 | 2.85E11 | 4.60E4 | 6.80E1 | 4.90E3 | 0 | 5.00E-4 | 14 | 1.00E-6 | Belt Sea |
| 37 | 1.48E12 | 1.80E4 | 5.80E-2 | 0 | 0 | 5.00E-4 | 41 | 1.00E-6 | Bothnian Bay |
| 38 | 4.89E12 | 6.00E4 | 1.10E-1 | 0 | 0 | 5.00E-4 | 62 | 1.00E-6 | Bothnian Sea |
| 39 | 3.79E12 | 4.60E4 | 3.60E0 | 0 | 0 | 5.00E-4 | 49 | 1.00E-6 | Baltic Sea West (Surface) |
| 40 | 6.97E12 | 8.50E4 | 0 | 0 | 0 | 5.00E-4 | 515 | 1.00E6 | Baltic Sea East (Surface) |
| 41 | 7.70E11 | 0 | 0 | 0 | 0 | 5.00E-4 | 108 | 1.00E-6 | Baltic Sea West (Deep Waters) |
| 42 | 1.53E12 | 0 | 0 | 0 | 0 | 5.00E-4 | 114 | 1.00E-6 | Baltic Sea East (Deep Waters) |
| 43 | 1.10E12 | 1.30E4 | 0 | 0 | 0 | 5.00E-4 | 57 | 1.00E-6 | Gulf of Finland |
| 44 | 4.05E11 | 5.00E3 | 0 | 0 | 0 | 5.00E-4 | 25 | 1.00E-6 | Gulf of Riga |

Annex 3

| Élément | Facteurs de concentration (Kd) (Bq/l)/(Bq/m3) | | | | Période (an) | Kd (Bq/l)/(Bq/m3) | | Fils 1 | % | Fils 2 | Fc (Sv/Bq) |
|---------|--|-----------|-----------|--------|-----------------|----------------------|--------|--------|------|--------|---------------|
| | Poisson | Crustacés | Mollusque | Algue | | régional | local | | | | |
| Th-231 | 6.00E2 | 1.00E3 | 1.00E3 | 2.00E2 | 2.91E-3 | 5.00E6 | 2.00E6 | Pa-231 | 1 | • | 4.90E-10 |
| Th-232 | 6.00E2 | 1.00E3 | 1.00E3 | 2.00E2 | 1.41E10 | 5.00E6 | 2.00E6 | Ra-228 | 1 | • | 1.80E-6 |
| Th-234 | 6.00E2 | 1.00E3 | 1.00E3 | 2.00E2 | 6.60E-2 | 5.00E6 | 2.00E6 | U-234 | 1 | • | 5.70E-9 |
| Pa-231 | 5.00E1 | 1.00E1 | 5.00E2 | 1.00E2 | 3.28E4 | 1.00E6 | 1.00E6 | Ac-227 | 1 | • | 1.40E-6 |
| Pa-233 | 5.00E1 | 1.00E1 | 5.00E2 | 1.00E2 | 7.39E-2 | 1.00E6 | 1.00E6 | U-233 | 1 | • | 1.40E-9 |
| Np-237 | 1.00E1 | 1.00E2 | 4.00E2 | 5.00E1 | 2.14E6 | 5.00E3 | 5.00E3 | Pa-233 | 1 | • | 6.40E-7 |
| Np-239 | 1.00E1 | 1.00E2 | 4.00E2 | 5.00E1 | 6.43E-3 | 5.00E3 | 5.00E3 | Pu-239 | 1 | • | 1.20E-9 |
| U-232 | 1.00 | 1.00E1 | 3.00E1 | 1.00E2 | 7.20E1 | 5.00E2 | 1.00E3 | Th-228 | 1 | • | 1.70E-7 |
| U-233 | 1.00 | 1.00E1 | 3.00E1 | 1.00E2 | 1.59E5 | 5.00E2 | 1.00E3 | Th-229 | 1 | • | 4.00E-8 |
| U-234 | 1.00 | 1.00E1 | 3.00E1 | 1.00E2 | 2.45E5 | 5.00E2 | 1.00E3 | Th-230 | 1 | • | 3.90E-8 |
| U-235 | 1.00 | 1.00E1 | 3.00E1 | 1.00E2 | 7.04E8 | 5.00E2 | 1.00E3 | Th-231 | 1 | • | 3.80E-8 |
| U-236 | 1.00 | 1.00E1 | 3.00E1 | 1.00E2 | 2.34E7 | 5.00E2 | 1.00E3 | Th-232 | 1 | • | 3.70E-8 |
| U-237 | 1.00 | 1.00E1 | 3.00E1 | 1.00E2 | 1.85E-2 | 5.00E2 | 1.00E3 | Np-237 | 1 | • | 7.30E-10 |
| U-238 | 1.00 | 1.00E1 | 3.00E1 | 1.00E2 | 4.47E9 | 5.00E2 | 1.00E3 | Th-234 | 1 | • | 3.60E-8 |
| Pu-238 | 4.00E1 | 3.00E2 | 3.00E3 | 2.00E3 | 8.77E1 | 1.00E5 | 1.00E5 | U-234 | 1 | • | 5.10E-7 |
| Pu-239 | 4.00E1 | 3.00E2 | 3.00E3 | 2.00E3 | 2.41E4 | 1.00E5 | 1.00E5 | U-235 | 1 | • | 5.60E-7 |
| Pu-240 | 4.00E1 | 3.00E2 | 3.00E3 | 2.00E3 | 6.57E3 | 1.00E5 | 1.00E5 | U-236 | 1 | • | 5.60E-7 |
| Pu-241 | 4.00E1 | 3.00E2 | 3.00E3 | 2.00E3 | 1.44E1 | 1.00E5 | 1.00E5 | Am-241 | 0.99 | U-237 | 1.10E-8 |
| Pu-242 | 4.00E1 | 3.00E2 | 3.00E3 | 2.00E3 | 3.76E5 | 1.00E5 | 1.00E5 | U-238 | 1 | • | 5.30E-7 |
| Am-241 | 5.00E1 | 5.00E2 | 2.00E4 | 8.00E3 | 4.33E2 | 2.00E6 | 2.00E6 | Np-237 | 1 | • | 5.70E-7 |
| Am-243 | 5.00E1 | 5.00E2 | 2.00E4 | 8.00E3 | 7.37E3 | 2.00E6 | 2.00E6 | Np-239 | 1 | • | 5.70E-7 |
| Cm-242 | 5.00E1 | 5.00E2 | 3.00E4 | 8.00E3 | 4.46E-1 | 2.00E6 | 2.00E6 | Pu-238 | 1 | • | 2.40E-8 |
| Cm-243 | 5.00E1 | 5.00E2 | 3.00E4 | 8.00E3 | 2.85E1 | 2.00E6 | 2.00E6 | Pu-239 | 0.99 | Am-243 | 4.00E-7 |
| Cm-244 | 5.00E1 | 5.00E2 | 3.00E4 | 8.00E3 | 1.81E1 | 2.00E6 | 2.00E6 | Pu-240 | 1 | • | 3.20E-7 |

APPENDIX II. INPUT DATA FOR MINORSKY CALCULATIONS

Contents

| | |
|---|------|
| Appendix II. Input Data for Minorsky Calculations | II-1 |
| II.1 Introduction..... | II-1 |
| II.2 Accident Case Data | II-1 |
| II.2.1 Bow Angle..... | II-2 |
| II.2.2 Rake Angle..... | II-3 |
| II.2.3 Shell Plate Thickness | II-3 |
| II.3 Merchant Vessel Fleet Distribution | II-4 |
| II.4 Addenda | II-4 |

Figures

| | |
|-------------------------------|------|
| Figure II.1. Bow Angles. | II-2 |
| Figure II.2. Rake Angle. | II-3 |

APPENDIX II. INPUT DATA FOR MINORSKY CALCULATIONS

II.1 Introduction

In Section 6.0, Probability of Deep Hull Penetration, Minorsky's correlation of collision damage with collision energy was revalidated. The revalidation both identified seven of the nine ship collisions that entered Minorsky's original correlation and added to the correlation data for nine modern ship collisions. For some of the modern collisions, values for all of the parameters required by Minorsky's correlation or for its use to estimate the probability of deep hull penetration during ship collisions were not directly available from published literature. Where parameter values were lacking, they were developed by staff at Engineering Computer Optecnomics (ECO), Inc. This appendix describes the analyses performed by ECO and documents their results.

II.2 Accident Case Data

ECO maintains a staff of highly qualified naval architects, system analysts, and data management specialists who perform data analysis and data reduction functions, including the generation of new and maintenance of existing proprietary databases. ECO is recognized both in the United States and abroad for its data collection and analytical studies and services associated with all forms of marine systems and marine entities and particularly oil spill incidents. Over the years, the company's data management staff developed and now continuously maintain a series of databases that reflect many years of investigative research into the causes, characteristics, and circumstances associated with marine accidents.

Among these databases are: ECOTANKTM, a database of worldwide tank ship accidents beginning in 1969; ECOCASTM, a database of ship casualties in U.S. ports and contiguous offshore waters; ECOSPILLTM, a database of spills of oil and other hazardous polluting substances onto the navigable waters of the United States regardless of source; ECOSPTM, a database that compiles the characteristics of all of the major ports of the United States; and ECOTRAFTM, a database of traffic levels and patterns within all major ports of the United States. ECO not only maintains these databases but also continuously refines and improves the databases and analysis capabilities by participating in numerous and varied risk and safety analyses associated with the marine transportation of oil, chemicals, and other hazardous materials. All of the databases are remarkably comprehensive, reliable, versatile, and are valuable repositories of marine system data that are readily available for our exclusive use in marine risk and other marine systems analyses.

Initially, an accident listing was extracted from a review of NTSB marine accident reports covering the period 1972 to present. From this listing, ten accident cases were selected for modeling using the Minorsky method. In reviewing these cases, it was necessary to determine specific conditions and parameters for each vessel, i.e., drafts, displacement, and speed. Detailed reading of the actual case files was performed to determine the necessary parameters. Calculations were performed to determine most probable displacement at the time of the accident. In several cases, time sequence plots were performed to correlate witness testimony to the vessel's speed and engine order telegraph. From this analysis, the most probable speed at the time of the accident was determined.

To the initial listing provided by Sandia, ECO added more recent accident cases. The most recent case occurred July 1, 1995, and remains incomplete at the time of this report because critical data has not been released by the ship's owner. Photographic documentation is appended to the report in Addendum IIa to show graphically the side-shell penetration, the tearing/slicing effect of the main deck,

and shear strake on the striking vessel. Photographs also show the lack of any strength provided by the cargo hatch covers. In this case, penetration to the centerline or one-half the beam is clearly visible. Photographs are credited to the USCG.

Addendum IIb contains summary data sheets for 17 accidents where the striking vessels speed was ten (10) knots or greater. Addendum IIc contains summary data sheets for ten accidents where the striking vessels speed was less than ten (10) knots.

II.2.1 Bow Angle

To account for the various types of ships and their typical construction, a review of differing bow shapes was performed. Four general categories of bow shapes for merchant ships exist for tanker/bulker, general cargo, container ships, and passenger ships.

The bow angle is necessary to calculate the surface area of impact of the collision. The following analysis explains the methodology used to quantify the bow angle by ship type.

Ocean-going merchant ships range from 300 to over 1,000 feet in length. The collision bulkhead is placed at a distance of 5 percent of the overall ship length from the bow. For a 400-foot vessel, the collision bulkhead would be placed 30 feet from the stern. Based on the freeboard of a loaded cargo ship, the expected impact point would be at the main deck level. Therefore, the bow angle (Θ) was measured at the main deck by drawing a line perpendicular to the centerline at a point 20 feet aft of the bow. At the points where the 20-foot perpendicular intersected the hull, tangents were drawn and extended to intersect the centerline of the hull. The angle formed by the two tangents is the bow angle (ϕ). The bow half angle is formed by one tangent line intersecting the hull centerline. Figure II.1 depicts these angles.

Allowing for numerous variations in hull design, the angles for each category of ship type are considered accurate to within ± 3 degrees. Addendum IId contains a summary of the merchant ship bow angle analysis for the four ship types.

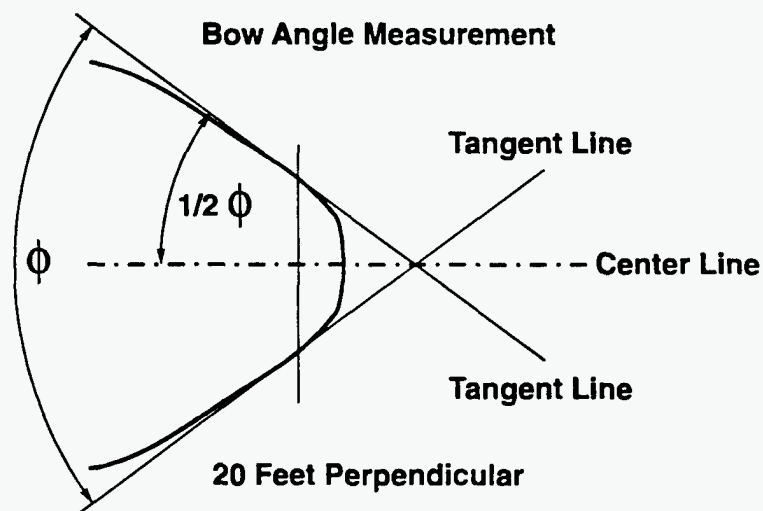


Figure II.1. Bow Angles.

II.2.2 Rake Angle

The impact during a vessel collision is a function of the bow shape. The bow angle was discussed above. Also to be considered is the rake of the bow, or the amount that the bow is inclined from the vertical.

Commercial ships are designed with the stem of the bow inclined from the vertical. The angle formed by the waterline of the vessel and the line drawn from the waterline at the hull to the forwardmost point on the bow is defined as the rake angle (α).

Figure II.2 depicts the definition of the rake angle of the bow of a ship.

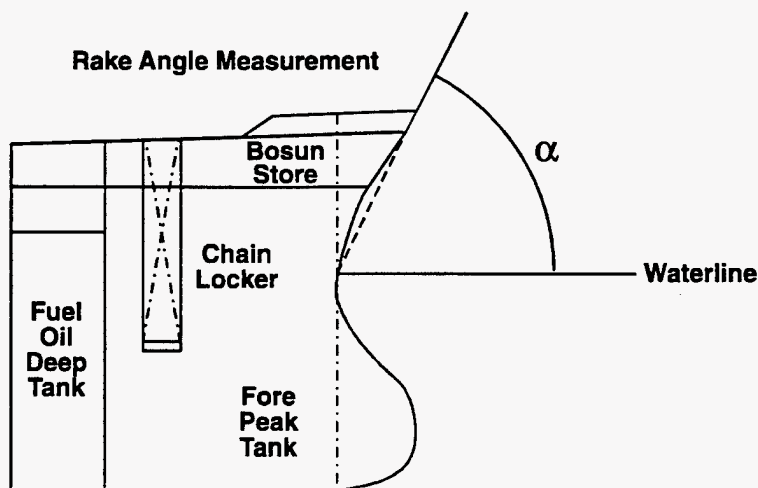


Figure II.2. Rake Angle.

Rake angles for each category of ship type are summarized in Addendum IId. Allowing for numerous variations in hull design, the angles within each category of ship type are considered accurate to within ± 5 degrees.

II.2.3 Shell Plate Thickness

In determining the resistance to penetration and energy absorbed in a collision, the side-shell plate thickness is an important factor. For the accidents being considered, an estimate of the side shell thickness was required.

Since the accident reports do not normally address the structural characteristics of the ship construction, an approach to estimate the side-shell thickness was established. It was decided to compare the specific ships in question to the structural rules required by the American Bureau of Shipping (ABS). This review was performed as if the ships were being constructed under current ABS classification requirements. The analysis provided a minimum shell-plate thickness while avoiding a very intensive research and analysis of individual ship construction plans. A summary of estimated side-shell thickness is shown in Addendum IIe.

II.3 Merchant Vessel Fleet Distribution

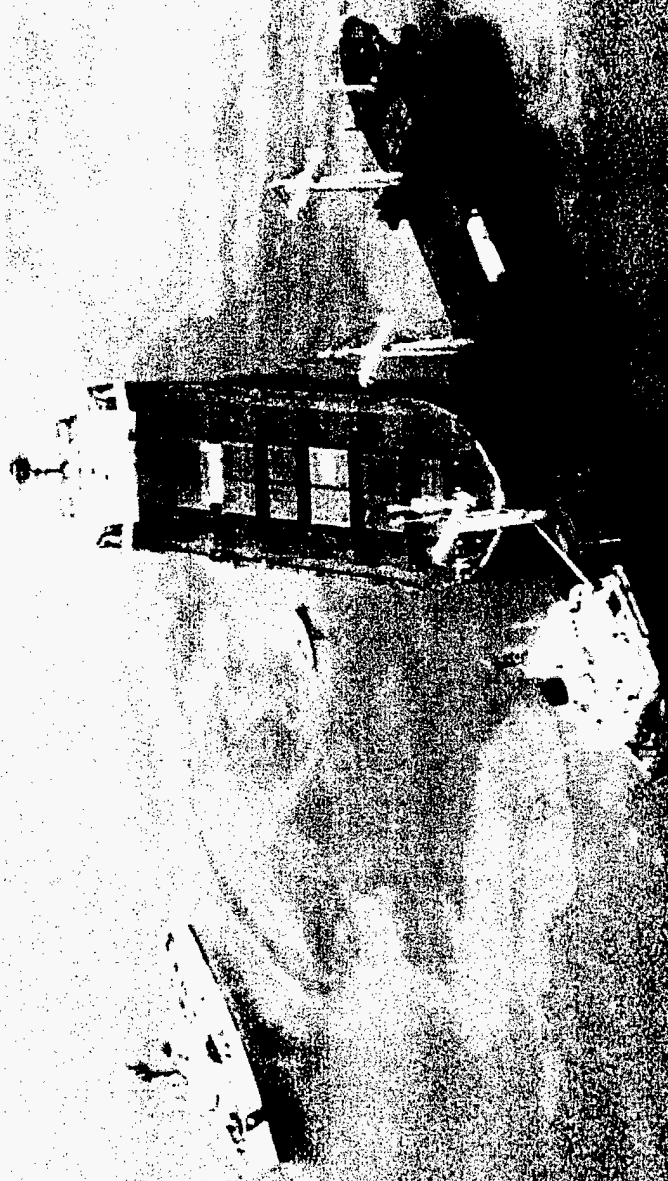
To determine the likelihood of a marine accident, the type of vessels that comprise the world merchant fleet is required. The best estimate of the total world merchant fleet is 50,000 vessels with approximately 25,000 being greater than 1,000 gross tons. A distribution of merchant vessels by four ship types was desired for Sandia's overall risk assessment.

The U.S. Maritime Administration publishes an annual abstract of steam and motor ships that have a gross tonnage greater than 1,000 tons. This abstract was analyzed to produce the distribution desired. The exclusion of vessels less than 1,000 gross tons was considered insignificant since their size would generally dictate their use would be confined to harbors and short coastal routes.

The distribution of merchant vessels greater than 1,000 tons is shown in Addendum II.f.

II.4 Addenda

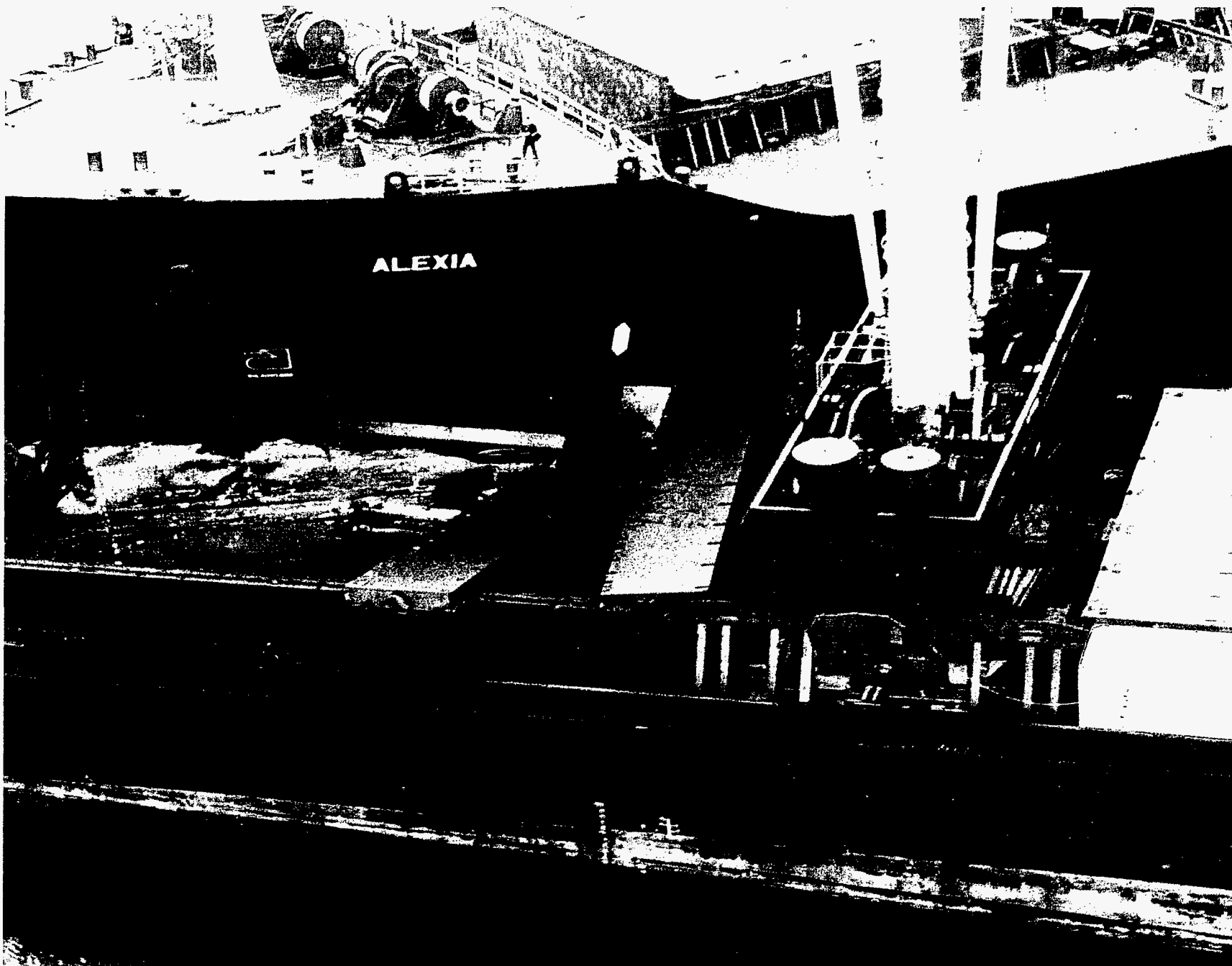
- IIa. Photographs of Collision July 1, 1995
- IIb. Vessel Accident Data, Velocity ≥ 10 knots
- IIc. Vessel Accident Data, Velocity < 10 knots
- IId. Bow Angle and Rake Angle Analysis by Ship Type
- IIe. Side-Shell Thickness
- IIf. Merchant Fleet Distribution



Addendum IIa. Photographs of Collision July 1, 1995 (Page 1 of 5).



Addendum IIa. Photographs of Collision July 1, 1995 (Page 2 of 5).



Addendum IIa. Photographs of Collision July 1, 1995 (Page 3 of 5).



Addendum IIa. Photographs of Collision July 1, 1995 (Page 4 of 5).



Addendum Ila. Photographs of Collision July 1, 1995 (Page 5 of 5).

ATLANTIC OCEAN, OFF NANTUCKET ISLAND - JULY 25, 1956

Striking Vessel

Name: STOCKHOLM
Type: Passenger Liner

Deadweight: 4,700 tons
Displacement: 16,500 tons
Length, Overall: 525.17 ft.
Breadth: 69.08 ft.
Depth: 38.5 ft.
Mean Draft: 24.6 ft.

Impact Angle: 90 degrees
Damage Length: 30 ft.
Damage Height: 29 ft.

Speed: 18.0 knots

Struck Vessel

Name: ANDREA DORIA
Type: Passenger Liner

Deadweight: 8,145 tons
Displacement: 21,200 tons
Length, Overall: 697.0 ft.
Breadth: 89.92 ft.
Depth: 50.08 ft.
Mean Draft: 18.78 ft.

Damage Penetration: 30 ft.
Damage Length: 50 ft.
Damage Height: 29 ft.

Speed: 22.0 knots

Revised 6/12/95

SAN FRANCISCO BAY ENTRANCE - JANUARY 18, 1971

Striking Vessel

Name: ARIZONA STANDARD
Type: Tanker

Deadweight: 17,350 tons
Displacement: 22,578 tons
Length, Overall: 504.0 ft.
Breadth: 68.2 ft.
Depth: 39.2 ft.
Mean Draft: 31.0 ft.

Impact Angle: 45 degrees
Damage Length: 17.0 ft.
Damage Height: 39.2 ft.

Speed: 11.4 knots

Struck Vessel

Name: OREGON STANDARD
Type: Tanker

Deadweight: 17,265 tons
Displacement: 22,575 tons
Length, Overall: 504.0 ft.
Breadth: 68.2 ft.
Depth: 39.2 ft.
Mean Draft: 31.0 ft.

Damage Penetration: 12.0 ft.
Damage Length: 72.0 ft.
Damage Height: 39.2 ft.

Speed: 4.0 knots

PUNTA INDIO CHANNEL, RIVER PLATE - MAY 11, 1972**Striking Vessel**

Name: ROYSTON GRANGE
Type: Refrigerator/Passenger

Deadweight: 10,385 tons
Displacement: 14,660 tons
Length, Overall: 489.0 ft.
Breadth: 65.7 ft.
Depth: 35.3 ft.
Mean Draft: 22.5 ft.

Impact Angle: 40 degrees
Damage Length: 110.0 ft.*
Damage Height: 30.0 ft.*

Speed: 13.0 knots

* Estimated damage

Struck Vessel

Name: TIEN CHEE
Type: Tanker

Deadweight: 18,750 tons
Displacement: 25,975 tons
Length, Overall: 579.6 ft.
Breadth: 70.0 ft.
Depth: 39.8 ft.
Mean Draft: 29.6 ft.

Damage Penetration: 10.0 ft.*
Damage Length: 100.0 ft.*
Damage Height: 30.0 ft.*

Speed: 11.0 knots

* Estimated damage

OFF THE COAST OF S. AFRICA, BETWEEN ALPHARD BANKS AND YZERVARKPUNT - AUGUST 21, 1972

Striking Vessel

Name: OSWEGO GUARDIAN
Type: Tanker

Deadweight: 95,608 tons
Displacement: 109,870 tons
Length, Overall: 899.6 ft.
Breadth: 127.9 ft.
Depth: 62.0 ft.
Mean Draft: 43.7 ft.

Impact Angle: 50 degrees
Damage Length: 25.0 ft.*
Damage Height: 43.0 ft.*

Speed: 16.0 knots

* Estimated damage based on
OSWEGO GUARDIAN striking approx.
18 foot below the main deck of the
TEXANITA

Struck Vessel

Name: TEXANITA
Type: Tanker

Deadweight: 100,613 tons
Displacement: 62,075 tons*
Length, Overall: 872.7 ft.
Breadth: 127.8 ft.
Depth: 61.3 ft.
Mean Draft: 25.0 ft.**

Damage Penetration: 25.0 ft.***
Damage Length: 80.0 ft.***
Damage Height: 43.0 ft.***

Speed: 15.0 knots

* Vessel in ballast condition

** Ballast condition draft

*** Estimated damage

Addendum IIb. Vessel Accident Data, Velocity \geq 10 Knots (Page 4 of 17).

NEW YORK HARBOR - JUNE 2, 1973**Striking Vessel**

Name: C.V. SEA WITCH
Type: Container Vessel

Deadweight: 16,343 tons
Displacement: 26,670 tons
Length, Overall: 610.0 ft.
Breadth: 78.2 ft.
Depth: 54.5 ft.
Mean Draft: 27.3 ft.

Impact Angle: 60 degrees
Damage Length: 21.0 ft.
Damage Height: 36.0 ft.

Speed: 15.5 knots

Struck Vessel

Name: ESSO BRUSSELS
Type: Tanker

Deadweight: 43,121 tons
Displacement: 52,500 tons
Length, Overall: 699.5 ft.
Breadth: 97.3 ft.
Depth: 49.3 ft.
Mean Draft: 38.0 ft.

Damage Penetration: 25.0 ft.
Damage Length: 40.0 ft.
Damage Height: 36.0 ft.

Speed: 0.0 knots (Anchored)

Striking Vessel

Name: Stolt Viking
Type: Tanker

Deadweight: 21,150 tons
Displacement: 28,500 tons
Length, Overall: 565.0 ft.
Breadth: 72.2 ft.
Depth: 42.2 ft.
Mean Draft: 33.2 ft. (max.)

Impact Angle: 45 degrees
Damage Length: No damage
Damage Height: No damage

Speed: 12.0 knots

Struck Vessel

Name: Candy Bar
Type: Crewboat (aluminum)

Deadweight: N/A
Displacement: 72 tons
Length, Overall: 95.0 ft.
Breadth: 21.0 ft.
Depth: 8.9 ft.
Mean Draft: 3.8 ft.

Damage Penetration: 21.0 ft. (cut in half)
Damage Length: cut in half
Damage Height: 8.9 ft.

Speed: 14.0 knots

CHESAPEAKE BAY, MOUTH OF THE POTOMAC RIVER, MARYLAND - OCTOBER 20, 1978

Striking Vessel

Name: SANTA CRUZ II
Type: General Cargo

Deadweight: 20,373 tons
Displacement: 25,855 tons
Length, Overall: 520.0 ft.
Breadth: 74.0 ft.
Depth: 44.0 ft.
Mean Draft: 32.5 ft.

Impact Angle: 5 degrees
Damage Length: Indentation
Damage Height: Indentation

Speed: 13.5 knots

Struck Vessel

Name: CUYAHOGA
Type: USCG Cutter

Deadweight: N/A
Displacement: 460 tons
Length, Overall: 125.0 ft.
Breadth: 24.0 ft.
Depth: 18.0 ft.
Mean Draft: 10.0 ft.

Damage Penetration: 10.0 ft.
Damage Length: 15.0 ft.
Damage Height: 10.0 ft.

Speed: 11.3 knots

ATLANTIC OCEAN, SE OF CAPE COD - JUNE 18, 1979

Striking Vessel

Name: EXXON CHESTER
Type: Tanker

Deadweight: 29,210 tons
Displacement: 36,630 tons
Length, Overall: 627.9 ft.
Breadth: 82.7 ft.
Depth: 42.5 ft.
Mean Draft: 33.6 ft.

Impact Angle: 60 degrees
Damage Length: 31.0 ft.
Damage Height: 40 ft.

Speed: 10.0 knots

Struck Vessel

Name: REGAL SWORD
Type: Bulk Carrier

Deadweight: 27,464 tons
Displacement: 34,714 tons
Length, Overall: 576.9 ft.
Breadth: 75.0 ft.
Depth: 48.6 ft.
Mean Draft: 36.0 ft.

Damage Penetration: 20.0 ft.
Damage Length: 150.0 ft.
Damage Height: 25.0 ft.

Speed: 12.0 knots

TAMPA BAY - JANUARY 28, 1980

Striking Vessel

Name: CAPRICORN
 Type: Tanker

 Deadweight: 24,796 tons
 Displacement: 29,950 tons
 Length, Overall: 604.9 ft.
 Breadth: 75.2 ft.
 Depth: 41.8 ft.
 Mean Draft: 31.5 ft.

Impact Angle: 180± 5 degrees
 Damage Length: Hawse pipe/anchor damage
 Damage Height: Hawse pipe/anchor damage

Speed: 12.0 knots

Struck Vessel

Name: BLACKTHORN
 Type: USCG Buoy Tender

 Deadweight: N/A
 Displacement: 1,025 tons
 Length, Overall: 180.0 ft.
 Breadth: 37.0 ft.
 Depth: 17.3 ft.
 Mean Draft: 12.8 ft.

Damage Penetration: 4.0 ft.
 Damage Length: 80.0 ft.
 Damage Height: 10.0 ft.

Speed: 7.5 knots

LOWER MISSISSIPPI RIVER, NEAR VENICE, LOUISIANA - NOVEMBER 24, 1980

Striking Vessel

Name: COASTAL TRANSPORT
Type: Chemical Tanker

Deadweight: 14,428 tons
Displacement: 20,160 tons*
Length, Overall: 490.0 ft.
Breadth: 64.0 ft.
Depth: 38.0 ft.
Mean Draft: 30.0 ft.**

Impact Angle: 90 degrees
Damage Length: Stem to fr. 110
Damage Height: 22.0 ft.

Speed: 17.3 knots

* Full load displacement
** Max draft

Struck Vessel

Name: SALLEE P.
Type: Offshore Supply Vessel

Deadweight: N/A
Displacement: 395 tons*
Length, Overall: 115.0 ft.
Breadth: 26.0 ft.
Depth: 8.0 ft.
Mean Draft: 7.0 ft.**

Damage Penetration: 20.0 ft.
Damage Length: 34.0 ft.
Damage Height: 8.0 ft.

Speed: 14.0 knots

* Displacement of vessel in ballast condition
** Ballast condition draft

MISSISSIPPI RIVER - DECEMBER 27, 1980**Striking Vessel**

Name: PISCES
Type: Tanker

Deadweight: 24,438 tons
Displacement: 31,070 tons
Length, Overall: 604.9 ft.
Breadth: 75.3 ft.
Depth: 41.8 ft.
Mean Draft: 33.3 ft.

Impact Angle: 90 degrees
Damage Length: 45.0 ft.
Damage Height: 50.0 ft.

Speed: 11.5 knots

Struck Vessel

Name: TRADE MASTER
Type: Bulk Carrier

Deadweight: 33,448 tons
Displacement: 41,768 tons
Length, Overall: 628.3 ft.
Breadth: 86.9 ft.
Depth: 50.2 ft.
Mean Draft: 37.0 ft.

Damage Penetration: 18.0 ft.
Damage Length: 55.0 ft.
Damage Height: 50.0 ft.

Speed: 11.1 knots

ATLANTIC OCEAN - MAY 6, 1981

Striking Vessel

Name: LASH ATLANTICO
Type: Barge Carrier

Deadweight: 29,820 tons
Displacement: 44,606 tons
Length, Overall: 819.8 ft.
Breadth: 100.2 ft.
Depth: 60.0 ft.
Mean Draft: 32.1 ft.

Impact Angle: 120 degrees
Damage Length: 70.0 ft.
Damage Height: 30.0 ft.

Speed: 18.0 knots

Struck Vessel

Name: HELLENIC CARRIER
Type: General Cargo

Deadweight: 15,153 tons
Displacement: 18,725 tons
Length, Overall: 470.0 ft.
Breadth: 67.1 ft.
Depth: 38.5 ft.
Mean Draft: 20.8 ft.

Damage Penetration: 30.0 ft.
Damage Length: 70.0 ft.
Damage Height: 32.0 ft.

Speed: 14.0 knots

GULF OF MEXICO - FEBRUARY 19, 1982**Striking Vessel**

Name: DELTA NORTE
 Type: Barge Carrier

Deadweight: 41,223 tons
 Displacement: 57,800 tons
 Length, Overall: 893.1 ft.
 Breadth: 100.2 ft.
 Depth: 60.0 ft.
 Mean Draft: 34.0 ft.

Impact Angle: 45 degrees
 Damage Length: 42.0 ft.
 Damage Height: 40.0 ft.

Speed: 19.0 knots

Struck Vessel

Name: AFRICAN PIONEER
 Type: General Cargo

Deadweight: 12,391 tons
 Displacement: 18,600 tons
 Length, Overall: 495.0 ft.
 Breadth: 71.4 ft.
 Depth: 39.7 ft.
 Mean Draft: 18.3 ft.

Damage Penetration: 30.0 ft.
 Damage Length: 80.0 ft.
 Damage Height: 33.0 ft.

Speed: 15.0 knots

RHODE ISLAND SOUND - JULY 2, 1983

Striking Vessel

Name: YANKEE
Type: Passenger Vessel/General Cargo

Deadweight: N/A
Displacement: 450 tons*
Length, Overall: 136.5 ft.
Breadth: 29.0 ft.
Depth: 9.5 ft.
Mean Draft: 7.5 ft.**

Impact Angle: 70 degrees
Damage Length: 10.0 ft.
Damage Height: 15.0 ft.

Speed: 11.5 knots

* Displacement is estimated at a draft
of 7.5 ft.

** Estimated vessel draft at 7.5 ft.

Struck Vessel

Name: HARBEL TAPPER
Type: General Cargo

Deadweight: N/A
Displacement: 17,525 tons*
Length, Overall: 435.0 ft.
Breadth: 72.0 ft.
Depth: 35.0 ft.
Mean Draft: 26.5 ft.**

Damage Penetration: 0.0 ft.
Damage Length: Indentation only
Damage Height: Indentation only

Speed: 5.0 knots

* Displacement is estimated at a draft
of 26.5 ft.

** Estimated vessel draft at 26.5 ft.

GALVESTON BAY ENTRANCE - NOVEMBER 10, 1988**Striking Vessel**

Name: FIGARO
 Type: Auto Carrier

 Deadweight: 27,764 tons
 Displacement: 35,894 tons
 Length, Overall: 649.6 ft.
 Breadth: 105.9 ft.
 Depth: 102.4 ft.
 Mean Draft: 29.8 ft.

Impact Angle: 30.0 degrees
 Damage Length: 72.0 ft.
 Damage Height: 70.0 ft. (port side)

Speed: 10.0 knots

Struck Vessel

Name: CAMARGUE
 Type: Tanker

 Deadweight: 133,360 tons
 Displacement: 158,210 tons
 Length, Overall: 918.9 ft.
 Breadth: 135.0 ft.
 Depth: 72.0 ft.
 Mean Draft: 36.4 ft.

Damage Penetration: 12.0 ft. (from bulbous bow)
 Damage Length: 75.0 ft.
 Damage Height: 45.0 ft.

Speed: 10.0 knots

LOWER MISSISSIPPI - MARCH 24, 1993

Striking Vessel

Name: ATTICOS
Type: Bulk Carrier

Deadweight: 29,165 tons (Ballast condition)
Displacement: 17,176 tons
Length, Overall: 593.1 ft.
Breadth: 75.9 ft.
Depth: 47.6 ft.
Mean Draft: 15.1 ft. (Ballast condition)

Impact Angle: 120 degrees
Damage Length: Minor damage, port side bulbous bow
Damage Height: 16.0 ft.

Speed: 10.5 knots

Struck Vessel

Name: GALVESTON
Type: Offshore Supply Vessel

Deadweight: N/A
Displacement: 630 tons
Length, Overall: 180.0 ft.
Breadth: 40.0 ft.
Depth: 14.3 ft.
Mean Draft: 8.2 ft.

Damage Penetration: 12.0 ft.
Damage Length: 15.0 ft.
Damage Height: 14.3 ft.

Speed: 13.5 knots

PORT PUSAN - MAY 2, 1994

Striking Vessel

Name: HANJIN HONGKONG
Type: Containership

Deadweight: 20,000 tons
Displacement: 27,780 tons
Length, Overall: 796.6 ft.
Breadth: 105.6 ft.
Depth: 62.3 ft.
Mean Draft: 17.1 ft.

Impact Angle: 90 degrees
Damage Length: 55.0 ft.
Damage Height: 62.3 ft.

Speed: 10.0 knots

Struck Vessel

Name: PRESIDENT WASHINGTON
Type: Containership

Deadweight: 49,310 tons
Displacement: 56,534 tons
Length, Overall: 860.2 ft.
Breadth: 105.8 ft.
Depth: 66.0 ft.
Mean Draft: 38.1 ft.

Damage Penetration: 55.0 ft.
Damage Length: 105.6 ft.
Damage Height: 40.0 ft.

Speed: 6.0 knots

BAY OF TOKYO, JAPAN - NOVEMBER 9, 1974

Striking Vessel

Name: PACIFIC ARES
Type: General Cargo

Deadweight: N/A
Displacement: 21,620 tons
Length, Overall: 505.5 ft.
Breadth: 72.8 ft.
Depth: 39.7 ft.
Mean Draft: 28.8 ft.

Impact Angle: 90 degrees
Damage Length: 40.0 ft.
Damage Height: 35.0 ft.

Speed: 5.5 knots

Struck Vessel

Name: YUYO MARU NO. 10
Type: Tanker

Deadweight: 52,836 tons
Displacement: 73,790 tons
Length, Overall: 740.3 ft.
Breadth: 117.4 ft.
Depth: 68.1 ft.
Mean Draft: 39.1 ft.

Damage Penetration: 15.0 ft.
Damage Length: 78.7 ft.
Damage Height: 35.0 ft.

Speed: 10.0 knots

MISSISSIPPI RIVER, PILOTTOWN, LOUISIANA - OCTOBER 3, 1978

Striking Vessel

Name: TEXACO IOWA
Type: Tanker

Deadweight: 41,282 tons
Displacement: 53,850 tons
Length, Overall: 699.5 ft.
Breadth: 97.0 ft.
Depth: 49.0 ft.
Mean Draft: 38.6 ft.

Impact Angle: 15 degrees
Damage Length: 30.0 ft.
Damage Height: 1.0 ft.

Speed: 8.0 knots

Struck Vessel

Name: BURMAH SPAR
Type: Tanker

Deadweight: 74,350 tons
Displacement: 81,135 tons
Length, Overall: 785.0 ft.
Breadth: 121.0 ft.
Depth: 54.0 ft.
Mean Draft: 40.0 ft.

Damage Penetration: 0.0 ft.
Damage Length: Indentation only
Damage Height: Indentation only

Speed: 6.0 knots

Striking Vessel

Name: MARITIME JUSTICE
Type: Bulk Carrier

Deadweight: 34,196 tons
Displacement: 41,089 tons
Length, Overall: 608.0 ft.
Breadth: 85.0 ft.
Depth: 51.0 ft.
Mean Draft: 31.3 ft.

Impact Angle: 0 degrees
Damage Length: 30.0 ft.
Damage Height: 20.0 ft.

Speed: 7.2 knots

Struck Vessel

Name: IRENE S. LEMOS
Type: Bulk Carrier

Deadweight: 43,285 tons
Displacement: 44,910 tons*
Length, Overall: 657.0 ft.
Breadth: 95.0 ft.
Depth: 53.0 ft.
Mean Draft: 34.5 ft.**

Damage Penetration: 25.0 ft.
Damage Length: 33.0 ft.
Damage Height: 20.0 ft.

Speed: 8.0 knots

* Light loaded (max. draft @ 39 ft.)

** Max. draft is 39 ft.

NECHES RIVER, NEAR BEAUMONT, TEXAS - FEBRUARY 25, 1979

Striking Vessel

Name: MOBIL VIGILANT
Type: Tanker

Deadweight: 53,490 tons
Displacement: 56,950 tons
Length, Overall: 735.0 ft.
Breadth: 104.0 ft.
Depth: 51.0 ft.
Mean Draft: 36.3 ft.

Impact Angle: 42 degrees
Damage Length: 45.0 ft.
Damage Height: 20.0 ft.

Speed: 4.0 knots

Struck Vessel

Name: MARINE DUVAL
Type: Tanker

Deadweight: 24,734 tons
Displacement: 34,224 tons
Length, Overall: 612.0 ft.
Breadth: 80.0 ft.
Depth: 42.0 ft.
Mean Draft: 33.4 ft.

Damage Penetration: 18.0 ft.
Damage Length: 160.0 ft.
Damage Height: 20.0 ft.

Speed: 6.6 knots

Striking Vessel

Name: FROTALESTE
Type: Bulk Carrier

Deadweight: 24,622 tons
Displacement: 30,753 tons*
Length, Overall: 582.2 ft.
Breadth: 75.7 ft.
Depth: 45.9 ft.
Mean Draft: 33.1 ft.**

Impact Angle: 135 degrees
Damage Length: 150.0 ft.
Damage Height: 40.0 ft.

Speed: 7.4 knots

* Load condition not given.

Displacement taken at max.

** Load draft not given. Draft is
at max. displacement

Struck Vessel

Name: CUNENE
Type: General Cargo

Deadweight: 16,311 tons
Displacement: 18,050 tons*
Length, Overall: 522.7 ft.
Breadth: 69.5 ft.
Depth: 44.1 ft.
Mean Draft: 25.0 ft**

Damage Penetration: 12.0 ft.
Damage Length: 22.0 ft.
Damage Height: 40.0 ft.

Speed: 0.0 knots (anchored)

* Vessel in ballast condition. Assumed
a 25 ft. ballast draft. Displacement
is estimated at a 25 ft. draft.

** Estimated ballast draft at 25.0 ft.

UNDER GREATER NEW ORLEANS BRIDGE AT NEW ORLEANS, LOUISIANA - MARCH 29, 1980

Striking Vessel

Name: NATCHEZ
Type: Sternwheel Passenger

Deadweight: N/A
Displacement: 1,550 tons
Length, Overall: 237.5 ft.
Breadth: 40.0 ft.
Depth: 7.8 ft.
Mean Draft: 6.0 ft.

Impact Angle: 55 degrees
Damage Length: 20.0 ft.
Damage Height: 8.0 ft.

Speed: 6.0 knots

Struck Vessel

Name: EXXON BALTIMORE
Type: Tanker

Deadweight: 50,311 tons
Displacement: 62,852 tons
Length, Overall: 743.0 ft.
Breadth: 102.0 ft.
Depth: 50.0 ft.
Mean Draft: 38.5 ft.

Damage Penetration: 2.0 ft.
Damage Length: 34.0 ft.
Damage Height: 2.5 ft.

Speed: 15.8 knots

MISSISSIPPI RIVER, GULF OUTLET NEAR SHELL BEACH, LOUISIANA - JULY 22, 1980

Striking Vessel

Name: SEADANIEL
Type: Bulk Carrier

Deadweight: N/A
Displacement: 28,300 tons
Length, Overall: 551.2 ft.
Breadth: 75.0 ft.
Depth: 46.4 ft.
Mean Draft: 32.0 ft.

Impact Angle: 45 degrees
Damage Length: 35.0 ft.
Damage Height: 30.0 ft.

Speed: 6.0 knots

Struck Vessel

Name: TESTBANK
Type: Containership

Deadweight: N/A
Displacement: 18,060 tons*
Length, Overall: 467.5 ft.
Breadth: 68.9 ft.
Depth: 35.5 ft.
Mean Draft: 28.0 ft.**

Damage Penetration: 10.0 ft.
Damage Length: 45.0 ft.
Damage Height: 30.0 ft.

Speed: 4.0 knots

* Vessels displacement at a draft of 28.0 ft.

** Assumed vessels load at draft of 28.0 ft.

SEATTLE HARBOR, WASHINGTON - JANUARY 13, 1981

Striking Vessel

Name: KLAHOWYA
 Type: Ferry

 Deadweight: N/A
 Displacement: 1,334 tons
 Length, Overall: 310.0 ft.
 Breadth: 73.0 ft.
 Depth: 17.0 ft.
 Mean Draft: N/A

Impact Angle: 40 degrees
 Damage Length: 30.0 ft.
 Damage Height: 17.0 ft.

Speed: 10.0 knots

Struck Vessel

Name: SANKOGRain
 Type: General Cargo/Vehicle freighter

 Deadweight: 20,138 tons
 Displacement: 13,570 tons*
 Length, Overall: 514.0 ft.
 Breadth: 75.0 ft.
 Depth: 44.3 ft.
 Mean Draft: 19.2 ft.**

Damage Penetration: 0.0 ft.
 Damage Length: Indentation only
 Damage Height: Intendation only

Speed: 2.0 knots

* Ballast condition displacement

** Draft of ballast condition

UPPER NEW YORK BAY - MAY 6, 1981

Striking Vessel

Name: HØEGH ORCHID
Type: General Cargo

Deadweight: 18,207 tons
Displacement: 26,450 tons*
Length, Overall: 599.8 ft.
Breadth: 67.7 ft.
Depth: 41.3 ft.
Mean Draft: 30.8 ft.**

Impact Angle: 90 degrees
Damage Length: 6.5 ft.
Damage Height: 6.0 ft.

Speed: 4.0 knots

* Vessel at time of accident operating at less than full load. Displacement number above is max. displacement.

** Max. draft of vessel

Struck Vessel

Name: AMERICAN LEGION
Type: Ferry

Deadweight: N/A
Displacement: 5,025 tons*
Length, Overall: 294.0 ft.
Breadth: 69.0 ft.
Depth: 20.6 ft.
Mean Draft: 14.3 ft.**

Damage Penetration: 15.0 ft.
Damage Length: 9.0 ft.
Damage Height: 50.0 ft.

Speed: 2.0 knots

* Max. displacement

** Max. draft

UPPER NEW YORK BAY - FEBRUARY 18, 1988

Striking Vessel

Name: MAERSK NEPTUNE
Type: Tanker

Deadweight: 68,800 tons
Displacement: 85,100 tons
Length, Overall: 811.1 ft.
Breadth: 105.5 ft.
Depth: 57.1 ft.
Mean Draft: 43.2 ft.

Impact Angle: 45 degrees
Damage Length: Bow indentation only
Damage Height: Bow indentation only

Speed: 1.5 knots

Struck Vessel

Name: MONT FORT
Type: Bulk Carrier

Deadweight: 26,748 tons
Displacement: 34,868 tons
Length, Overall: 600.6 ft.
Breadth: 73.7 ft.
Depth: 46.6 ft.
Mean Draft: 34.5 ft.

Damage Penetration: 10.0 ft.
Damage Length: 16.0 ft.
Damage Height: 34.0 ft.

Speed: 0.0 knots (Anchored)

BOW ANGLE (Θ) ANALYSIS*

| SHIP DISPLACEMENT (X1,000 TONS) | | CATEGORY OF SHIP TYPE | | | |
|------------------------------------|------------|--------------------------|------------------------------|--------------------------------|----------------------|
| | | TANKER/BULKER <15 KTS | GENERAL CARGO 15 - 20 KTS | CONTAINER SHIPS 20 - 25 KTS | PASSENGER 25+ KTS |
| class 1 | 0-5 | 28 | 29 | 17 | 17 |
| class 2 | 5-10 | 28 | 29 | 17 | 17 |
| class 3 | 10-20 | 30 | 20 | 17 | 17 |
| class 4 | 20-30 | 30 | 20 | 17 | 17 |
| class 5 | 30-40 | 38 | 20 | 17 | 17 |
| class 6 | 40-50 | 38 | 20 | 17 | 17 |
| class 7 | 50-60 | 38 | 20 | 17 | 17 |
| class 8 | 60-70 | 38 | 20 | 17 | 17 |
| class 9 | 70-80 | 38 | 20 | 17 | |
| class 10 | 80-150 | 38 | 20 | 17 | |
| class 11 | 150 and up | 38 | | | |

- * Angles reported are half angles ($1/2 \Theta$)

| RAKE ANGLE (α) | |
|-------------------------|-----|
| Tanker/Bulker | 7.4 |
| General Cargo | 7.6 |
| Container Ship | 6.3 |
| Passenger | 5.4 |

VESSEL SIDE SHELL THICKNESS

| STRUCK SHIP | DISPLACEMENT | LENGTH | BREADTH | DEPTH | TYPE | BEST ESTIMATED* SIDE SHELL THICKNESS (INCHES) |
|------------------|--------------|--------|---------|--------|-----------------|---|
| ESSO GREENSBORO | 21800 | 504.0' | 68.0' | 39.3' | T-2 TANKER | 3/4 |
| TULLAHOMA | 21900 | 504.0' | 68.0' | 39.3' | T-2 TANKER | 3/4 |
| GULF GLOW | 21900 | 504.0' | 68.0' | 39.3' | T-2 TANKER | 3/4 |
| MOJAVE | 5600 | 417.6' | 56.8' | 37.2' | LIBERTY CARGO | 3/4 |
| CATAWBA FORD | 21800 | 504.0' | 68.0' | 39.3' | T-2 TANKER | 3/4 |
| DAVID E. DAY | 8700 | 504.0' | 68.0' | 39.3' | T-2 SE A1 | 3/4 |
| ANDRIA DORIA | 28140 | 697.0' | 89.9' | 50.08' | PASS. | 3/4 |
| ESSO BRUSSELS | 52500 | 699.5' | 97.3' | 49.3' | TANKER | 3/4 |
| TRADE MASTER | 41768 | 628.3' | 86.9' | 50.2' | BULK CARRIER | 3/4 |
| HELLENIE CARRIER | 18725 | 470.0' | 67.1' | 38.5' | GEN. CARGO | 5/8 |
| CAMARQUE | 158210 | 918.9' | 135.0' | 72.0' | TANKER | 7/8 |
| AFRICAN PIONEER | 18600 | 495.0' | 71.4' | 39.7' | GEN. CARGO | 5/8 |
| OREGON STANDARD | 22575 | 504.0' | 68.2' | 39.2' | TANKER | 3/4 |
| CUNENE | 18050 | 522.7' | 69.5' | 44.1' | GEN. CARGO | 5/8 |
| GALVESTON | 630 | 180.0' | 40.0' | 14.3' | OFFSHORE SUPPLY | 3/8 |

MERCHANT FLEET DISTRIBUTION*

OCEAN GOING STEAM AND MOTOR SHIPS OF 1,000 GROSS TONS AND GREATER AS OF JULY 1995

| TOTAL VESSELS** | CATEGORY OF SHIP TYPE | | |
|-----------------|--------------------------|------------------------------|----------------------|
| | TANKER/BULKER <15 KTS | GENERAL CARGO 15 - 20 KTS | PASSENGER 25+ KTS |

25,374 11,421 10,852 2,713 388

PERCENTAGE OF TOTAL 45.0 42.8 10.7 1.5

*Excludes ships operating on the Great Lakes and inland waterways and special types such as channel ships, icebreakers, cable ships, etc., and merchant owned by any military force.

** Vessels less than 1,000 gross tons total approximately 25,000 worldwide.

APPENDIX III. MERCHANT VESSEL SPEEDS IN COMMERCIAL PORTS

Contents

| | |
|--|-------|
| Appendix III. Merchant Vessel Speeds in Commercial Ports | III-1 |
| III.1 Introduction..... | III-1 |
| III.2 Port of Charleston, South Carolina | III-1 |
| III.2.1 Prominent Features | III-1 |
| III.2.2 Upper Cooper River..... | III-2 |
| III.2.3 Pilotage..... | III-2 |
| III.2.4 Port Speed Assessment | III-2 |
| III.3 Summary | III-3 |
| III.4 Bibliography | III-3 |

Figures

| | |
|---|-------|
| Figure III.1. Principal Features of the Port of Charleston. | III-4 |
| Figure III.2. Navigation Channels in the Port of Charleston | III-5 |

APPENDIX III. MERCHANT VESSEL SPEEDS IN COMMERCIAL PORTS

III.1 Introduction

Vessel speeds in the open ocean are usually substantially greater than vessel speeds in a port. Because collision damage depends strongly on vessel speed at the time of a ship collision, merchant vessel speeds in three areas of a typical commercial port were investigated. The areas investigated were (1) the approach from the sea to the sea buoy; (2) harbor transit; and (3) maneuvering in the terminal and off-loading pier area.

The Port of Charleston, South Carolina, was chosen for investigation because shipments of spent European research reactor fuel will be off-loaded at this port in the future. The Port of Charleston has both commercial container unloading facilities and a controlled U.S. military waterfront pier facility. By generalizing the vessel speed results developed for the Port of Charleston, ranges of speeds that apply to the major regions of other ports are estimated below.

III.2 Port of Charleston, South Carolina

The Port of Charleston, South Carolina, is a historic seaport that dates to the earliest days of colonial settlement. Charleston is the largest city and port in South Carolina and is located at the intersection of the Cooper, Ashley, and Wando Rivers. Charleston is the central distribution point for a rich agricultural district. Numerous manufacturing plants are located in and near the city. Major imports are: building cement, plywood, wool, bananas, nonferrous ores, chemicals, fertilizers, frozen meats, automobiles, steel products, naval stores, and petroleum products. Principal exports consist of soybeans, clay, paper products, corn, woodpulp, lumber, heavy machinery, chemicals, fertilizer, textiles, automobiles, and general cargo. Charleston is a busy commercial port averaging more than 4,200 ship movements in 1995.

III.2.1 Prominent Features

Entrance to the Port of Charleston begins at the sea buoy located approximately 10 miles offshore. The harbor entrance is defined by converging jetties that extend seaward for nearly 3 miles. Harbor navigation is aided by prominent landmarks, towers, tanks, lighthouses, and navigational ranges. Navigation in clear weather is generally routine. The narrow channels that exist are influenced by tidal currents that can range up to 2.5 knots, and in severe storm conditions, can approach 5 knots. Large commercial ships of deep drafts can be affected by the current as they maneuver in the harbor and proceed upriver to a terminal facility. The upriver transit requires passing beneath the twin spans of the Route 17 highway bridges and beneath the Mark Clark Bridge near North Charleston. The width of the channel is 200 yards, which restricts shipping to a single direction. Drum Island, which supports the western end of the Route 17 bridges, affects navigation by obscuring vessels downbound in the Cooper River. At the northernmost end of Drum Island, the Cooper River joins the Wando River. There are cross currents on the ebb tide from the confluence of the Cooper and Wando Rivers. Safe navigation dictates that vessels should make every effort to avoid meeting at the Drum Island Turn, one-half mile north of the Route 17 highway bridges. Commercial vessels must communicate and establish firm proposals for meeting or passing in a timely manner so that the vessel stemming the tide can hold in a safe position to allow safe passage of the vessel with the fair tide.

III.2.2 Upper Cooper River

The Cooper River north of Charleston has several areas of significant navigational difficulty where extreme caution must be exercised. The area of Shipyard Creek produces high velocity currents on ebb tides. Up-bound low-powered vessels and tugs with deep draft bows are strongly cautioned not to transit this area except on a flood tide. Also, in the area of Daniel Island Reach, the tankships moored to the oil terminal are susceptible to current surges and suction from the close passing of deep-draft vessels.

Prudent seamanship dictates that the tankships moored at the terminal facilities should employ the maximum mooring lines including wire ropes and winches with manually or hydraulically set brakes. Close attention to the radio broadcast intentions of transiting deep-draft vessels will enable mooring lines to be tended during their passage. Poor handling vessels should have tug assistance when transiting this area to avoid collision with tank vessels moored at the oil terminals. Current effects tend to set across the channel on both flood and ebb tides.

III.2.3 Pilotage

Pilotage is compulsory for all foreign vessels and for all U.S. vessels under register in foreign trade. Government vessels such as Navy and Coast Guard ships are exempt from pilotage; however, their commanding officers frequently request pilots in an advisory capacity. From the sea buoy, a vessel transiting up the Cooper River to the Naval Weapons Station can expect to make in excess of 20 course changes to navigate the channel.

The Port of Charleston continues to experience growth in waterborne commerce. Increases are shown in all categories. In the past five years, the average monthly vessel arrivals have increased from 128 to 155. The mean draft of vessels arriving has increased from 28.04 feet in CY1991 to a mean draft of 29.17 feet in CY1995. The average gross tonnage of merchant vessels was 26,536 tons in CY1991 and increased to 28,649 tons in CY1995. According to U.S. Army Corps of Engineers' statistics on waterborne commerce, the Port of Charleston ranked 53rd in CY1991 and 51st in CY1994 when more than 10.8 million tons of cargo was handled by the port. The Port of Charleston has an excellent safety record despite increased traffic volume and larger ships. This can be attributed to the dedication and skill of the pilots who guide these vessels into and out of the harbor.

III.2.4 Port Speed Assessment

Vessel speeds have been investigated in the areas of approaching the harbor entrance from the sea, transiting the harbor, and maneuvering in the terminal areas. As a vessel approaches from sea, it must slow in the vicinity of the sea buoy to take on board a pilot. Once the pilot is safely aboard, the vessel would proceed inbound in the channel and increase speed to approximately 15 knots. The vessel must travel approximately 7 miles from the sea buoy until it enters the harbor entrance jetties. During this inbound transit, it is common to experience cross currents tending to push the vessel north or south of the entrance to the jetties. Upon entering the jetties, speed would be reduced to 8–10 knots as the vessel proceeded into the center of the harbor. If proceeding up river above the Route 17 highway bridges, the vessel's speed would be further reduced to 5–7 knots to transit beneath the bridges. Once clear of the bridges, the remaining transit to the terminal would continue at the speed of 5–7 knots because of the channel construction and close proximity of moored vessels. The minimum speed for large merchant vessels to maintain proper steering control is within the range of 5–7 knots depending on hull design and depth of the channel.

III.3 Summary

Vessel speed is a function of the topography of the port. Charleston, because of its narrow and winding channel, greatly limits harbor transit speed. While navigating from the Charleston sea buoy, a vessel is required to make in excess of 20 course changes as it follows the serpentine channel up the Cooper River to the Ordnance Terminal and the U.S. Naval Weapons Station. Large open water ports such as New York, Norfolk, and San Francisco would permit greater inner harbor transit speeds. As a general rule, it would be anticipated that vessel speeds would fall in the following ranges:

| | |
|--------------------------|---------------------------|
| Approach to sea buoy: | Maximum speed 17–25 knots |
| Harbor transit: | 8–15 knots |
| Maneuvering at terminal: | 5–7 knots |

III.4 Bibliography

1. Charleston Branch Pilots' Association
2. United States Coast Pilot, Region 4
3. National Oceanic and Atmospheric Agency Charts 11524, 11523, and 11521
4. U.S. Coast Guard Marine Safety Office, Charleston, South Carolina
5. U.S. Corps of Engineers, New Orleans, Louisiana

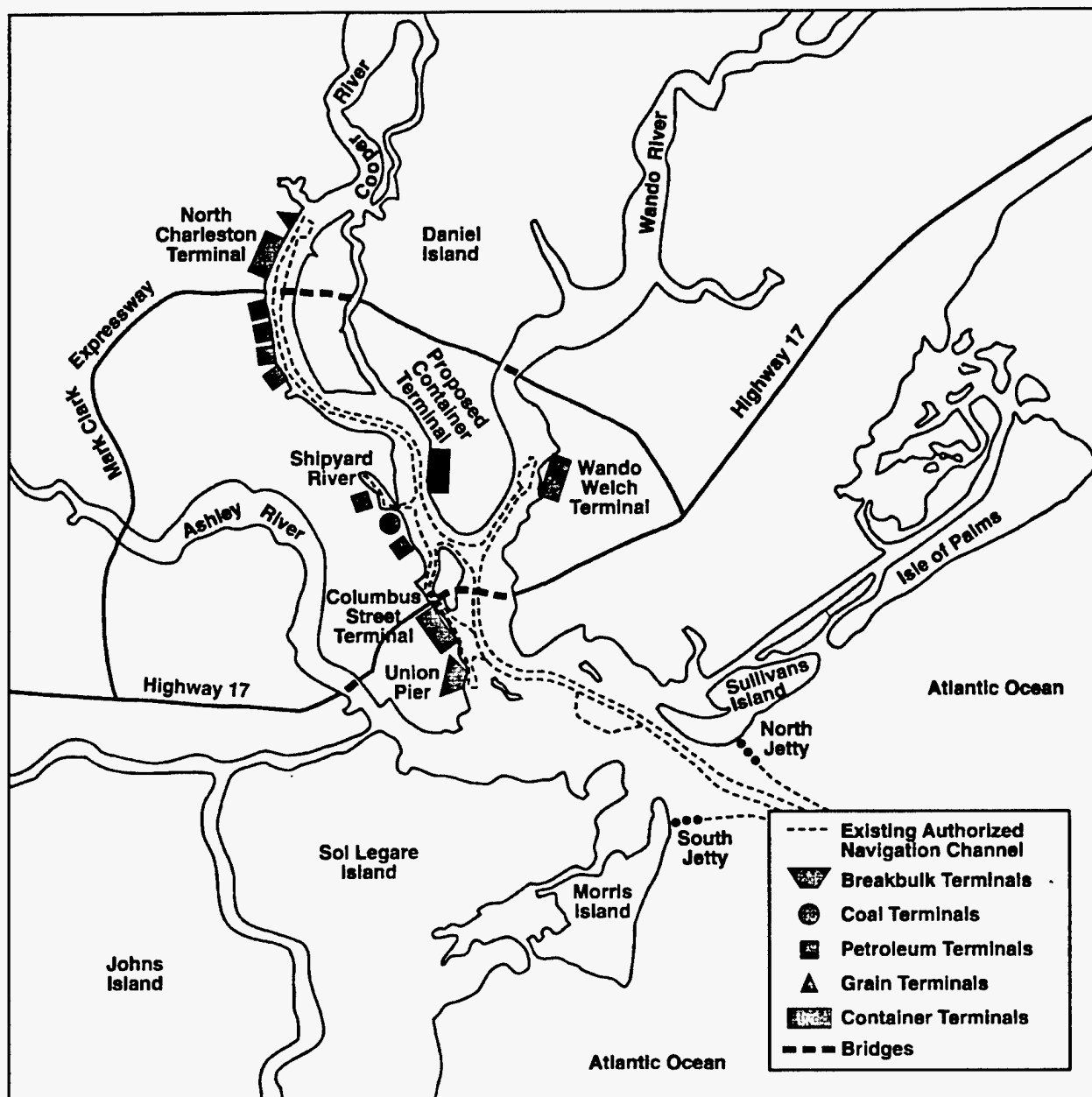


Figure III.1. Principal Features of the Port of Charleston.

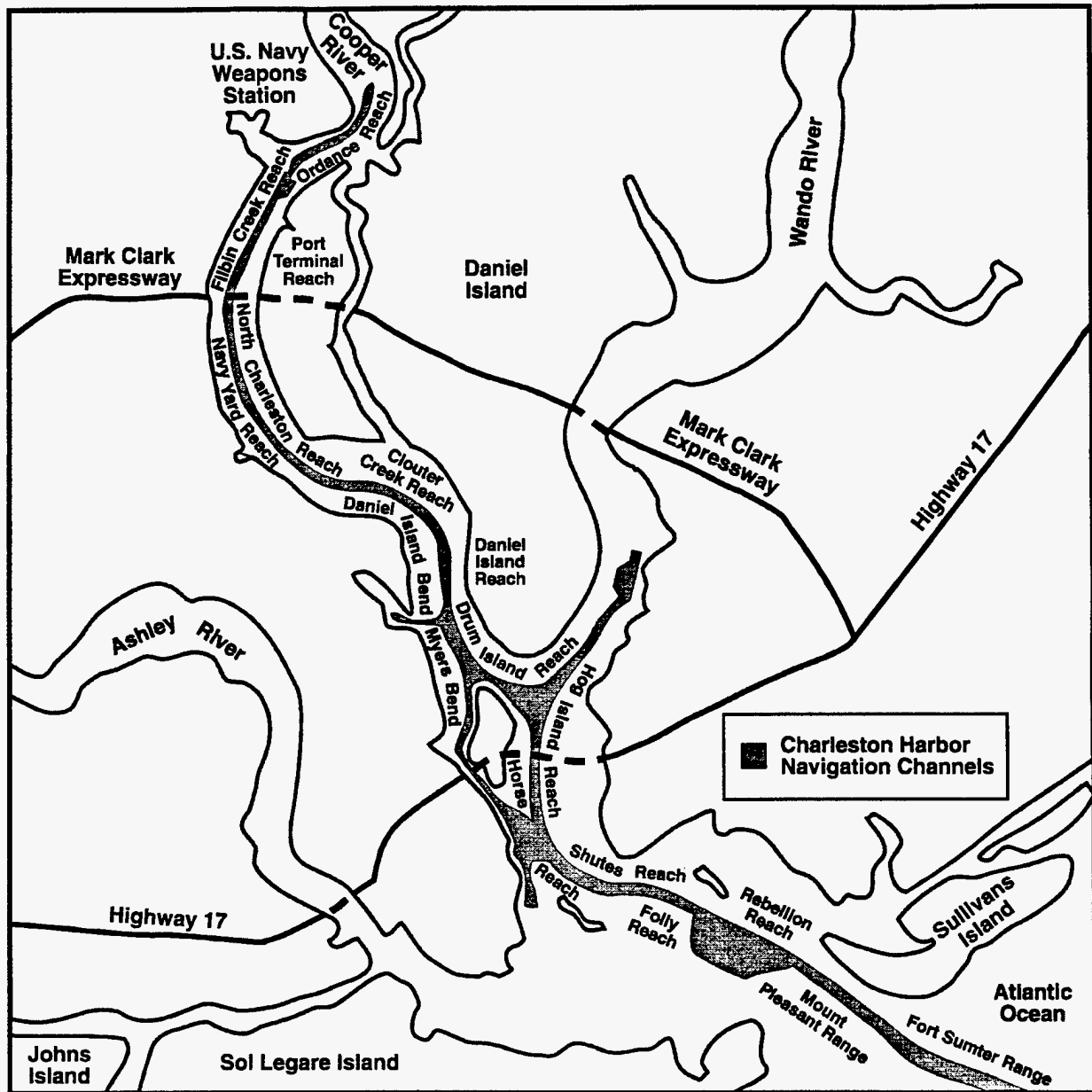


Figure III.2. Navigation Channels in the Port of Charleston.

APPENDIX IV. CASK-TO-ENVIRONMENTAL RELEASE FRACTIONS

Table of Contents

| | |
|---|------|
| 1.0 INTRODUCTION | 1-1 |
| 2.0 SYSTEM DESCRIPTIONS | 2-1 |
| 2.1 Description of TN-12 Spent Fuel Shipping Cask | 2-1 |
| 2.2 Description of PWR Spent Fuel | 2-1 |
| 3.0 MELCOR CODE DESCRIPTION | 3-1 |
| 4.0 MELCOR INPUT MODEL DESCRIPTION | 4-1 |
| 4.1 Fuel Rod Depressurization Model | 4-1 |
| 4.2 Shipping Cask Hydraulic Model | 4-4 |
| 4.3 Shipping Cask Thermal Model | 4-9 |
| 4.3.1 Normal Operating Environmental Conditions | 4-10 |
| 4.3.2 Engulfing Pool Fire Conditions | 4-10 |
| 4.3.3 Cooling Fin Model | 4-10 |
| 4.3.4 Steel Shell - Basket Gap | 4-16 |
| 4.3.5 Basket | 4-18 |
| 4.3.6 Basket - Fuel Gap | 4-21 |
| 4.3.7 Homogenized Fuel | 4-23 |
| 4.3.8 Convective Heat Transport Between Interior Surfaces and the Cask Atmospheres | 4-24 |
| 4.3.9 Axial Heat Conduction to End Regions | 4-25 |
| 4.4 Radionuclide Release and Transport Models | 4-26 |
| 4.4.1 Radionuclide Species | 4-27 |
| 4.4.2 Description of Radionuclide Sources | 4-29 |
| 4.4.3 Aerosol Dynamics | 4-33 |
| 4.4.4 Radionuclide Deposition Surfaces | 4-35 |
| 5.0 MODEL VALIDATION | 5-1 |
| 5.1 Validation of the Fin Cooling Model | 5-1 |
| 5.2 Validation of the Thermal Model During Normal Operating Conditions | 5-3 |
| 6.0 BASE SEVERE ACCIDENT SCENARIOS | 6-1 |
| 6.1 Descriptions of the Base Scenarios | 6-1 |
| 6.2 Overall Fission Product Transport Results for the Base Scenarios | 6-2 |
| 6.3 Base Scenario Hydrodynamic and Heat Transport Results | 6-5 |
| 6.4 Base Scenario Radionuclide Transport Results | 6-12 |
| 7.0 PARAMETER SENSITIVITY ANALYSES | 7-1 |
| 7.1 Sensitivity of Fuel Release Fractions | 7-1 |
| 7.2 Sensitivity of Cask Seal Failure Size | 7-1 |
| 7.3 Sensitivity of Rod Failure Fraction | 7-4 |
| 7.4 Sensitivity of Axial Failure Location | 7-4 |
| 7.5 Sensitivity of Radionuclide Transport Parameters | 7-6 |
| 7.6 Fire Enhancement of Radionuclide Transport From Cask | 7-6 |
| 8.0 SUMMARY OF FINDINGS | 8-1 |
| 9.0 REFERENCES | 9-1 |
| ADDENDUM | AD-1 |

APPENDIX IV. CASK-TO-ENVIRONMENTAL RELEASE FRACTIONS

1.0 INTRODUCTION

If a ship collision or a shipboard fire were to damage a RAM cask being transported on the ship, radioactive vapors and/or aerosols could be released from the cask to the environment. For each radionuclide in the cask inventory, the magnitude of its release is usually estimated as the product of three quantities:

- (1) The cask inventory of the radionuclide,
- (2) The fraction of that inventory that is released into the cask atmosphere from the radioactive material being carried in the cask, and
- (3) The fraction of the amount released to the cask atmosphere that escapes from the cask to the environment (the cask-to-environment release fraction).

For example, if the cask is transporting spent reactor fuel, then the amount of radioactive cesium released to the atmosphere is the product of the amount of radioactive cesium in the fuel pellets in the fuel rods being transported in the cask *times* the fraction of that amount that escapes from the rods to the cask atmosphere *times* the fraction of that amount that escapes from the cask to the environment.

Release of radionuclides into the cask atmosphere does not automatically mean escape to the environment. Instead, condensation of radioactive vapors and deposition of radioactive aerosols onto interior cask surfaces will cause large quantities of the radionuclides that escape from the fuel pellets into the cask atmosphere to be retained inside of the cask. Because condensation of vapors and deposition of aerosols can be efficient processes, a study of these processes was conducted in order to develop estimates of the magnitude of the cask-to-environment release fraction for several important accident environments.

Three accident scenarios were studied:

- (1) A severe ship collision that subjects the RAM cask to mechanical loads that cause the failure of both the cask and some of the fuel rods being transported in the cask;
- (2) A severe ship collision that subjects the RAM cask first to mechanical loads that cause the failure of both the cask and some of the fuel rods being transported in the cask and then to a fully engulfing 4-hour 1200°C fire; and
- (3) A severe ship fire not caused by a ship collision that subjects the RAM cask to a fully engulfing 4-hour 1200°C fire that causes the fuel rods in the cask to fail by burst rupture.

For this study, release of radioactive gases, vapors, and aerosols from spent power reactor fuel carried in a Transnuclear TN-125 cask [1], and the transport of these species through the cask to the environment, was examined for a range of accident conditions. Five radioactive species were examined: noble gases, CsOH, CsI, TeO, and fuel fines. MELCOR calculations were performed in order to estimate values of the cask-to-environment release fraction for a range of cask failures and failure conditions.

MELCOR is a compartment code that implements a full suite of thermal-hydraulic and fission product transport processes [2]. Simple parametric models were implemented in MELCOR to simulate the release of radionuclides from the fuel rods into the cask atmosphere following rod failure due to the mechanical or thermal loads generated by the ship collision or ship fire. Transport of radionuclides from the cask atmosphere through the cask failure to the environment was assumed to be caused by two processes: (1) by depressurization of the cask following its pressurization by helium released from the rods upon rod failure, and (2) by expansion of helium due to heating by an engulfing fire. Cask depressurization, thermal expansion of cask gases, condensation of vapors, and deposition of aerosols released to the cask atmosphere were all simulated using the default set of models implemented in the MELCOR code. These calculations developed estimates of the dependence of cask-to-environment release fraction values on the size of the cask failure and the temperature of the cask. The size of the cask failure was used as a surrogate for the magnitude of the mechanical damage inflicted on the cask by the ship collision. The temperature of the cask was used as a surrogate for the effects of a ship hold fire on the cask and its contents.

2.0 SYSTEM DESCRIPTIONS

The system examined by these calculations was the Transnuclear, Inc., TN-12 Model 125 (TN-125) shipping cask and its contents (internal structures and spent fuel). The Transnuclear TN-125 cask was designed to transport spent power reactor fuel on land by rail or at sea in ships. All information about the design and performance of this cask was taken from the cask's Safety Analysis Report (SAR) [1].

2.1 Description of TN-12 Spent Fuel Shipping Cask

The shell of the TN-125 cask is a cylindrical carbon steel (stainless steel clad) vessel 4.6 m (15 ft) in length with inside and outside diameters of 1.2 m and 1.8 m (4 and 6 ft), respectively. A neutron shield consisting of a 0.1 m (4 in) thick hydrogenous resin layer surrounds the shell. Heat removal from the vessel is enhanced by approximately 60,000 nickel-chromium plated copper fins which are welded to the outside surface of the shell, penetrate through the resin layer, and extend into the ambient environment. An internal basket assembly containing 12 lodgments holds the spent fuel assemblies. The spent fuel is transported dry with either air or nitrogen gas filling the cask interior. The cask is equipped with a 0.36 m (14 in) thick lid bolted to the shell, lifting and support trunnions, and balsa and oak wood filled shock-absorbing covers at each end for insulation and impact protection. The cask design is illustrated in two drawings copied from the SAR, Figures 2-1 and 2-2.

Rows of cooling fins are formed from sheets by cutting the sheets nearly through from one side for each individual fin (i.e., leaving the fins connected at their bases). Then each fin is bent outward from the sheet and twisted 90° so that after mounting on the cask each fin will be oriented at right angles to the cylindrical axis of the cask. A total of 288 fin strips are welded to the steel shell of each TN-125 cask. Each fin extends 0.33 m (1.1 ft) from the steel shell (0.22 m beyond the resin layer) with a cross section (length x thickness) of 19 mm by 3 mm. The resin, an inert thermal insulator, will char during a fire but is self extinguishing. The copper fins have a thermal conductivity approximately 200 times greater than that of the resin, therefore heat transport from the vessel is dominated by heat conduction through the fins. The fins expel energy to the environment by means of radiative heat transfer and natural convective cooling.

The internal basket assembly consists of several components aligned by 8 pins and assembled by 4 tie rods with nuts that lock in place. The basket has 12 square lodgments, 0.227 m long, designed to hold PWR fuel assemblies. The basket is assembled as four quadrants separated by free space in the shape of a cross. Perforated stainless steel plates, 5 mm thick, are placed inside the cross-region to reinforce the basket assembly. The lodgment walls are formed by an arrangement of stainless steel wire mesh boxes containing sintered B₄C-Cu plates for neutron shielding which are cast in an aluminum alloy. The length of the aluminum basket that is in contact with the internal wall of the cask shell is approximately 4 m. The exterior of the basket and the interior of the shell are machined with a tolerance sufficient to ensure a radial gap of between 1 and 2 mm at 20 °C. The radial gap decreases at higher temperatures because the aluminum basket expands faster with temperature increases than does the steel shell. The cask loaded with 12 fuel assemblies has a free volume of 2.68 m³.

2.2 Description of PWR Spent Fuel

The Westinghouse 15x15 fuel assembly design was selected for this investigation. This assembly contains 204 fuel rods with an outside diameter of 0.011 m (0.422 in) and a 3.66 m (12 ft) active fuel length. The fuel pins are formed of stacks of sintered uranium oxide pellets enclosed in a Zircaloy tube with welded plugs closing the ends. Space is provided in each fuel rod at its upper end for a gas plenum. An Inconel spring is placed in each gas plenum to hold the stack of fuel pellets against the lower end of the rod. The fuel rods are fabricated so that there is space, the fuel-cladding gap, between the fuel pellets and the Zircaloy cladding. The pellets are cylindrical in shape with a slight dish in each end surface to allow greater expansion of pellets along their axis than occurs at their cylindrical surface. Thus the free space within each fuel rod includes the gas plenum, the fuel-cladding gap, and the dish spaces between the pellets. This space is filled with pressurized helium during fabrication to reduce stress to the cladding when the rods are subjected to the reactor operating pressures which are typically about 15.5 Mpa (2250 psia).

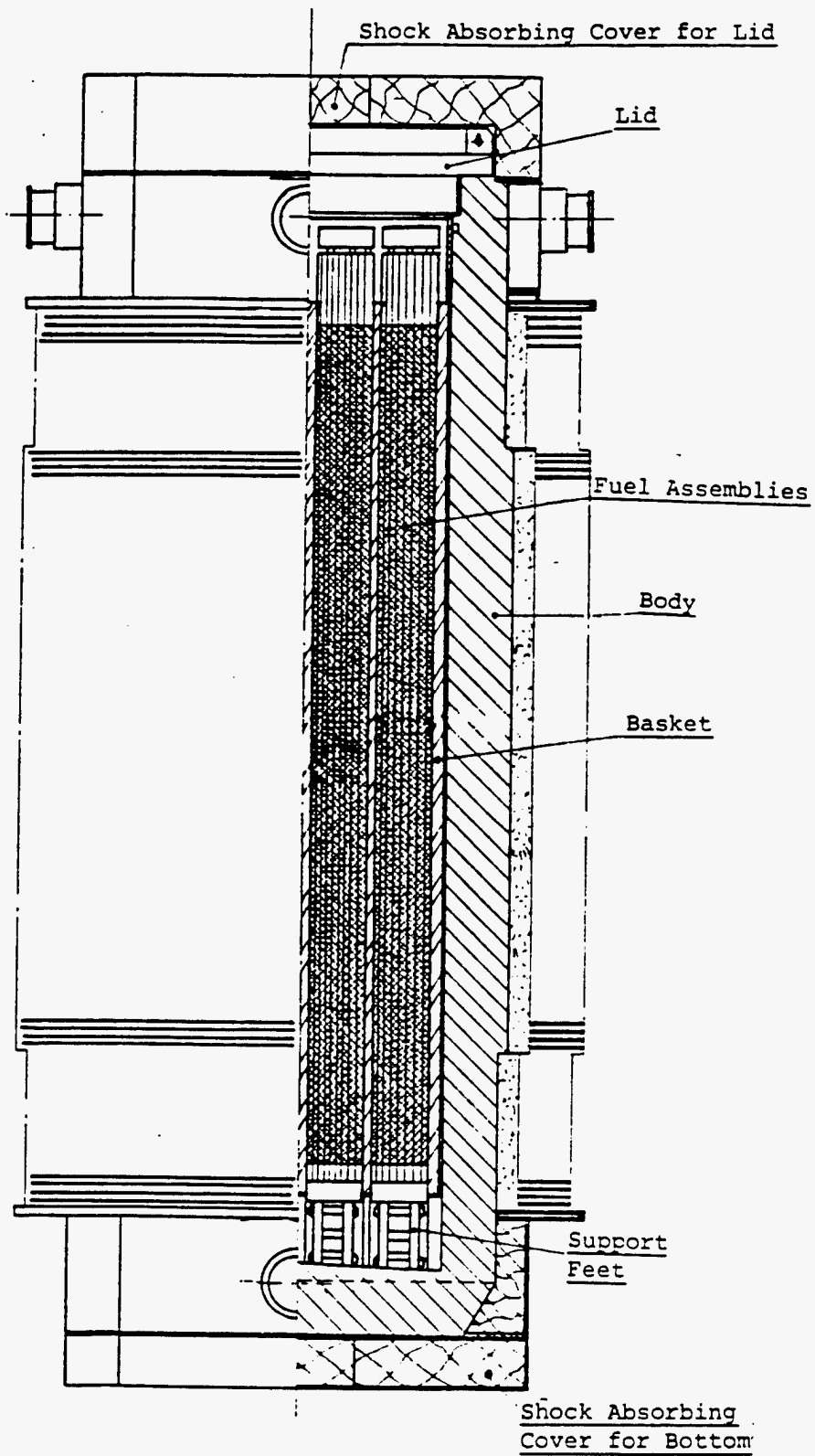


Figure 2-1: TN-125 Package Assembly

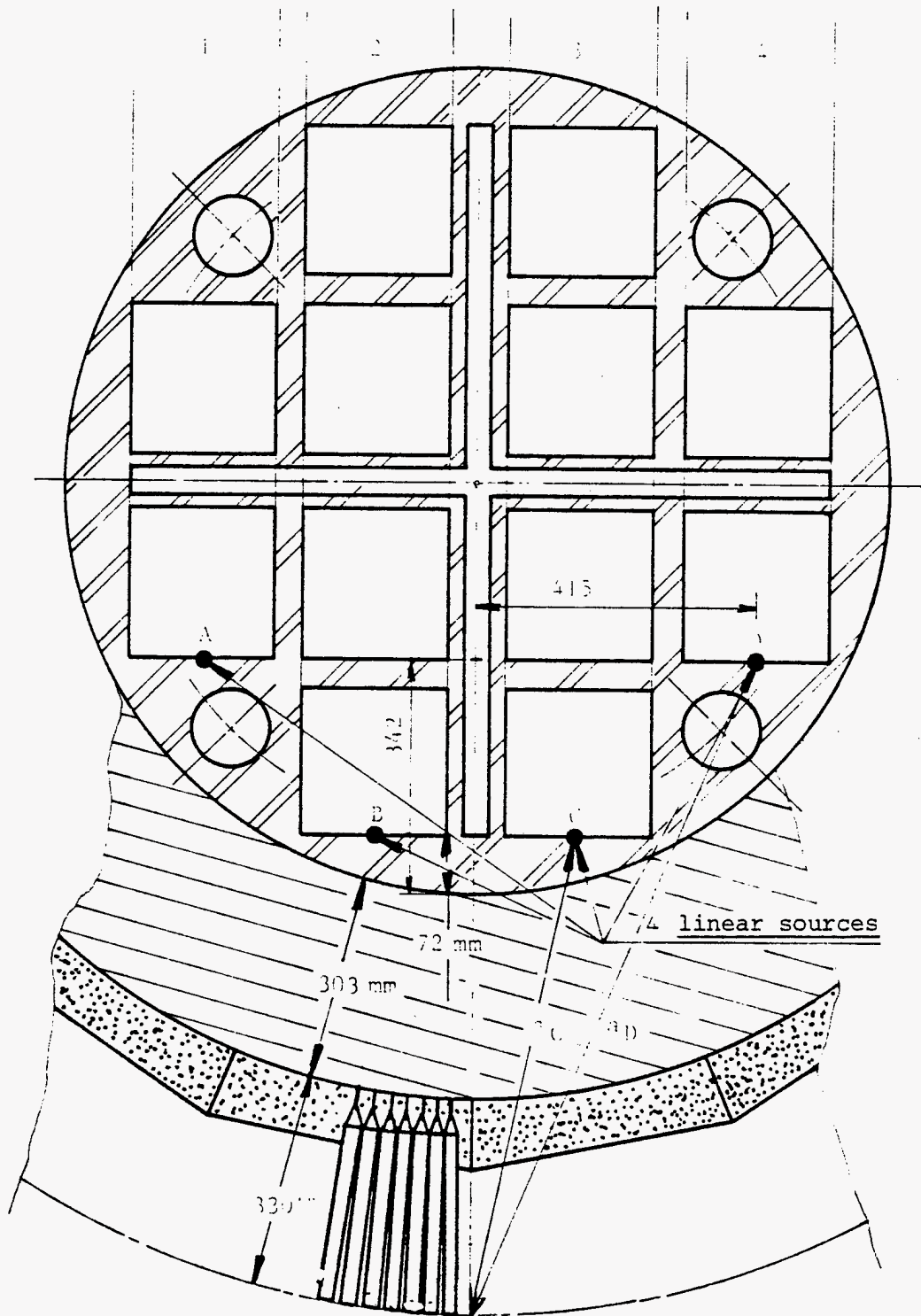


Figure 2-2: TN-125 Basket Cross Section

3.0 MELCOR CODE DESCRIPTION

The MELCOR code developed at Sandia National Laboratories for the U. S. Nuclear Regulatory Commission is a fully integrated computer code that models the progression of severe accidents in light water reactor nuclear power plants [2]. The entire spectrum of severe accident phenomena, including the reactor coolant system and the containment thermal-hydraulic response; nuclear core heatup, degradation and relocation; and fission product release and transport, is treated in MELCOR in a unified framework for both boiling and pressurized water reactors. MELCOR was designed to facilitate sensitivity and uncertainty analyses. MELCOR was subjected to a peer review in 1992 [3] and has been subjected to model validation studies throughout its development.

The MELCOR code was adapted to simulate the TN-12 spent fuel shipping cask through user input (no code modifications were needed) by activating only the applicable code models, specifically the thermal-hydraulic models and the radionuclide transport models. The core meltdown models, for example, remained dormant.

The thermal-hydraulic behavior is modeled with a lumped sum approach using control volumes connected by flow paths. Each volume is defined spatially by its volume versus altitude, may contain a gravitationally separated pool of single or two-phase water, and an atmosphere consisting of any combination of water vapor, suspended water droplets or noncondensable gases. The pool and the atmosphere are each individually treated by equilibrium thermodynamics such that they have equal pressures but may have unequal temperatures. (Pools of water were not simulated in this study.) Noncondensable gases are modeled as ideal gases with temperature dependent specific heat capacities.

The flow paths connect volumes and define paths for moving hydrodynamic materials. Flow within the paths is treated as adiabatic but not, in general, isotropic. Materials do not reside within the flow paths, and do not transfer heat within the flow path. The flow paths may represent either a pipe-like connection in a tank-and-tube model or a cell boundary in a finite-difference model, allowing considerable modeling flexibility.

The governing thermal-hydraulic equations are the equations of conservation of mass, momentum, and energy. As is typical of lumped-parameter codes, the kinetic energy term in the energy equation and the momentum flux term in the momentum equation are omitted on the assumption that MELCOR calculations will model volume-averaged flows in the far subsonic range making these terms unimportant here. Component models exist for special flow conditions such as two-phase flow momentum exchange and phase separation. Critical flow models are included to predict critical flows at such locations as pipe breaks.

The transfer of heat between control volume atmospheres and pools and their surrounding surfaces are modeled using heat structures. These heat structures can include reactor system components such as pressure vessels, internal support structures, pipes, and steam generator tubes and containment components such as walls, floors, beams, and equipment. In this study, the heat structures were used to model the cask shell, resin, fins, basket, and fuel rods. Heat transfer within a heat structure is modeled as one-dimensional heat conduction. Many options are available to model surface heat transfer.

The MELCOR code contains models to predict the transport and behavior of radionuclide vapors and aerosols that directly couple to the thermal-hydraulic models. The MELCOR models group radionuclides into elemental classes with chemical properties such that they show similar transport and deposition behavior. Each group is then tracked as a single element or compound. These radionuclides may exist in either a vapor or an aerosol form and may combine with other non-radioactive materials such as aerosols formed during the melting of structural materials. Each radionuclide class is defined with its own distinct properties. The aerosol dynamics models were adapted from the multicomponent MAEROS code [4]. The condensation and evaporation of vapors from heat structures and aerosols is evaluated by equations adapted from the TRAP-MELT code [5]. Radionuclide aerosols and vapors may deposit directly on surfaces such as heat structures and water pools and aerosols may agglomerate and settle. The particle coagulation processes modeled include Brownian diffusion, gravitational settling, and turbulent impaction. The aerosol deposition processes modeled include gravity, diffusion, thermophoresis, and diffusiophoresis. Resuspension was not modeled. MELCOR has other models for pools, sprays, filters, and vapor chemistry.

4.0 MELCOR INPUT MODEL DESCRIPTION

A MELCOR input model was developed that focused on those cask design features that were anticipated to affect fission product release from the fuel, fission product transport from the rod to the cask and from the cask to the environment, and fission product deposition onto surfaces along transport paths. The major physical processes that required modeling included: the depressurization of failed fuel rods and the associated release of radioactive materials from the rods; the convective transport of aerosolized or vaporized radionuclides throughout the cask interior and their deposition either within the cask or their release to the environment; and the input of heat from a postulated exterior pool fire and from the radioactive decay of radionuclides in the spent fuel. Modeling of heat transport is important because surface and gas temperatures strongly affect radionuclide transport and deposition. Heat transport processes modeled included: conductive heat transport through cask components; convective and radiative heat transport from the cask fins to the environment or from a pool fire to the fins; and convective and radiative heat transport inside the cask. The cask hydraulic input model included: the depressurization gas flows from failed fuel rods, the subsequent pressurization of the cask, and the depressurization of the cask to the environment through a postulated failed cask seal. The fission products released from the fuel were followed until they were either deposited somewhere within the cask or transported from the cask to the environment. MELCOR Version 1.8.3-PS was used to analyze the TN-125 shipping cask without any code modifications, i.e., all of these physical processes and transport paths were modeled using existing user input options.

4.1 Fuel Rod Depressurization Model

Accurate modeling of the depressurization of failed spent fuel rods is potentially very complex, i.e., the depressurization rate depends upon a number of poorly known parameters which are likely to differ from fuel rod to fuel rod. Unlike new fuel with its clearly defined cladding gap, irradiated fuel pellets and their cladding have undergone physical and dimensional changes. Fuel pellets crack and swell, the cladding creeps down onto the pellets, and the original cladding gap may disappear completely with its free volume relocating into pellet interiors in the form of cracks and voids (bubbles). Impact forces from postulated collisions could further fragment the pellets increasing the amount of fuel fines present in the rods. Whereas new fuel would depressurize by helium flows through the cladding gap to the location of cladding failure, the depressurization flows from spent fuel must pass through the cracks in the fragmented fuel pellets. The flow resistance depends on the spectrum of crack widths and shapes, and on an effective flow length which is likely significantly longer than the linear geometric length of fuel parallel to the flow pathway through the network of cracks. Entrainment of fine particles of fuel in the depressurization flows may lead to the plugging of cracks which would diminish subsequent flows and fission product release from failed rods to the cask interior.

The depressurization flow will also depend upon the location of cladding failure, i.e., a fuel rod failing in its upper plenum region which contains roughly 40% of its gas volume will depressurize faster than a rod failing at its bottom end from where more of the rod gas must work its way through the cracks in the pellets before reaching the failure location. Because fuel rod failure is somewhat more likely near the rod center than near its ends, the failure location and the size of the failures should each be described using probability functions. According to Reference 6, rupture hole sizes, produced during fuel rod failure experiments, were estimated to be about 2 mm² in area and less than 1 cm in length.

The pressurized PWR fuel rods transported in the shipping cask were postulated to fail either directly by collision impact forces or indirectly by over pressurization due to heat from an engulfing pool fire surrounding the cask. A TN-125 cask fully loaded with 12 Westinghouse 15 x 15 spend fuel assemblies contains 2448 fuel rods (12 x 204). During a ship collision, a large fraction of the fuel rods within the TN-125 cask are expected to fail. The conservative assumption is to assume that all 2448 fuel rods fail.

The scope of this study did not allow the development of a detailed and accurate fuel rod depressurization model, even if one is possible with available data. Further, a detailed model was not required for the postulated accident scenarios of greatest interest, i.e., scenarios where the cask seal failure results in a relatively small hole size. For these scenarios, the cask depressurizes much slower than the fuel rods, therefore the accuracy with which fuel rod depressurization is modeled does not significantly affect the retention of radionuclides within the cask.

A relatively simple fuel rod depressurization model was developed for this study. The model treated gas flow from all of the failed fuel rods as a single equivalent flow. The model was developed from limited data using engineering judgement, and was refined by performing trial calculations. The model consists of one control volume that represents the combined gas volume within all the failed rods and one flow path simulating friction and form losses. The model assumes that all rod gases must flow through the same flow resistance which is obviously not the case since the gases are distributed throughout the crack network within the pellets in the rod.

Experimentation with the spent fuel rod model indicated that spent fuel rods would most likely depressurize within a few minutes; whereas a model of a new unirradiated (fresh) fuel rod with a fuel-cladding gap that has not closed up, predicted depressurization in a few seconds if the cladding rupture area is roughly equivalent to or is larger than the gap area. Moreover, it may be possible for fine fuel fragments to partially block the cladding rupture thereby causing the depressurization to take a significantly longer time, however this was not deemed very likely to happen to a significant number of rods. In reality, there will likely be a spectrum of depressurization times if all 2448 fuel rods in a fully loaded cask failed. Some rods may depressurize in seconds and a few may take tens of minutes. The probability distribution is likely to center around the first couple of minutes and have a long tail that extends to much longer times.

The parameters of the fuel rod depressurization flow model are listed in Table 4-1 for both an irradiated spent fuel rod, where depressurization flow is through a network of cracks in the irradiated pellets, and for a new unirradiated fuel rod, where depressurization flow is through the fuel cladding gap. The parameter values for irradiated fuel were based on new fuel design parameters from the Zion Updated Final Safety Analysis Report (UFSAR) [7], on scaling cracks and cladding gaps shown in pictures of spent fuel cross-sections [Figures I-12 and I-13 of Reference 6], and on engineering judgment.

Several assumptions were required to complete this model. The cross sectional flow area of a spent fuel rod was assumed bounded by the sum of the cross sectional areas of the individual cracks in a pellet. Whereas, the cross sectional flow area of a new fuel rod was taken to be the cross sectional area of the fuel-cladding gap. Since many of these cracks effectively dead end and many of the cracks are too narrow to support significant flow, the effective flow area of a spent fuel rod must be significantly reduced from that of a new fuel rod. Based on the referenced pictures of spent fuel pellets, an effective flow area of 10% of the original fuel-cladding gap area was used in the rod depressurization model. In a similar manner, the effective flow path length was estimated to be 50% longer than the linear geometric length of the fuel; the flow hydraulic diameter was based on flow through cracks with an effective width of 10% of the cladding thickness; a form loss coefficient of 10 was applied to flow through each of 240 fuel pellets; and the surface roughness was 25% of the crack width. The size of the cladding rupture was assumed to not add any additional flow resistance. The total flow resistance for the old fuel, as modeled, is 430 times larger than the flow resistance of new fuel.

The free gas volume for a Westinghouse 15 x 15 fuel rod was estimated using data from the Zion FSAR. It was assumed that the total free gas volume of a spent fuel rod is the same as its unirradiated free volume. The total free space within a new fuel rod includes the volume of the upper gas plenum, the volume of the fuel-cladding gap, and the volume of the dish spaces between individual fuel pellets. The total volume was estimated, as shown in Table 4-2, by subtracting the volume of fuel and the volume of the Inconel spring from the internal volume of the cladding tube. The fuel volume was estimated from the total core load using the UO_2 95%-theoretical density of 10.5 gm/cm^3 . The spring volume was estimated to be 1 cm^3 per rod. The calculation of the free gas volume is relatively sensitive to the accuracy of dimensions used. The free gas volume of 34 cm^3 is deemed an overestimate because the spring volume is likely an underestimate. Thus, the estimate of free gas volume is believed to be conservative with respect to its affect on depressurization. The free gas volume distribution is 42.1, 30.2, and 27.7% for upper gas plenum, the fuel-cladding gap, and the pellet dishes, respectively.

PWR fuel rods are generally filled with helium during fabrication to reduce stress to the cladding when the rods are subjected to reactor operating pressures which are typically about 2250 psia. The as-fabricated fuel rod pressure varies with fuel rod design. The TN-125 SAR states that the initial helium pressure for a Westinghouse 15 x 15 fuel rod is 6.5 MPa (943 psia) but fails to specify the temperature of the rod during the filling procedure. The SAR further states that the fuel rod pressure is 7.6 MPa (1102 psia) at 38°C (100°F) after irradiation when rod gases

Table 4-1: Fuel Rod Depressurization Flow Parameters

| Parameter | Units | New Fuel | Irradiated and Fragmented Fuel | Assumptions and Comment for Modeling Irradiated Fuel |
|---------------------------|-----------------|--|---|--|
| Gas Volume | m ³ | 0.0833 | 0.0833 (2448 rods) | 34 cm ³ /rod |
| Gas Pressure | MPa | 17.1 | 20 | At 538 °C (1000 °F) |
| Flow Area | m ² | 6.88 x 10 ⁻³ (Fuel-Clad Gap) | 6.878 x 10 ⁻⁴ (2448 rods) | Effective Area for Irradiated Fuel = 10% of New Fuel Gap Area |
| Length of Flow | m | 3.66 (Active Fuel Length) | 5.49 | Effective Flow Length = 150% of Active Fuel Length |
| Hydraulic Diameter | m | 1.9 x 10 ⁻⁴ (Fuel-Clad Gap) | 1.2 x 10 ⁻⁴ | Effective Width of Crack Flow Pathways = 10% of Clad Thickness |
| Form Loss Coefficient | - | 2 | 2400 | K=10 for each of the 240 fuel pellets in a rod |
| Surface Roughness | m | 1.5 x 10 ⁻⁵ | 1.5 x 10 ⁻⁵ | 25% of Crack Width |
| Roughness/Diameter | - | 0.081 | 0.125 | |
| Friction Factor | - | 0.093 | 0.118 | |
| Friction Loss Coefficient | - | 1776 | 5244 | |
| Total Loss Coefficient | - | 1787 | 7644 | |
| Flow Resistance | m ⁻⁴ | 1.88 x 10 ⁷ | 8.08 x 10 ⁹ | Ratio = 430 |

include fission product gases in addition to the original helium fill gas. If the 6.5 MPa pressure was also measured at 38 °C, then the production of fission product gases causes rod pressures to increase by about 17 percent. The TN-125 SAR states that during normal transport, rod temperatures are about 538 °C and thus rod pressures are about 20 MPa (2901 psia). Because spent fuel pressures at a normal reactor operating temperature of 371 °C (700 °F) are about 15.7 MPa (2280 psia), this pressure increase is in good agreement with the perfect gas law. Accordingly, the fuel rods in the rod depressurization model were all initialized at 20 MPa and 538 °C which is deemed to be conservative with respect to fission product release from failed rods.

Table 4-2: Fuel Rod Free Gas Volume Estimate

| Dimensions | (cm) |
|---------------------------|--------------------|
| Active Fuel Length | 365.8 |
| Gas Plenum Length | 20.3 |
| Cladding Outside Diameter | 1.072 |
| Cladding Thickness | 0.062 |
| Cladding Inside Diameter | 0.948 |
| Pellet Diameter | 0.929 |
| Volumes | (cm ³) |
| Inside Cladding Tube | 272.7 |
| Uranium Oxide Fuel | 237.7 |
| Inconel Spring | 1 |
| Free Gas Volume | 34.0 |

The TN-125 SAR notes that during transportation fuel assemblies may contain control rods. A review of several PWR FSARs indicated that control rods are also filled with pressurized helium. However, since there are no more than 20 control rods per assembly and pressurization data was not readily available for control rods, depressurization of control rods was not considered in these calculations.

Rod depressurization times and helium flow velocities through the hole in the failed rod for fuel rods that contain fresh and spent fuel as calculated using the fuel rod depressurization model are shown in Figures 4-1a and 4-1b. The results shown were calculated assuming that the cask had not failed and that all of the 2448 fuel rods had failed simultaneously. Full depressurization of a spent fuel rod, as modeled, takes about 3 minutes, whereas a new fuel rod depressurizes in a few seconds.

The free gas volume within the TN-125 cask when fully loaded with 12 Westinghouse 15 x 15 fuel assemblies is 2.68 m³ [1]. During transport, this volume is pressurized to 0.05 MPa (half atmosphere) with nitrogen gas. If during a ship collision all the fuel rods fail and depressurize into the internal volume of the TN-125 cask, then the resulting equilibrium pressure in the cask would be 0.64 MPa (93 psia). Moreover, as Figure 4-1b shows, the helium flow velocities through the spent fuel pellets is fast enough that fuel fines located along the flow pathway would likely be entrained into the gas flow.

Although, there is considerable uncertainty in the actual performance of spent fuel during depressurization, this model indicates that depressurization is relatively rapid compared to the depressurization of a failed shipping cask with a slow leak to the environment through a small hole. Therefore, this simplified fuel rod depressurization model is judged to be adequate to support the primary objectives of this study.

4.2 Shipping Cask Hydraulic Model

The transport of radionuclides as aerosols and vapors from the location where they are expelled from the failed fuel rods to and through the failed cask seal to the environment occurs by convective transport through the cask. Further, the deposition of radionuclides within the cask depends upon the convective flow paths within the cask that are followed by the radionuclides. Convective flow through the cask would be driven by the depressurization helium flows from the ruptured fuel rods and/or by thermal expansion of cask and rod gases due to heating of the shipping cask by a postulated engulfing pool fire. The calculations performed verified that total convective gas

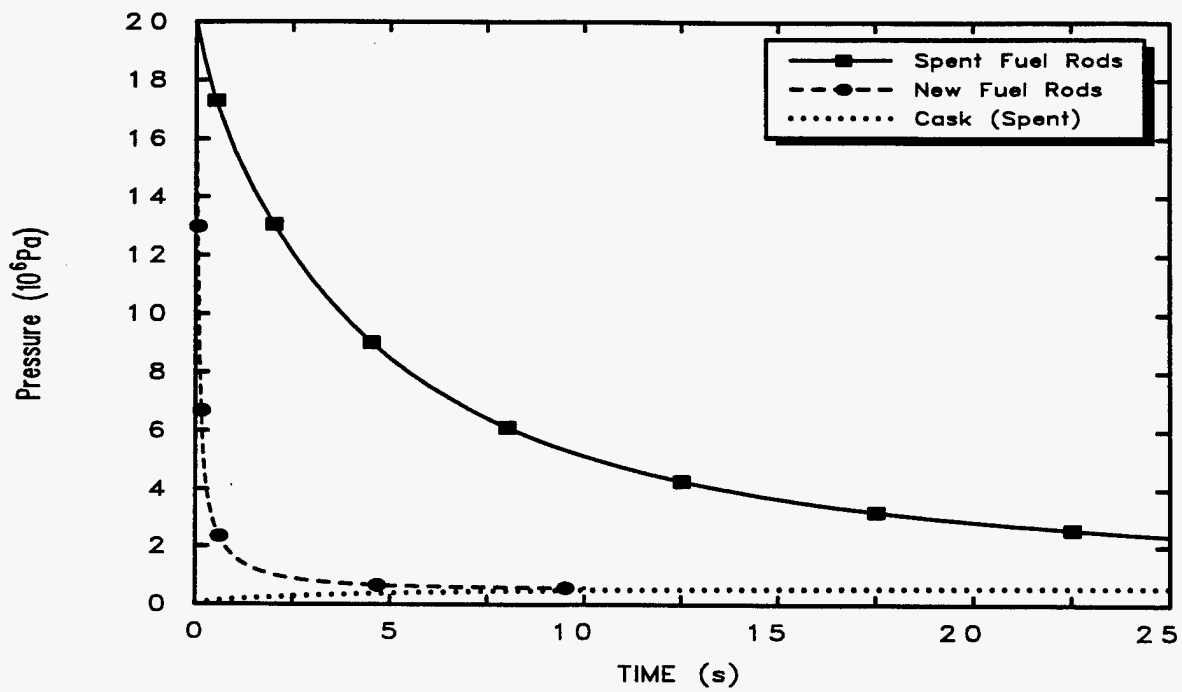


Figure 4-1a: Fuel Rod Depressurization

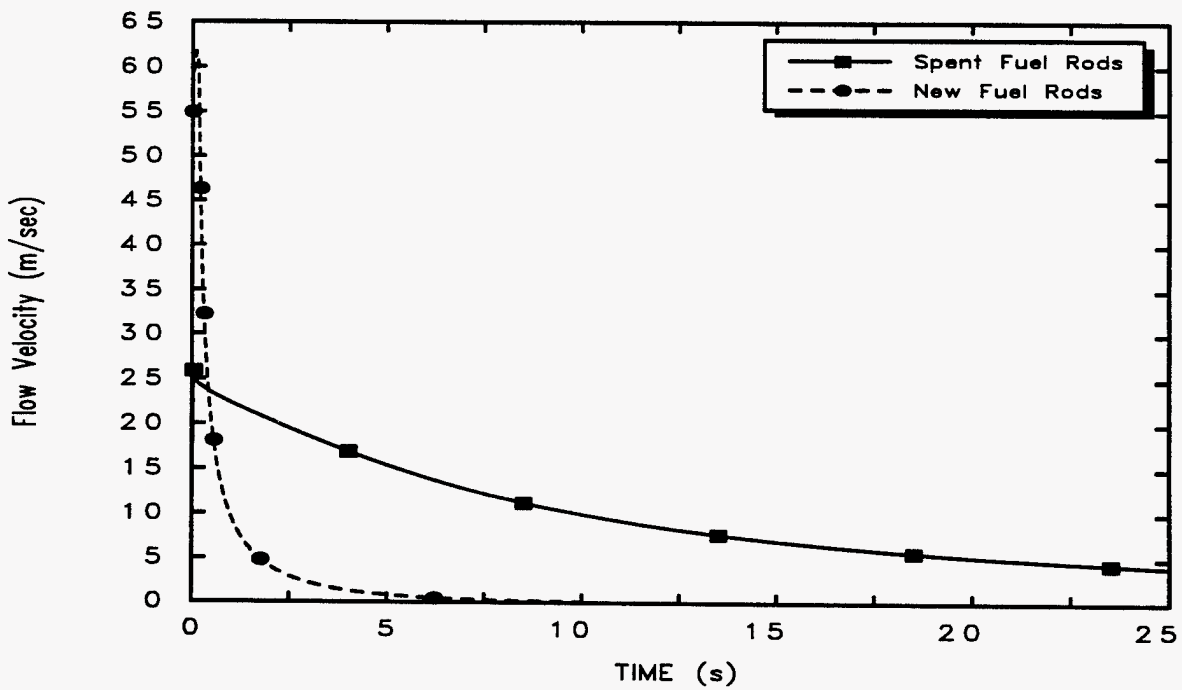


Figure 4-1b: Fuel Rod Helium Flow Velocity

flows would be dominated by the fuel rod depressurization flows. Since many radionuclide deposition and coagulation processes are strongly dependent upon surface and gas temperatures, the cask hydraulic model had to be coupled with the cask thermal model described in the Section 4.3. In fact, some important radionuclide species will be volatile at the temperatures encountered in the accident scenarios studied.

The TN-125 shipping cask, which is normally operated with an 0.05 MPa (1/2 atmosphere) nitrogen atmosphere, will be pressurized by the helium expelled from failed fuel rods. The amount of pressurization and the subsequent dispersion and deposition of radionuclides within the cask will depend upon the number of fuel rods failed and the size of the failure of the cask seal. A slower cask depressurization provides more time for radionuclides to deposit on cask interior surfaces before the pressurized gases leak from the cask, carrying radioactive aerosols and vapors with them. Thus, longer cask depressurization times reduce fission product releases to the environment.

For the MELCOR input, the free space within the TN-125 cask interior was subdivided into eight control volumes as shown in Figure 4-2. The volumes were designated with a letter "V" followed by a number. Each control volume is characterized by individual values of gas pressure, gas temperature, and radionuclide densities. Table 4-3 provides the volume and initial temperature of each control volume.

Table 4-3: Hydraulic Model Control Volumes

| Identifier | Volume Description | Volume (m ³) | Initial Temperature (°C) |
|------------|-----------------------------------|--------------------------|--------------------------|
| V1 | Fuel Lodgment - Upper Section | 0.325 | 477 |
| V2 | Fuel Lodgment - Upper Mid Section | 0.325 | 477 |
| V3 | Fuel Lodgment - Center Section | 0.325 | 477 |
| V4 | Fuel Lodgment - Lower Mid Section | 0.325 | 477 |
| V5 | Fuel Lodgment - Bottom Section | 0.325 | 477 |
| V6 | Lower Cask Region | 0.23 | 165 |
| V7 | Basket Center Space (Cross) | 0.591 | 279 |
| V8 | Upper Cask Region | 0.233 | 165 |

The 12 fuel assembly lodgments were modeled using five control volumes that represented all the free space within the fuel assemblies and all the free space between the assemblies and the lodgment walls. Each lodgment, which is slightly longer than a fuel assembly, is a solid-walled square box open on each end. Thus, the fuel rod depressurization flows can only exit the lodgments at its ends. The lodgments were combined into one equivalent composite lodgment because their behaviors were expected to be similar during the postulated scenarios studied. Eight of the lodgments are symmetrically located around the outer portion of the basket and 4 are located towards the center of the basket (see Figure 2-2). In order to model the cask with one-dimensional thermal and engulfing pool fire models, the 8 outer and the 4 inner assemblies needed to be treated alike. A review of heat transport analyses performed with two-dimensional heat transport codes [6] showed that conduction of heat through the basket was rapid enough compared to heat transport from fuel rods to the basket that the temperatures of the inner 4 lodgments and the fuel assemblies they contain would be close enough to the temperatures of the 8 outer lodgments and their fuel assemblies that all of the lodgments and assemblies could be treated identically for the purposes of this study.

Subdividing the representative lodgments into a set of five axial control volumes allowed the MELCOR code to predict radionuclide densities along the length of the fuel assemblies. Obviously these densities and deposition rates should be highest near the location of the postulated fuel rod ruptures. In fact, the majority of the deposition of fuel fines was found within the control volume containing the rupture location. The remaining free space regions, i.e., the free space below the basket, the free space above the basket, and the free space interior to the basket, were each adequately described by a single control volume. The free spaces of the basket interior were dominated by the space

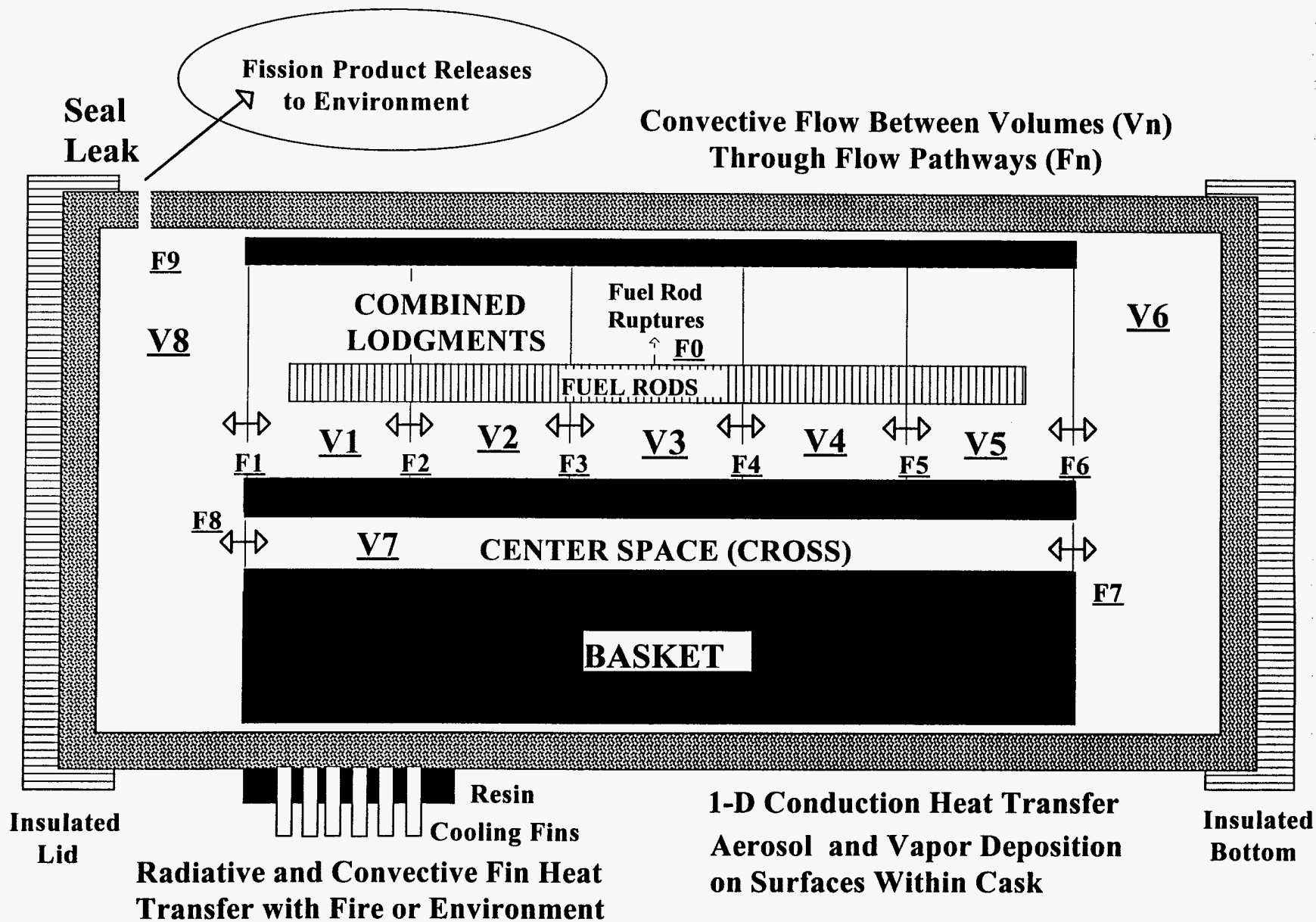


Figure 4-2: TN12 Shipping Cask Hydraulic Model

within the basket cross. Flows through the bottom region and the basket cross and the corresponding radionuclide deposition within these spaces were subordinate to the flows exiting the lodgments to the upper region containing the leak through the cask seal.

Control volumes were connected by means of flow paths designated with the letter "F" followed by a number. These flow paths are shown in Figure 4-2 and the values of their flow parameters are provided in Table 4-4. Flows move through the channels of the fuel assemblies with little resistance, as expected, because the fuel assemblies were designed to minimize pressure losses during reactor operation (the flow resistance is defined as the sum of the form and friction loss coefficients divided by two times the flow area squared.). The primary resistance to flow through these channels is caused by the grid assemblies that hold the rods in place. A form loss coefficient of 1.2 was applied to each grid assembly. The center cross space, by contrast, has a much larger resistance to flow due to the 48 perforated steel plates placed at intervals inside the cross region to reinforce the basket assembly.

Table 4-4: Hydraulic Model Flow Pathways

| Identifier | Pathway Description | Flow Area (m ²) | Form Loss Coefficient | Friction Term | Flow Resistance (m ⁻⁴) |
|----------------|---|-----------------------------|-----------------------|---------------|------------------------------------|
| F0 | Fuel Rod Ruptures | 6.88×10^{-4} | 2400 | 5244 | 8.1×10^9 |
| F1 | Exit from Fuel Lodgments into Cask Upper Region | 0.398 | 1.5 | 0.48 | 6.3 |
| F2, F3, F4, F5 | Intermediate Lodgment Pathways | 0.398 | 2.4 | 0.96 | 10.6 |
| F6 | Entrance to Fuel Lodgments from Bottom Region | 0.398 | 1.5 | 0.48 | 6.3 |
| F7 | Entrance to Cross from Cask Bottom Region | 0.189 | 200 | 0.64 | 2820 |
| F8 | Exit From Cross into Cask Upper Region | 0.189 | 200 | 0.64 | 2820 |
| F9-S | Small Cask Seal Leak | $4. \times 10^{-6}$ | 5 | 7 | 3.8×10^{11} |
| F9-L | Large Cask Seal Leak | $1. \times 10^{-4}$ | 5 | 7 | 6.0×10^8 |

Flow through the gap between the basket and the inner steel surface of the cask shell was not modeled. The basket and vessel were machined to ensure a radial gap between 1 and 2 mm at 20 °C. However, the inner vessel wall temperature, when operated at peak conditions of 12 fuel assemblies with 10 kW of decay power per assembly, would be about 216 °C and would become considerably hotter when the cask is heated by a postulated engulfing pool fire. Since the aluminum basket expands faster with temperature increases than does the steel vessel, this gap would be much smaller or could even disappear during the accident scenarios studied. The SAR stated that the basket to vessel radial gap was estimated to be 0.135 mm at 216 °C. In any case, flow through the basket-vessel gap would be minor and would not significantly impact the results.

Two different cask seal leak paths are shown in Table 4-4, i.e., F9-S and F9-L, which respectively represent a small and a large cask seal failure. Two different types of cask pressurization and radionuclide release behavior are characterized by these paths. The smaller path has a flow area of 4 mm² and the larger path has an area of 100 mm². Their flow resistances simply vary with the square of their flow areas. The smaller leak path has a flow resistance almost 50 times greater than the fuel rod depressurization resistance obtained using the fuel rod depressurization model. Therefore, the cask would be expected to pressurize upon fuel rod depressurization. The larger leak path has a lower resistance than the fuel rod failure path, however since the fuel rods are initially at high pressure, the cask would still be expected to pressurize but would then depressurize rather quickly. The MELCOR calculations verified this expected behavior.

The hydraulic shipping cask model also included a model to control the gas temperature in the free space immediately surrounding the cask. This gas temperature determined the rate of convective and radiative heat transfer to and from the cask fins. When a fully engulfing fire was postulated, the temperature of the gasses in this region

was set to the average temperature of the fire. When a pool fire was not postulated, the temperature of this region was set to an appropriate ambient environmental temperature. Further, the flow of gasses through this region removed heat rejected from the cask, thereby preventing a temperature buildup.

4.3 Shipping Cask Thermal Model

A thermal model was developed that predicted both the surface and the gas temperatures within the cask which are needed by the MELCOR models that predict radionuclide deposition and transport. Cask pressurization and depressurization were both temperature dependent processes. Several of the radionuclide deposition transport processes were also temperature dependent. Radionuclide species, such as CsOH and CsI, were volatile at some of the temperatures encountered in the accident scenarios studied. Thus, both aerosol and vapor processes, especially the temperature dependence of their vapor pressures, affected their deposition and transport. The heat transport processes which required modeling within the TN12 cask included:

- heat exchange between the cooling fins and the ambient environment during normal operation including solar insolation,
- heating of these fins by a postulated fully engulfing pool fire,
- heat conduction through the fins, resin layer, and steel shell of the cask,
- heat transport through the gap between the cask and the basket,
- heat conduction through the basket,
- heat transport through the gap between the basket lodgment walls and the fuel assemblies,
- heat transport within the fuel assemblies,
- convective heat transport from the fuel rods to the lodgment gases,
- convective heat transport from the lodgment gases to the lodgment walls,
- and heat transport to structures in the end regions of the cask.

The heat transport processes modeled directly by the MELCOR code include one-dimensional heat conduction through structures and heat transfer between the surfaces of these structures and their surrounding atmospheres by convective and radiative processes. Other heat transport processes, such as surface to surface radiative heat transfer can be modeled indirectly by implementing the appropriate equations into MELCOR's unique control function logic and applying the computed heat fluxes to the appropriate structures using the surface boundary conditions selected for those structures.

Since some heat transport processes, such as the two-dimensional nature of the basket heat conduction, were beyond the capability of the MELCOR code, several key assumptions were required in developing the cask thermal model. These assumptions included:

- the cask along the length of the basket was treated as a one-dimensional symmetric cylinder that had a uniform diameter and wall thickness along its entire shell length,
- axial heat conduction was neglected except for conduction through the steel shell of the cask to its end regions,
- the 2-D basket, resin layer, and cooling fins were modeled as equivalent 1-D heat conducting cylinders,
- the fuel assemblies were treated as 1-D cylinders of homogenized fuel,
- the homogenized fuel properties for assemblies shipped in helium were used rather than properties for assemblies shipped in nitrogen because properties for assemblies homogenized in nitrogen were not readily available (properties were homogenized with a detailed two-dimensional heat conduction code, not MELCOR),
- the basket thermal conductivity is high enough that all 12 fuel assemblies behave identically regardless of their location within the basket,
- the peak rated decay heat power of 120 kW for the cask contents was used and this heat was dissipated from the cask entirely through the cask's cooling fins,
- the decay power was uniformly distributed along the length of the fuel rods,
- the basket to cask radial gap was kept at a constant 0.135 mm (value specified in SAR for normal operating conditions),

- heat losses from the cask through the ends were neglected, because of the low thermal conductivity of the balsa wood impact limiters,
- the impact limiters are not damaged during any collision accident scenario,
- the resin was inert, although it would char during a fire, and
- gamma radiation heat transport was neglected.

The TN-125 thermal model is shown schematically in Figure 4-3. Details of the specific sub-models are now presented.

4.3.1 Normal Operating Environmental Conditions

The 10 CFR 71.71 [8] conditions of normal transport were used to specify the environmental conditions surrounding the TN-125 shipping cask except when the cask was engulfed by a postulated pool fire. Ambient temperature and pressure were set to 38 °C (100 °F) and to the pressure of a standard atmosphere. Full solar insolation of 1354 W/m² [6] was applied uniformly to the cask at the tips of the fins having an effective combined surface area of 31.24 m². 10 CFR 71.71 provides a normal transport solar insolation of 400 g-cal/cm² over a 12 hour period which converts to an average flux of 388 W/m². The solar flux of 1354 W/m², therefore represents a middle of the day solar flux. This solar insolation was applied before and after a surrounding pool fire but not during the fire, i.e., it was assumed that the fire and smoke would prevent the solar flux from reaching the cask.

4.3.2 Engulfing Pool Fire Conditions

The conditions of the pool fire determine the rate of convective and radiative heat transport to the cask cooling fins. The temperature of the fire in the TN-125 thermal model was a user specified input value. For all of the TN-125 calculations the temperature was specified as either 800 or 1200 °C. The heat flux to the cask fins was determined from an experimental correlation from Reference 9 which was developed for large cylinder calorimeters in open pool fires, for conditions where the calorimeters were cold relative to fire. This correlation was recommended by the lead author of Reference 9 as the most appropriate correlation for this study. This correlation provides a surface heat that was applied uniformly to the cask fin tip surface area. The pool fire correlation used is given by the following equation.

$$q_{cold} = 10.56 + 0.0597 T_{fire} + 6.97 \times 10^{-5} T_{fire}^2$$

where q_{cold} = the heat flux to a cold surface, kW/m²

T_{fire} = the fire temperature, °C

4.3.3 Cooling Fin Model

The copper cooling fins were an important part of the ability of the shipping cask to dissipate the decay heat released by the fission products in the spent fuel. The fins were welded to the outside surface of the steel shell of the cask, passed radially through the 4 inch thick hydrogenous resin neutron shield, and then extended into the ambient environment. Each fin was 0.33 m in length with about 1/3 of its length embedded in the resin layer and 2/3 extending into the ambient atmosphere. Cask cooling was accomplished by conducting heat up through the fins, then convecting or radiating the heat from fin surfaces to the environment. At normal operating conditions, convective processes dominated. During the postulated fire scenarios, the fire heat flux was radiated and convected to the fins with the radiative processes dominating. Since the approximately 60,000 fins were closely spaced, the radiative heat transport process principally involved only the tips of the fins and the environment, i.e., the geometric view factors from the fire to the interior resin and interior portions of the fin surfaces were small compared to the view factor from the fire to the fin tips. Conversely, the view factor from the resin surface to the atmosphere was small compared to the view factor from the fin tips to the atmosphere. In fact, the majority of the radiative heat exchange between an engulfing fire and the fins was from the fire to the outer couple of centimeters of the fins.

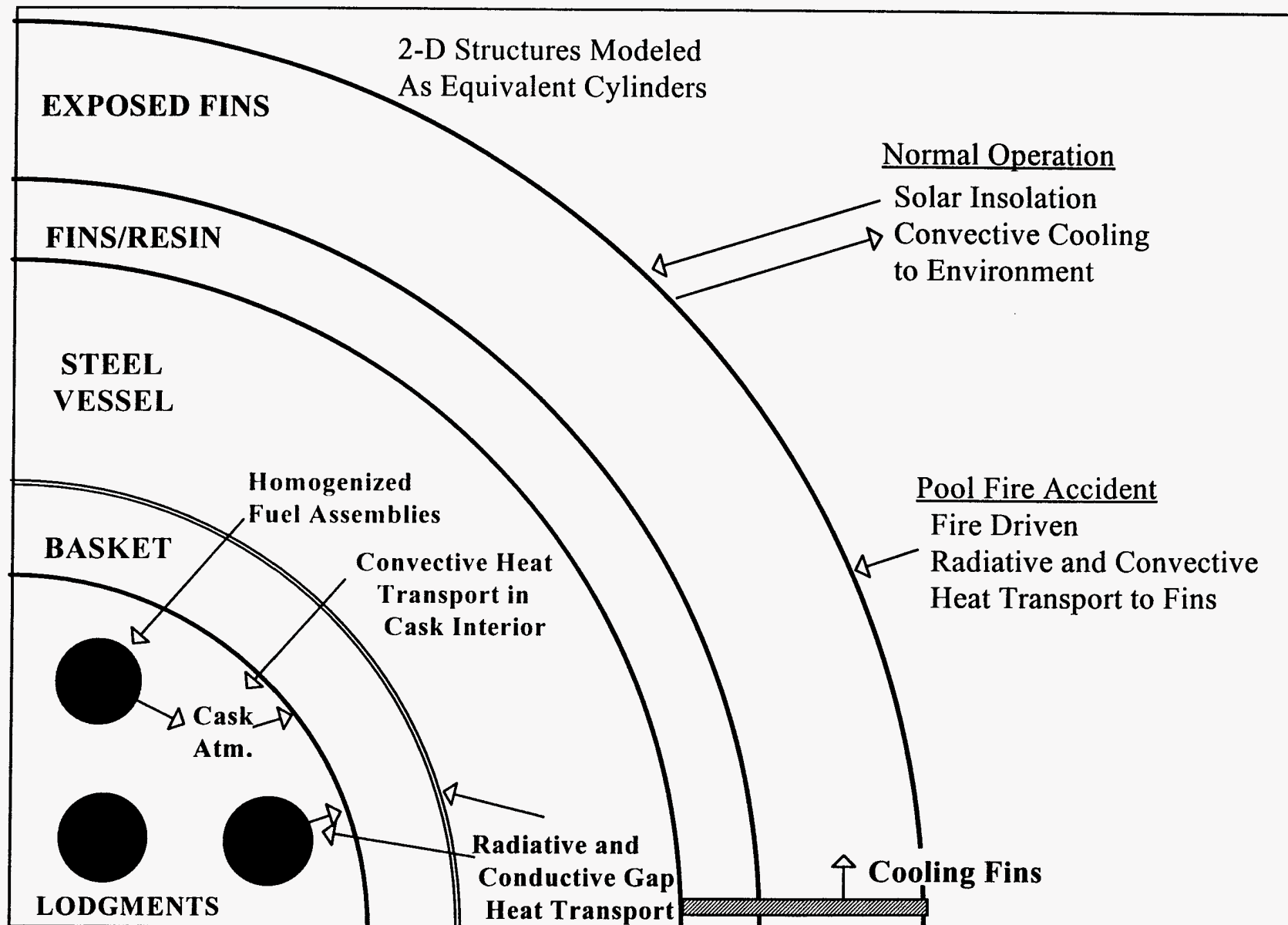


Figure 4-3: TN12 Shipping Cask Thermal Model

The fin heat transport model as illustrated in Figure 4-3 included: two equivalent conducting cylinders, the first simulating the resin layer and the first third of the fin lengths and the second simulating the two-thirds of the fin lengths that extend beyond the resin layer surface. The sum of the thicknesses of these two layers, i.e., 0.11 and 0.22 m, respectively, sum to the overall length of the fins, 0.33 m. The thermal properties of these two layers were set to values that (1) caused the amount of heat conducted through the layers to be the same as the amount that would be conducted through the fins under steady state normal transport conditions and (2) made the layers together have the same heat capacitance as the resin and fins have together. Heat was conducted between the steel shell and the resin-fin layer and between the resin-fin layer and the exposed fin layer with thermal resistances of zero assigned to their junctions. Since the majority of the radiative heat exchange was from the outer tips of the fins, heat radiating to or from the fins was simply applied to the outer surface of the exposed fin equivalent layer.

The convective heat exchange between the fins and the environment was considerably more complex to model since the convection process took place along the complete length of the exposed fins. An analytical steady state fin equation was developed to determine the heat convected to or from the fins along the length of the fin. This convected energy was either added to or taken from the equivalent cylinder heat structure using the internal energy source option of the MELCOR heat structure models. This fin model was shown to accurately predict fin cooling under steady state normal transport conditions and the model was deemed sufficient for the transient conditions of an engulfing pool fire because fin heating by the fire occurred predominantly by radiative heat transport to the fin tips followed by conduction to the cask body through the fins.

The textbook [10] differential equation for a one-dimensional uniform cross sectional area fin exposed to a surrounding fluid was solved using the initial conditions required by this model, i.e., the base temperature of the fin and the radiative heat flux to the fin tip are known. The textbook differential equation is:

$$\frac{d^2}{dx^2} T(x) = C \cdot (T(x) - T_o)$$

where $T(x)$ = the fin temperature as a function of the distance from base,
 T_o = the ambient temperature,
 C = hP/kA ,
 h = the convective heat transfer coefficient,
 P = the fin perimeter,
 k = the thermal conductivity of the fin,
 A = the cross sectional area of the fin.

The boundary conditions applicable to the TN-125 fins involved in a pool fire are:

$$T(0) = T_b$$

$$\frac{dT}{dx}(L) = \frac{q_r}{k \cdot A}$$

where T_b = the fin temperature at its base,
 L = the length of the fin,
 q_r = the total heat radiated from the tip of the fin.

This equation was solved for the temperature along the length of the fin.

$$T(x) = T_o + (T_b - T_o) \cdot \cosh(\sqrt{C} \cdot x) - \frac{\left[(T_b - T_o) \cdot \sinh(\sqrt{C} \cdot L) + \frac{q_r}{\sqrt{C} \cdot k \cdot A} \right] \cdot \sinh(\sqrt{C} \cdot x)}{\cosh(\sqrt{C} \cdot L)}$$

The heat convected from the fin, q_c , was found by subtracting the heat radiated away from the fin from the heat conducted through the base of the fin.

$$q_c = -k \cdot A \cdot \frac{dT(0)}{dx} - q_r$$

and

$$q_c = \frac{k \cdot A \cdot \left[(T_b - T_o) \cdot \sinh(\sqrt{C} \cdot L) + \frac{q_r}{\sqrt{C} \cdot k \cdot A} \right] \cdot \sqrt{C}}{\cosh(\sqrt{C} \cdot L)} - q_r$$

The total heat convected from the cask was:

$$Q_c = N_{fins} \cdot q_c$$

where Q_c = the total heat convected away from the cask,
 N_{fins} = the total number of fins welded to the cask.

The equivalent cylinder heat structure used to simulate the exposed fins was subdivided into 15 equally spaced segments. The distribution of the convected heat among the 15 segments was determined by:

$$f_n = \frac{h \cdot P \cdot \Delta x \cdot (T_n(x) - T_o)}{\sum_{i=1}^{15} [h \cdot P \cdot \Delta x \cdot (T_i(x) - T_o)]}$$

where f_n = the fraction of the total convected heat lost from each segment n ,
 Δx = the width of each segment.

During normal operation, the solar insolation was subtracted from the radiative cooling at the tips of the fins to obtain the total heat radiated away from the cask.

$$Q_r(\text{normal}) = \epsilon \cdot \sigma \cdot A_{\text{cask}} \cdot (T_{\text{fin}}^4 - T_o^4) - Q_{\text{solar}}$$

where Q_r = the total heat radiated from the fins,
 Q_{solar} = the total solar insolation to the cask,
 A_{cask} = the area of a cylinder defined by the tips of the fins,
 T_{fin} = the temperature at the tip of the fins,
 T_o = the ambient temperature,
 ϵ_{fin} = the effective emissivity of the fins,
 σ = the Stefan-Boltzmann constant.

The TN-125 fins are fabricated from copper plated with a nickel-chromium alloy. The emissivity of oxidized nickel ranges from 0.59 to 0.86. The TN-125 SAR used a value of 0.08 for the emissivity of the fins. However, the effective emissivity of the fin tips must include the effect of the spaces between the fin tips, i.e., these spaces would act as near black bodies to heat radiated into them. Approximately 11% of the cylinder defined by the fin tips was actually fin tip surface area. Applying the nickel-chromium emissivity to the 11% and a value of one to the other 89%, provided an effective emissivity for the fins that ranged between about 0.9 for non-oxidized and 0.97 for oxidized fins. An emissivity of 0.9 was used during this study.

The pool-fire correlation (q_{cold}) models an experimental heat flux to a large cold cylinder located within a test fire. The use of the term cold implies that the radiative heat lost from the cylinder back to the fire was not significant. During an engulfing pool fire, radiative heating of the cask was determined using a modified version of the pool fire correlation. Because the fins of a shipping cask engulfed by a pool fire would heat to temperatures near the average temperature of the fire, the experimental correlation for heating of the fins (pool fire correlation) was modified by multiplying the correlation by the ratio of the difference between the emissive powers of the fire and the heated fins and the difference between the emissive powers of the fire and the cold fins. Further, since the correlation measured the total heat flux to a large cylinder, a small amount of this energy was convected heat. Therefore, another modification to the correlation deleted an estimate of this convected heat prior to applying the emissive power ratio. The modified correlation is:

$$Q_r(\text{fire}) = A_{\text{cask}} \left[q_{\text{cold}} - h_{\text{fire}} (T_{\text{fire}} - T_{\text{cold}}) \right] \cdot \left(\frac{T_{\text{fire}}^4 - T_{\text{fin}}^4}{T_{\text{fire}}^4 - T_{\text{cold}}^4} \right)$$

where q_{cold} = the fire heat flux to a large cold cylinder,
 T_{fire} = the temperature of the fire,
 T_{fin} = the temperature of the fins in an engulfing fire,
 T_{cold} = the temperature of the cold cylinder,
 h_{cold} = the fire convective heat transfer coefficient.

The convective correction to the correlation had a relatively minor effect on the results but was included for completeness. The fire convection heat transfer coefficient was estimated to be $6 \text{ W/m}^2\text{°K}$ for the flow and temperatures conditions of an engulfing pool fire. The results from this equation were relatively insensitive to the temperature used for the cold cylinder, therefore a nominal value of 100 °C was used.

Heat conduction through the equivalent resin-fin layer was dominated by the conduction through the copper fins. The thermal conductivity of the copper was about 200 times that of the resin. Since the spaces occupied by the resin between the fins were relatively thin, the resin temperatures were expected to generally follow the temperatures of the fins. The properties of pure copper at 20 °C were used for the fins. The thermal conductivity of the resin was specified as $1/200$ that of the temperature dependent copper thermal conductivity. The SAR provided a density of 1500 kg/m^3 for the resin but the resin specific heat capacity was not known. Therefore, it was estimated from the specific heat capacities of several other organic polymers [11]. The heat capacities of these polymers suggested use of a value of 2000 J/kg°K for the heat capacity of the resin.

The effective density and specific heat capacities of the resin-fin equivalent layer were determined by volume averaging the properties of the copper fins and the resin. The volume-averaged equations were:

$$\rho_{\text{eq}} = \frac{\rho_{\text{cu}} \cdot V_{\text{cu}} + \rho_{\text{resin}} \cdot V_{\text{resin}}}{V_{\text{cu}} + V_{\text{resin}}}$$

and

$$C_{p\ eq} = \frac{\rho_{cu} \cdot C_{p\ cu} \cdot V_{cu} + \rho_{resin} \cdot C_{p\ resin} \cdot V_{resin}}{\rho_{eq} \cdot (V_{cu} + V_{resin})}$$

where ρ_{eq} = the density of the equivalent layer,
 ρ_{cu} = the density of pure copper,
 ρ_{resin} = the density of the resin,
 V_{cu} = the volume of the copper fins within the layer,
 V_{resin} = the volume of the resin,
 $C_{p\ eq}$ = the specific heat capacity of the equivalent layer,
 $C_{p\ cu}$ = the specific heat capacity of pure copper,
 $C_{p\ resin}$ = the specific heat capacity of the resin.

The effective thermal conductivity of the resin-fin equivalent layer was determined by summing the parallel thermal resistances of the fins and the resin to obtain an effective thermal resistance for the resin-fin layer and from that the thermal conductivity of the cylindrical equivalent layer. The equation for the effective thermal conductivity was:

$$k_{eq}(T) = \frac{\ln\left(\frac{r_o}{r_i}\right)}{2 \cdot \pi \cdot L_{cask} \cdot \Delta r} \cdot (k_{cu}(T) \cdot A_{fins} + k_{resin} \cdot A_{resin})$$

where $k_{eq}(T)$ = temperature dependent thermal conductivity of the equivalent layer,
 $k_{cu}(T)$ = temperature dependent thermal conductivity of pure copper,
 k_{resin} = the thermal conductivity of the resin,
 A_{fins} = the total cross sectional area of the fins,
 A_{resin} = the total cross sectional area of the resin,
 L_{cask} = the length of the portion of the cask with fins,
 r_o = the outer radius of the resin-fin layer,
 r_i = the inner radius of the resin-fin layer,
 Δr = the thickness of the resin-fin layer.

The equivalent properties for the exposed fins were obtained in a similar manner using the following equations:

$$\rho_{eq} = \frac{\rho_{cu} \cdot V_{cu}}{V_{layer}}$$

$$C_{p\ eq} = \frac{\rho_{cu} \cdot C_{p\ cu} \cdot V_{cu}}{\rho_{eq} \cdot V_{layer}}$$

$$k_{eq}(T) = \frac{\ln\left(\frac{r_o}{r_i}\right)}{2 \cdot \pi \cdot L_{cask} \cdot \Delta r} \cdot k_{cu}(T) \cdot A_{fins}$$

where V_{layer} = the total volume of the exposed fin layer.

The values of the thermal properties used to model heat conduction through the resin-fin and exposed fin equivalent layers are shown in Table 4-5.

The fin model was validated by using the model to simulate an experimental verification of the heat dissipation capabilities of the TN-125 cask. This validation is discussed in Section 5.1.

4.3.4 Steel Shell - Basket Gap

Cooling of the spent fuel or its heating by a surrounding pool fire requires the transport of heat across the radial gap between the basket assembly and the steel shell of the shipping cask. The width of this gap depends upon the temperatures of the basket and the shell. The basket and vessel were machined to ensure a radial gap between 1 and 2 mm at 20 °C. The inner vessel wall temperature, when the cask is transporting 12 fuel assemblies having 10 kW of decay power per assembly, was estimated in the SAR to be 216 °C. This temperature would certainly become hotter with the cask engulfed by a postulated pool fire. Since the aluminum basket expands faster with temperature increases than does the steel shell, the gap between the basket and the cask shell would likely decrease during the fire accident scenarios studied here. The SAR predicted a basket to vessel radial gap of 0.135 mm at 216 °C; however their prediction was based on the extrapolation of the coefficients of expansion beyond their ranges of validity. The basket could conceivably come into contact with the steel shell during a postulated fire scenario. Despite this possibility, the SAR radial gap of 0.135 mm was used throughout these calculations.

Table 4-5: Resin and Copper Fin Thermal Properties

| Property | Pure Copper | Resin | Resin-Fin Equivalent Layer | Exposed Fin Equivalent Layer |
|----------------------------------|-------------|-------|----------------------------|------------------------------|
| Density (kg/m ³) | 8950 | 1500 | 2540 | 1070 |
| Specific Heat Capacity (J/kg °K) | 383 | 2000 | 1200 | 383 |
| Conductivity (W/m °K) | | | | |
| 0 °C | 386 | 1.93 | 55.7 | 46.3 |
| 100 °C | 379 | 1.90 | 54.7 | 45.5 |
| 200 °C | 374 | 1.87 | 54.0 | 44.9 |
| 300 °C | 369 | 1.84 | 53.2 | 44.2 |
| 400 °C | 363 | 1.82 | 52.5 | 43.6 |
| 600 °C | 353 | 1.77 | 51.0 | 42.4 |

The basket-shell gap heat transport model included models for conductive and convective heat transport by the gas within the gap, and radiative heat transport across the gap, i.e., the total gap heat transport was the sum of the three components. The sign of the heat transport was positive for spent fuel cooling when heat transport is from the cask to the environment.

$$Q_{\text{gap}} = Q_{\text{cond}} - Q_{\text{rad}} - Q_{\text{conv}}$$

where Q_{gap} = the total gap heat transport,
 Q_{cond} = the conductive heat transport through the gap gas,
 Q_{rad} = the radiative heat transport across the gap,
 Q_{conv} = the convective heat transport through the gap gas.

Gap heat transport dominated the conductive process during normal spent fuel transport conditions. The conductive model used herein was simply the equation for heat conduction through a cylinder using the temperature dependent thermal conductivity of nitrogen gas from Reference 10 for nitrogen at the pressure of one standard atmosphere.

$$Q_{\text{cond}} = \frac{2 \cdot \pi \cdot k_n(T_{\text{gas}}) \cdot L \cdot (T_{\text{basket}} - T_{\text{shell}})}{\ln \left(\frac{r_{\text{basket}} + \Delta_{\text{gap}}}{r_{\text{basket}}} \right)}$$

where Q_{cond} = the conductive heat transport through the gap gas,
 $kn(T_{\text{gas}})$ = the temperature dependent thermal conductivity of nitrogen gas,
 L = the length of the basket-shell gap,
 T_{gas} = the temperature of the gas within the gap,
 T_{basket} = the temperature of the outer basket surface,
 T_{shell} = the temperature of the inner steel shell,
 r_{basket} = the outer radius of the basket,
 Δ_{gap} = the thickness of the gap (0.135 mm).

Radiative heat transport also contributed significantly to the heat transport across the gap during normal spent fuel transport conditions. The radiative contribution was even more significant during postulated accident scenarios involving a pool fire. The equation for radiative heat transport across a radial gap is:

$$Q_{\text{rad}} = \frac{2 \cdot \pi \cdot r_{\text{basket}} \cdot L \cdot \sigma \cdot (T_{\text{basket}}^4 - T_{\text{shell}}^4)}{\left[\frac{1}{\epsilon_{\text{basket}}} + \left(\frac{r_{\text{basket}}}{r_{\text{basket}} + \Delta_{\text{gap}}} \right) \cdot \left(\frac{1}{\epsilon_{\text{shell}}} - 1 \right) \right]}$$

where Q_{rad} = the radiative heat transport through the gap gas,
 ϵ_{basket} = the emissivity of the outer basket surface,
 ϵ_{shell} = the emissivity of the inner steel shell surface,
 σ = the Stefan-Boltzmann constant.

The thermal analyses presented in the TN-125 SAR used an emissivity of 0.55 for both the aluminum basket and the stainless steel clad cask shell. This value seemed too high for both surfaces. The largest emissivity listed for aluminum in the tables of References 10 and 12 is 0.33 for heavily oxidized aluminum at a temperature of 540 °C. The largest emissivity for stainless steel was 0.39 at a temperature of 820 °C. Since the gap heat transport was dominated by conduction (refer to Section 5.2) through the gas and information was not available regarding the actual surface conditions of the structures, the SAR value of 0.55 was used in the MELCOR input model. This emissivity produced slightly conservative results for the fire scenarios since the value likely overestimated the heat transport to the interior of the cask slightly.

Convective heat transport through the gases in the gap volume was modeled assuming (1) that the gap volume was not connected to any other volume in the cask model (i.e., that convective gas flow through the gap was negligible), and (2) that the properties of nitrogen would reasonably represent the properties of the gap gases. Given these assumptions, convective heat transport across the gap was modeled using two equations, one treating transport from the basket to gap gases, and the second transport from the gases to the cask shell. In both equations, heat was convected from the hotter surface to the gas and from the gas to the colder surface.

$$Q_{\text{conv}} = 2 \cdot \pi \cdot r_{\text{basket}} \cdot L \cdot h_{\text{mc}} \cdot (T_{\text{basket}} - T_{\text{gas}})$$

$$Q_{\text{conv}} = 2 \cdot \pi \cdot r_{\text{basket}} \cdot L \cdot h_{\text{mc}} \cdot (T_{\text{gas}} - T_{\text{shell}})$$

where Q_{conv} = the convective heat transport through the gap gas,
 h_{mc} = the convective heat transfer coefficient calculated by MELCOR.

The potential turbulence and pressurization of the gap gas resulting from fuel rod depressurization was not modeled because of the uncertainties associated with knowing the flow resistances through the gap and the relative unimportance of the convective heat transport across the gap. The affect of the gap pressurization on the thermal conductivity of the nitrogen gas was also not modeled. However, the increased thermal conductivity of a pressurized gas would have enhanced the conductive heat transport to the spent fuel during a fire scenario. This model deficiency likely did not impact the overall study conclusions.

In the MELCOR input model, a boundary surface input option (MELCOR heat structure Option 7) was used for the outer basket and the inner steel shell surfaces. This option applied both a surface power and a convective heat transfer to the surfaces. The conductive and radiative heat transport calculated by the equations above were removed from the outer basket surface as a negative surface power and applied to the inner steel shell as a positive surface power (during normal operating conditions). Further, the normal transport temperatures predicted by this model were in good agreement with those presented in the SAR (see Section 5.2).

4.3.5 Basket

The internal basket assembly of the TN-125 cask contains 12 square lodgments designed to hold PWR fuel assemblies (a cross section was shown in Figure 2-2). The assembly had an outer diameter of 1.218 m and the length in contact with the internal wall of the cask shell was 3.995 m. The square lodgments measured 0.227 m on each side. The basket was assembled from four individual sectors separated by a central free space in the shape of a cross. Perforated stainless steel 5 mm thick plates positioned along the vertical axis of the basket inside the cross region reinforce the basket assembly. The lodgment walls are formed by an arrangement of stainless steel wire mesh boxes containing sintered B₄C-Cu plates for neutron shielding. The B₄C-Cu plates are cast in aluminum alloy. The basket components were aligned by 8 pins and connected by 4 tie rods with locking nuts.

An accurate treatment of heat conduction through this basket would require a 2-D model of the structure. Since the MELCOR code used in this study has only 1-D heat conduction capability, the basket was modeled using an equivalent cylinder approach, i.e., the equivalent cylinder was assigned heat transfer properties that caused it to conduct the same quantity of heat from the lodgment walls as would be conducted by a 2-D model. A further implication of the 1-D MELCOR model was that all of the lodgment walls were assumed to be at the same temperature regardless of their radial location.

The acceptability of the 1-D equivalent cylinder approach was based upon an observation of the results of a similar 2-D calculation presented in Reference 6. These 2-D results illustrated that the temperatures of the inner fuel assemblies of a 21-assembly cask were similar to those of the outer assemblies. The implication of this observation was that the fuel-to-basket and the basket-to-shell thermal resistances were much larger than the resistance to conduction through the basket, which means that there is little variation in temperature along the radius of the basket.

The preferred method of benchmarking the equivalent cylinder model is to compare its performance with either experimental results or with a 2-D calculation for the same basket. Neither experimental data nor a 2-D calculation was available for the TN-125 cask. Therefore, the 1-D model relied heavily on engineering judgment. However, since the overall conclusions of this study were not highly sensitive to the predictions of this model, this 1-D equivalent cylinder model was deemed adequate for the purposes of this study.

The dimensions of the equivalent cylinder were the outside diameter and length of the basket and an inside diameter which yields a cylinder volume that equals the volume of the basket (1.218 m, 3.995 m, and 0.9655 m, respectively). The total mass and displacement volume of the basket, provided in the SAR, were 5740 kg and 1.73 m³, respectively. Therefore, the average density of the equivalent cylinder was this mass divided by the displacement volume, i.e., 3318 kg/m³.

The principal materials used to fabricate the basket were aluminum alloy, stainless steel, and copper containing boron carbide (B₄C-Cu plates). Once the quantity of copper was estimated from the dimensions of the B₄C-Cu plates, the volumes of the aluminum alloy and stainless steel were deduced from the total mass and volume. The resulting material composition of the basket is shown in Table 4-6.

Table 4-6: Composition of Basket

| Material | Density (kg/m ³) | Mass (kg) | Volume (m ³) |
|-----------------|---------------------------------|--------------|-----------------------------|
| Aluminum Alloy | 2650 | 3639 | 1.37 |
| Stainless Steel | 7860 | 1425 | 0.18 |
| Copper | 3850 | 676 | 0.18 |
| Totals | 3318 (ave) | 5740 | 1.73 |

The specific heat capacity for the basket was developed by assuming that the stainless steel and the copper components were uniformly distributed within the aluminum alloy.

$$Cp_{basket} = \frac{\rho_{al} \cdot Cp_{al} \cdot V_{al} + \rho_{ss} \cdot Cp_{ss} \cdot V_{ss} + \rho_{cu} \cdot Cp_{cu} \cdot V_{cu}}{\rho_{basket} \cdot V_{basket}}$$

where Cp_{basket} = the effective specific heat capacity for the basket,
 ρ_{al} = the density of the aluminum alloy,
 ρ_{ss} = the density of stainless steel,
 ρ_{cu} = the density of copper,
 ρ_{basket} = the average density of basket,
 Cp_{al} = the specific heat capacity of the aluminum alloy,
 Cp_{ss} = the specific heat capacity of stainless steel,
 Cp_{cu} = the specific heat capacity of copper,
 V_{al} = the volume of the aluminum alloy,
 V_{ss} = the volume of stainless steel,
 V_{cu} = the volume of copper,
 V_{basket} = the total displacement volume of basket.

The variation with temperature of the resulting specific heat capacities is shown in Table 4-7. The basket heat capacity was dominated by the heat capacity of the aluminum alloy. Since the type of aluminum alloy was not specified in the SAR, the temperature dependent heat capacity of pure aluminum was used to determine the basket heat capacity. Note that specific heat capacities for stainless steel and copper were assumed constant for the determination of the basket heat capacity. Because the basket temperatures exceeded the melting temperature of aluminum during extreme fire scenario conditions, the latent heat of fusion was incorporated into the aluminum heat capacity table (at 661 °C) to simulate basket melting (Melt relocation was not modeled.).

Heat conduction within the basket generally flows through the panels forming the walls of the spent fuel lodgments. Each of these panels includes a B₄C-Cu plate and stainless steel wire mesh embedded in aluminum alloy. The heat conduction through one of these panels was modeled as three parallel heat conducting surfaces. Thus, the thermal conductivity for heat conduction through a panel is:

$$k_{panel} = \frac{V_{al} \cdot k_{al} + V_{ss} \cdot k_{ss} + V_{cu} \cdot k_{cu}}{V_{basket}}$$

where k_{panel} = the effective thermal conductivity for a basket panel,
 k_{al} = the thermal conductivity of the aluminum alloy,
 k_{ss} = the thermal conductivity of stainless steel,
 k_{cu} = the thermal conductivity of copper,
 V_{al} = the volume of the aluminum alloy,
 V_{ss} = the volume of stainless steel,
 V_{cu} = the volume of copper,
 V_{basket} = the total displacement volume of basket.

Table 4-7: Basket Specific Heat Capacities

| Temperature (°C) | Pure Aluminum (J/kg-°K) | Stainless Steel (J/kg-°K) | Pure Copper (J/kg-°K) | Basket (J/kg-°K) |
|---------------------|----------------------------|------------------------------|--------------------------|---------------------|
| 0 | 892.6 | 460.5 | 400.0 | 726.9 |
| 40 | 910.2 | 460.5 | 400.0 | 738.0 |
| 80 | 928.1 | 460.5 | 400.0 | 749.4 |
| 120 | 946.0 | 460.5 | 400.0 | 760.7 |
| 160 | 964.1 | 460.5 | 400.0 | 772.2 |
| 200 | 982.2 | 460.5 | 400.0 | 783.7 |
| 240 | 1000.6 | 460.5 | 400.0 | 795.3 |
| 280 | 1018.2 | 460.5 | 400.0 | 806.5 |
| 320 | 1037.6 | 460.5 | 400.0 | 818.8 |
| 360 | 1056.3 | 460.5 | 400.0 | 830.6 |
| 400 | 1075.1 | 460.5 | 400.0 | 842.5 |
| 440 | 1094.1 | 460.5 | 400.0 | 854.6 |
| 480 | 1113.2 | 460.5 | 400.0 | 866.7 |
| 520 | 1132.4 | 460.5 | 400.0 | 878.9 |
| 560 | 1151.7 | 460.5 | 400.0 | 891.1 |
| 600 | 1171.2 | 460.5 | 400.0 | 903.5 |
| 640 | 1190.8 | 460.5 | 400.0 | 915.9 |
| 660 | 1200.6 | 460.5 | 400.0 | 922.1 |
| 661 | 40980 | 460.5 | 400.0 | 26137 |
| 670 | 40980 | 460.5 | 400.0 | 26137 |
| 671 | 1176.5 | 460.5 | 400.0 | 906.8 |
| 2000 | 1176.5 | 460.5 | 400.0 | 906.8 |

The heat conduction along these panels to each of the 48 lodgment wall sections was approximated by summing the contribution to each wall section and then adjusting the properties of the equivalent cylinder to match this sum. It was assumed that the contribution to each wall section could be determined from an estimated conduction length and a conduction area. The lengths and areas were estimated from a detailed engineering drawing in the SAR showing the details and dimensions of a quarter section of the basket. This process is illustrated by the following equation.

$$\frac{Q_{\text{tot}}}{\Delta T} = \frac{2 \cdot \pi \cdot L \cdot k_{\text{basket}}}{\ln\left(\frac{r_o}{r_i}\right)} = \sum_{i=1}^{48} \frac{k_{\text{panel}} \cdot A_{c_i}}{l_{c_i}}$$

where Q_{tot} = the total heat conducted through the basket,
 ΔT = the temperature difference across the basket,
 k_{basket} = the effective thermal conductivity of the equivalent cylinder basket,
 k_{panel} = the thermal conductivity of a lodgment wall panel,
 A_{c_i} = the effective heat conduction area for heat flow to a specific panel,
 l_{c_i} = the effective heat conduction length for heat flow to a specific panel,
 L = the length of the basket,
 r_o = the outer diameter of the basket,
 r_i = the inner diameter of the equivalent basket cylinder.

The resulting thermal conductivity for the equivalent basket cylinder is then:

$$k_{\text{basket}} = \left(\frac{48}{2 \cdot \pi}\right) \cdot \ln\left(\frac{r_o}{r_i}\right) \cdot k_{\text{panel}} \cdot \chi_{\text{ave}}$$

where

$$\chi_{\text{ave}} = \left(\frac{1}{48}\right) \cdot \sum_{i=1}^{48} \frac{\Delta t_i}{l_{c_i}}$$

and Δt_i = the effective heat conduction area divided by the basket length.

The value of χ_{ave} was estimated to be 0.053 and there is understandably a rather large uncertainty associated with the estimate. Had experimental data or an appropriate 2-D calculation been available, this estimate could have been determined from a comparison of the 1-D MELCOR model with the data or 2-D calculation. Since neither of these were available, the estimate was used without further substantiation. This estimate resulted in the effective basket thermal conductivities shown in Table 4-8.

4.3.6 Basket - Fuel Gap

The heat transport from the outer fuel rods to the lodgment walls was dominated by the radiative process but with a significant contribution from conduction through the nitrogen gas. This order of importance was the reverse of the order of importance for the basket-shell gap heat transport where conduction was dominant because the gap width between the fuel and the lodgment walls was about 46 times the gap width between the basket and the cask shell. For both gaps, the thermal resistance to conductive heat transport increases linearly with gap width.

Table 4-8: Basket Thermal Conductivities

| Temperature °C | Thermal Conductivities (J/kg-K) | | | | |
|-------------------|------------------------------------|-----------------|--------|-------|--------|
| | Aluminum | Stainless Steel | Copper | Panel | Basket |
| 0 | 159.2 | 16.3 | 385.9 | 167.2 | 15.7 |
| 20 | 164.4 | 16.3 | 385.9 | 171.3 | 16.1 |
| 100 | 181.7 | 17.3 | 379.0 | 184.5 | 17.4 |
| 200 | 193.8 | 17.3 | 373.8 | 193.5 | 18.2 |
| 300 | 201.0 | 19.0 | 368.6 | 198.9 | 18.7 |
| 400 | 205.0 | 19.0 | 363.4 | 201.5 | 19.0 |
| 600 | 206.0 | 22.5 | 353.1 | 201.7 | 19.0 |
| 2000 | 206.0 | 31.2 | 353.1 | 202.6 | 19.1 |

Convective heat transport was relatively minor except possibly during the relatively brief period of fuel rod depressurization. The convective heat transport process was, however, important in determining the temperatures of the gases in the channels between the fuel rods which in turn was important to the transport of volatile radionuclide species. The convective process is discussed in Section 4.3.8.

The radiative heat transport was determined by:

$$Q_{\text{rad}} = \frac{4 \cdot W_{\text{lodg}} \cdot L_{\text{fuel}} \cdot \sigma \cdot (T_{\text{fuel}}^4 - T_{\text{lodg}}^4)}{\left(\frac{1}{\epsilon_{\text{fuel}}} + \frac{1}{\epsilon_{\text{lodg}}} - 1 \right)}$$

where Q_{rad} = the radiative heat transport from the fuel to lodgment walls,
 W_{lodg} = the width of a spent fuel lodgment,
 L_{fuel} = the length of the active fuel,
 T_{fuel} = the temperature of the outer fuel,
 T_{lodg} = the temperature of the lodgment walls,
 ϵ_{fuel} = the emissivity of the outer fuel rods,
 ϵ_{lodg} = the emissivity of the lodgment walls,
 σ = the Stefan-Boltzmann constant.

The emissivity of 0.8 measured for typical PWR spent fuel [6] was used for the outer fuel rods and the SAR emissivity of 0.55 for basket surfaces was used for the lodgment walls.

The conductive heat transport was determined by:

$$Q_{\text{cond}} = \frac{4 \cdot W_{\text{lodg}} \cdot L_{\text{fuel}}}{\Delta_{\text{gap}}} \cdot k_n(T_{\text{gas}}) \cdot (T_{\text{fuel}} - T_{\text{lodg}})$$

where Q_{cond} = the conductive heat transport from the fuel to lodgment walls,
 W_{lodg} = the width of a spent fuel lodgment,
 L_{fuel} = the length of the active fuel,
 T_{fuel} = the temperature of the outer fuel,
 T_{lodg} = the temperature of the lodgment walls,

$k_n(T_{gas})$ = the temperature dependent thermal conductivity of nitrogen gas,
 T_{gas} = the temperature of gas in the fuel-lodgment wall gap,
 Δ_{gap} = the gap width.

The above equations were used to calculate the heat removed by radiative and conductive heat transfer from the surface of the equivalent cylinder used to represent a single fuel assembly. Because the TN-125 cask basket holds 12 fuel assemblies, this amount of heat was then scaled by a factor of twelve before it was deposited onto the inner surface of the equivalent cylinder simulating the basket.

4.3.7 Homogenized Fuel

The heat transport cooling the spent fuel assemblies involved the interaction of conductive, convective, and radiative heat transport among the individual fuel pins and the gases filling the spaces between the fuel rods. Heat conduction occurred both within the individual fuel rods and between rods through the surrounding gases. Heat was convected from the center of the fuel assembly to the outer regions by the circulation of gases. Heat was radiated from each fuel rod to other rods with a net radiative heat transport from the hotter center rods to the cooler outer rods. During normal transport conditions the convective heat transport tended to be minor compared to the heat conducted and radiated through the circulating gases.

Performing rod-to-rod conductive and radiative heat transport calculations is a complex process beyond the scope of this study. Therefore, the spent fuel assemblies were modeled as a single homogenized material structure that has a volume that equals the volume of the space occupied by the actual spent fuel assemblies.

Homogenized material properties for a 15 x 15 PWR spent fuel assembly in a helium environment were available in References 6. The density and the temperature dependent heat capacity of the homogenized equivalent cylinder were specified so that the homogenized structure had the same total mass and heat capacitance as that of the spent fuel assembly. In Reference 6, an effective temperature-dependent thermal conductivity for the homogenized spent fuel structure was derived using a 2-D finite-element thermal analysis code capable of modeling the rod-to-rod heat transport. These effective conductivities, which are a function of the complex interplay of conduction, convection, and radiation in the fuel pin array, were verified by comparison to temperatures measured in an instrumented spent fuel assembly. The material properties adapted from Reference 6 are shown in Table 4-9.

Table 4-9: Effective Thermal Properties of Homogenized Spent Fuel

| Temperature (°C) | Density (kg/m ³) | Specific Heat Capacity (J/kg-°C) | Thermal Conductivity (W/m-°C) |
|---------------------|---------------------------------|--|-------------------------------------|
| 24 | 4135 | 258 | 0.39 |
| 93 | 4135 | 269 | 0.50 |
| 260 | 4135 | 294 | 0.78 |
| 538 | 4135 | 306 | 1.23 |
| 815 | 4135 | 318 | 1.68 |
| 1093 | 4135 | 329 | 2.14 |

Since homogenized material properties were not available for a fuel assembly immersed in nitrogen gas, the helium homogenized spent fuel thermal properties were applied to the 1-D MELCOR spent fuel model for the TN-125 cask despite the fact that the TN-125 spent fuel was transported in nitrogen rather than helium. The use of homogenized properties for an assembly immersed in helium rather than nitrogen tended to over predict heat transport because the thermal conductivity of nitrogen gas is only about 18% of the thermal conductivity of helium. However, because of the spacing between the fuel rods (3.6 mm between nearest neighbors and 9.5 mm between diagonal neighbors), the

rod-to-rod radiative heat transport likely contributed more to the rod-to-rod heat transport than the conductive process. While the conductive heat transport was over predicted by a factor of about 5, the overall heat transport was probably only over predicted by a factor less than 2.

The primary impact of using the helium homogenized conductivity rather than a nitrogen-homogenized conductivity was in the prediction of the peak fuel temperatures at the center of the assembly, i.e., the predicted peak fuel temperatures would have been greater using a nitrogen homogenized thermal conductivity. But, the conductive process would have been compensated somewhat by the radiative process as the fuel temperature gradient increased. The spent fuel temperatures would have been increased until all of the decay heat was transported from the assembly. In retrospect, this model deficiency was not deemed to have significantly impacted study predictions of radionuclide transport.

The 1-D MELCOR spent fuel model consisted of 12 identical equivalent cylinders of a material represented by the helium homogenized thermal properties and with the fission product decay heat of 10 kW per assembly applied uniformly throughout the cylinders. The cylinders were cooled by radiative and conductive heat transfer to the lodgment walls and by convective heat transport to the nitrogen gas that surrounds each assembly. Axial heat transport within the fuel assemblies was not deemed important and was not modeled.

4.3.8 Convective Heat Transport Between Interior Surfaces and the Cask Atmospheres

Convective heat transport within the fuel assemblies and the spent fuel lodgments had relatively little impact on the heating and cooling of the spent fuel and of the shipping cask. This was particularly true during the conditions of normal transport with gas circulation driven by natural circulation processes since there was little driving force for natural circulation within the horizontally oriented shipping cask. Convection could be somewhat more important during the period of fuel rod depressurization where forced flow conditions existed, however this period was brief enough that its impact on the overall heating and cooling of the spent fuel was minor. The convective heat transport process was, however, important in determining the temperatures of the gases in the channels between the fuel rods that strongly affected the transport of volatile radionuclide species.

The MELCOR code contains models to predict convective heat transfer from the heat structures modeled. These models provide useful predictions only if they use the real surface areas of the structures modeled. Because the basket was modeled as an equivalent cylinder and the rods as homogenized cylinders, the surface areas of these simplified representations, especially the surface area of the equivalent cylinder used to represent the basket, are quite different from their real surface areas. Because the surface areas of these simplified heat structures were quite different from the surface areas of the actual structures they represented, convective heat transport from these structures as modeled by MELCOR would not have been realistic. This problem was resolved by deactivating convective heat transport to the lodgment atmospheres, as normally calculated by MELCOR, and implementing a more realistic model using MELCOR's control logic capabilities.

MELCOR control logic was used to calculate the heat convected to the lodgment atmospheres from the fuel rods and the lodgment walls. Because the equation used to calculate heat convection used the real surface areas of the fuel rods and the basket, its predictions of convective heat transport rates are reasonable. The heat calculated using the real surface areas of the rod and the basket was then added to the lodgment control volume atmospheres as a heat source and simultaneously removed from the structures that generated the heat (the fuel rods and the lodgment walls).

Convective heat transport to the atmospheres of the five axial lodgment volumes was predicted using:

$$Q_{c_i} = \left(\frac{12}{5}\right) \cdot \left[A_{rod} \cdot h_{rod} \cdot \sum_{j=1}^9 f_{v_j} (T_{f_j} - T_{g_i}) + A_{lodg} \cdot h_{lodg} \cdot (T_{lodg} - T_{g_i}) \right]$$

| | | |
|-------|------------|--|
| where | Q_{c_i} | = the convective heat transport to the lodgment gases, |
| | A_{rod} | = the active-fuel cladding surface area for each fuel assembly, |
| | h_{rod} | = a nominal convective heat transfer coefficient for normal transport, |
| | fv_j | = the volume fraction of each finite fuel interval j, |
| | T_{f_j} | = the temperature of each finite fuel interval j, |
| | T_{g_i} | = the temperature of lodgment atmosphere volume i, |
| | A_{lodg} | = the lodgment wall surface area around each fuel assembly, |
| | h_{lodg} | = a nominal convective heat transfer coefficient for normal transport, |
| | T_{lodg} | = the temperature of the lodgment walls. |

The 12/5 constant in this equation apportions the convective heat generated by the 12 fuel assemblies over the 5 lodgment control volumes that contain the assemblies. The homogenized fuel cylinder used to model the fuel assemblies was divided along its radius into 9 volumes separated by 10 equally spaced nodes. Nominal but realistic heat transport coefficients of 0.2 and 0.28 W/m²-K respectively, were applied to the fuel rods and to the lodgment walls. Constant heat transfer coefficients were used, rather than a correlation, because the constants provided needed numerical stability to the model and their values predicted reasonable results. During normal transport conditions, use of these constant coefficients in the preceding equation predicted a lodgment atmosphere temperature of 443 °C when the maximum fuel, outer fuel, and lodgment wall temperatures were 569, 375, and 279 °C, respectively. Thus, this model provided a reasonable temperature to the radionuclide transport models.

The temperature of the gases in the control volume that represents the center cross-region of the basket was predicted in a similar manner by:

$$Q_{cross} = A_{cross} \cdot h_{cross} \cdot (T_{lodg} - T_{g_{cross}})$$

| | | |
|-------|-----------------|---|
| where | Q_{cross} | = the convective heat transport to the center cross region gases, |
| | A_{cross} | = the surface area within the cross region, |
| | h_{cross} | = the convective heat transfer coefficient for the cross region, |
| | T_{lodg} | = the temperature of the lodgment walls, |
| | $T_{g_{cross}}$ | = the temperature of the cross region gases. |

The convective heat transfer coefficient, h_{cross} , calculated using the following turbulent natural circulation convective correlation for a horizontal cylinder [10], was found adequate for cross-region although the natural circulation may not always be turbulent.

$$h_{cross} = 1.24 \left(T_{lodg} - T_{g_{cross}} \right)^{\frac{1}{3}}$$

Convective heat transport in the two end regions of the cask was estimated using simple convective heat exchange between the end region heat structures and their respective atmospheres. Since the surface areas of these structures as modeled reasonably represented their actual surface areas, the end region convective heat transport was predicted using MELCOR's normal convective heat transport model.

4.3.9 Axial Heat Conduction to End Regions

The end regions of the TN-125 cask are surrounded by balsa and oak wood filled shock-absorbing covers to provide insulation and impact protection during transport. Thus, heat conduction through the base and lid of the cask (in the axial direction) is minor compared to heat conduction through the walls of the cask (in the radial direction) via cask fins. Because of this, in the TN-125 SAR, heat conduction is modeled as a 2-D problem that neglects the axial direction. Although heat transport through cask end structures can be neglected, because these structures have significant interior surface areas and are significantly cooler than the shell of the cask, radionuclide deposition onto

these structures is important, especially onto interior lid surfaces as cask failure usually occurs by failure of the lid seal. Therefore, to support the modeling of radionuclide deposition, models were needed to predict the temperatures of the atmosphere and surfaces along flow paths that connect lodgment control volumes to cask end region control volumes, particularly the lid region control volume.

Four cask end structures receive heat by conduction from the cask shell: the upper lid, the cask bottom, and the two portions of the cask shell that extend past the top and bottom of the fuel rods. These structures were modeled as simple 1-D heat structures. Convective heat transport was applied to their inner surfaces and an insulated boundary condition to their outer surfaces.

Since these end structures were physically connected to the steel shell of the cask, heat was conducted through the shell to the end structures. The following simple conduction equation simulated this conduction heat transport to the 1-D heat structure that represented each end of the cask.

$$Q_{\text{end}} = \frac{A_{\text{shell}}}{\Delta x} \cdot k_{\text{steel}}(T) \cdot (T_{\text{shell}} - T_{\text{end}})$$

where Q_{end} = the axial conductive heat transport to an end structure,
 A_{shell} = the cross sectional area of the shell at the end regions,
 Δx = a characteristic conduction length,
 $k_{\text{steel}}(T)$ = the temperature dependent thermal conductivity of the steel shell,
 T_{shell} = the average center section temperature of the steel shell,
 T_{end} = the average temperature of the end structure.

The heat conducted from the cask shell to each end structure was applied to each structure as an internal energy source term and simultaneously removed from the steel shell. One quarter of the active fuel length plus the distance from the end of the active fuel to the end structure was used as the characteristic conduction length. The performance of this simple model was sufficient to predict reasonable normal transport temperatures for the end structures (actual temperatures were not provided by the SAR). Further, during postulated fire accident scenario calculations, the temperature of the end structures slowly but steadily increased as would be expected.

4.4 Radionuclide Release and Transport Models

The primary objective of this study was to develop insights into the potential retention of fission products by the TN-125 shipping cask after their escape from PWR spent fuel rods to the cask interior due to rod failure during a postulated severe accident. Upon failure, rod depressurization would cause the helium and any gasborne fission products trapped in the rod to be expelled from the rod into the cask interior. The fission products expelled into the cask interior by rod depressurization would exist in three physical forms: aerosolized solid particles, noble gases, and vapors. The aerosolized solid particles would be comprised primarily of small particles of UO_2 , called fuel fines. Because they have the composition of bulk fuel, fuel fines will contain all of the radionuclides produced from the fissioning of UO_2 . The quantity of fuel fines released from a spent fuel rod may depend strongly upon the extent to which fuel pellets have been fragmented during the accident by collision impact forces.

The transport of fission products from their point of release from the fuel rods, through the cask interior to a failed cask seal, and then through the failed cask seal to the environment would likely be predominantly driven by the depressurization flow of helium gases from the failed spent fuel rods. Conversely, the retention of the fuel fines and of fission product vapors within the cask interior would depend upon the relative depressurization rates of the fuel rods and the cask, i.e., the slower the cask depressurizes, the more time is available for fission products, other than the noble gases, to deposit onto cask interior surfaces where they would likely remain.

Therefore, MELCOR's radionuclide models must analyze the behavior of gases, vapors, and aerosols as each is transported through the control volumes used to represent the interior of a TN-125 cask. To do this MELCOR must be provided with a list of the fission products to be treated, the physical forms in which they can exist (fixed gases, vapors, aerosols), their initial amounts, the dependence on temperature of the vapor pressure of volatile species, the initial size distribution of aerosols, and the characteristics of the surfaces onto which these species may deposit. Given this information, MELCOR's radionuclide transport models will keep track of the variation with time of the concentrations of each species in the gas phase and on surfaces, thereby developing the basis for calculating the fraction of each specie that escapes the cask to the environment.

4.4.1 Radionuclide Species

The transport of three types of fission products was modeled in the TN-12 shipping cask study, i.e., 1) species that always exist as gases (noble gases) at the temperatures of postulated transportation accidents, 2) species that always exist as solids (aerosols) at these temperatures, and 3) volatile species capable of existing in both the vapor and solid phases at transportation accident temperatures. Spent fuel contains a number of hazardous fission products. Table 4-10 lists fission products and nuclear fuel species existing in PWR spent fuel in sufficient quantities 5 years after removal from the reactor that can contribute significantly to postulated radiological risks [6 and 13].

Table 4-10: Risk Dominant Radionuclides in 5-Year Old PWR Spent Fuel

| Physical States | Radionuclide Species |
|------------------------------------|---|
| Always Exists in Gas Phase | ^3H , ^{85}Kr |
| Exist in Either Gas or Solid Phase | ^{134}Cs , ^{137}Cs , ^{129}I , ^{106}Ru , ^{125}Te |
| Always Exists in Solid Phase | ^{241}Am , ^{137}Ba , ^{144}Ce , ^{244}Cm , ^{60}Co , ^{154}Eu , ^{155}Eu , ^{238}Pu , ^{239}Pu , ^{240}Pu , ^{241}Pu , ^{90}Sr , ^{235}U , ^{238}U , ^{90}Y |

Krypton will of course always exist only in the gas phase since it is one of the noble gases. Further, it does not chemically react or adhere to surfaces. Its release to the environment would therefore be governed by its dilution due to mixing with cask gases and the rate of leakage of those gases to the environment. When cask pressurization due to rod failure is high, cask failure should cause large amounts of krypton to be released to the environment. Because krypton transports only as a gas, its behavior was used to develop a baseline for evaluating the cask retention of other species that were subject to deposition onto cask surfaces.

When present as tritium gas (HT), tritium (T), like krypton, will be gaseous at all accident temperatures. However unlike krypton, tritium gas can be converted to a condensable vapor, HTO, by exchange of hydrogen with H_2O or by reaction with oxidizing agents. At elevated temperatures, tritium can also react with Zircaloy cladding to form a hydride of zirconium, thereby binding it to the clad. Despite the complexities of the behavior of tritium, it was not included in the MELCOR input model because it is not present in spent fuel in large amounts.

The species listed as always solid during transport accident scenarios were all treated as aerosols, hereafter referred to as "fuel fines". These fuel fines are particles that have fragmented away from the fuel pellets. The bulk of these particles consist of UO_2 with fission products and plutonium embedded in the particles. Because all aerosols transport by the same processes, the behavior of fission products that transport as aerosols is wholly governed by the dynamics of aerosolized particles, therefore these are simply modeled as fuel fines.

Five isotopes are listed in Table 4-10 as existing in either a vapor or a solid phase depending upon the temperature. Since these isotopes are generally highly chemically reactive, they will exist primarily as chemical compounds and

the volatility of those chemical compounds will determine whether they transport as vapors or as aerosols.

Because elemental cesium is highly reactive, cesium atoms are expected to react with other atoms in the fuel matrix to form molecular species. Thus, cesium atoms will tend to form Cs_2O by picking up oxygen from the UO_2 fuel. Some fraction of the cesium atoms will combine with Iodine-129 to form CsI . The ^{129}I isotope itself was not considered a major contributor to overall radiological risk because of the activity level associated with its long half life. (Note that the high risk iodine isotopes, ^{131}I and ^{133}I , have decayed away until their activity levels in 5 year old spent fuel do not contribute significantly to overall transportation risk.) If iodine were to exist in the elemental form in a TN-125 cask, it would exist in the vapor form at the cask's normal transport temperatures. Since the shipping cask is operated with an inert nitrogen atmosphere, conversion of Cs atoms or Cs_2O molecules to CsOH , as would generally occur in the steam environment of a reactor accident, will occur only if these species are exposed to water vapor. Exposure to water vapor can occur if water was left in the cask when it was loaded in the reactor water storage pool, or if water formed by a fire is drawn into the failed transportation cask.

Ruthenium is a refractory metal and some ruthenium oxides are moderately volatile. Because of its symmetric structure, the oxide RuO_4 is very volatile [14]. The portion of ruthenium forming RuO_4 and its stability during transportation accident conditions are unknown.

The spent fuel likely still contains some tellurium that would oxidize to form TeO . TeO is volatile at the higher temperatures potentially encountered during a pool fire accident scenario.

Insufficient data were available to model Cs_2O and RuO_4 . The RuO_4 is not likely a major contributor to the overall risk because spent fuel contains a relatively smaller quantity of ruthenium and not all of the ruthenium in spent fuel will be converted to RuO_4 even if the fuel is exposed to air while hot. Therefore, the transport of ruthenium from the cask will usually be governed by transport in fuel fines.

Since cesium is the radionuclide most likely to dominate overall risk and Cs_2O would likely be an important form of cesium in a spent fuel transportation accident, the lack of vapor pressure data for Cs_2O is a deficiency of this study. Because vapor pressure data for Cs_2O was not available, Cs_2O was not explicitly modeled during the MELCOR calculations performed for this study. The volatility of Cs_2O is apparent from vitrification work performed at the Savannah River Plant [15] and from the melting point of Cs_2O . The Cs_2O melting point of 490°C (in nitrogen) is in between the melting points of CsOH and CsI , 273 and 626°C , respectively [16]. This suggests that the volatility of Cs_2O would be between that of CsOH and CsI and that the cask retention of CsOH and CsI are reasonable models for the cask retention of Cs_2O .

Some cesium may remain in the fuel fines in the form of uranates such as $\text{Cs}_2\text{U}_5\text{O}_{16}$, and $\text{Cs}_2\text{U}_4\text{O}_{13}$ [17]. If formed, these compounds will be transported as constituents of fuel fines.

The radionuclides actually included in the MELCOR input model are shown in Table 4-11. The vapor pressures of the three volatile species modeled are shown in Figure 4-4.

Table 4-11: Radionuclides Included in the MELCOR Input Model

| Radionuclide | Volatility |
|-----------------|--------------|
| Kr | Always Vapor |
| CsOH | Volatile |
| CsI | Volatile |
| TeO | Volatile |
| UO ₂ | Always Solid |

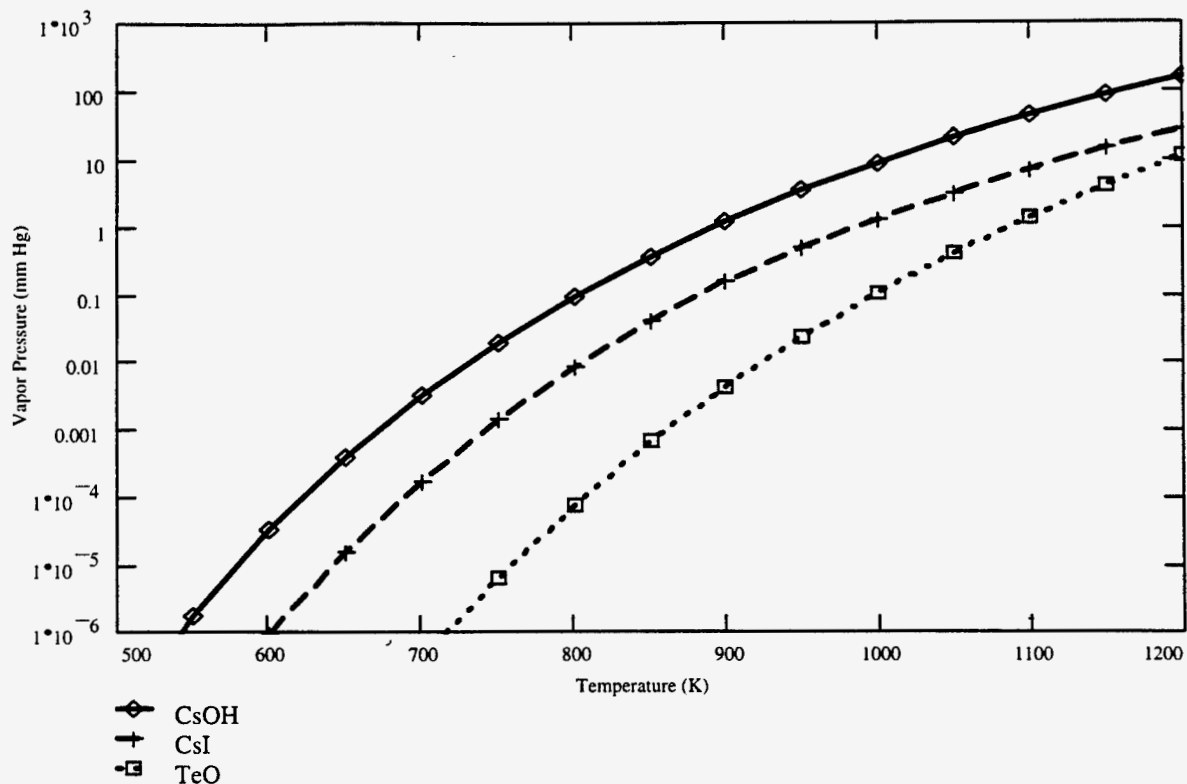


Figure 4-4: RN Vapor Pressures

4.4.2 Description of Radionuclide Sources

The amount of radioactivity (M) released to the environment when a RAM cask is involved in a transportation accident is the product of three numbers: the cask inventory (I) which can be calculated quite precisely, the fraction of that inventory that is released to the interior of the cask (R_{fuel}), and the fraction of that release that escapes from the cask to the environment (R_{cask}). Thus, $M = I R_{\text{fuel}} R_{\text{cask}}$.

Because fuel pellets can be fragmented when the RAM cask in which they are being transported is subjected to a collision, the amount of fuel fines available for release during a transportation accident may be significantly greater than the amount that was present prior to the collision. Thus, for fuel fines, the value of R_{fuel} for transportation accidents is quite uncertain.

The release fraction for fuel fines from spent fuel rods that have not been subjected to collision forces was experimentally determined by Lorenz [6]. The Lorenz experiments suggested that the quantity of fuel fines ejected from spent fuel rods upon depressurization would be somewhat less than 0.003% of the total fuel inventory [6].

Three accident scenarios were examined by this study:

- a collision scenario without a fire,
- a fire scenario without a collision, and
- a combination collision and fire scenario.

The fire without a collision scenario assumed that the amount of fuel fines present in the fuel rods prior to the transportation accident was not increased by collision-induced fragmentation of fuel pellets during the accident. Whereas, both scenarios with a collision assumed that pellet fragmentation took place as a result of the collision.

The size of the radionuclide source from the rods to the cask interior was also examined by a parameter sensitivity study.

The fire without a collision scenario used a fuel-to-cask release fraction of $R_{\text{fuel}} = 3 \times 10^{-5}$ because collision induced fragmentation was not postulated. In the two scenarios that involved a collision, a fuel-to-cask release fraction of $R_{\text{fuel}} = 2 \times 10^{-4}$ was used in the base case calculations and parameter sensitivity calculations used a value of 1×10^{-5} as a lower bound and a value of 1×10^{-3} as an upper bound. The upper bound value of 1×10^{-3} was obtained from experiments where shaped charges were used to explosively breach a shipping cask and where the largest release of aerosolized fuel for full length fuel rods was 9.8×10^{-4} of the fuel inventory [6]. This upper bound value of 1×10^{-3} is not necessarily an absolute upper bound, but was deemed a reasonable upper bound for this study. The base case value of 2×10^{-4} was determined from the following equation.

$$R_{\text{fuel}} = R_{\text{non}} + F_{\text{rod}} \cdot F_{\text{aero}} \cdot F_{\text{trans}}$$

where R_{fuel} = the fraction of the fuel inventory ejected as aerosolized fuel fines,
 R_{non} = the non-fragmented ejection fraction of 3×10^{-5} ,
 F_{rod} = the fraction of the rod fragmented,
 F_{aero} = the fraction of each pellet which becomes aerosolized fines,
 F_{trans} = the fraction of the aerosolized fines transported from the rods.

A value for fuel fines of $R_{\text{fuel}} = 2 \times 10^{-4}$ was computed by assuming that 20% of the pellets along the length of each fuel rod were fragmented by the collision forces; that 2% of the mass of each fragmented pellet was converted to fuel fines; and that 4% of the fines were ejected from the rods upon rod depressurization, i.e., $3 \times 10^{-5} + 0.2 \times 0.02 \times 0.04 = 2 \times 10^{-4}$. Only 20% of the pellets in a rod were assumed to fragment because only 20% of the rod length was assumed to experience collision forces during a transportation accident. Experiments [18] which subjected depleted UO_2 pellets to impact forces and measured the size distribution of the resulting debris, indicated that the fraction of the debris that was in particles small enough to be transported as aerosols was on the order of 2%. The fraction of aerosols that escape from the rods to the interior of the cask was based on the observation that fuel swelling converts the original rod gap volume to internal crack volume in the pellets. As initial gap volume is about 4 percent of initial fuel volume, after fuel swelling, the crack network in the pellets will constitute about 4 percent of the volume of each pellet. Therefore, if only the aerosolized debris lying within or near the pellet crack network can be transported from the rod, while other debris remains trapped within the pellets, then the fraction of the aerosolized debris that escapes the rod will be about 4 percent.

In an actual collision, the impact forces and the resulting fragmentation of fuel pellets would vary from rod to rod and with axial position along each rod. In addition, the physical processes governing the transport of particles through the crack network in the fuel pellets, to the failure in the rod, and through that hole to the cask interior would be very complex and difficult to model. Despite these complexities, the simple model just described was used for two reasons: first, because a better simple approach was not available, and second, because this approach yielded a reasonable range (3×10^{-5} to 1×10^{-3}) and central estimate (2×10^{-4}) for the values of the release fraction for fuel fines from the rod to the cask interior. Note that the central estimate value of 2×10^{-4} is 6.67 times the no-fragmentation value of 3×10^{-5} and 1/5 of the explosive upper bound value of 1×10^{-3} . Thus, this value is approximately the geometric mean of the range.

The release of gases and vapors from a failed rod will differ from that of fuel fines. Gas and vapor transport from a failed fuel rod depends primarily upon the flow of rod gases into the cask and has little or no dependence on crack volumes, widths, and particle diameters which control the transport of aerosols from rods. Gaseous species migrate within the fuel pellets and rods and may concentrate in pellet voids or the gas plenum of rods. Some cesium would exist as vapors in the fuel voids and the rod plenums while non-volatile cesium species would still be entrained in the fuel. Upon cladding rupture, a burst of volatile cesium species would escape from the gas plenum and fuel voids to the cask interior. Following this burst release, gases and vapors would continue to be released by diffusion, however the diffusional releases would in general be much smaller than the burst releases for temperatures encountered in transportation accidents.

The complexity of modeling these release processes, especially collision induced fuel fragmentation, was beyond the scope of this study. Therefore, a simpler approach was employed. Since this study focused on the retention in the cask of fission products released into the cask from failed rods, the MELCOR input model simply released a small tracer quantity of each radioactive gas and vapor of interest and tracked the specie to determine its release fraction (R_{cask}) from the cask to the environment. The radionuclide source quantities used in the MELCOR input model for the basic scenarios where all of the fuel rods were postulated to fail are shown in Table 4-12.

Table 4-12: Scenario Radionuclide Source Terms

| Species | Accident Scenarios without Fuel Fragmentation | Accident Scenario with Fuel Fragmentation |
|------------|---|--|
| Kr | 0.15 gm | 1 gm |
| CsOH | 0.15 gm | 1 gm |
| CsI | 0.15 gm | 1 gm |
| TeO | 0.15 gm | 1 gm |
| Fuel Fines | 0.1833 kg (3×10^{-5} of total fuel mass) | 1.222 kg (2×10^{-4} of total fuel mass) |

A TN-125 shipping cask fully loaded with 12 PWR spent fuel assemblies (2448 fuel rods) would contain 6109 kg of UO_2 fuel. The 1 gm tracer mass for the gas and vapor species used for the accident scenario that treated fines production by fuel fragmentation was a somewhat arbitrary selection. If a more realistic value is determined later, the 1 gm release mass can be scaled to a more realistic value for the mass of gas or vapor species released from the rods to the cask. The 0.15 gm release mass used for scenarios that did not treat fuel fragmentation due to collision forces makes the ratio of gas and vapor masses for these two cases the same as the ratio of fuel fine masses for the two cases, i.e., $0.15 = 3 \times 10^{-5} / 2 \times 10^{-4}$.

The size distribution of the aerosolized fuel fines sourced into cask for the MELCOR calculations was represented by a log-normal distribution. Based on a review of the data presented in Reference 6, the log-normal distribution selected had a mass mean diameter (MMD) of 2 μm and a geometric standard deviation (GSD) of 2.5. A parameter sensitivity study later determined that this distribution was more than adequate. Within each MELCOR calculation, this size distribution was subdivided into size sections such that the ratio of the upper bound diameter to the lower bound diameter of each section was a constant. The particle sizes ranged from 0.01 μm to 1000 μm . The resulting sectional size distribution is shown in Figure 4-5.

Each radionuclide was introduced into each calculation as a source term to the atmosphere of the lodgment volume into which the fuel rods were postulated to fail. The radionuclide mass was introduced into that lodgment volume at a uniform rate for 100 seconds. The mass of each radionuclide species introduced is listed in Table 4-12. Division of this mass by 100 seconds gives the uniform rate of introduction for the particular species. For collision induced fuel rod failures, introduction of the source term began at time zero and ended at 100 seconds and for fire induced failures, introduction began at 4 hours and ended 100 seconds later. Thus, the timing of the radionuclide sources roughly corresponded to the depressurization time of the fuel rods. In reality, the rate that the radionuclides would be released from the rods could be anything but uniform. However, there does not appear to be any data available on the uniformity or non-uniformity of these source rates. Moreover, this crude radionuclide source model is adequate for all accident scenarios where cask depressurization took significantly longer than the 100 seconds used to source the radionuclides into the cask.

The radionuclide source-timing model, i.e., the uniform rate for 100 seconds, was revised because it caused some secondary counterintuitive trends. A description of the revised model and its impact on the study results and conclusions is found in the Addendum.

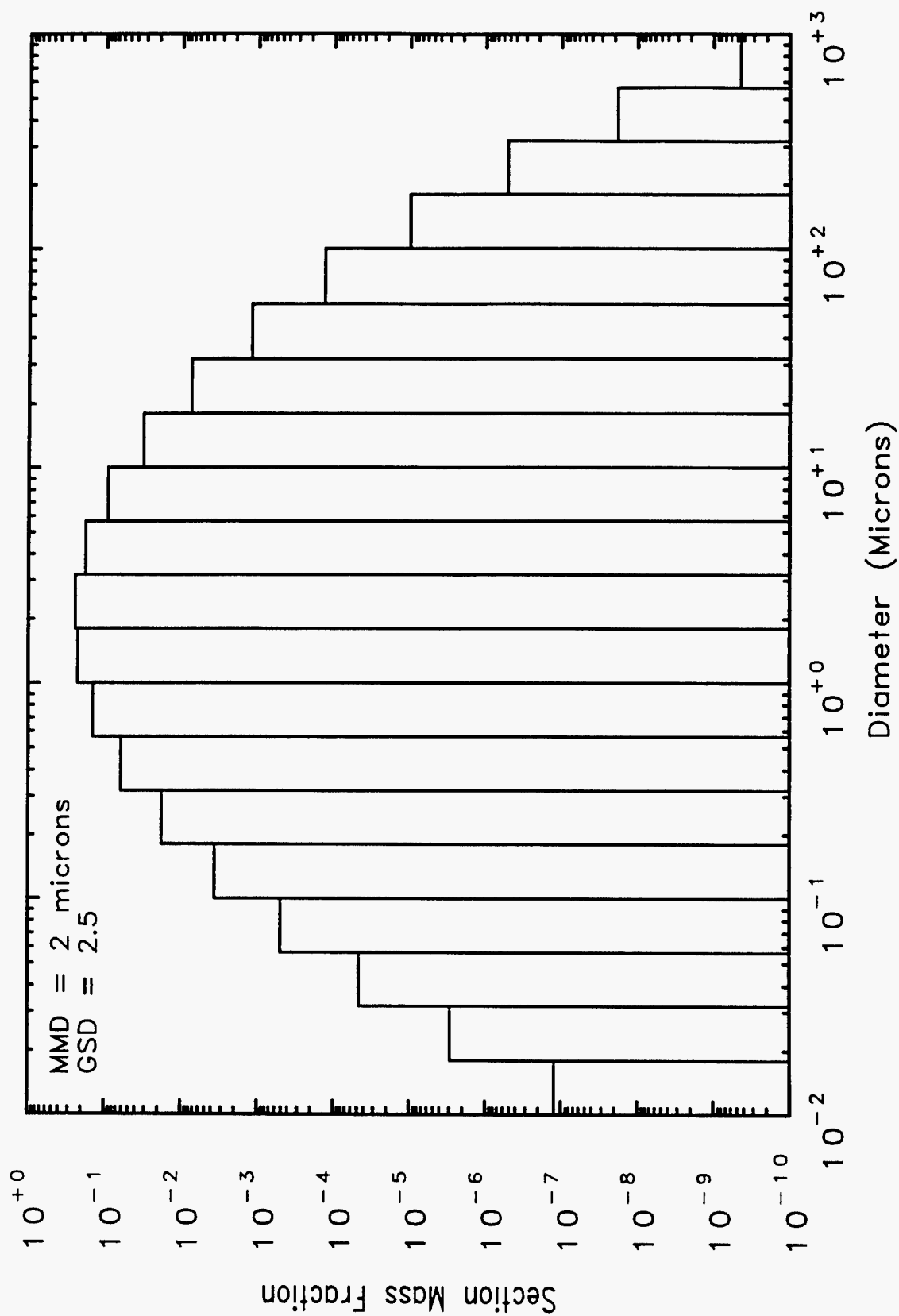


Figure 4-5: Initial Size Distribution of Fuel Fine

The radionuclides were introduced into the center axial lodgment atmosphere in all three of the basic scenarios because the axial center location was deemed the most probable location for the spent fuel rods to fail. One of the parameter sensitivity studies examined the effect of introducing the radionuclides into the other four lodgment atmospheres. In general, moving the rod failure location closer to the failed cask seal, decreased transport pathway lengths, which decreased fission product deposition along this path and as a consequence increased fission product release from the cask to the environment. In reality, if all of the 2448 fuel rods were to fail, the axial failure locations of the rods would be best described by a probability distribution. If such a probability distribution could be determined, then the source terms of future calculations should introduce the appropriate fraction of the sources into each of the five axial lodgment atmospheres.

4.4.3 Aerosol Dynamics

The MELCOR code requires a number of input parameters that are used as constants in the MAEROS aerosol dynamics equations that govern the prediction of aerosol coagulation, deposition, and transport. Reference 19 was heavily relied upon for guidance in determining an appropriate value for these input parameters. The numbers selected for each of these parameters are shown in Table 4-13.

The solid density of all individual aerosol particles in the calculation is the nominal density and only one nominal density is allowed by the MELCOR aerosol dynamics model. The gravitational settling of particles is directly proportional to this particle density. The 95% theoretical density for UO_2 fuel was used because most of the aerosol mass would be UO_2 .

The dynamic and coagulation aerosol shape factors are used in the aerosol dynamics model to account for the effects of non-spherical particles. A shape factor of one implies a spherical particle. The shape factor then increases as the particles become more non-spherical. A non-spherical particle will not fall as fast as a spherical particle of the same mass and density because of its increased aerodynamic drag and the non-spherical particle will be more likely to collide with another particle. These two effects tend to counteract one another in the aerosol dynamics model, i.e., non-spherical particles fall slower but the greater collision frequency causes the particle to coagulate into larger particles which in turn fall faster than their smaller constituent parts. Both shape factors were specified as one because the particles making up the fuel fines were not expected to have highly non-spherical shapes and data regarding the effective shape factors of UO_2 particles was not available.

A particle mobility correlation in the aerosol dynamics model uses the particle slip coefficient as a constant in that correlation. The particle mobility accounts for particle motions that cannot be deduced by treating the gas phase as a continuum. These motions primarily effect the smaller particles. The mobility correlation employed by the MAEROS equations used a value of 1.257 for this constant but the MELCOR code allows the user to alter this constant. The value of the original constant, 1.257, was used in this MELCOR input model for lack of any justification to do otherwise.

A particle sticking coefficient of one assumes that once particles come in contact, they will remain in contact, i.e., the particles will be held together by the Van der Waals intermolecular forces between the particles. Based on discussions in Reference 19, it was deemed likely that UO_2 particles would stick together upon making contact, therefore a particle sticking coefficient of one was used in this study.

The turbulent energy dissipation rate directly effects the rate of turbulent coagulation of aerosol particles. The rate of $0.001 \text{ m}^2/\text{s}^3$ used in this study represents the lower end of the uncertainty range for nuclear power plant containment analyses. For reactor accidents, the turbulent energy dissipation rate is related in some sense to the reactor power level. Therefore, for transportation accidents, because the decay heat power level in aged spent fuel is rather modest compared to the power associated with a nuclear power severe accident, use of a turbulent energy dissipation rate that corresponds to the low end of the range of rates calculated for reactor accidents seems appropriate. Using this rate may underestimate the aerosol coagulation rate somewhat.

The ratio of the gas thermal conductivity to the thermal conductivity of the particles is used by the algorithm that predicts thermophoretic deposition in the aerosol dynamics model. The ratio of nitrogen gas thermal conductivity to the thermal conductivity of irradiated UO_2 fuel was estimated to be about 0.008.

The thermal accommodation coefficient is another constant in the thermophoretic deposition algorithm. This coefficient is nearly always in the range of 0 to 1. Thermal accommodation coefficients have been measured for only a few materials and must be considered uncertain. The MELCOR default value of 1.0 was used for this study. Information presented in Reference 19 indicated that the appropriate number for particles in nitrogen gas is likely greater than 0.6 and that data for glass surfaces and cold nitrogen gas suggests a number of about 0.7. In retrospect, a coefficient of about 0.8 would probably have been more justified, however, using a 0.8 would not have significantly affected the overall results.

Table 4-13: Aerosol Dynamics Constants

| Parameter | MELCOR Input |
|--|--------------------------------------|
| Nominal Density of Aerosol Particles | 10500 kg/m ³ |
| Aerosol Dynamic Shape Factor | 1. |
| Aerosol Coagulation Shape Factor | 1. |
| Particle Slip Coefficient | 1.257 |
| Particle Sticking Coefficient | 1. |
| Turbulent Dissipation Rate | 0.001 m ² /s ³ |
| Gas to Particle Thermal Conductivity Ratio | 0.008 |
| Thermal Accommodation Coefficient | 1. |
| Diffusion Boundary Layer Thickness | 1 x 10 ⁻⁵ m |

The aerosol dynamics model in MELCOR includes the diffusive deposition of particles onto surfaces through a boundary layer with a thickness taken to be a constant, i.e., independent of flow conditions and particle size. Diffusion often tends to dominate the deposition of submicron particles but becomes relatively unimportant for the deposition of larger particles. The MELCOR default value of 10⁻⁵ m was used in this study. A sensitivity calculation using a value of 10⁻⁴ m was run to determine the relative importance of this parameter. Cask fission product retention was nearly identical for the two calculations, indicating that the calculations were not very sensitive to this parameter.

The overall effect of these parameters on the aerosol dynamics in the TN-125 cask during normal transport conditions was examined by plotting the variation with particle size of the coagulation and deposition kernels used by the MAEROS equations. The coagulation kernels for a 2 μm particle interacting with other particles of various sizes are shown in Figure 4-6. When this 2 μm particle interacted with a particle smaller than about 1 μm , the brownian coagulation process clearly dominated. But when this particle interacted with a particle larger than about 1 μm , the gravitational process dominated. The gravitational process involves a larger particle falling faster than a smaller particle, thereby sweeping the smaller particles out as it falls. Since two particles of the same size and shape will fall at the same velocity, the gravitational deposition kernel goes to zero at 2×10^{-6} m (the width of this dip in the gravitational kernel was a function of number of points plotted). Over the range of particle sizes examined, the turbulent coagulation process was the least important process relative to the 2 μm reference particle. However, the turbulent process did tend to dominate the interactions between the very small and the very large particles which was not very important in this study because there was not much mass distributed into either the very small or the very large particle size sections.

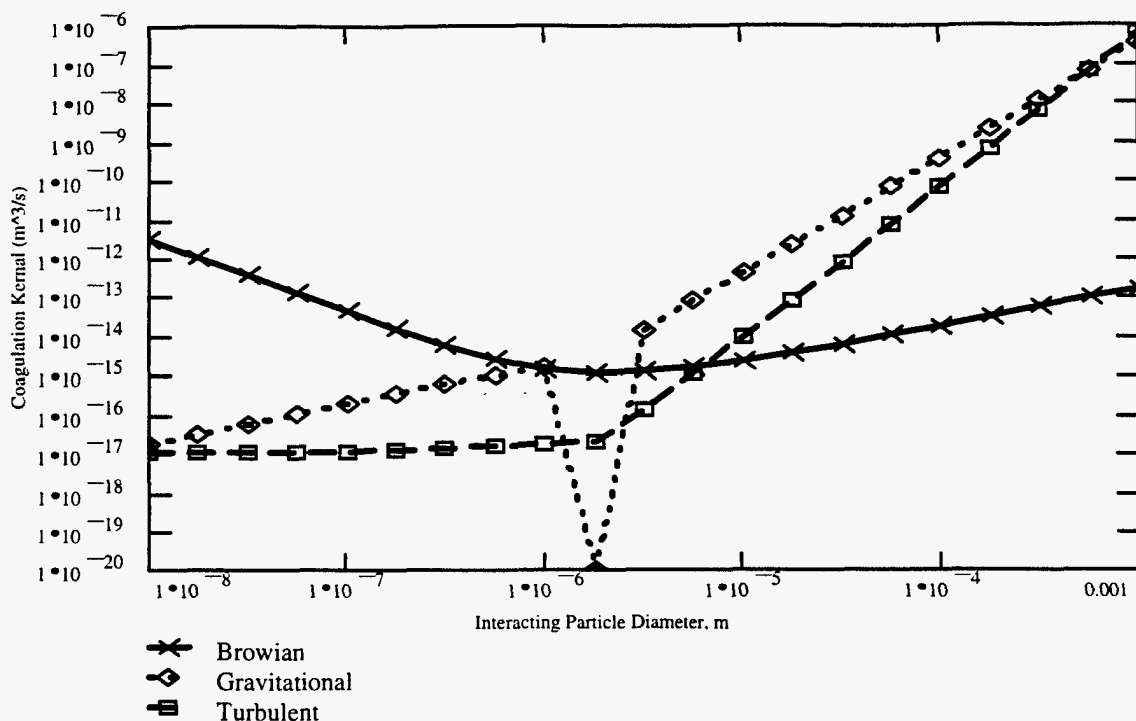


Figure 4-6: Coagulation Kernels (2 mic.)

The variation with particle size of the MAEROS deposition kernels is shown in Figure 4-7. Diffusive deposition dominated for particles smaller than about $0.4 \mu m$, while for larger particles, gravitational deposition dominated. Most of the aerosol mass was in particles larger than $0.4 \mu m$. Thermophoresis was relatively unimportant to this study. The relative importance of these deposition processes is more clearly shown by a linear plot of their fractional contribution to total deposition. These fractional contributions are shown in Figure 4-8.

Based on the MAEROS equations for the dominant processes, the aerosol dynamics parameters likely to have had the greatest impact on the overall aerosol transport from the TN-125 cask would be the nominal particle density, the dynamic and coagulation shape factors, and the particle slip and sticking coefficients. It was deemed unlikely that the uncertainties associated with the values selected for these parameters significantly effected the overall aerosol transport results. The higher temperatures associated with a fire accident scenario would alter these plots somewhat but not the conclusions regarding the dominant processes.

4.4.4 Radionuclide Deposition Surfaces

It was important to describe the interior shipping cask surface areas, including their sizes, orientations, locations, and temperatures, relatively accurately to properly predict radionuclide deposition within the cask. The surface areas associated with the equivalent heat structures created in the thermal model to predict heat transport through the basket and into the fuel were not at all adequate to predict the deposition of radionuclides onto these structures. For example and most importantly, in a real TN-125 cask all of the spent fuel rod cladding surface area will be available for radionuclide deposition but the area associated with the equivalent homogenized fuel cylinder used to represent the rods as a heat structure only had about 11% of the true total cladding surface area. Thus, using the equivalent cylinder surface area would have drastically underpredicted deposition onto the cladding. Further, the outer temperature of the equivalent cylinder did not correspond well to the temperatures of the interior fuel rods. To work around these problems, the surface areas associated with the equivalent cylinders, i.e., fuel homogenized cylinders, and the lodgment walls, were deactivated in the radionuclide deposition model to prevent deposition onto those surfaces. (The MELCOR radionuclide deposition model allows each individual heat structure to be specified in the

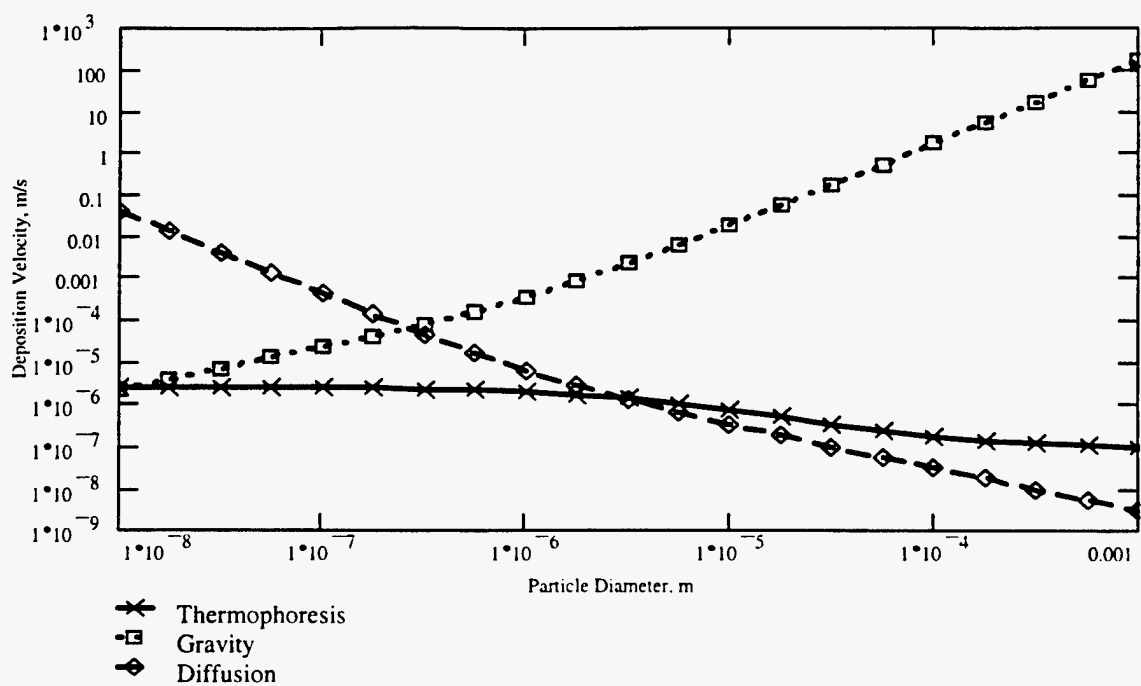


Figure 4-7: Deposition Kernels

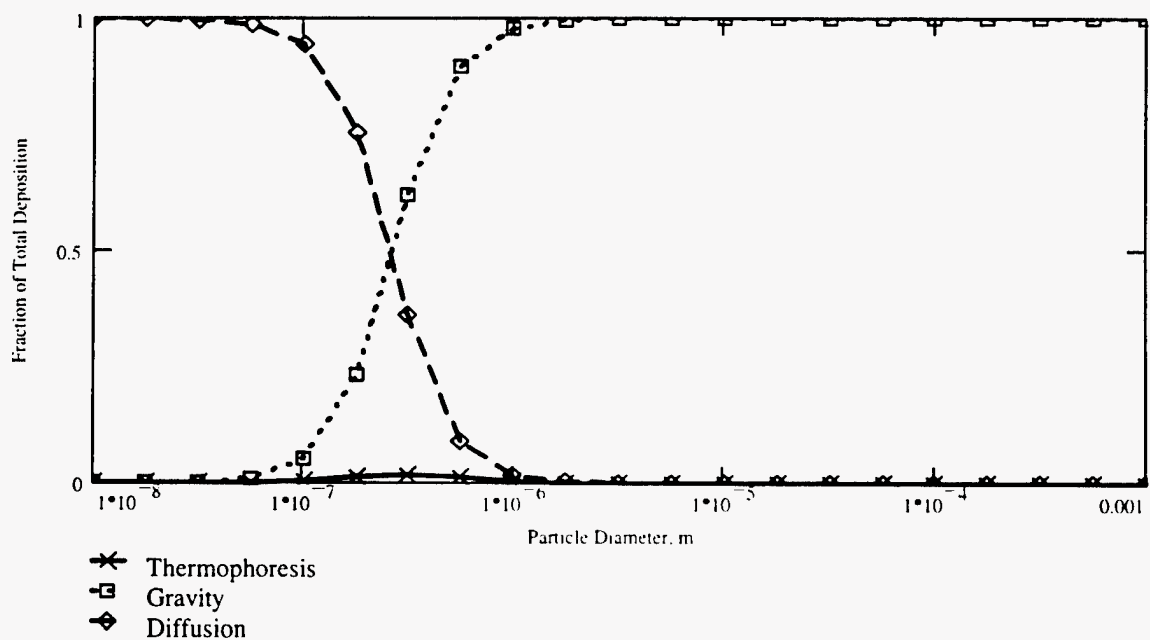


Figure 4-8: Deposition Fractions

input model as either active or inactive with regard to radionuclide deposition.) Then, additional thermally passive heat structures with surface areas, orientations, locations, and temperatures were added to the set of heat structures input to MELCOR to support modeling of radionuclide deposition.

Thermally passive heat structures were designed such that their presence in the calculation would not impact the shipping cask heat transport or the temperatures of thermally active structures. Each thermally passive structure inserted into the input model consisted of a thin slab with high thermal conductivity and low heat capacity. Thus, passive heat structures were poor reservoirs of heat and had front and back surface temperatures that were nearly identical. One surface of each passive structure was maintained at a temperature appropriate for modeling deposition of vapors onto the structure (a temperature close to the surface temperature of the real surface to which it corresponded), and the other surface had a convective surface boundary condition with a convective coefficient set near zero to prevent any actual convective heat transfer from or to the passive structure. The temperature maintained surface was specified as radionuclide inactive while the convective surface, which had a temperature nearly identical to that of the radionuclide inactive surface, was active with regard to fission product deposition. Thus, this thermally passive but radionuclide active surface became a radionuclide deposition surface area without impacting cask heat transport.

A total of 45 passive heat structures were used to simulate the fuel rod cladding surfaces. There were nine passive heat structures in each of the five lodgment control volumes. The temperature of the surfaces of each of the nine passive structures tracked identically the temperature of one of the nine radial segments of the homogenized equivalent cylinder used to represent heat transport by the fuel rods contained within a fuel assembly. Thus, all of the true cladding surface area was implemented for radionuclide deposition and the areas and temperatures of each of these surfaces were about the same as the areas and temperatures of the set of rods that they represented.

All radionuclide deposition surfaces must be declared in the MELCOR input as a ceiling, as a wall, or as a floor so that the model for gravitational settling will know how to treat gravitational deposition of particles onto each structure. Aerosol particles removed by gravitational settling are deposited only onto the floor areas in each control volume. During transport, the fuel rods in a TN-125 cask will be oriented horizontally. Thus, each rod will have a small surface area onto which particles would be deposited by gravitational settling. Nevertheless, to avoid having to subdivide rod surface area into floor, wall, and ceiling surfaces, the fuel rods in this study were treated as vertical walls. Thus, the radionuclides removed by gravitational settling in lodgment control volumes were deposited only onto the floor surfaces of those volumes and not onto the surfaces of control rod structures contained in those volumes.

With regard to fission product deposition, the lodgment wall surfaces were simulated by passive heat structures in a manner similar to that used to simulate control rods, except that lodgment surfaces were subdivided by orientation, as well as, by axial lodgment volume. A total of 15 lodgment wall passive heat structures were defined, i.e., a ceiling, a wall, and a floor for each of the 5 axial lodgment control volumes. It was assumed that the basket in the TN-125 cask was oriented such that the walls of the lodgments were either vertical or horizontal surfaces, i.e., one side of each lodgment was a ceiling, two sides were walls, and one side was a floor. The temperatures of the lodgment wall passive structures used to treat fission product deposition were driven by the inner surface temperature of the equivalent cylinder that represented the cask basket.

The interior surfaces of the cask lid, and bottom, and the center cross-region space in the basket were simulated by 2, 2, and 5 heat structures, respectively. Although during transport, most interior lid and bottom surfaces will have vertical orientations (walls), each surface will have some area that is oriented horizontally (floor surface area) and thus be subject to gravitational deposition. Therefore, a small horizontal passive surface area was added to each end structure to provide a location for gravitational deposition to occur. The temperature of the center cross surfaces was driven by the inner basket temperature and the end surfaces were driven by the respective end surface temperatures of the active heat structures that represented these cask components.

Deposition in the basket-shell gap was not modeled because the gap width and the flow through the gap were so uncertain. Not modeling radionuclide deposition in this gap, although probably conservative, was not expected to significantly impact the overall deposition results because gas flow through the basket-shell gap is so small that

fission product deposition to surfaces in the basket-shell gap should also be very small. Therefore, most particle deposition should take place onto lodgment and cladding surface and little onto shell surfaces.

All of the surface areas modeled for radionuclide deposition in the cask interior are shown in Table 4-14 by component and orientation. As the table shows, because their total surface area is so large, cladding surface areas will clearly dominate deposition.

Table 4-14: Radionuclide Deposition Surface Areas

| Component | Surface Areas by Orientation (m ²) | | | |
|--------------------|--|---------------|------------------|-------|
| | Horizontal Ceiling | Vertical Wall | Horizontal Floor | Total |
| Fuel Rod Cladding | 0 | 301.6 | 0 | 301.6 |
| Lodgment Walls | 10.9 | 21.8 | 10.9 | 43.6 |
| Top Lid End | 0 | 1.6 | 0.2 | 1.8 |
| Center Cross Space | 4.8 | 26.7 | 4.8 | 36.3 |
| Basket-Shell Gap | 0 | 0 | 0 | 0 |
| Bottom End | 0 | 1.8 | 0.2 | 2.0 |
| Total | 15.7 | 353.5 | 16.1 | 385.3 |

5.0 MODEL VALIDATION

Two methods were used to benchmark and validate the MELCOR shipping cask input model to increase confidence in these study results. First, the SAR included a discussion of an experimental verification of the heat dissipation capabilities of the TN-125 package that was directly applicable to the cooling fin input model. Secondly, the SAR presented calculations of the normal operating temperatures for a mid-cask cross section. These temperatures were compared to temperatures computed by MELCOR when the input model was run as a steady state calculation. Both the similarities and the differences between these two sets of temperatures added credibility to the models.

5.1 Validation of the Fin Cooling Model

Transnuclear, Inc. built a full scale test model of a 0.513 m axial section of the finned zone of the TN-125 cask to verify the thermal performance of the fins [1]. This full scale cask section was heated by electrical heaters placed inside the model. The heat input to the interior of the model simulated steady state heat input to the inner surface of the shell of the TN-125 cask and transport of that heat through the fins to the surrounding ambient atmosphere. The steel shell of the TN-125 cask was simulated by 2 concentric shells of mild steel separated by a 3 mm thick cement layer. The heaters were spaced regularly around the inner concentric shell at a distance approximately 10 mm from the wall of the inner shell. The lateral (end) faces of the model were equipped with circular glass wool filled drums to insulate the ends so that the cooling of the fins could be approximated by one-dimensional heat transport. The cooling fins on the model were of the same design as those on the cask. The test apparatus was not enclosed or exposed to solar insolation. During the test, the model was oriented with its cylindrical axis parallel to the ground. The experiment was instrumented with numerous thermocouples and a voltmeter and ammeter to measure the power to the heaters. The measured power delivered to the heaters of 14,700 Watts corresponded to the decay power of a fully loaded TN-125 cask. Therefore, the measured fin temperatures of the model should be about the same as the real temperatures of the fins on a fully loaded shipping cask.

This fin heat dissipation test was simulated with the MELCOR code using only the thermal model of the cask shell, resin layer, and fins. Power was introduced to the calculation as a heat source to the atmosphere of the cask interior. The computed fin temperatures were then compared to the experimental temperatures to validate the cooling fin model.

The test apparatus was cooled by ambient air, which flowed around the circumference of the cask up over its fins. This flow was driven by natural convection that forced air to flow around and through the fins from the underside to the topside of the test apparatus. Since the air was cooler when passing over the lower fins than when passing over the upper fins, the resulting experimental temperatures were not symmetrical around the circumference of the test apparatus. The experimental temperatures compared to the MELCOR results were therefore circumferential averages. As reported in the TN-125 SAR, although a convective heat transfer coefficient of $2.5 \text{ W/m}^2/\text{K}$ was deduced from the experimental data, a convective coefficient of 3.2 was applied to the TN-125 cask for normal transport conditions (the SAR did explain this difference).

The effective overall fin convective heat transfer coefficient was adjusted in the MELCOR cooling fin benchmark calculation to get the best temperature agreement with the experiment. A coefficient of $2.8 \text{ W/m}^2/\text{K}$ provided excellent agreement with the test data. The calculated fin temperatures were found to decrease about $1.8 \text{ }^\circ\text{K}$ for each $0.1 \text{ W/m}^2/\text{K}$ increase in the convective heat transfer coefficient. The comparison of the MELCOR temperatures to the experimental temperatures is shown in Figure 5-1. The largest deviation in the comparison was at the fin tips where MELCOR predicted a $5 \text{ }^\circ\text{C}$ higher temperature than the SAR reported. The SAR reported an average fin tip temperature of $80 \text{ }^\circ\text{C}$. However, the temperature distribution around the experimental apparatus indicated that the average temperature could easily be $85 \text{ }^\circ\text{C}$ as predicted by the MELCOR model. The uncertainty in the test results was probably significantly larger than the difference between the MELCOR results and the test results. Further, the experimental uncertainty would have been the greatest at the fin tips.

This fin heat dissipation benchmark calculation verified the MELCOR input models capability to predict heat transfer through the fins during normal transport conditions. Therefore, the convective heat transfer coefficient of $2.8 \text{ W/m}^2/\text{K}$ was implemented in the MELCOR input model and used to model all scenarios that didn't involve a

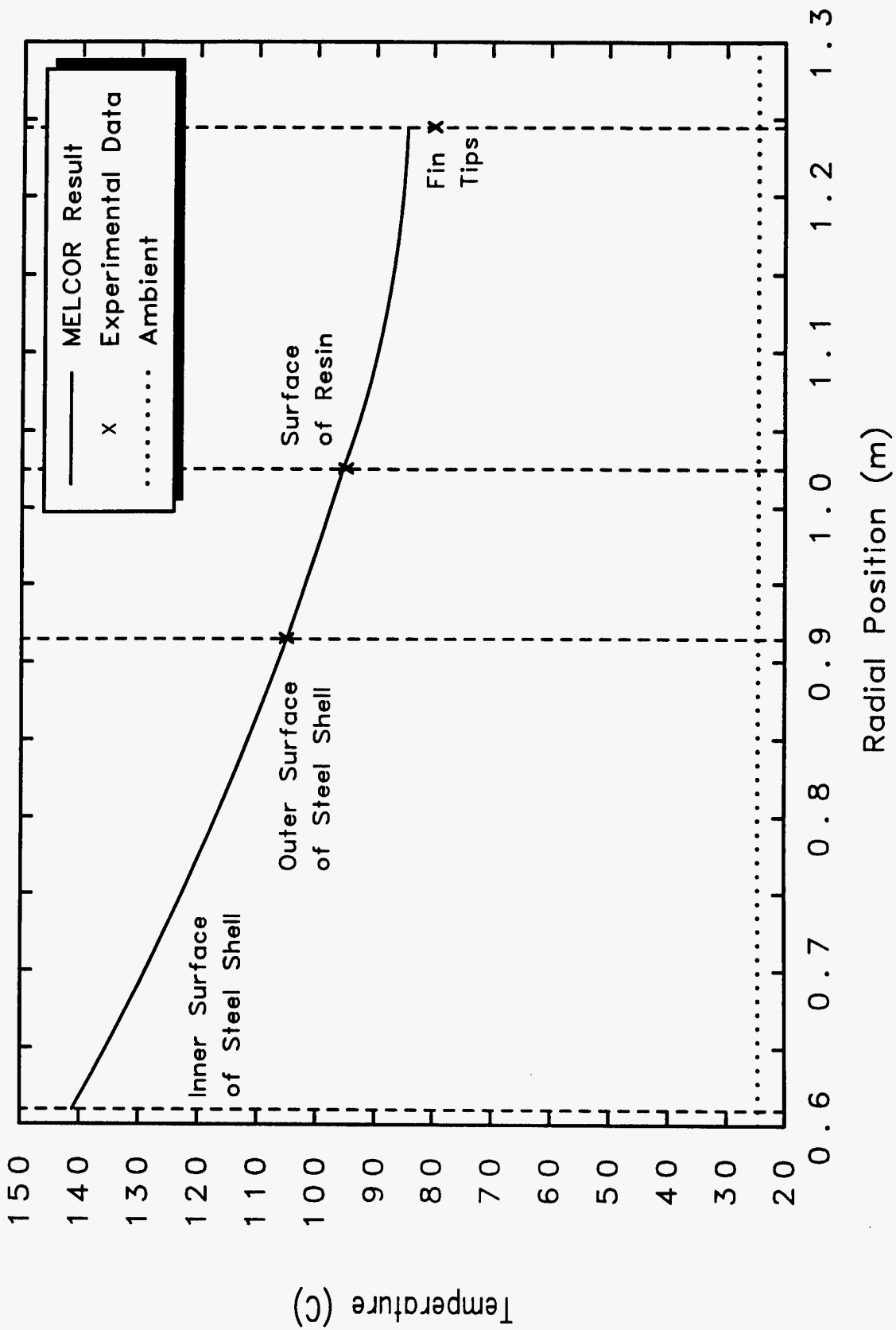


Figure 5-1: MELCOR Model Steady-State Fin Benchmark

fire. During a fire scenario, the fin heat transfer was dominated by radiative heat transfer to the fin tips and then conductive heat transfer through the fin to the steel shell. Therefore, this model validation does not directly apply to fire conditions. However, the benchmark calculation does provide some indirect validation to the fin model for fire conditions.

5.2 Validation of the Thermal Model During Normal Operating Conditions

The MELCOR input model for the TN-125 shipping cask was run in the steady state mode until model parameters, especially temperatures, achieved their steady state values for the conditions of normal transport. To avoid this initialization process, all subsequent normal transport calculations were run using the steady state values obtained from this calculation. In addition, all subsequent normal transport calculations were started 2000 seconds prior to the time of the hypothetical accident so that the values of all parameters that had been initialized to steady state values could adjust to the exact steady state values characteristic of the current calculation. The relative importance of the radiative, conductive, and convective processes within the gaps and on the cask exterior are shown in Table 5-1.

Table 5-1: Relative Importance of Heat Transport Processes During Normal Transport Conditions

| Heat Transport Process | Heat Transported from Cask, kW | | |
|----------------------------------|--------------------------------|---------------------------|------------------------------|
| | Spent Fuel to Basket Gap | Basket to Steel Shell Gap | Cask Exterior to Environment |
| Radiative Heat Transport | 91.7 | 3.9 | 23.6 |
| Conductive Heat Transport | 28.1 | 116.1 | 0 |
| Convective Heat Transport | 0.2 | 0.04 | 138.7 |
| Solar Insolation | 0 | 0 | -42.3 |
| Total | 120 | 120 | 120 |

The SAR provided estimates of the normal operating temperatures for a mid-cask cross section. These estimated temperatures appeared to all be computed by hand rather than by computer codes. The steady state temperatures computed by MELCOR were compared to these SAR temperatures as a validation of the MELCOR input model. Comparing the MELCOR results to hand calculated results is not as definitive as comparing to experimental data or to a more detailed computer calculation, but the comparison and the explanation of the differences still provided additional credibility to the MELCOR input model. The temperatures at specific radial locations are compared in Table 5-2 and the differential temperatures across components are compared in Table 5-3.

Both the MELCOR and the SAR calculations assumed the same ambient temperature of 38 °C and a constant decay heat power of 120 kW. The component temperatures computed by MELCOR were in good agreement with those presented in the SAR ($\Delta T = 3$ to 8 °C) for the following cask components, the shell, the basket, and the lodgment walls, and also for lodgment gases and for cask gases. As fin, resin and shell temperatures predicted by MELCOR were all slightly higher than those given in the SAR, the MELCOR model appeared to be slightly less efficient at cooling the cask than was the SAR model. In contrast to the good agreement for the fins, resin layer, and cask shell, the temperatures predicted by MELCOR for outer and inner fuel differed substantially from the temperatures given in the SAR ($\Delta T = -45$ and 51 °C, respectively).

Table 5-3 shows that the same pattern of results was obtained for differential temperatures, which agreed well (small ratios) for all differences except the basket to spent fuel gap for which a ratio of 0.66 was obtained. The SAR calculation overpredicted the temperature required to drive the 120 kW of power across the gap between the outer fuel rods and the lodgment walls for two reasons. First, the SAR calculation did not include the conductive heat transport through the nitrogen gas which in the MELCOR calculation accounted for 23% of the heat transport across this gap. Second, the SAR calculation used an emissivity of 0.55 for the fuel whereas the MELCOR calculation used 0.8. Both used 0.55 for the emissivity of the lodgment walls. The SAR emissivity of 0.55 rather than 0.8 for fuel

results in about a 20% reduction in radiative heat transport for the same surface temperatures. Since the spent fuel emissivity of 0.8 was a measured value for typical PWR spent fuel [6] and conductive heat transport through the gas was a significant contributor, the outer fuel temperature calculated by MELCOR is clearly more valid than the SAR temperature.

Table 5-2: Comparison of MELCOR and SAR Normal Transport Temperatures

| Location | Temperatures (°C) | | |
|-------------------|-----------------------|---------------------------|------------|
| | MELCOR | Safety Analysis Report | Difference |
| Ambient | 38 | 38 | 0 |
| Tip of Fins | 121 | 116 | +5 |
| Resin Surface | 130 | 124 | +6 |
| Outer Steel Shell | 140 | 134 | +6 |
| Inner Steel Shell | 193 | 188 | +5 |
| Outer Basket | 219 | 216 | +3 |
| Lodgment Walls | 279 | 275 | +4 |
| Outer Fuel | 376 | 421 | -45 |
| Inner Fuel | 569 | 518 | +51 |
| Lodgment Gases | 443 | 472 | -29 |
| Average Cask gas | 359 | 367 | -8 |

Table 5-3: Comparison of MELCOR and SAR Normal Transport Differential Temperatures

| Component | Differential Temperatures (°C) | | |
|---------------------------|------------------------------------|------------------------------|-------------|
| | MELCOR | Safety Analysis Report | Ratio |
| Fin Tips to Environment | 83 | 78 | 1.06 |
| Exposed Fins | 9 | 8 | 1.13 |
| Resin Layer | 10 | 10 | 1.00 |
| Steel Shell | 53 | 54 | 0.98 |
| Steel Shell to Basket Gap | 26 | 28 | 0.93 |
| Basket | 60 | 59 | 1.02 |
| Basket to Spent Fuel Gap | 97 | 146 | 0.66 |
| Fuel Assembly | 193 | 97 | 1.99 |
| Total | 531 | 480 | 1.11 |

The MELCOR input model predicted an inner fuel temperature that was 51 °C hotter than the temperature reported in the SAR despite the fact the outer temperature predicted by MELCOR was 45 °C colder than the SAR temperature. In other words, the MELCOR calculation predicted a temperature drop across the fuel assembly of 193 °C rather than the 97 °C drop reported in the SAR. The MELCOR homogenized model for heat transport within a fuel assembly was presented in Section 4.3.7. The SAR model was so vaguely discussed that it was not possible to reliably evaluate the validity of the model. However, the SAR description of the model discussed a direct radiative heat exchange between the center rods of the assembly and the lodgment walls. In reality the radiative heat exchange within a 15x15 rod array involves a network calculation with each rod interacting with all of the other rods. However, the rod-to-rod geometric view factor drops rapidly when the rods are more than about a rod-pitch away

from each other. Thus, rod-to-rod calculations usually only consider rod-to-rod radiative exchange within about 4 rod-pitches of each other. Thus the geometric view factor from the center rods to the lodgment walls is extremely small. The SAR energy exchange between the center rods and the lodgment walls implied a geometric view factor of about 0.04 with both the fuel and lodgment wall emissivities set at 0.55. This is clearly questionable at best. Further, the SAR model did not consider conductive heat transport through the nitrogen gas.

Since the MELCOR inner-to-outer fuel temperature difference agrees with analyses present in Reference 6 and the SAR analyses is clearly deficient, the MELCOR temperatures should be accepted as the more valid temperatures. To further support this conclusion, an additional verification of the MELCOR fuel temperatures was performed using the following simple textbook [10] equation for a cylinder with a uniformly distributed heat source.

$$\Delta T_{\text{fuel}} = \frac{q_{\text{dh}} \cdot r_{\text{fuel}}^2}{4 \cdot k_{\text{fuel}}}$$

where ΔT_{fuel} = the difference between the center and outer fuel temperatures,
 q_{dh} = the decay heat power density,
 r_{fuel} = the equivalent radius of the fuel assembly,
 k_{fuel} = the temperature dependent thermal conductivity of the steel shell.

With a uniformly distributed 120 kW decay heat power and the helium homogenized thermal conductivity of 1.13 W/m-°C (see Table 4-9) for a volume averaged fuel temperature of 476.6 °C, this equation predicts a temperature differential of 192.5 °C, i.e., the same difference as predicted by MELCOR.

This temperature difference is, of course, an underprediction because the shipping cask actually contains nitrogen gas rather than helium, and because nitrogen homogenized thermal conductivities were not available and thus couldn't be used. However, if the nitrogen homogenized thermal conductivity is about 0.8 W/m-°C (about 70% of the helium conductivity), then this equation would predict a temperature difference of 272 °C, thereby suggesting that the actual fuel temperatures were about 80 °C hotter than those used in this study.

The actual peak fuel temperature used in this study may also be somewhat underpredicted because an emissivity of 0.55 was used for the aluminum lodgment walls where a value of about 0.2 might have been more realistic. An emissivity of 0.2 would have reduced the importance of gap radiative heat transport, particularly between the basket and the spent fuel. A value of 0.55 was used in the MELCOR input model to be consistent with the SAR. However, in retrospect, 0.2 probably should have been used. Also in retrospect, the temperature drop across the basket was probably overpredicted by the estimated parameters used to determine a 1-D equivalent thermal conductivity for the basket (see Section 4.3.5). Although the MELCOR and SAR predictions of 60 and 59 °C temperature drops were in good agreement, the 2-D calculations of Reference 6 indicated that this temperature drop might well have been as low as a few degrees. Taking an overall look at the calculated results, the actual peak fuel temperatures were likely a few tens of degrees higher than those used in this study. In light of the preceding comparisons, it was concluded that the predictions of the MELCOR thermal model were quite adequate for the purpose of predicting radionuclide transport within the TN-125 shipping cask. That is, the model deficiencies discussed above were not deemed likely to significantly impact the overall radionuclide transport results.

6.0 BASE SEVERE ACCIDENT SCENARIOS

Three basic shipping cask severe accident scenarios were investigated using the MELCOR input model described above to gain insights into the retention of fission products by the shipping cask once those fission products were released from failed spent fuel rods. A number of parameters were varied during the investigation to determine which conditions or calculational uncertainties most influenced the retention of fission products by the cask.

6.1 Descriptions of the Base Scenarios

The three basic accident scenarios studied were a fire without a collision, a collision without a fire, and a collision that causes a fire. Principal scenario characteristics are presented in Table 6-1.

Table 6-1: Basic Severe Shipping Cask Accident Scenarios Studied

| ACCIDENT SCENARIO | FIRE CONDITIONS | TIME OF ROD/CASK FAILURE | FUEL RELEASE FRACTION FROM RODS TO CASK |
|--------------------------|-------------------|--------------------------|---|
| Collision Without a Fire | No Fire | At Collision | 2×10^{-4} (Collision Induced Fragmentation) |
| Collision With a Fire | 3 Hour 1200 °C | At Collision | 2×10^{-4} (Collision Induced Fragmentation) |
| Fire Without a Collision | 3 Hour 1200 °C | 4 Hours After Ignition | 3×10^{-5} (Lorenz, No Fragmentation) |

In collision damage scenarios, the accidents were initiated by some hypothetical transportation accident that fails the shipping cask seal and all of the spent fuel rods contained within the cask. For collision scenarios that lead to fires, a fully engulfing 1200 °C 3-hour pool fire was postulated to ignite at the time of the collision. In the collision without a pool fire scenario, the transport of radionuclides from the cask was principally driven by spent fuel rod depressurization flows and in the scenarios with a fire, the transport was enhanced by the thermal expansion of gases within the cask as the result of heating by the fire.

In the fire induced damage scenario, the accident was initiated by the hypothetical fire that was assumed to burn steadily at 1200 °C for 3 hours before burning itself out. No collision damage to the cask or the spent fuel rods was assumed. Following fire burnout, the interior of the cask continued to heat as a thermal front caused by fire heating moved inwards. At 4 hours, all of the fuel rods were postulated to fail by burst rupture due to overpressurization caused from fire induced heating of rod gases. The cask was subsequently postulated to fail due to a thermally degraded cask seal at the time the cask was pressurized by the depressurization of helium from the failed fuel rods.

Several important parameters were common to all the basic scenarios. All three basic accident scenarios postulated that all of the fuel rods failed and that they failed at their axial midpoints. Since (a) the size of the hole in the postulated failed cask seal depends upon the extent of the collision damage, (b) there were no real guidelines for determining the size of that hole, and (c) the size the hole greatly impacted the results, two cask seal failure hole sizes were postulated for each of the three scenarios, i.e., a relatively modest hole of 4 mm² and a relatively large hole of 100 mm². The radionuclide aerosols released from the spent fuel rods had a log-normal size distribution with a 2 µm mass medium diameter and a standard deviation of 2.5.

Other parameters were varied to determine the sensitivity of the cask retention of fission products to the values selected for these parameters. Parameters varied during the sensitivity studies of the collision scenario without a fire included:

- the spent fuel release fractions from 10^{-5} to 10^{-3} ,
- the cask seal leak size from 0.1 to 100 mm²,
- the fraction of the spent fuel rods which failed at collision from 0 to 100%,
- the axial location of rod failures, and
- selected radionuclide parameters.

The fire temperature and fire duration were both varied in the scenario that postulated collision induced damage and a fully engulfing pool fire.

6.2 Overall Fission Product Transport Results for the Base Scenarios

The base scenario cask retention fractions are shown in Tables 6-2 and 6-3 respectively for the 4 and 100 mm² cask seal leak sizes. Separate cask retention fractions were determined for each radionuclide species studied, i.e., Kr, CsOH, CsI, TeO, and fuel fines (particulates) and for the helium gas expelled from the fuel rods. Since fission product species that remain in the solid phase throughout the course of an accident scenario (e.g., oxides of Co, Sr, and Ce) transport only as constituents of fuel fines, their cask retention fractions are identical to those calculated for the fuel fines.

Table 6-2: Base Scenario Results for a 4 mm² Cask Seal Leak Area

| FRACTIONS OF RADIONUCLIDES RETAINED WITHIN CASK | | | | | | |
|---|-------|-------|--------|--------|--------|------------|
| ACCIDENT SCENARIO | He | Kr | CsOH | CsI | TeO | Fuel Fines |
| Collision Without a Fire | 0.216 | 0.111 | 0.9994 | 0.9987 | 0.9858 | 0.9835 |
| Collision With a Fire | 0.158 | 0.082 | 0.9955 | 0.9957 | 0.9851 | 0.9833 |
| Fire Without a Collision | 0.164 | 0.180 | 0.589 | 0.587 | 0.731 | 0.972 |

Table 6-3: Base Scenario Results for a 100 mm² Cask Seal Leak Area

| FRACTIONS OF RADIONUCLIDES RETAINED WITHIN CASK | | | | | | |
|---|-------|-------|-------|-------|-------|------------|
| ACCIDENT SCENARIO | He | Kr | CsOH | CsI | TeO | Fuel Fines |
| Collision Without a Fire | 0.222 | 0.264 | 0.805 | 0.771 | 0.754 | 0.746 |
| Collision With a Fire | 0.160 | 0.151 | 0.754 | 0.721 | 0.716 | 0.708 |
| Fire Without a Collision | 0.162 | 0.189 | 0.417 | 0.321 | 0.331 | 0.667 |

Inspection of Tables 6-2 and 6-3 shows that, as expected, retention of noble gases (Kr) is much less than retention of fuel fines (particulates), and that retention of condensable vapors (CsOH, CsI, and TeO) is similar to that of fuel fines for collision and collision plus fire scenarios and much reduced for fire only scenarios. In addition, retention of all species, except the noble gases, is higher for the scenarios with a 4 mm² cask seal leak area than it is for the scenarios with a 100 mm² leak area.

Several trends seem counterintuitive. First, Kr retention is greater for the 100 mm² leak scenarios than for the 4 mm² leak scenarios. Second, adding a fire to the collision scenario decreases Kr retention much more for the 100 mm² scenarios than for the 4 mm² scenarios. Third, even though CsOH is more volatile than CsI, its retention during fire only scenarios is the same or greater than that of CsI.

The behavior of Kr was complicated by imperfect modeling of the release of radionuclide species from the failed fuel rods. Although Kr and He flow rates during rod depressurization should behave similarly, they don't because Kr was sourced into the cask interior at a constant rate over a 100 second time period while He flows from a rod volume into the cask through a resistance (an orifice that represents the retarding effect of the spent fuel matrix on gas flow through that matrix) with a rate that decreases exponentially with time over a time period of about 150 seconds. Consequently, when cask and therefore rod depressurization is rapid, as is the case when the leak area is 100 mm², the gas flow into the cask is low in Kr during the early portions and rich in Kr during later portions of the 150 sec He rod depressurization period. The relative flow rates of He and Kr during rod depressurization means that the gas flows from the cask to the environment during rod depressurization contain concentrations of Kr that are much lower than they would be if Kr were not sourced into the cask at a uniform rate. Consequently, retention of Kr for 100 mm² scenarios is higher than it ought to be both absolutely and relative to the retention of Kr predicted for 4 mm² scenarios.

The behavior of Kr associated with the imperfect modeling of its release into the cask is illustrated by comparing the behavior the cask retention fractions for He to those of Kr in Tables 6-2 and 6-3. Realistically these two gasses would behave identically if the concentrations of Kr in the He atmosphere of the rods were uniform, i.e., the mass of Kr per mass of He passing through the rod breach is constant. These He retention fractions show nearly the same behavior for the 4 and 100 mm² cask seal leak sizes. Further, the effect of adding a fire to the collision scenario was nearly the same for the 4 and 100 mm² cask seal leak sizes.

The imperfect behavior noted for the Kr must be extended to the other species as well since those species were also introduced into the cask at a constant rate over a 100 second period. Thus the roughness of this model introduced calculational uncertainty into the predicted transport of all of the radionuclide species. The degree of uncertainty for each radionuclide species is directly related to how rapidly that species deposited onto surfaces near the breach of the rods, i.e., the more rapid the species deposited, the less impact the imperfect model had on the predicted release of the species from the cask. Therefore, the discrepancy noted above for Kr relative to He, indicates the maximum uncertainty in the cask retention fractions associated with the roughness of the radionuclide source model, i.e., the uncertainty associated with the transport of Kr which was on the order of 10 to 20%, should be considerably higher than the corresponding uncertainty associated with the fuel fines which tended to deposit almost immediately upon being expelled from the rods. In retrospect, the radionuclides source model should have been designed to introduce the radionuclides species into the He atmosphere of the fuel rods prior to their postulated failure, however the overall conclusions of this study are still valid.

The radionuclide source timing model, i.e., the uniform rate for 100 seconds, was revised as a results of these observations so that the model introduces each radionuclide species into the fuel channels in direct proportion to the rate of helium flow from the fuel rod breach. The base cases were rerun with this revised model and those revised results are found in the Addendum.

Another potential uncertainty potentially impacting this study is that the diffusion of one gas species through another gas is not modeled in the MELCOR code. During the longer duration accident scenarios, the Kr and the airborne vapors could realistically relocate within the cask despite the lack of convective flows by means of this diffusion process. This process would most likely increase the retention of vapor radionuclide species over the retention predicted without considering diffusion because with diffusion, these vapors could find colder surfaces to condense onto more rapidly than predicted herein due to convective flows. This source of uncertainty indicates conservatism for the predicted results reported herein, i.e., including a diffusion model would tend to increase the predicted retention of the vapor species. Note that this diffusion would not significantly impact the transport of the solid aerosol particles due to the relative short times that these aerosol particles are airborne.

The enhanced retention of CsOH relative to CsI in fire only scenarios is caused by the fact that, for these calculations, CsI usually rapidly condenses to the solid phase and then transports as an aerosol, while CsOH, because

of its greater volatility, usually transports as a vapor. Consequently, because vapor deposition onto cold cask surfaces is much more rapid than aerosol deposition onto all cask surfaces, despite its greater volatility, retention of CsOH is sometimes greater than retention of CsI, at least when CsOH but not CsI reaches a cold surface while still a vapor. In particular, this result is observed for the 100 mm² fire only scenario where the retention fraction for CsOH is 0.417 while that of CsI is only 0.321.

Most of the fuel fines were retained within the cask, especially for a small cask seal leak, where times for particle deposition are lengthy. Despite the high depressurization flow rates, the cask retention fractions were also quite high, 2/3 to 3/4, for the large leak because particle deposition onto spent fuel assemblies and lodgment surfaces near the location where the rods ruptured was efficient.

Adding a fully engulfing pool fire to the collision (collision plus fire scenarios) had only a relatively minor effect on the cask retention fractions because most of the radionuclides remaining within the cask after the completion of cask depressurization were present as aerosols that had deposited onto interior surfaces. Thus, when the thermal front generated by the pool fire reached the interior of the cask, despite some movement of volatile species from hotter surfaces to colder surfaces, there was not enough thermal driving force to transport these volatile species from the cask through the seal leak to the environment. The modest reduction in noble gas retention in the fire/collision scenario, relative to the collision only scenario, was due to the thermal expansion of interior gases by thermal heating.

The cask retention fractions were significantly lower for the volatile species in the fire without collision scenario than in the other scenarios because the interior surfaces and gases were already at elevated temperatures when the fuel rods ruptured releasing these species into the cask. The colder end surfaces were also at more elevated temperatures, thereby reducing their effectiveness for vapor deposition. In this scenario, a much higher portion of the volatile species were transported in the vapor form at a time when the cask was undergoing depressurization and the lodgment walls and the fuel rod claddings were hot enough so that vapor deposition to these surfaces was not important. However, since the postulated releases from the fuel rods were much smaller because they were not assumed to reflect the occurrence of fuel fragmentation, the masses of radionuclides released to the environment were still considerably less for this fire scenario than for the collision or collision plus fire scenarios.

The fraction of the fuel being transported by the shipping cask that was predicted to enter the environment for the base case scenarios is shown in Table 6-4. These insights are discussed further in the following report sections.

Table 6-4: Base Scenario Fines Released to Environment

| FRACTIONS OF TOTAL FUEL MASS RELEASED TO ENVIRONMENT AS FINES | | |
|--|--|--|
| ACCIDENT SCENARIO | 4 mm² Cask Seal Leak | 100 mm² Cask Seal Leak |
| Collision Without a Fire | 3.30 x 10 ⁻⁶ | 5.08 x 10 ⁻⁵ |
| Collision With a Fire | 3.34 x 10 ⁻⁶ | 5.84 x 10 ⁻⁵ |
| Fire Without a Collision | 8.40 x 10 ⁻⁷ | 9.99 x 10 ⁻⁶ |

In retrospect, a forth basic scenario should probably have been postulated in which all of the spent fuel rods failed as a results of collision impact forces but the cask seal remained intact until fire induced thermal degradation caused the seal to fail at 4 hours. In this scenario, the volatile radionuclides associated with fragmented fuel would be primarily in the airborne vapor phase at the time the cask seal failed resulting in the combination of a relatively high release of cesium species from the fuel rods and a relatively low retention of those species by the shipping cask, i.e., a potentially much worse scenario than the three base scenarios reported herein. If the cesium released from fragmented spent fuel rods were 5 to 10 times higher than usually postulated for non-fragmented rods (Lorenz) and the cask retention fraction was in the range of 0.3 to 0.6, as calculated here for the fire induced damage scenario, then the cesium released to the environment might be several times higher than the result usually cited that uses the

results of Lorenz experiments to estimate release from the rods to the cask interior and then assumes a release fraction of one for release from the cask to the environment.

6.3 Base Scenario Hydrodynamic and Heat Transport Results

A sampling of the hydrodynamic and heat transport results for the base scenarios are presented in this section to provide further understanding of the radionuclide transport results.

The primary driving force for radionuclide transport from the PWR shipping cask was the helium depressurization flows from the ruptured fuel rods. The pressurization and depressurization of the shipping cask is shown in Figure 6-1 which is a plot of the cask pressures for both the collision induced damage and the fire induced damage scenarios with both a 4 and a 100 mm² cask seal leak. The cask was operated with a half an atmosphere of nitrogen at the normal transport temperatures. The fuel was postulated to fail at time zero in the collision scenario and at 4 hours in the fire scenario. The cask pressure increased slightly in the fire scenario prior to fuel rod ruptures due to thermal heating of the cask's nitrogen atmosphere. The cask took about 2 hours to depressurize when a 4 mm² cask seal leak was postulated but only a few minutes for a 100 mm² cask seal leak. The longer it took to depressurize the cask, the more time was available for the radionuclides to deposit onto interior surfaces which produces a higher retention of the radionuclides.

The circulation of gases within the cask determined the pathway of airborne radionuclides from their point of introduction into the cask to either the cask seal leak or a surface where they were deposited. Figures 6-2 and 6-3 present mass flow rates and velocities between cask volumes (i.e., through the flow paths that connect these volumes) for the collision without a fire scenario that had a 4 mm² seal leak area. Thus, these figures indicate the circulation of gases in the cask that occurs during this accident scenario. The figures show that during the first minute or two after rod failure, the gases expelled from the fuel rods flowed preferentially towards the failed lid end of the cask because at the initial high flow rates, the flow resistance through the center cross region was significantly higher than through the lodgments which inhibited gas flow into the center cross region. The distribution of aerosol particles deposited within the lodgment reflects this preferential flow pattern at the time when the aerosols were first introduced into the lodgments by rod failure. Because the seal leak has a small cross section (4 mm²), the flow velocity through this leak, which peaks at 360 m/sec, is very much greater than the flow velocities through any of the internal cask volumes (e.g., lodgments to cask lid region), which are all approximately 2×10^{-3} m/sec two minutes after rod failure. Because flow velocities between internal cask volumes were quite slow, the times available for aerosol deposition onto internal cask surfaces were relatively long and deposition was quite efficient. Consequently, aerosol retention fractions for this scenario are very large (0.9835).

The thermal response of the shipping cask involved in a 3 hour 1200 °C pool fire is shown in Figures 6-4 through 6-7. Figure 6-4 shows the variation with time of the temperatures of the fire, of a number of cask structures, and of the gases in the lodgment volumes (channel gases). While the fire was burning, outer cask structure temperatures increased rapidly with the tips of the fins approaching the temperature of the fire. The temperatures of cask interior structures increased more slowly. After the fire burned out at 3 hours, a thermal front continued to move inwards with the inner fuel temperature peaking at 836 °C at 6.7 hours. At about 4 hours, the temperature of the inner fuel rods exceeded the temperature range where typical PWR spent fuel rod claddings may rupture (725 to 750 °C, Reference 6). The outer fuel rod temperatures, which peaked at 703 °C, also approached this temperature range. The fuel baskets reached temperatures that exceeded the 660 °C melting temperature of aluminum at 3.8 hours. The effects of basket melting were not considered in this study and thus neither were its effects on radionuclide transport.

Figure 6-5 shows the total radiative and convective heat transport to the cask fins during the fire and the subsequent cooling following the fire. The heating of the cask by the fire was dominated by radiative processes but the cooling of the cask was dominated by convective processes. Figure 6-6 shows three internal cask heat transport rates, i.e., the total heat transport across the basket-to-shell gap, the fuel-to-basket gap, and the total heat conducted axially to the end structures. In this figure, outward flows of heat have positive signs. Thus, the heat transport across the

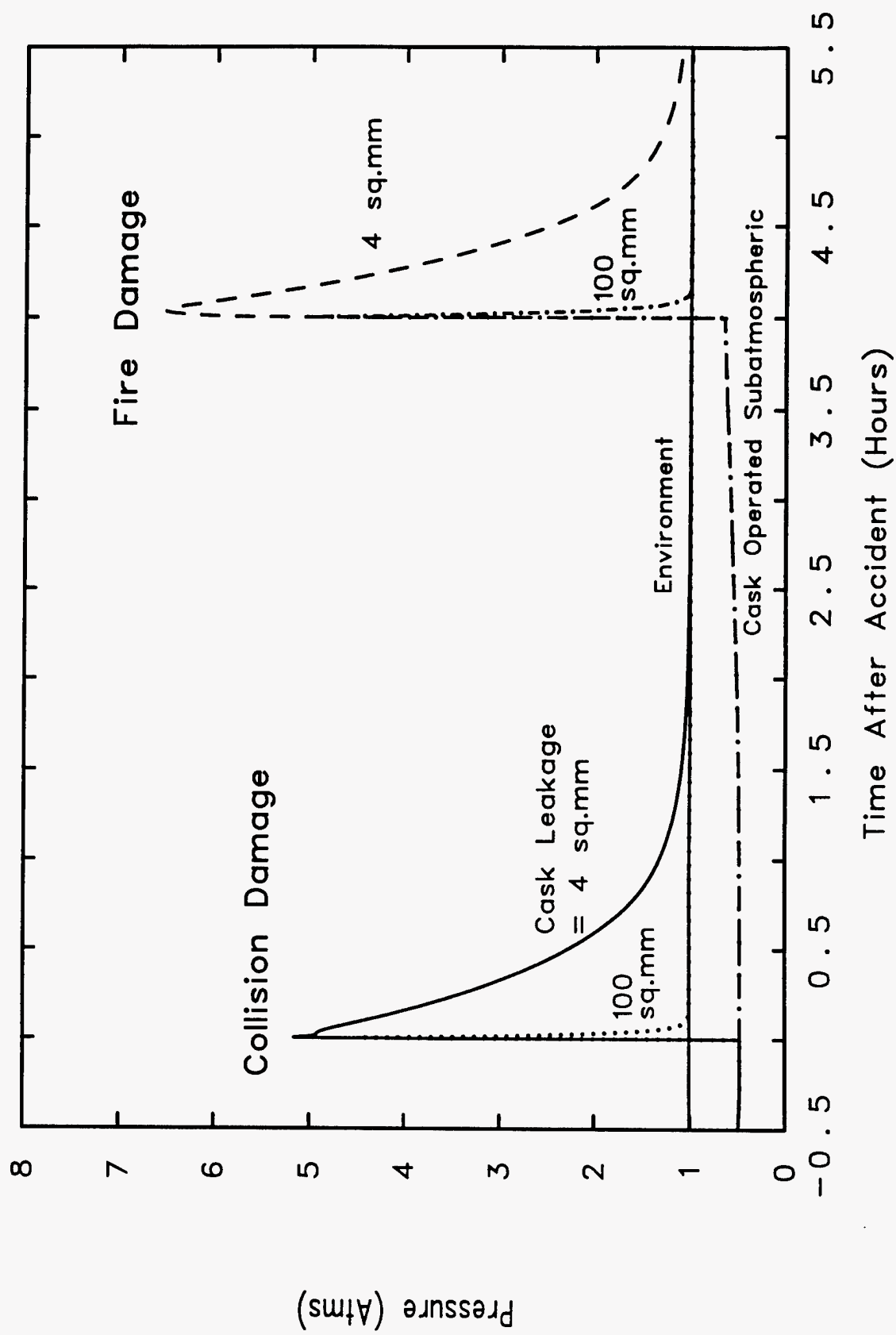


Figure 6-1: Basic Scenario Cask Pressures

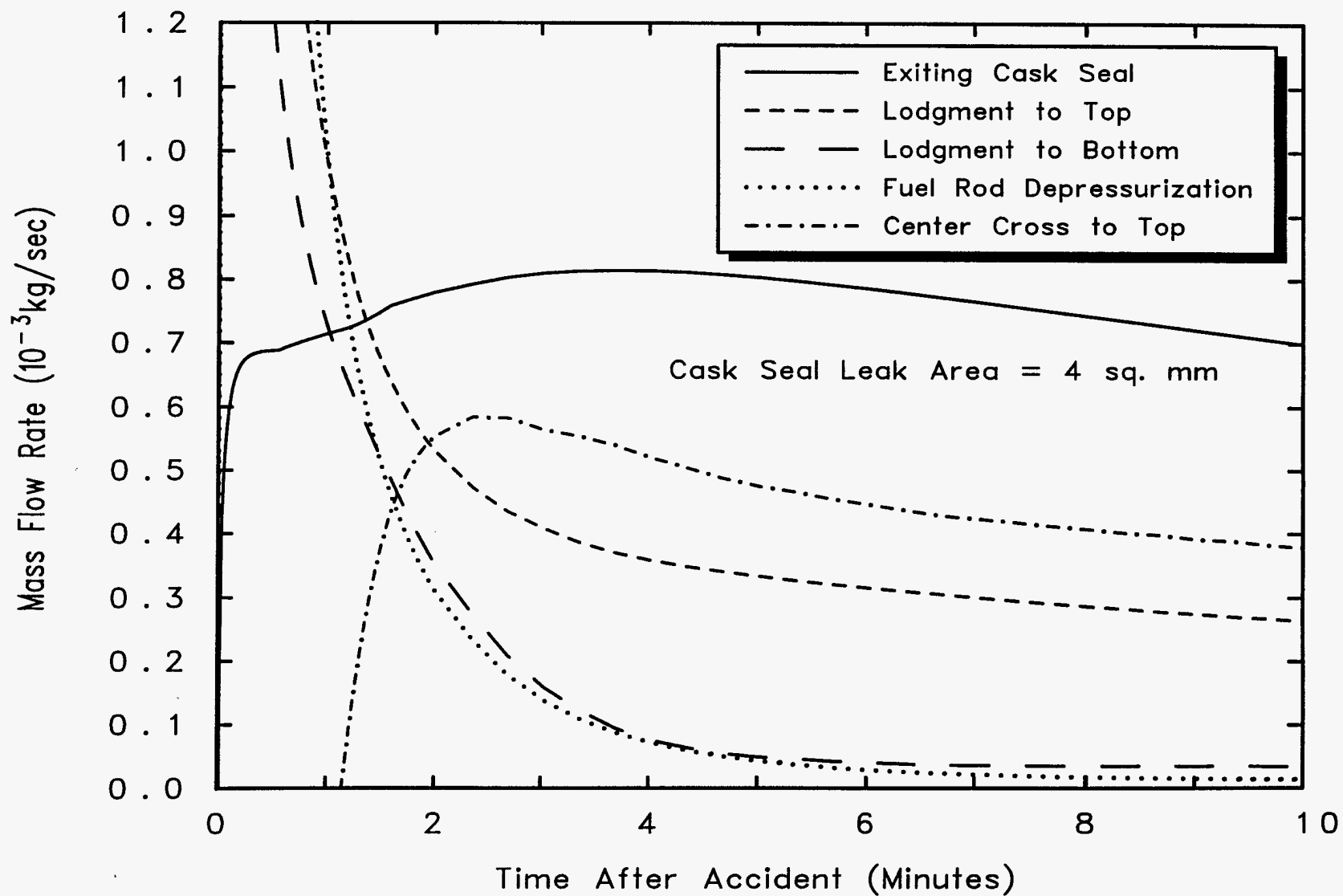


Figure 6-2: Collision Scenario Mass Flows

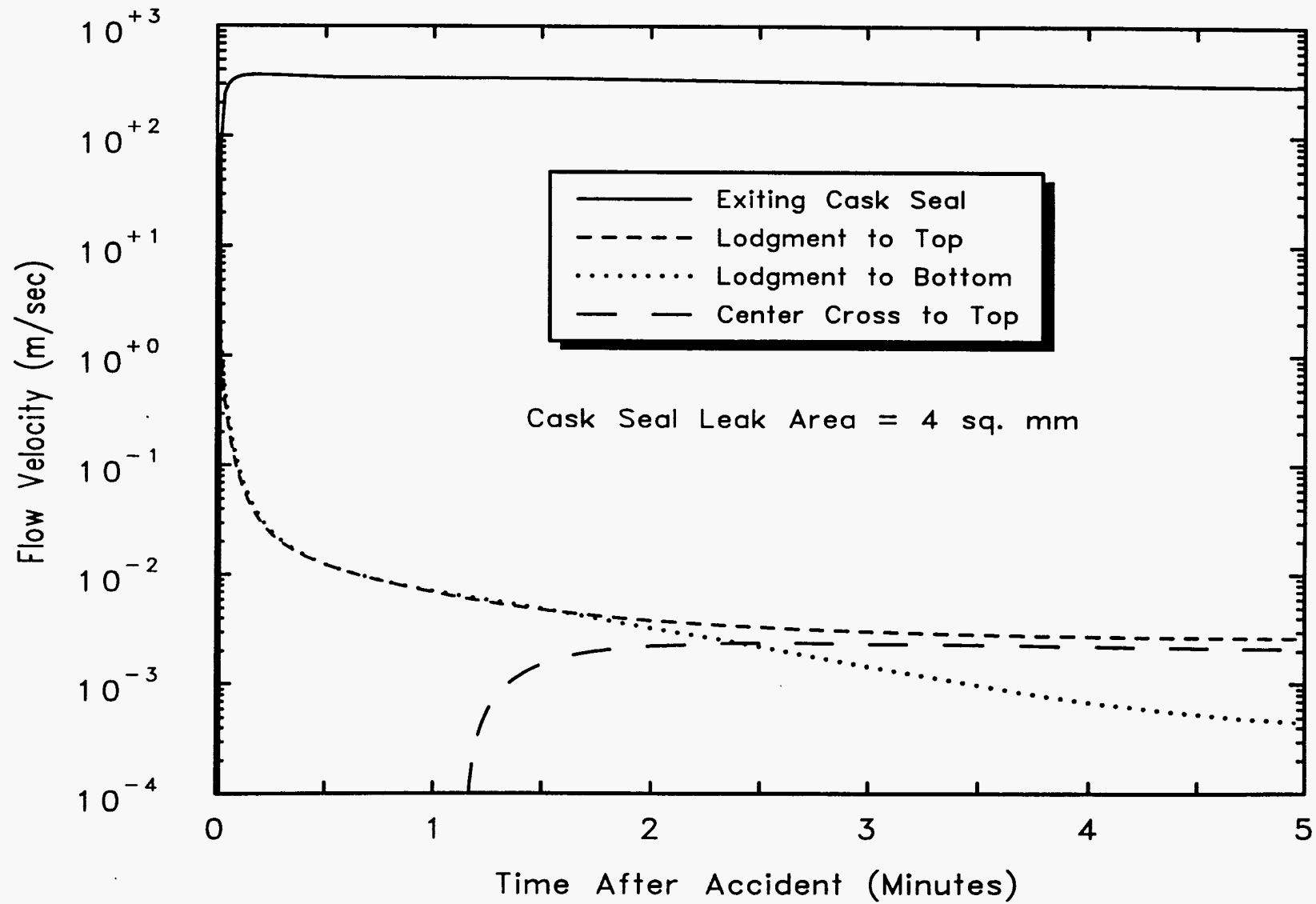


Figure 6-3: Collision Scenario Flow Velocities

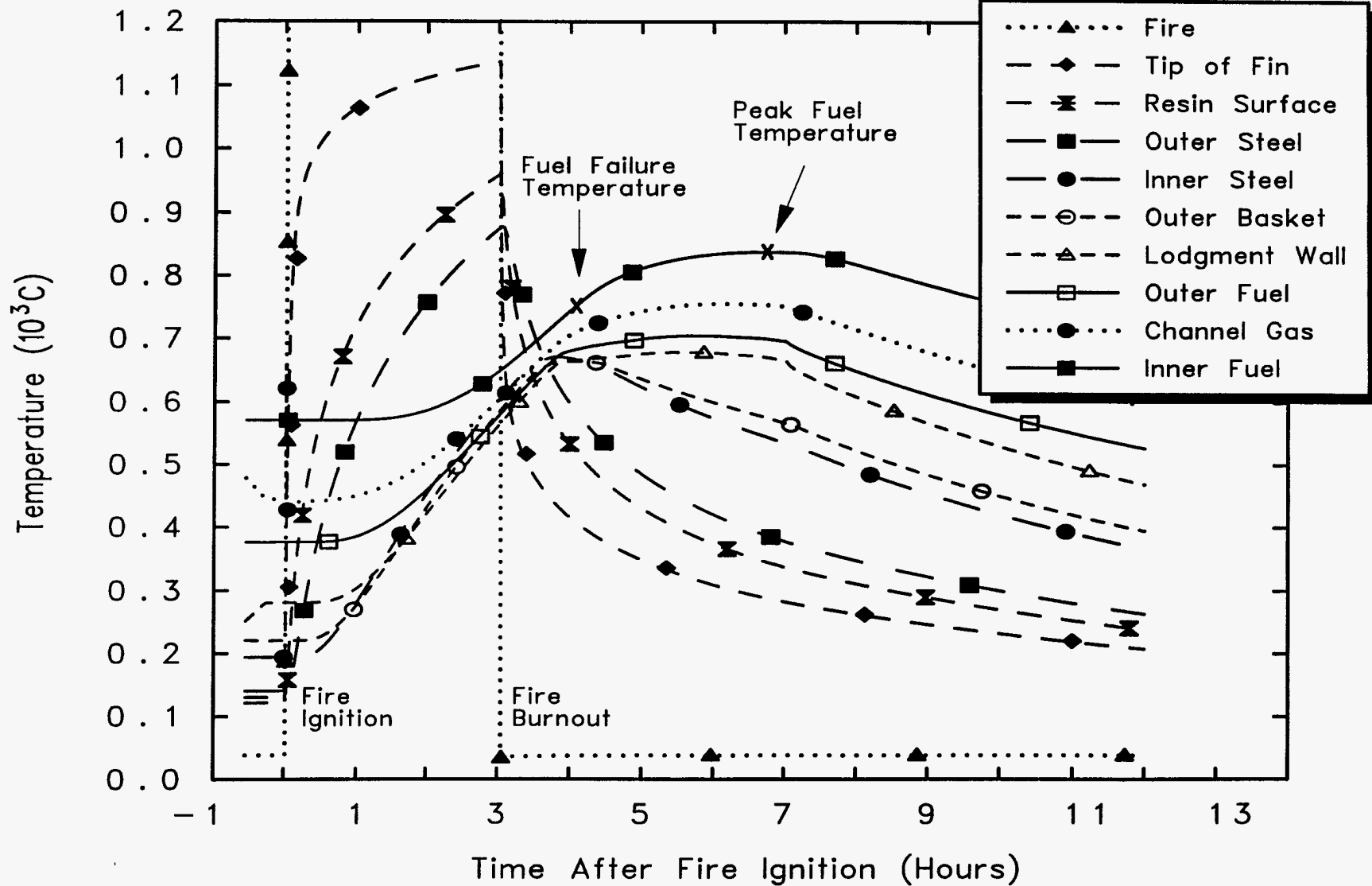


Figure 6-4: Cask Thermal Response to 3-Hour 1200°C Fire

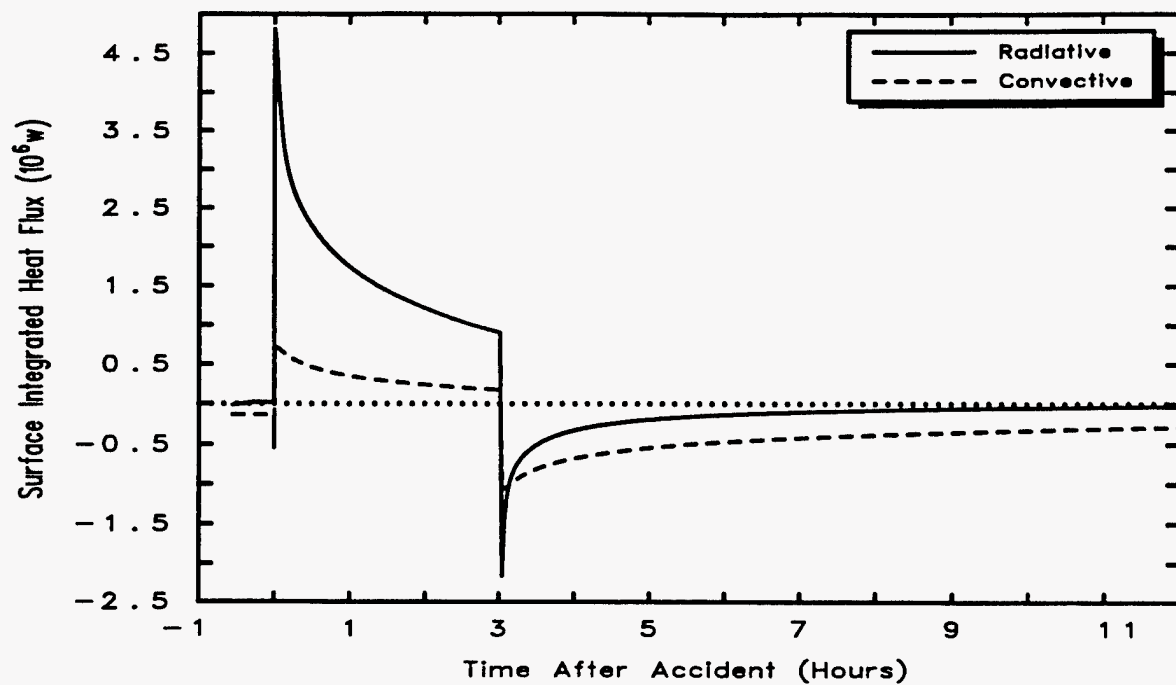


Figure 6-5: Total Heat Transfer to Fins

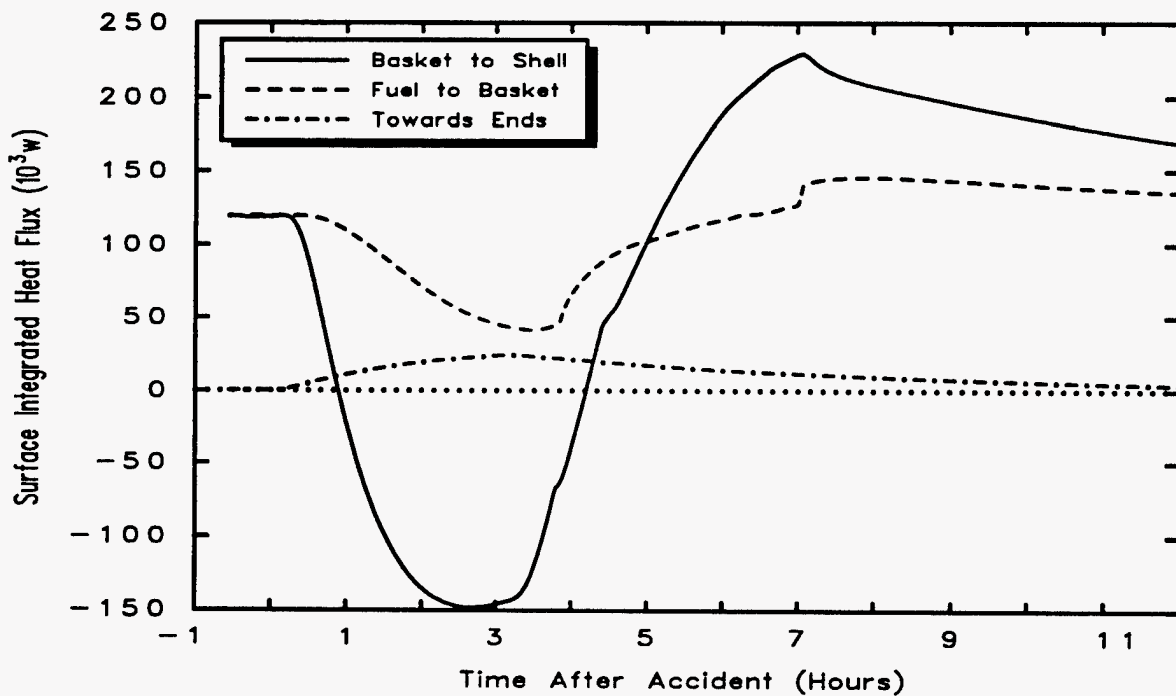


Figure 6-6: Heat Transfer Within Cask Interior

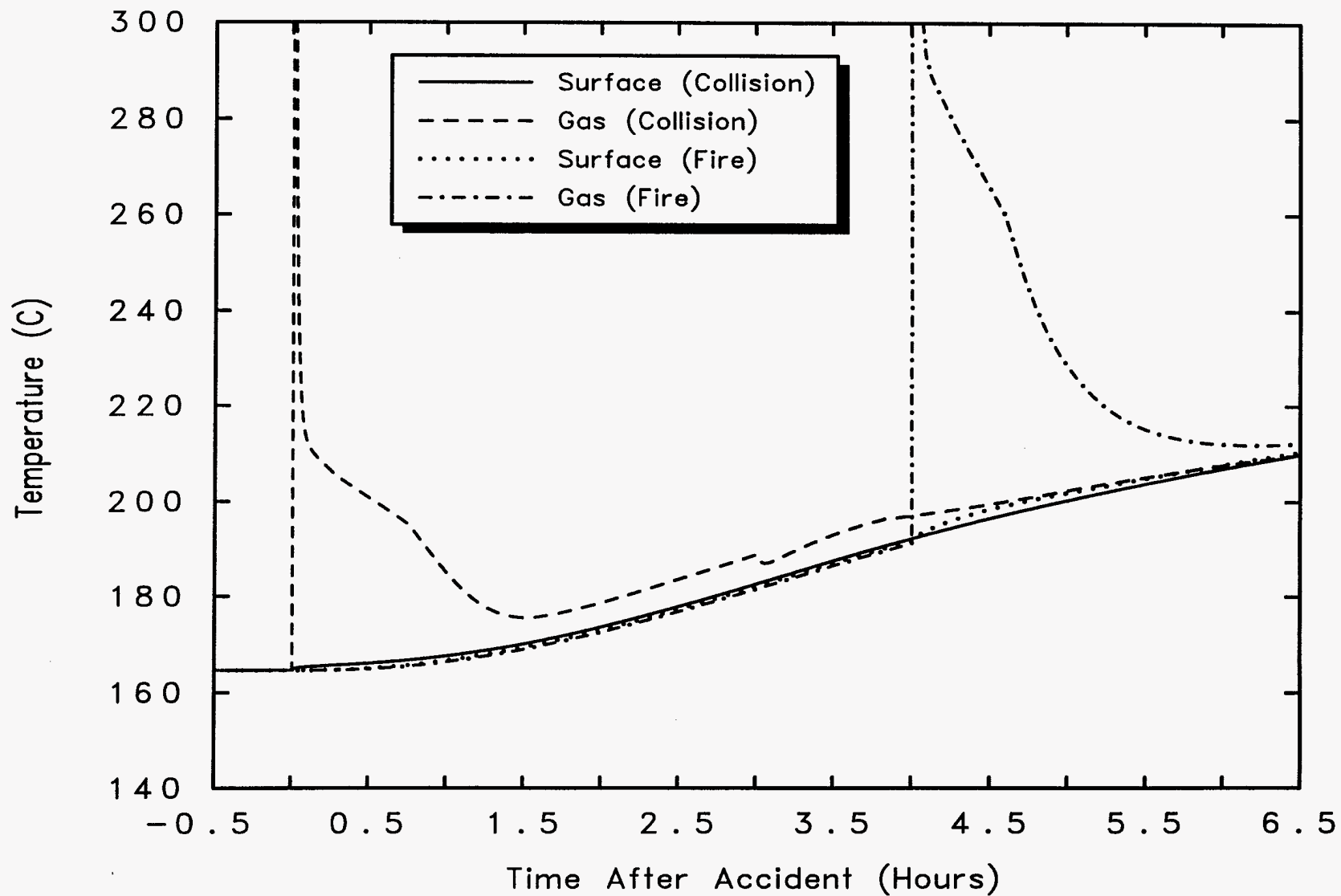


Figure 6-7: Temperatures in the Upper Lid Region

basket to shell gap is initially positive because initially heat is flowing outward from the fuel through the rods to cask structures, then it becomes negative as the heat front from the fire reaches internal cask structures, and finally it again becomes positive after the fire dies out. Because of the continuous input of heat due to radioactive decay, the heat transport rate from the fuel to the basket always remained positive, meaning the fuel was continually cooled even when the cask was engulfed by a pool fire.

The heat conducted towards cask end structures was much smaller than the heat transported radially, however this heat did increase the temperature of the end structures significantly. Figure 6-7 shows the temperature of the cask lid and the temperature of the gases in the lid end region for both the collision plus fire and the fire only scenarios. In both scenarios, when the rods fail, the temperature of the gases in the lid region rises rapidly as rod helium, previously heated by radioactive decay of fuel, is released by rod depressurization and then mixes with the nitrogen in the lid region. The fact that lid gas and surfaces temperatures for the fire only scenario track the lid surface temperature for the collision plus fire scenario until 4.0 hours, when the fuel rods fail in the fire only scenario, shows that lid surface and gas temperatures are principally driven by fire heating until helium is introduced into this region by rod depressurization. The end region surface temperatures were significantly warmer for the fire only scenario at the time of fuel rod failure than they were for the collision plus fire scenario, affecting the deposition of vapors and the solidification of gasborne vapors.

6.4 Base Scenario Radionuclide Transport Results

Radionuclide transport calculations are usually considered complete when all the radionuclides released from the cask inventory have either deposited onto surfaces or have escaped from the cask to the environment where they constitute a source term for consequence calculations. Aerosol particles once deposited onto a surface will remain on the surface unless a strong convective gas flow over the surface resuspended the particles. But once the fuel rods were fully depressurized, the gas flows within the cask were not large enough to resuspend particles. Deposited vapors will also remain on surfaces unless the temperature of those surfaces increases enough to cause revaporization.

The behavior of several radionuclide species is shown in Figures 6-8 and 6-9 for the accident scenarios where the seal leak area was 4 mm^2 . The aerosol particles sourced into the cask deposited rapidly onto cask surfaces. This behavior is depicted in Figure 6-8a for the collision without a fire scenario where most particles indeed deposited onto a surface within the first few minutes following fuel rod rupture.

(The slight discontinuity shown in Figure 6-8a at 100 seconds corresponded to the cessation of the aerosol source into the cask.) Inspection of the amounts of aerosols on vertical and horizontal surfaces showed that most of the aerosols deposited onto horizontal surfaces, which means that gravitational settling was the dominant deposition process. Table 6-5 shows the distribution of deposited fuel fines by final locations for the collision without fire scenario. Approximately 2/3 of the particles remained within the central axial lodgment volume into which they were initially sourced from the rods, and most of these aerosols were on the floor of this lodgment volume.

Figure 6-8b compares the behavior of a condensable vapor, CsOH, to that of a non-condensable gas, Kr, for the collision plus fire and fire only scenarios. In the collision plus fire scenario, the majority of the Kr was expelled from the cask during cask depressurization while most of the CsOH was rapidly deposited onto interior cask surfaces. Then later, well after the cask had depressurized, the deposited CsOH was revaporized from the surfaces where it was deposited due to heating of those surfaces by the fire. However, little of the revaporized CsOH escaped from the cask because there is no longer an efficient transport process available to carry the CsOH vapor out of the cask (depressurization is over and diffusion is inefficient). In the fire only scenario, the CsOH aerosols sourced into the cask vaporized quickly in the cask atmosphere that now was hot due to heating by the fire. Consequently, a larger fraction of the CsOH was expelled from the cask during cask depressurization. Thus, for the fire only scenario, the CsOH behavior was similar to that of Kr. Because fuel fragmentation was not postulated for the fire only scenario, which does not subject the cask to impact, the actual quantity of CsOH released to the environment was less than the amount released to the environment by the collision plus fire scenario where additional fuel fines and thus CsOH aerosols were assumed to be generated by fragmentation of fuel during the collision.

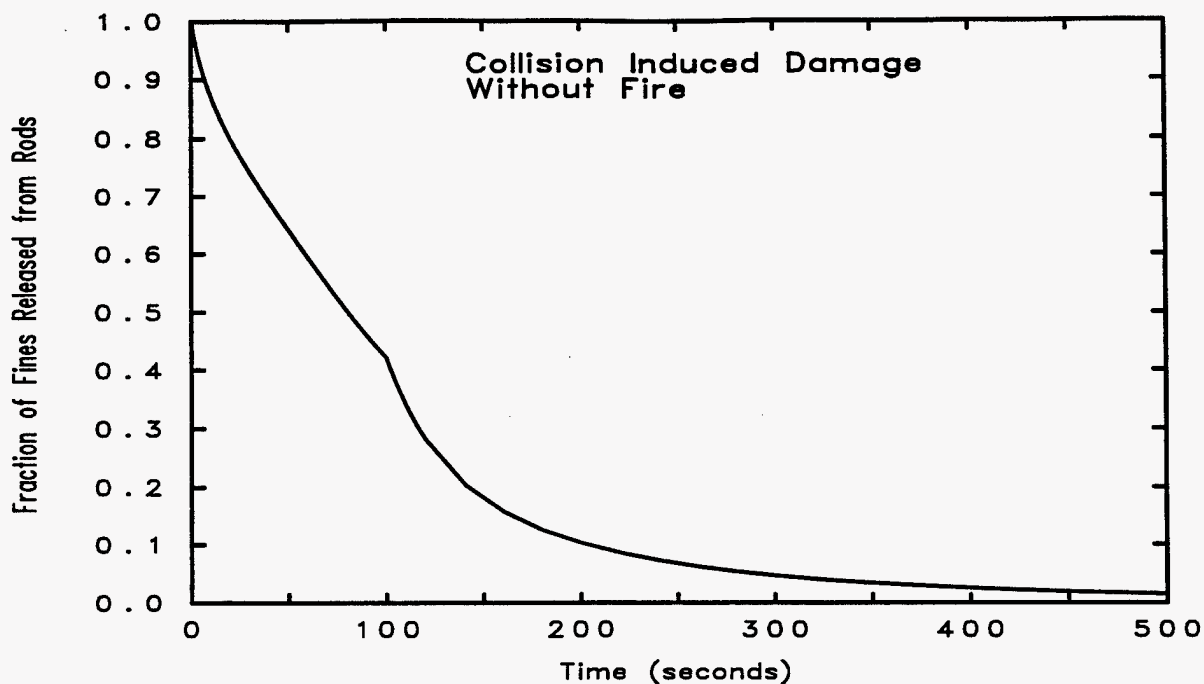


Figure 6-8a: Airborne Fuel Fines Within Cask

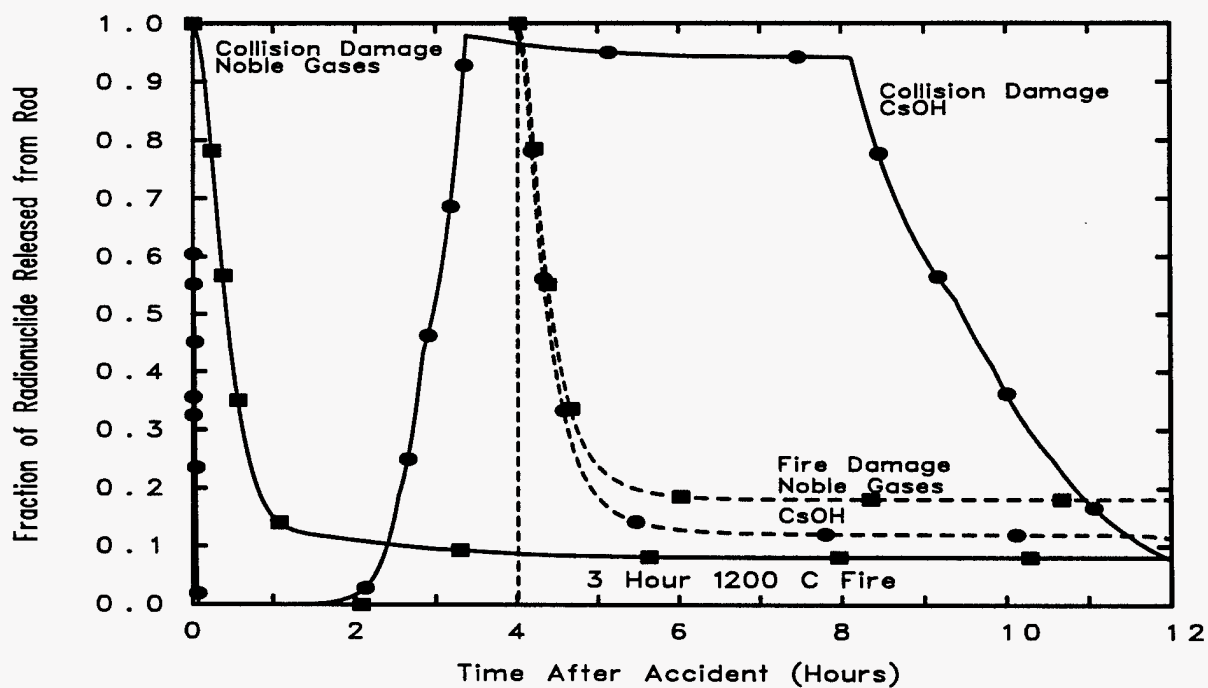


Figure 6-8b: Airborne Kr and CsOH Within Cask

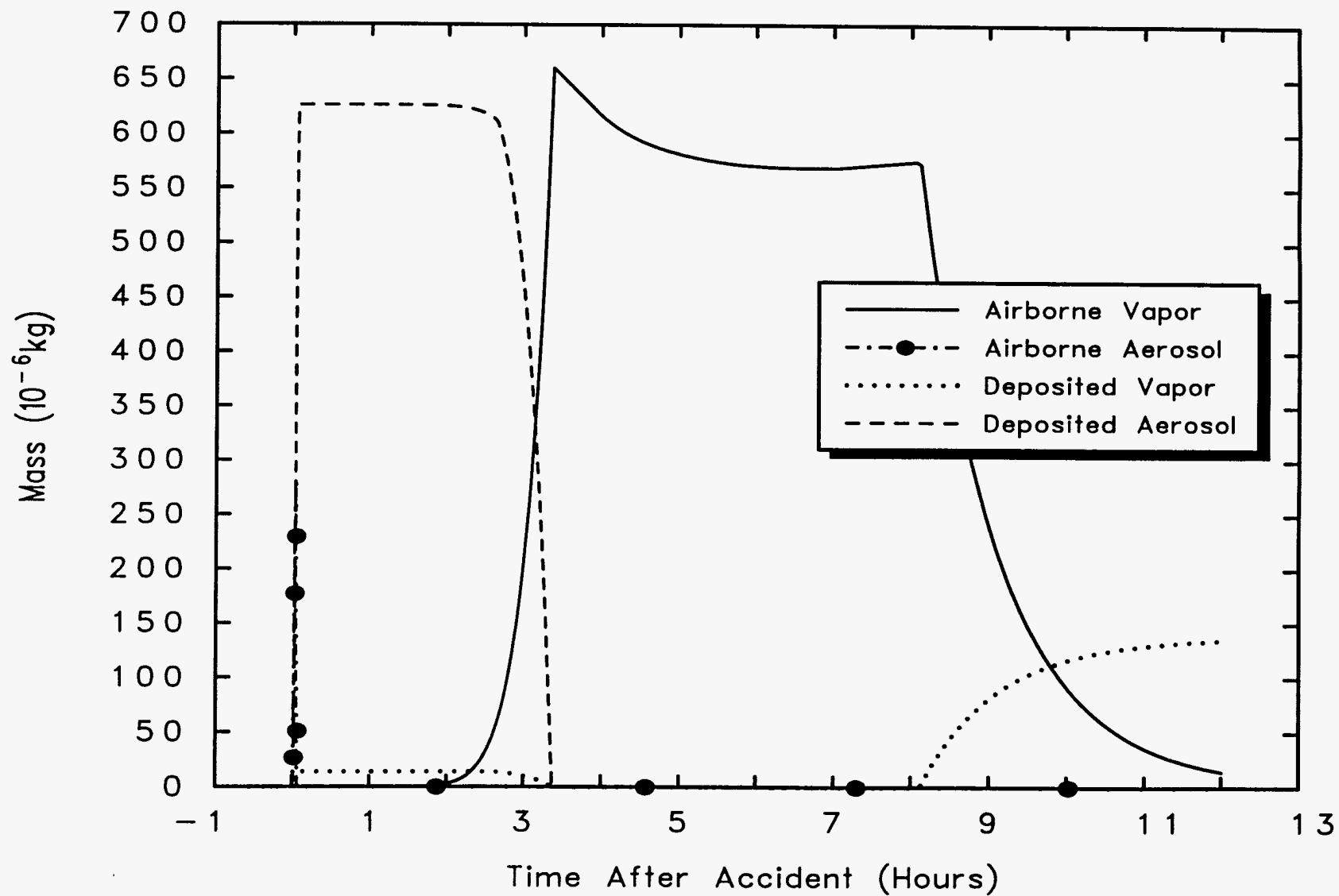


Figure 6-9: CsOH Mass in Center Lodgment Volume and Floor

Table 6-5: Final Distribution of Fuel Fines for the Collision without Fire Scenario

| LOCATION | Fuel Fines (Percent of Amount Released from Rods) |
|-------------------------------------|--|
| Lodgment - Gas Plenum Region | 3.6 |
| Lodgment - Mid Upper Region | 10.8 |
| Lodgment - Central Region | 66.5 |
| Lodgment - Mid Lower Region | 10.4 |
| Lodgment - Bottom End Region | 3.0 |
| Other Interior Regions | 4.1 |
| Released to Environment | 1.6 |

The behavior of the CsOH in the central axial lodgment volume during the collision plus fire scenario is further illustrated in Figure 6-9. This figure shows that the CsOH initially sourced into this volume as an aerosol rapidly deposited during the first few minutes of the scenario onto the horizontal lodgment floor where it remained until heating of lodgment surfaces by the fire caused CsOH aerosols to vaporize starting at about two hours into the scenario. Much later, at about eight hours, five hours after the fire ceased, cooling of lodgment surfaces begins to allow CsOH vapor to condense onto cool surfaces. Note that during the first three hours of the scenario, a small amount of CsOH was deposited as a vapor because some of the CsOH aerosols sourced into the central lodgment volume were vaporized upon release from hotter center fuel rods and therefore condensed onto cool lodgment walls as soon as they encountered those walls.

The timing of the release of fuel fines to the environment is illustrated in Figures 6-10a and 6-10b. For each of the three base scenarios, Figure 6-10a shows the time integrated amounts of fuel fines that escape from the cask to the environment expressed as a fraction of the fines initially released from the fuel rods into the cask. Figure 6-10b presents the same data expressed as a fraction of the total cask fuel mass. Figure 6-10a shows that the fraction of the fines released from the rods that escape to the environment is somewhat higher for the fire only scenario than it is for either the collision only or the collision plus fire scenario. Despite this, Figure 6-10b shows that the fraction of total fuel mass released to the environment during the fire only scenario is much smaller than the fraction released during the other two scenarios. As was noted previously, this slightly counterintuitive result is caused by the assumption that collision scenarios generate additional fuel fines by fragmenting fuel during the collision which means that there are significantly larger amounts of fuel fines available for release during the two collision scenarios than there are during the fire only scenario.

The timing of the releases of CsI and TeO to the environment is shown in Figures 6-11 and 6-12, respectively, again expressed as fractions of the mass of each radionuclide species released from the fuel rods into the cask. Figure 6-11 shows that a fire following a collision significantly increases CsI release compared to that produced by a collision without a fire. Release is increased because vaporization of CsI deposited on surfaces while cask gases are expanding due to heating by the fire causes a large amount of the vaporized CsI to be transported from the cask to the environment. The fire only results presented in the figure show that cask and rod failure after the cask has been heated to elevated temperatures greatly enhances CsI release to the environment. Release is increased because for the fire only scenario much more CsI is present as a vapor when cask depressurization takes place than is present for the collision only or the collision plus fire scenarios. Figure 6-12 presents similar results for TeO. This figure shows that release of TeO is not significantly increased when a collision leads to a fire. The TeO release to the environment for TeO does not show an enhancement similar to that of CsI because TeO is much less volatile than CsI. Thus, during both the collision only and the collision plus fire scenarios, TeO transports primarily as an

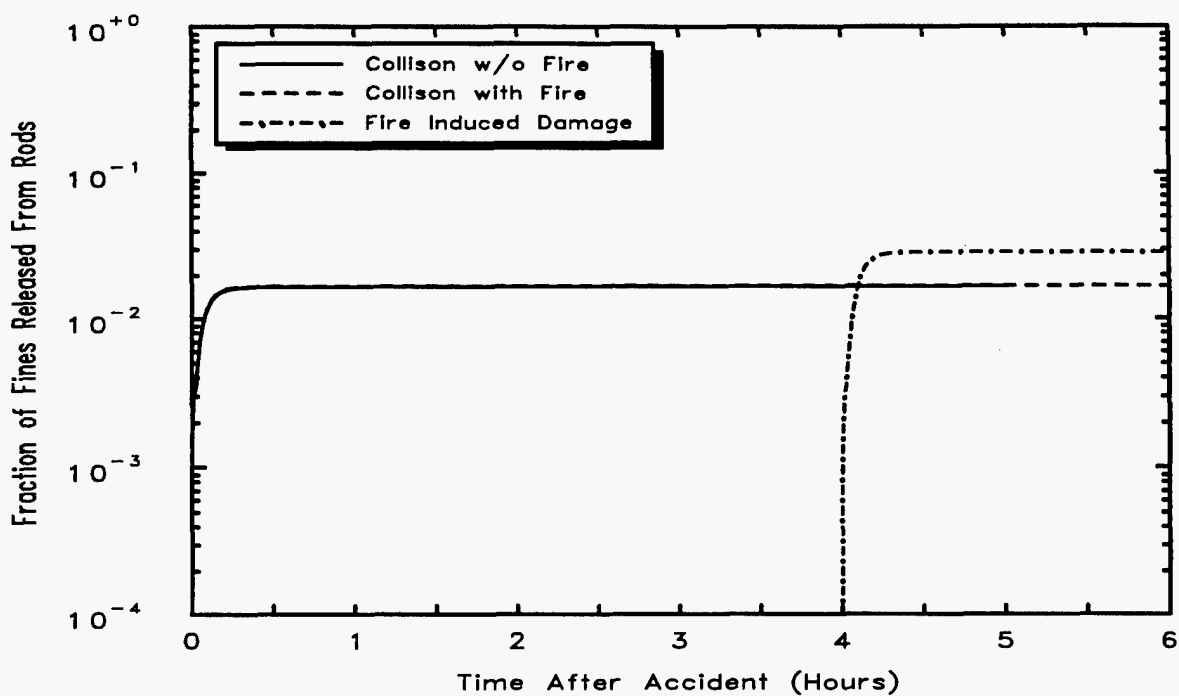


Figure 6-10a: Fuel Fines Released to Environment

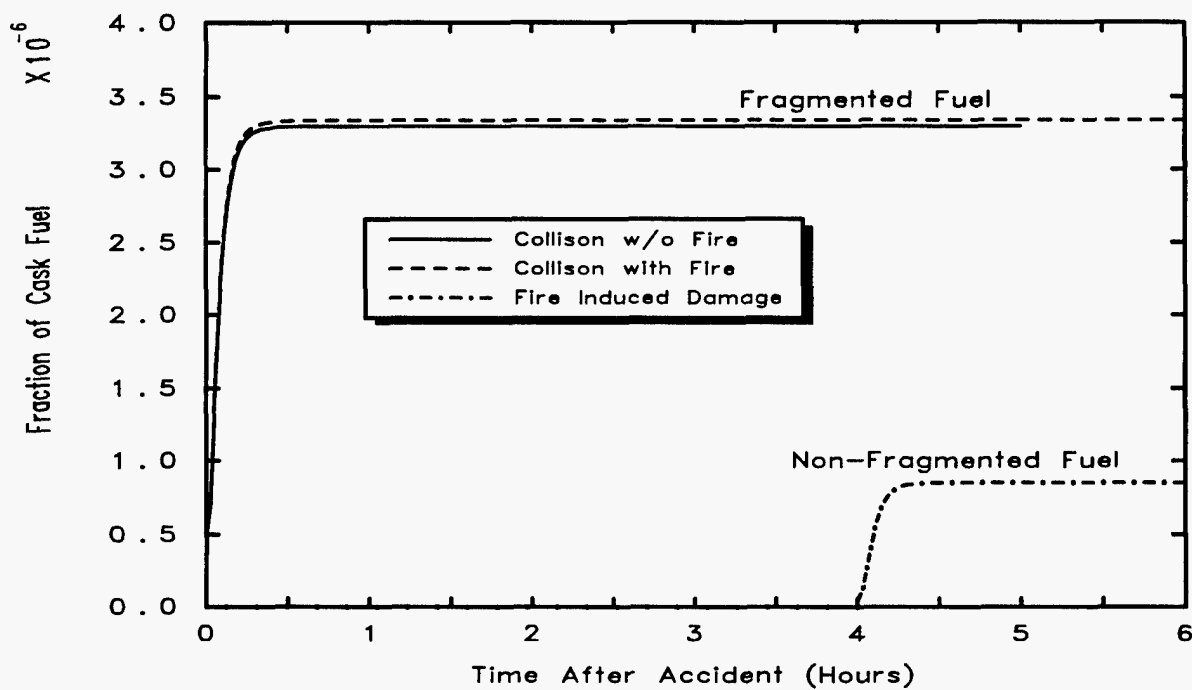


Figure 6-10b: Fuel Fines Released to Environment

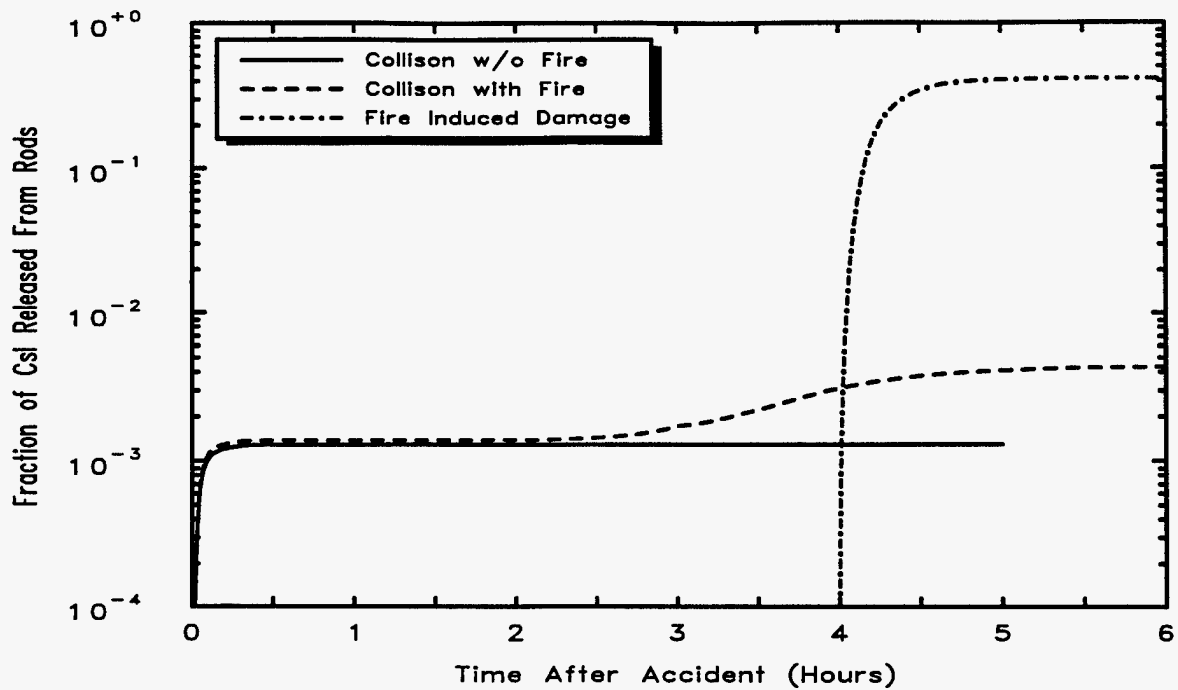


Figure 6-11: Csl Released to Environment

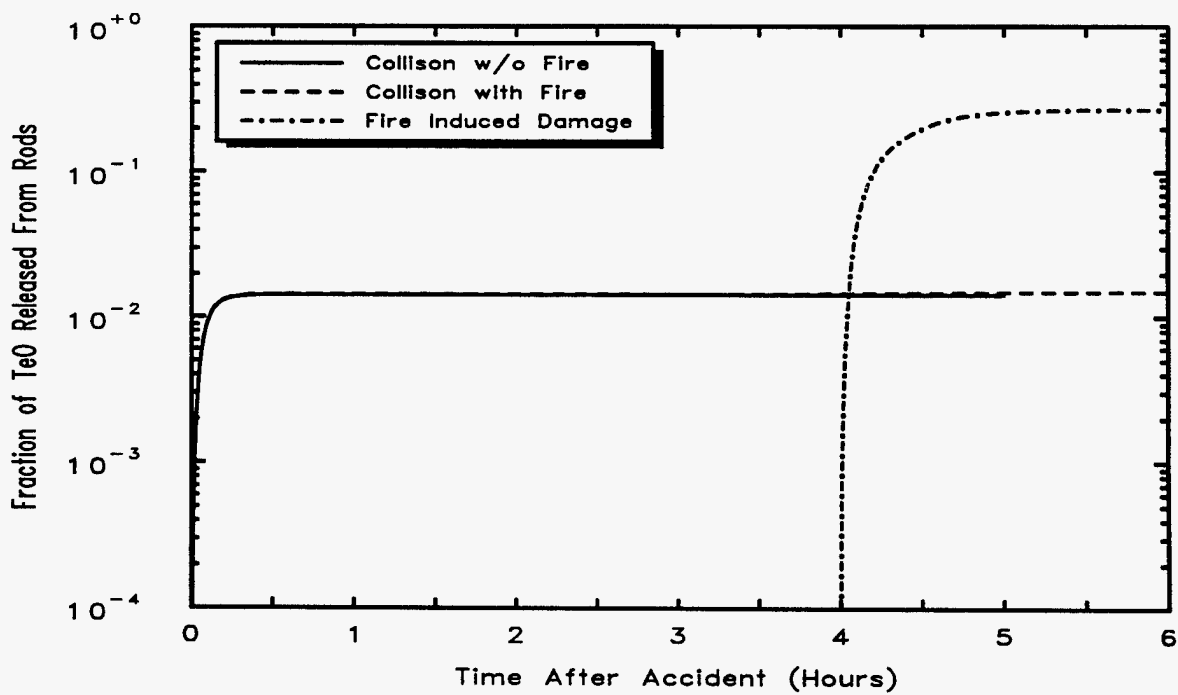


Figure 6-12: TeO Released to Environment

aerosol, which means that the fire has little effect on TeO release. The enhanced release of TeO obtained for the fire only scenario is the result of the simultaneous occurrence of rod and cask failures during the fire only scenario and the small amount of TeO that was vaporized was more effectively transported from the cask. Comparing the TeO in Figure 6-12 to the fuel fines in Figure 6-10a for the fire only scenario shows that the release of TeO to the environment was enhanced by vaporization.

The size distributions of the aerosol particles released into the environment are shown in Figure 6-13 for the collision only scenario for both the 4 mm² and the 100 mm² cask seal leaks. These size distributions are compared in the figure to the aerosol source distribution. The comparison shows that the environmental release distributions have fewer small and large particles than the original source distribution. Small particles are removed from the source distribution because they efficiently coagulate with larger particles. Large particles are removed because particle deposition in the cask occurs most efficiently by gravitational settling and gravitational settling removes larger particles more efficiently than smaller particles. Figure 6-13 shows that for the 100 mm² seal leak, coagulation empties the smallest size section and the deposition of the four largest size sections of the original source distribution, which had 20 size sections spanning the size range 10⁻² to 10³ microns. For the 4 mm² seal leak, one more size section is emptied on each side of the source distribution. The three aerosol size distributions depicted in Figure 6-13 can each be well represented by a log-normal distribution. The parameters that define these log-normal distributions are presented in Table 6-6.

Table 6-6: Aerosol Size Distribution Log-Normal Parameters

| Distribution | Mass Medium Diameter (microns) | Geometric Standard Deviation |
|---|---------------------------------------|-------------------------------------|
| Source | 2.0 | 2.5 |
| Environment - 4 mm² Seal Leak | 1.5 | 1.8 |
| Environment - 100 mm² Seal Leak | 1.7 | 1.9 |

Further understanding of fission product transport within the cask was gained by reviewing the final locations of the various radionuclide masses for the three base scenarios. Distributions of radionuclide masses by final location are presented in Tables 6-7, 6-8, and 6-9 for 4 mm² cask seal failures. These tables present the amounts and final locations of the radionuclides sourced into each of the three base case scenarios. Radionuclide amounts are expressed as fractions of the masses of radionuclides that were released from the fuel rods and sourced into the cask atmosphere. All of the locations were combined into four groups: (1) fuel rod cladding and lodgment wall surfaces, (2) all other cask interior surfaces, (3) the cask atmosphere (radionuclides still gasborne at the end of the calculation), and (4) the environment (radionuclides that escape from the cask).

Because CsOH, CsI, and TeO can exist both as aerosols and vapors, the fractions of these radionuclide species that were gasborne or deposited on surfaces at the end of the calculations are listed for both physical forms. This is physically reasonable for gasborne vapors and aerosols because they have physical forms that are clearly different. For deposited vapors and aerosols, the distinction is less clear as deposited vapors, if they solidify (crystallize) may not be clearly distinguishable from deposited aerosols. Even though deposited vapors and aerosols may not be physically distinguishable, tabulating each separately allows the fraction of the original aerosol that is converted to vapor during the course of the simulation to be displayed. Therefore, in Tables 6-7 through 6-9, deposited vapors and aerosols are separately tabulated.

Table 6-7 shows that for the collision only scenario, most (94.3%) of the fuel fines, which transport only as solid particles, remained within the fuel assembly lodgments. On the other hand, most of the noble gases (88.9%) were expelled from the cask with only 11.1% remaining in the cask atmosphere at the end of the scenario. Some

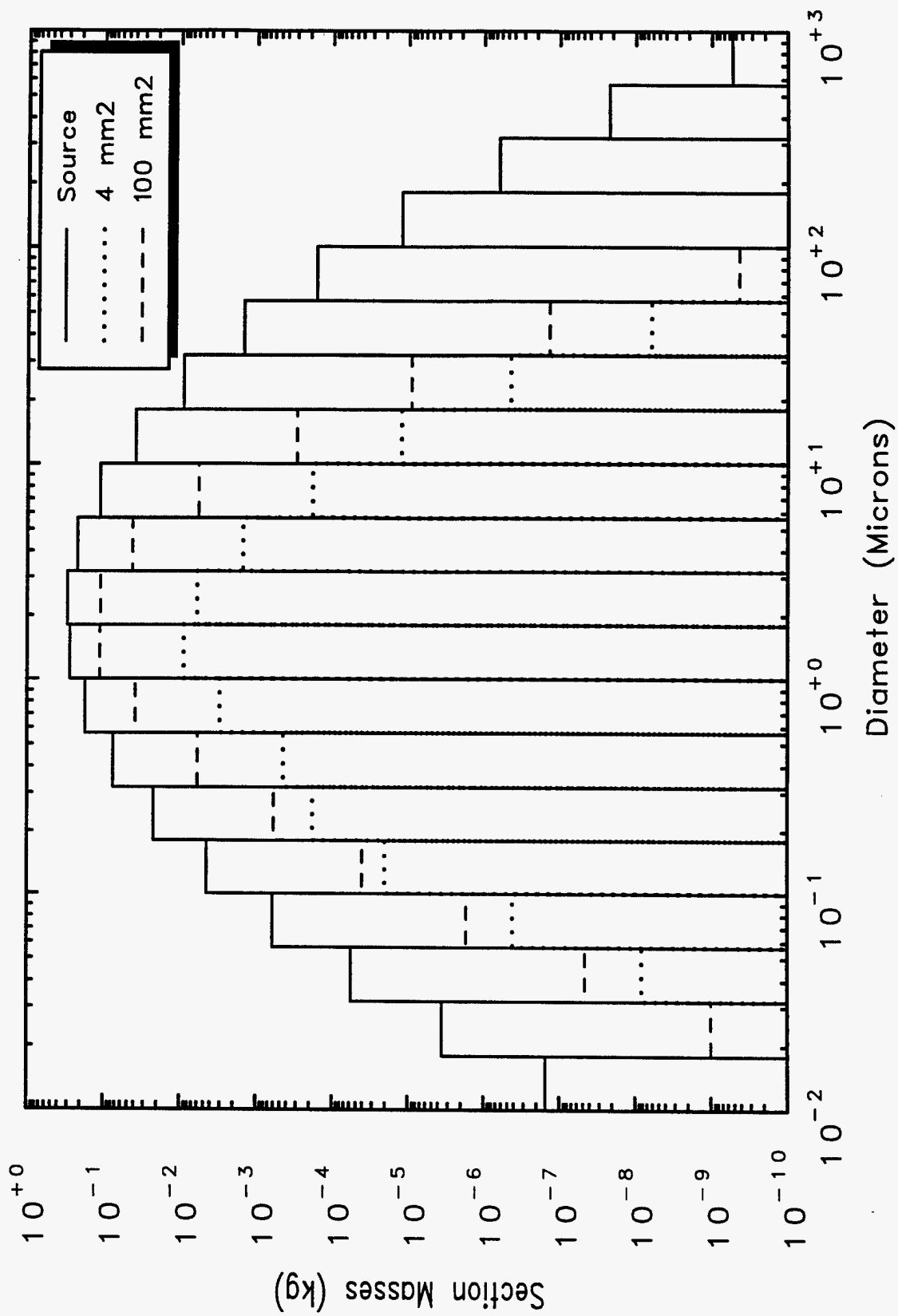


Figure 6-13: Aerosol Size Distributions

Table 6-7: Final Distribution of Radionuclides for Scenario with Collision Induced Damage, No Fire, and 4 mm² Seal Leak

| FINAL DISTRIBUTION OF RADIONUCLIDES FOR COLLISION INDUCED FAILURES W/O FIRE | | | | | | | | | | |
|---|-----------------------------|--------|-------|---------------------------------|---------|---------|----------------------|-------|-------|--------------|
| (Fractions of Total Radionuclide Released from Rods) | | | | | | | | | | |
| Location: | Fuel and Lodgments Surfaces | | | Other Surfaces of Cask Interior | | | Airborne Within Cask | | | Outside Cask |
| Species | Aerosol | Vapor | Total | Aerosol | Vapor | Total | Aerosol | Vapor | Total | Total |
| Kr | 0 | 0 | 0 | 0 | 0 | 0 | 0 | 0.111 | 0.111 | 0.889 |
| CsOH | 0.767 | 0.228 | 0.995 | 0.000909 | 0.00332 | 0.00423 | 0 | 0 | 0 | 0.000557 |
| CsI | 0.840 | 0.154 | 0.994 | 0.00316 | 0.00150 | 0.00465 | 0 | 0 | 0 | 0.00128 |
| TeO | 0.932 | 0.0320 | 0.964 | 0.0192 | 0.00266 | 0.0219 | 0 | 0 | 0 | 0.0142 |
| UO ₂ | 0.943 | 0 | 0.943 | 0.0406 | 0 | 0.0406 | 0 | 0 | 0 | 0.0165 |

Table 6-8: Final Distribution of Radionuclides for Collision Induced Damage With Fire and 4 mm² Seal Leak

| FINAL DISTRIBUTION OF RADIONUCLIDES FOR COLLISION INDUCED FAILURES WITH FIRE | | | | | | | | | | |
|--|-----------------------------|--------|-------|---------------------------------|----------|---------|----------------------|----------|----------|--------------|
| (Fractions of Total Radionuclide Released from Rods) | | | | | | | | | | |
| Location: | Fuel and Lodgments Surfaces | | | Other Surfaces of Cask Interior | | | Airborne Within Cask | | | Outside Cask |
| Species | Aerosol | Vapor | Total | Aerosol | Vapor | Total | Aerosol | Vapor | Total | Total |
| Kr | 0 | 0 | 0 | 0 | 0 | 0 | 0 | 0.0816 | 0.0816 | 0.918 |
| CsOH | 0 | 0.850 | 0.850 | 0.0669 | 0.000942 | 0.06785 | 0.00144 | 0.0757 | 0.0771 | 0.00448 |
| CsI | 0 | 0.938 | 0.938 | 0.0472 | 0.000374 | 0.04757 | 0.000174 | 0.00972 | 0.00989 | 0.00434 |
| TeO | 0.860 | 0.0964 | 0.956 | 0.000025 | 0.00458 | 0.00460 | 0 | 0.000031 | 0.000031 | 0.0149 |
| UO ₂ | 0.943 | 0 | 0.943 | 0.0406 | 0 | 0.0406 | 0 | 0 | 0 | 0.0167 |

Table 6-9: Final Distribution of Radionuclides for Scenario with Fire Induced Damage and 4 mm² Seal Leak

| FINAL DISTRIBUTION OF RADIONUCLIDES FOR THERMALLY INDUCED FAILURES | | | | | | | | | | |
|--|-----------------------------|--------|--------|---------------------------------|---------|--------|----------------------|----------|----------|--------------|
| (Fractions of Total Radionuclide Released from Rods) | | | | | | | | | | |
| Location: | Fuel and Lodgments Surfaces | | | Other Surfaces of Cask Interior | | | Airborne Within Cask | | | Outside Cask |
| Species | Aerosol | Vapor | Total | Aerosol | Vapor | Total | Aerosol | Vapor | Total | Total |
| Kr | 0 | 0 | 0 | 0 | 0 | 0 | 0 | 0.180 | 0.180 | 0.820 |
| CsOH | 0 | 0 | 0 | 0.463 | 0.0146 | 0.478 | 0.000634 | 0.111 | 0.112 | 0.410 |
| CsI | 0 | 0.0539 | 0.0539 | 0.466 | 0.00840 | 0.474 | 0.000305 | 0.0598 | 0.060 | 0.412 |
| TeO | 0.0314 | 0.307 | 0.338 | 0.386 | 0.00936 | 0.396 | 0 | 0.000181 | 0.000181 | 0.266 |
| UO ₂ | 0.927 | 0 | 0.927 | 0.0447 | 0 | 0.0447 | 0 | 0 | 0 | 0.0284 |

vaporization of the volatile species occurred during this scenario even though the cask temperatures reflected normal transport conditions (i.e., without any increase due to heating by a fire). The extent of vaporization (23.1% for CsOH, 15.6% for CsI, and 3.5% for TeO) of the three vaporizable aerosols initially sourced into the middle lodgment volume is consistent with the relative volatility of the species (see Figure 4-6) with the CsOH showing the most vaporization and TeO showing the least. Even though significant amounts of these three aerosol sources were converted to vapors, most of the sourced mass of these volatile species remained within the lodgment volumes (99.5% for CsOH, 99.4% for CsI, and 96.4% for TeO).

During the collision plus fire scenario, 94.3% of the fuel fines and 86.0% of the TeO were again retained primarily within the lodgments due to deposition as aerosols. Comparison of the collision plus fire results to the collision only results shows that the addition of a fire to the collision scenario has little effect on the amounts of aerosols that escape from the cask to the environment. Addition of a fire does effect the behavior of cesium species, CsOH and CsI, which now are retained in the lodgment volumes primarily as condensed vapors (85.0% of the CsOH and 93.8% of the CsI were retained in the lodgment volumes as condensed vapors), which means that after being sourced into the middle lodgment volume as aerosols, they were both largely vaporized before they encountered and then condensed onto cooler surfaces. The fire that followed the collision did enhance fission product release to the environment, e.g., the release of CsOH was a factor of 8 times higher than that predicted for the collision only scenario.

During the fire only scenario, the vaporization of the volatile species was much increased. This allowed most of the cesium species to be transported from the lodgment volumes to cask end regions where they either deposited on cask interior surfaces or escaped from the cask to the environment. Even the TeO species displayed a high degree of vapor transport in this scenario, which caused its fractional release to the environment to be much increased. In addition, release of fuel fines to the environment is also increased because cask depressurization takes place from a higher initial pressure due to heating of cask gases by the fire.

This concludes the discussion of the base scenario fission product transport results. Now several parameter sensitivity studies will be presented in the next sections for the parameters determined to have the largest impact on the transport of fission products from the TN-12 shipping cask.

7.0 PARAMETER SENSITIVITY ANALYSES

Single parameter sensitivity analyses were performed for the fuel release fractions, the size of the cask seal failure hole, the fraction of fuel rods failed, the axial location of the rod breach, selected radionuclide transport input parameters, and pool fire duration and temperature.

7.1 Sensitivity of Fuel Release Fractions

The quantity of fuel fines (small particles) available for release from failed fuel rods and the fraction of those particles that would be released upon rod failure are both poorly known (see discussion in Section 4.4.2). Although the fraction of spent fuel that is present as fuel fines at reactor shutdown has been measured, the amount of additional fines that would be produced when spent fuel being carried in a transportation cask is subjected to crush or impact forces by a transportation accident (e.g., a ship collision) is unknown. In addition, the fraction of the fines present at the time of rod failure that would be released due to resuspension from the fuel into the rod gases during rod depressurization is also poorly known. Because of these two uncertainties, the fraction of the fuel mass that would be released to the cask interior upon rod failure during a transportation accident is quite uncertain. Therefore, the fraction of the spent fuel released from the fuel rods into the shipping cask was varied to determine the impact of this uncertainty on the ability of the cask to retain these fuel particles once released into the cask. The fraction of fuel released into the cask was varied from 10^{-5} to 10^{-3} for the collision only scenario with a 4 mm^2 seal leak and the results are shown in Figures 7-1a and 7-1b. Figure 7-1a shows the fraction of fuel fines retained by the cask and Figure 7-1b shows the fraction of the fuel mass released to the environment.

Retention of fuel fines in the cask varies with the quantity of fines released from the rods into the cask interior because the rate of particle coagulation is strongly related to the density of aerosol particles in the cask atmosphere, i.e., particles are more likely to coagulate with other particles in a dense gasborne aerosol than in a sparse one. Then, as coagulation produces larger particles, gravitational settling removes these particles more efficiently than it removes the smaller particles from which they were formed. Therefore, Figure 7-1a shows that, as the release fraction for fuel fines and thus gasborne particle density was increased, the cask retention fraction also increased, but only slightly (from 0.97 when the fuel mass release fraction was 10^{-5} to 0.99 when that fraction was 10^{-3}). Figure 7-1b shows that the quantity of fines actually released from the cask also increased (by a factor of 33) as the fraction of fuel mass expelled from the rods increased from 10^{-5} to 10^{-3} , but not linearly as would be predicted if coagulation effects were ignored. To illustrate the impact of coagulation, Figures 7-1a and 7-1b also present results for calculations during which the MELCOR aerosol coagulation model was deactivated. Without coagulation, as would be expected, the cask retention fraction did not vary with the density of gasborne fuel fines, and the fuel release to the environment did vary linearly with the amount of fuel fines expelled from the failed spent fuel rods.

The fractions of fuel released as fuel fines that were used in the base case scenarios are also shown in Figures 7-1a and 7-1b. Those values were 2×10^{-4} for the collision only and the collision plus fire scenarios and consistent with the Lorenz experiments of 3×10^{-5} for the fire only scenario that assumed no impact fracturing of fuel.

7.2 Sensitivity of Cask Seal Failure Size

The size of the postulated failure of the cask seal (the hole size) was another major uncertainty in these analyses. Indeed, there probably is a spectrum of hole sizes for the likely range of accident scenarios. The hole size may range from a pin hole to perhaps the loss of the entire cask lid. However experts in cask design and testing believe that the hole size produced by collision accidents would most likely be a few square millimeters. A hole size of 4 mm^2 was therefore used in the base scenarios, and a much larger hole size of 100 mm^2 was used to illustrate the cask failure that might result from a very severe accident. In this sensitivity study, the cask seal leak hole size for the collision only scenario was varied from 0.1 to 100 mm^2 .

The results of this hole size sensitivity study are shown in Figure 7-2 for each of the radionuclide species modeled in this study. The ability of the cask to retain fuel fines, that is the cask retention fraction, decreased from over 99.9% for the small 0.1 mm^2 hole to 74.6% for the 100 mm^2 hole. The result for the base scenario value of 4 mm^2 is

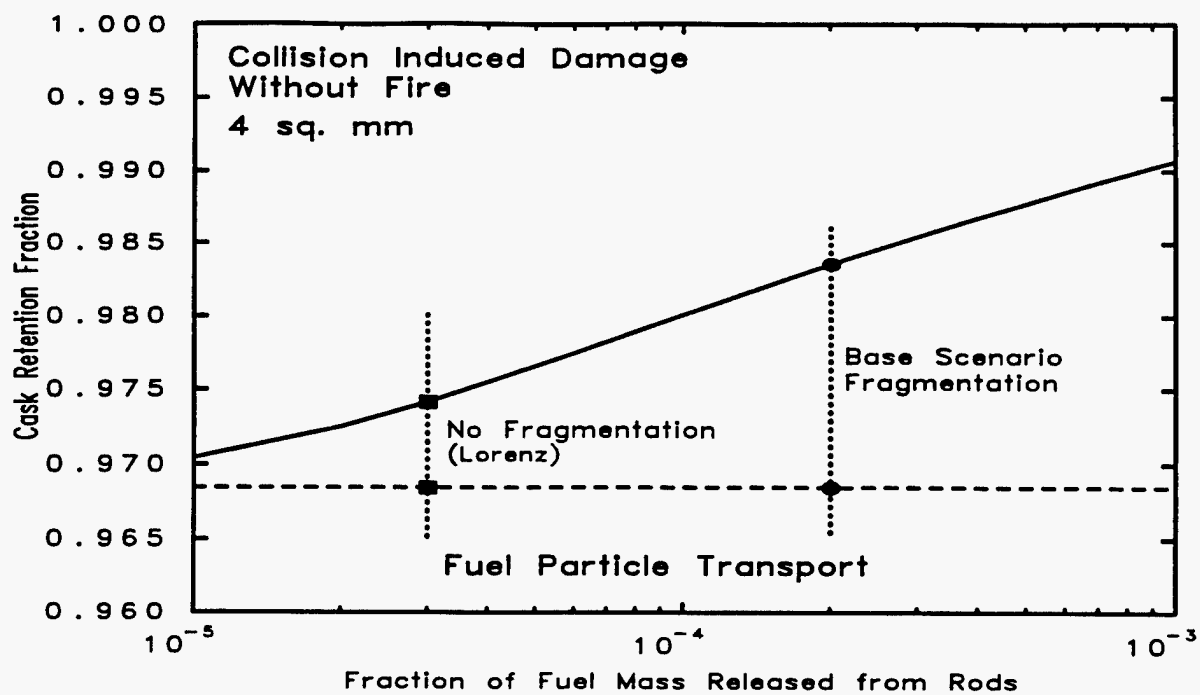


Figure 7-1a: Fuel Fragmentation Sensitivity

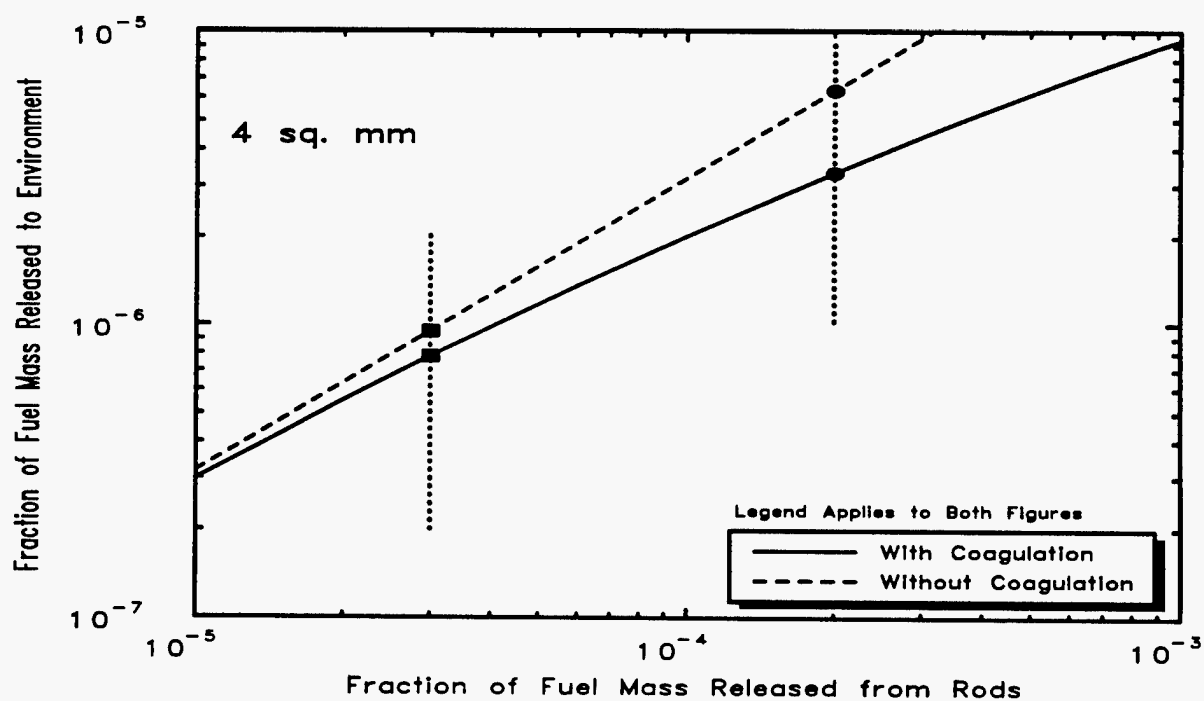


Figure 7-1b: Fuel Fragmentation Sensitivity

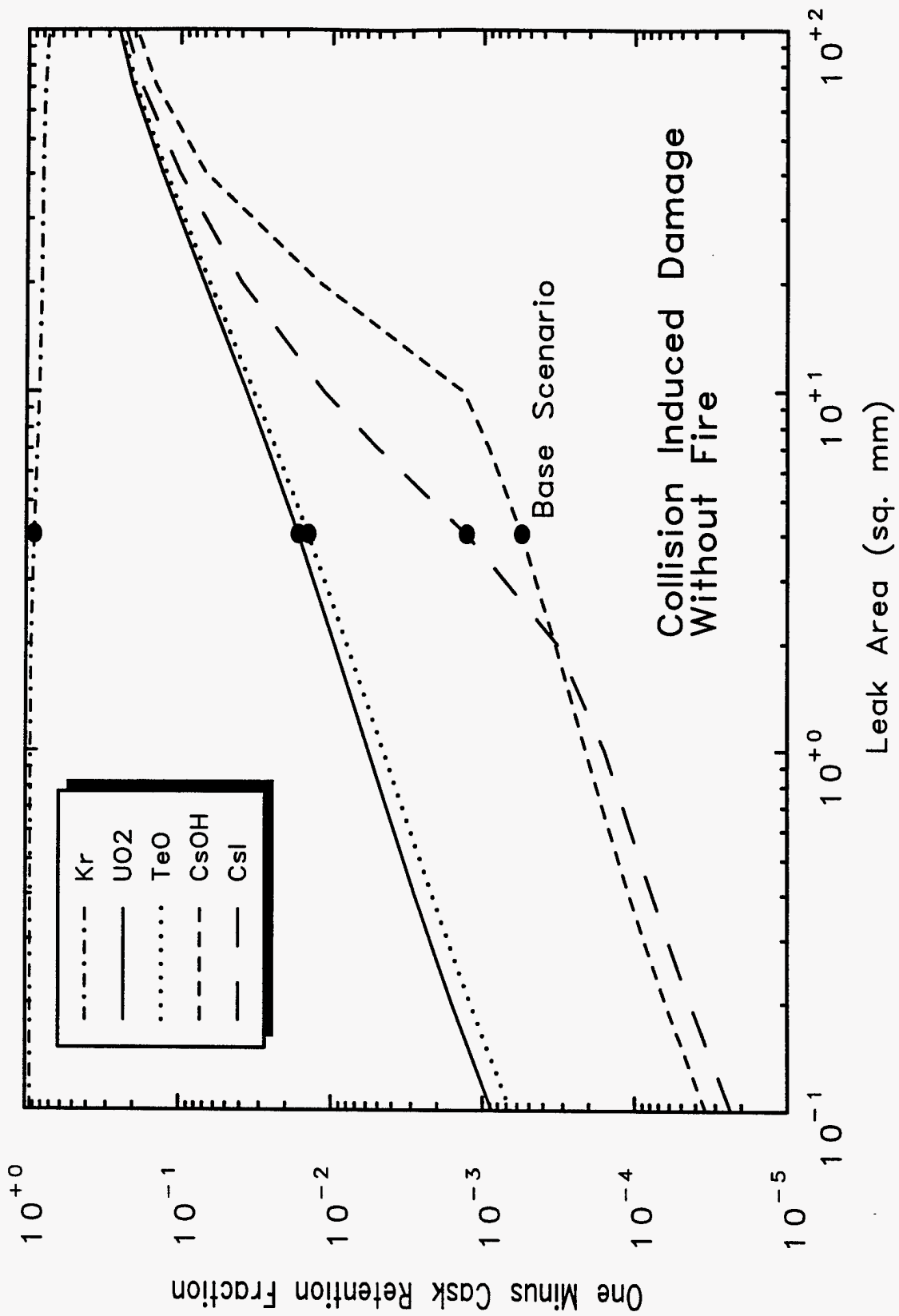


Figure 7-2: Cask Seal Failure Size Sensitivity

indicated in the figure. For hole sizes below 20 mm², the volatile species showed a higher cask retention than the fuel fines (see Section 6.4); however for the larger hole sizes, the volatile species began to behave more like the fuel fines due to the more rapid depressurization of the cask. Rapid depressurization decreases vapor retention by preventing vapor concentrations from increasing to levels where vapor condensation becomes important. Hole sizes larger than 100 mm² were not examined because for these hole sizes cask depressurization rates approach those of the fuel rods and therefore the uncertainty in the fuel rod depressurization rate tended to invalidate those results. Nevertheless, the results obtained suggest that, even if the cask were to lose its entire lid during a most unlikely collision, a substantial fraction of the fuel fines released from the rods would still be retained due to deposition within the fuel assembly lodgments.

The dependency of Kr retention on hole size was different than for the other radionuclides and somewhat counterintuitive, i.e., more Kr was retained in the cask at the larger hole sizes (shown in Figure 7-2). This behavior is related to the relative concentrations of Kr, helium and nitrogen gases in the cask during depressurization. For larger seal failures, the gases leaking from the cask tend towards higher concentrations of nitrogen because the fuel rods are still depressurizing as the cask depressurizes than would be the case for small seal failures where rod depressurization completes before significant cask depressurization occurs. However, this dependency was over emphasized in the original calculations due to the uniform-rate rod-depressurization model. The dependency remained in the revised calculations but was not nearly as pronounced (see Addendum).

7.3 Sensitivity of Rod Failure Fraction

The number of the 2448 spent fuel rods in a fully loaded TN-125 shipping cask that would actually fail during a postulated collision is another uncertain parameter. No cask test data is available that demonstrates rod failure during impact or crush tests, failure of rod cladding by ductile tearing or by material fracture is expected during severe impact events [6]. The number of rod failures would certainly depend on the magnitude of the collision impact forces that in turn depend upon the conditions postulated for a particular accident. Because of this uncertainty, the worst case condition of postulating that all of the fuel rods would fail during any collision was used in the base case collision scenarios, and sensitivity to that very conservative assumption was investigated by a sensitivity study.

The sensitivity of the retention of fuel fines to the number of rods that fail was studied by varying the fraction of the 2448 rods in the TN-125 cask that fail from 0 to 100 percent with 100 percent rod failure causing the release of fuel mass to equal the mass (1.222 kg) of the fuel fines sourced from the rods into the cask that was used in collision only and collision plus fire base case scenarios. Figures 7-3a and 7-3b present the results of this sensitivity study. Figure 7-3a shows how the fraction of fines retained by the cask and Figure 7-3b how the fraction of the fuel mass released to the environment varied as the fraction of failed rods was increased from 0 to 100 percent. Figure 7-3a shows that the cask retention fraction equals 1.0 until about 10 percent of the rods fail and then decreases slowly to about 0.98 when 100 percent of the rods fail. Since the TN-125 cask was operated at subatmospheric pressures, release of radioactivity to the environment does not become significant until about 10% of the rods have failed, because until then cask pressures remain subatmospheric. Since the base case scenarios postulated that the cask seal failed at the same time as the fuel rods failed, some ambient air flowed into the cask as the fuel rods depressurized which decreases the number of rods that must fail in order to increase cask pressures to ambient. Figure 7-3b shows that the fraction of fuel mass released to the environment increases linearly with the percent of rods that fail.

7.4 Sensitivity of Axial Failure Location

The location of rod failures along the rod axis is also uncertain. Although it is likely that a spent fuel rod would fail nearer its center than at its ends, in reality, the failure location should be described as a probability function, i.e., if a large number of the fuel rods in a cask were to fail, then certainly they would not all fail at their centers. The axial location of the fuel rod failure determines the length of the pathway that radionuclides must traverse before escaping from the cask. Radionuclides expelled from a rod failing at the gas plenum end of the rod near the cask lid would not have to travel as far as radionuclides expelled from the bottom end of the rod. Of course, longer escape pathways produce more deposition of vapors and aerosols onto internal cask surfaces.

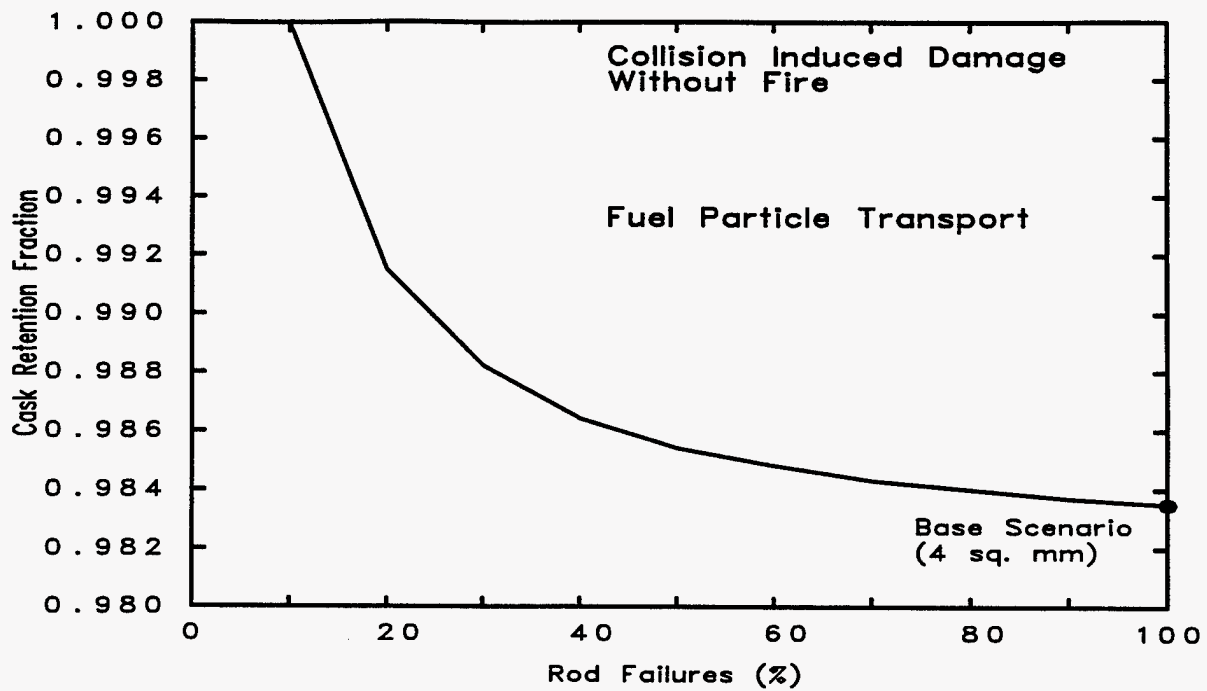


Figure 7-3a: Rod Failure Fraction Sensitivity

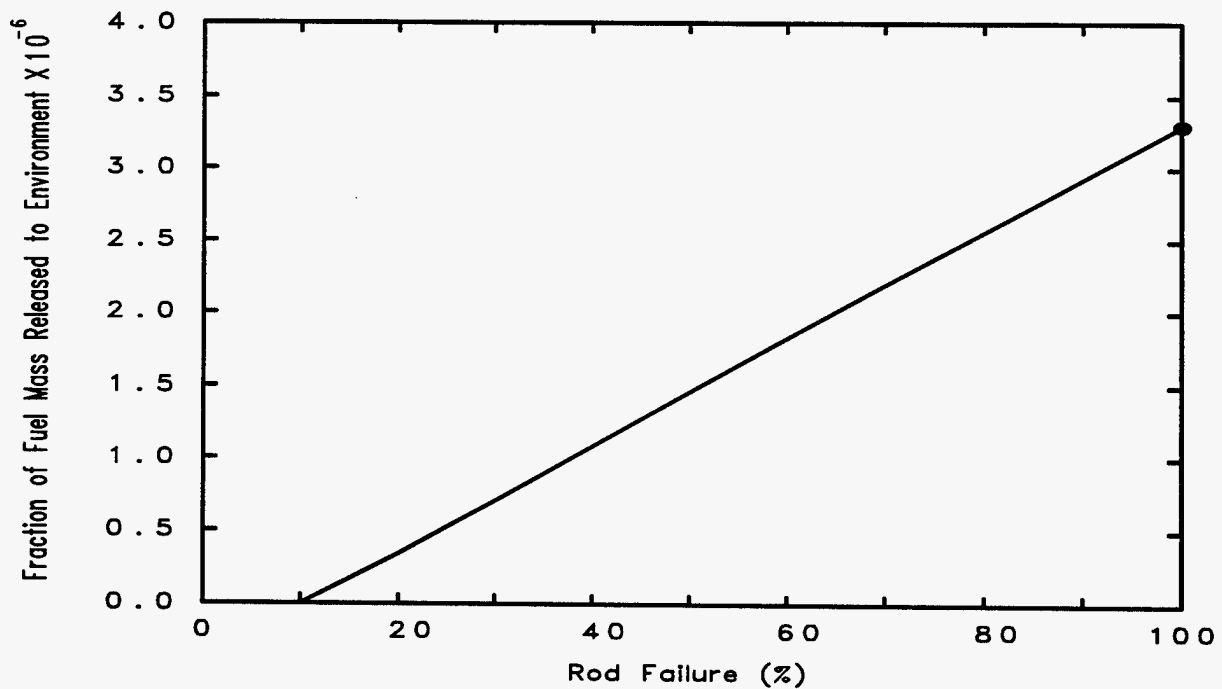


Figure 7-3b: Rod Failure Fraction Sensitivity

The effect of the axial location on the prediction of the ability of the cask to retain radionuclides was investigated for the collision only scenario by varying the location where the fuel rods were postulated to fail. Each of the five axial lodgment volumes was postulated as the location of rod rupture. These results are shown in Table 7-1 for both the 4 and the 100 mm² cask seal leak sizes. The results clearly show that cask retention of radionuclides is greater when the rod rupture location is further from the cask seal. For example, for the 4 mm² seal leak, the cask retention of fuel fines was 99% when the rod failures were located in the bottom lodgment volume and only 93% when they were located in the lodgment volume nearest to the rod gas plenums.

If an axially symmetrical location probability distribution were applied to the data in Table 7-1, it would somewhat reduce the prediction of cask retention because these retention fractions were not axially symmetrical. Even so, the cask retention of radionuclides, other than the noble gases, would likely remain relatively high, at least for small cask seal failure hole sizes.

7.5 Sensitivity of Radionuclide Transport Parameters

A radionuclide transport prediction depends upon several model input parameters which are relatively uncertain. The effect of parameter uncertainty on the cask retention of radionuclides was examined for three of these parameters. The parameters examined included the size distribution of the aerosol particles expelled from the fuel rods, the diffusion boundary layer thickness, and the mass of the volatile (CsOH and CsI) and noble gas (Kr) radionuclides expelled from the rods. Although other parameters could have been investigated, based on general aerosol transport experience, it was deemed unlikely that the uncertainty associated with the other transport parameters would significantly impact the overall cask retention results.

The size of the aerosol particles expelled from the fuel rods was examined by varying both the mass median diameter (MMD) and the geometric standard deviation (GSD) of the log-normal distribution used to describe the aerosol in the MELCOR input model (see Section 4.4.2). The MMD was varied from 1 to 3 μm (the base case value was 2 μm) and the GSD was altered from the base value of 2.5 up to a value of 6. These results are shown in Table 7-2. The cask retention was shown to be relatively insensitive to the values of these aerosol parameters when the values were near the base case values that were developed from experimental data.

The aerosol model diffusion boundary layer thickness was varied from the base value of 10^{-5} up to a value of 10^{-4} m. The change in the cask retention as a result of this change in the diffusion boundary layer thickness was minimal.

As explained in the MELCOR input model (Section 4.4.2), the masses of radionuclides other than the fuel fines were treated by simply introducing a relatively small mass of 10^{-3} kg of each radionuclide into the calculation. The uncertainty associated with this assumption was examined by varying the mass over several orders of magnitude, i.e., from 10^{-6} to 10^{-1} kg for each of these radionuclide species for the collision only scenario with a 4 mm² seal leak. The results of this sensitivity analyses are shown in Table 7-3.

These results show that the size of the source mass has a significant impact on the transport of the volatile species. Deposition of the radionuclides in the vapor form depends upon their partial pressures, i.e., the rate of deposition is a function of the difference between the concentration of the vapor species in the atmosphere and the saturation concentration of the vapor in the atmosphere at the temperature of deposition surface. Thus, the predicted cask retention fractions were higher for smaller quantities of the radionuclide species. For very large concentrations of the volatile species, the cask retention fractions approached the retention fraction of the fuel fines and there was enough of the volatile species in the aerosol form to slightly impact the transport of the fuel fines. (The mass of fuel fines was not varied during this sensitivity study.) The retention of the noble gases was not sensitive to the mass of noble gases expelled from the fuel rods.

In any case, the cask retention of volatile radionuclides for source masses within one order of magnitude of the base value of 10^{-3} kg was relatively insensitive to the source mass. Therefore, the overall cask retention results for the volatile species were deemed valid.

Table 7-1: Axial Rod Failure Location Sensitivity

| RESULTS OF FAILURE LOCATION CALCULATIONS | | | | | | | | | | |
|--|---------------------------------------|--------|--------|--------|-----------------|---|-------|-------|-------|-----------------|
| Location of Rod Failure | Final Cask Retention Fractions | | | | | | | | | |
| | Cask Leakage Area = 4 mm ² | | | | | Cask Leakage Area = 100 mm ² | | | | |
| | Kr | CsOH | CsI | TeO | UO ₂ | Kr | CsOH | CsI | TeO | UO ₂ |
| Gas Plenum End | 0.089 | 0.934 | 0.933 | 0.930 | 0.930 | 0.035 | 0.407 | 0.384 | 0.377 | 0.376 |
| Upper Intermediate | 0.092 | 0.979 | 0.974 | 0.968 | 0.967 | 0.103 | 0.627 | 0.595 | 0.585 | 0.581 |
| Central Rod | 0.111 | 0.9994 | 0.9987 | 0.9858 | 0.9835 | 0.264 | 0.805 | 0.771 | 0.754 | 0.746 |
| Lower Intermediate | 0.152 | 0.9997 | 0.9997 | 0.9940 | 0.9903 | 0.520 | 0.928 | 0.894 | 0.877 | 0.864 |
| Bottom End | 0.355 | 0.9996 | 0.9996 | 0.9962 | 0.9924 | 0.441 | 0.904 | 0.883 | 0.866 | 0.851 |

Table 7-2: Initial Aerosol Size Distribution Sensitivity

| RESULTS OF AEROSOL PARAMETERS CALCULATIONS | | | | | |
|--|------------------------------|--------|--------|--------|-----------------|
| Aerosol Paramter | Final Cask Release Fractions | | | | |
| | Kr | CsOH | CsI | TeO | UO ₂ |
| Mass Medium Diameter | | | | | |
| 1 micron | 0.1109 | 0.9998 | 0.9995 | 0.9900 | 0.9785 |
| 2 micron * | 0.1108 | 0.9998 | 0.9996 | 0.9932 | 0.9835 |
| 3 micron | 0.1108 | 0.9998 | 0.9997 | 0.9952 | 0.9872 |
| Standard Deviation | | | | | |
| 2.5 * | 0.1108 | 0.9998 | 0.9996 | 0.9932 | 0.9835 |
| 6.0 | 0.1108 | 0.9998 | 0.9997 | 0.9929 | 0.9839 |

* Base Parameter

Table 7-3: Cask Retention Sensitivity to Volatile Masses

| RESULTS OF FP MASS CALCULATIONS | | | | | |
|---------------------------------|--------------------------------|--------|--------|--------|-----------------|
| Mass of FP Released, Kg | Final Cask Retention Fractions | | | | |
| | Kr | CsOH | CsI | TeO | UO ₂ |
| 1E-06 | 0.111 | 0.9998 | 0.9998 | 0.9993 | 0.9835 |
| 1E-05 | 0.111 | 0.9998 | 0.9996 | 0.9931 | 0.9835 |
| 1E-04 | 0.111 | 0.9997 | 0.9994 | 0.9886 | 0.9835 |
| 1E-03 | 0.111 | 0.9994 | 0.9987 | 0.9858 | 0.9835 |
| 1E-02 | 0.112 | 0.9988 | 0.9919 | 0.9848 | 0.9837 |
| 1E-01 | 0.113 | 0.9929 | 0.9888 | 0.9854 | 0.9854 |

Base Value = 0.001 kg

7.6 Fire Enhancement of Radionuclide Transport From Cask

A pool fire surrounding a shipping cask which has been damaged by collision impact or crush forces can enhance the transport of radionuclides from the cask to the environment over the transport that would occur without a pool fire. If heat from the fire penetrates to the interior of the cask, surface and gas temperatures will increase which may cause condensed vapors and volatile components of both gasborne and deposited aerosols to vaporize. Further, the heated interior gases would expand, thereby expelling additional gases from the cask that would carry additional radionuclides with them to the environment.

The conditions of the postulated fire, i.e., the fire temperature and the fire duration, were additional uncertainties in this study. The temperature and duration of the fire depends upon a number of accident conditions including the quantity and type of fuel driving the fire, the supply of oxygen, and the overall configuration of the accident, e.g., partial or fully engulfing fire, the elevation of the cask in the fire, enclosed or non-enclosed fire, etc.

The collision only scenario was used to examine the uncertainty associated with the conditions of the fire. In this scenario, all of the fuel rods and the cask seal were postulated to fail during the collision with the seal failure producing a 4 mm² leak. Two fire temperatures, 800 and 1200 °C, were evaluated. An 800 °C fire was examined because 800 °C is the temperature of the standard regulatory fire. A 1200 °C fire was examined because this fire temperature represents a more extreme, near worst case fire temperature. A temperature of 1200 °C was used in the base case fire scenarios. The duration of each fire was varied from 0 to 5 hours. The base case fire scenarios assumed a fire duration of 3 hours.

The results of the study are shown in Figures 7-4a, and 7-4b for the 1200 °C fire and 7-5a, and 7-5b for the 800 °C fire. Figures 7-4a and 7-5a present for the 1200 and 800 °C fires, respectively, the maximum temperatures calculated during the entire simulation for the center and outer fuel and for the lodgment walls. These calculations were all run long enough to allow these temperatures to peak and then to decrease as the cask cooled again. Basket aluminum was predicted to soften or melt at about 2.6 and 4.4 hours for the 1200 and 800 °C fires, respectively. Basket slump or melting and its effect on radionuclide transport were not modeled in this study. The retention of radionuclide vapors and aerosols by the cask is shown in Figures 7-4b and 7-5b for the two fire temperatures. Retention is expressed as the fraction of the radionuclides expelled from the fuel rods that were also transported from the cask. These cask retention fractions can be compared to the base scenario results reported in Table 6-2.

Because fuel fines were assumed to be involatile (i.e., to transport only as aerosols), variation of fire duration from 1 to 5 hours had no significant effect on retention of fuel fines in the cask. Expansion of cask gases by fire heating should decrease aerosol retention. However, for the 4 mm² leak, the decrease is not large enough to be seen in Figure 7-4b and 7-5b. Because of its very low volatility, retention of TeO was also not significantly affected by fire duration for the 800 °C fire and was increased for the 1200 °C only very slightly and then only for fires with durations longer than 3 hours. Retention of CsOH and CsI was considerably decreased by increased fire duration. The decrease is caused by increasing vaporization of CsI and CsOH aerosols as fire duration increases and also by the heating of cold surfaces to temperatures where condensation of these vapors becomes negligible.

In the collision only scenario, a higher fraction of the volatile species than of fuel fines was retained because CsOH and CsI vapors condensed onto colder surfaces more readily than aerosol particles deposited onto all surfaces. As fire duration increased, heating of the surfaces onto which the vapors had condensed revaporized these species and then expansion of cask gases caused a small portion of the vapors to escape from the cask. However, as shown in Figures 7-4b and 7-5b, although transport of the volatile species was enhanced, retention of these species still did not exceed that of the fuel fines.

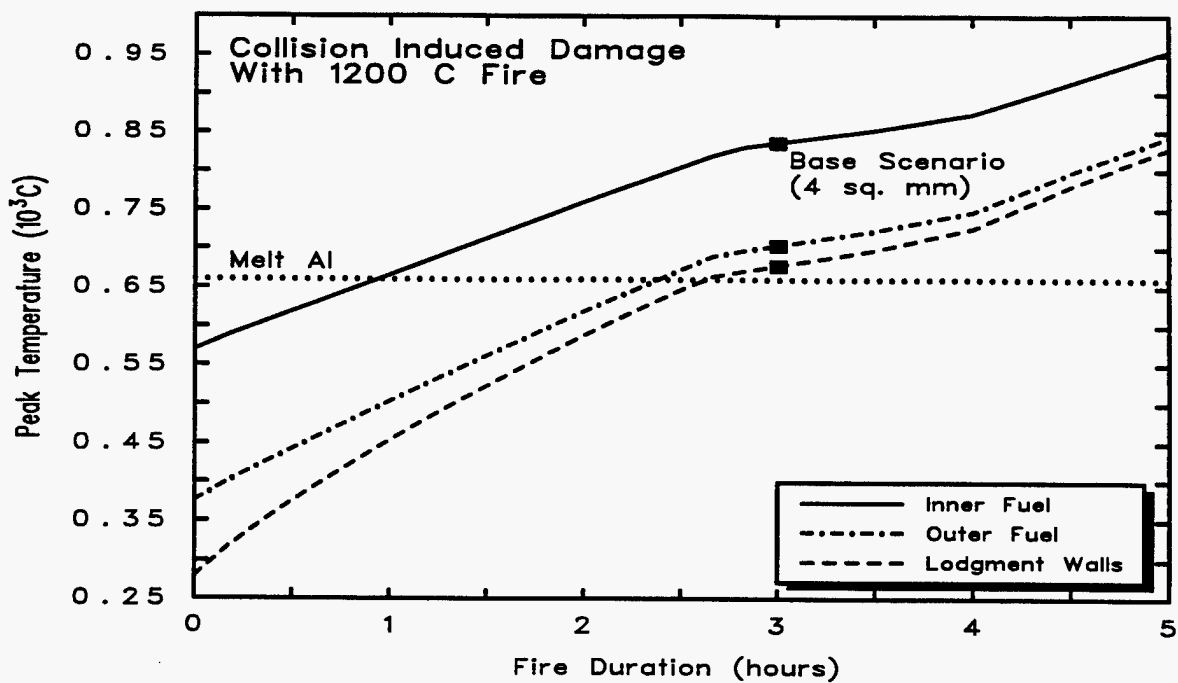


Figure 7-4a: Peak Cask Temperatures

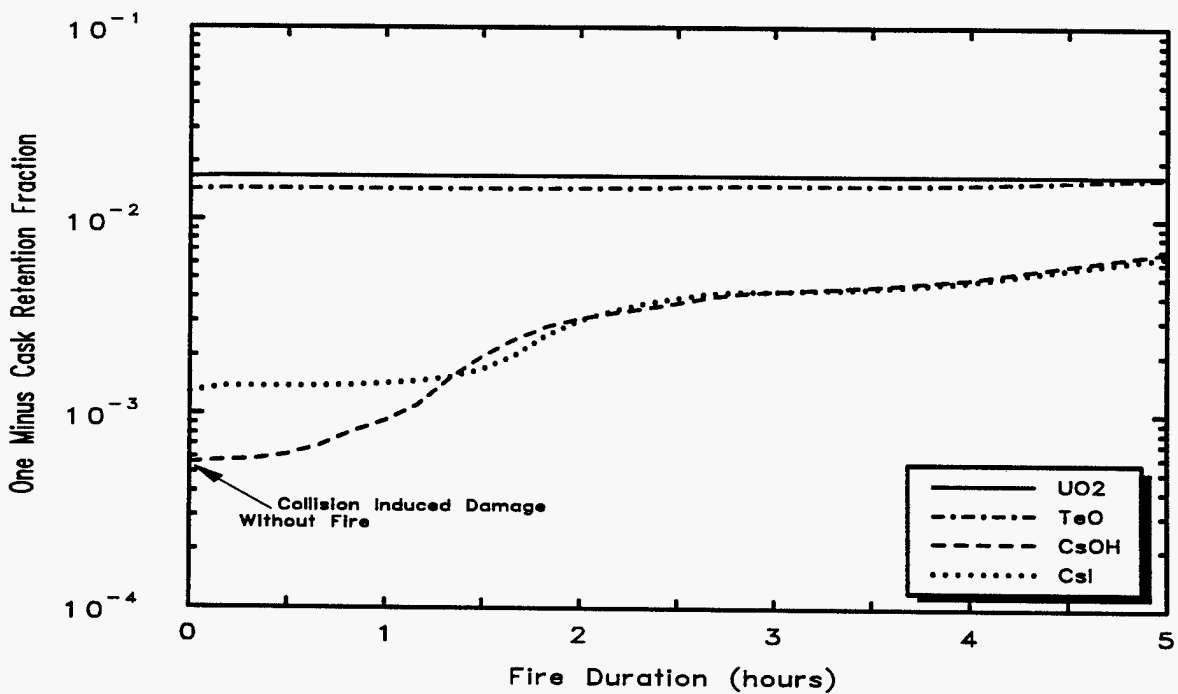


Figure 7-4b: Fire Enhancement of FP Transport

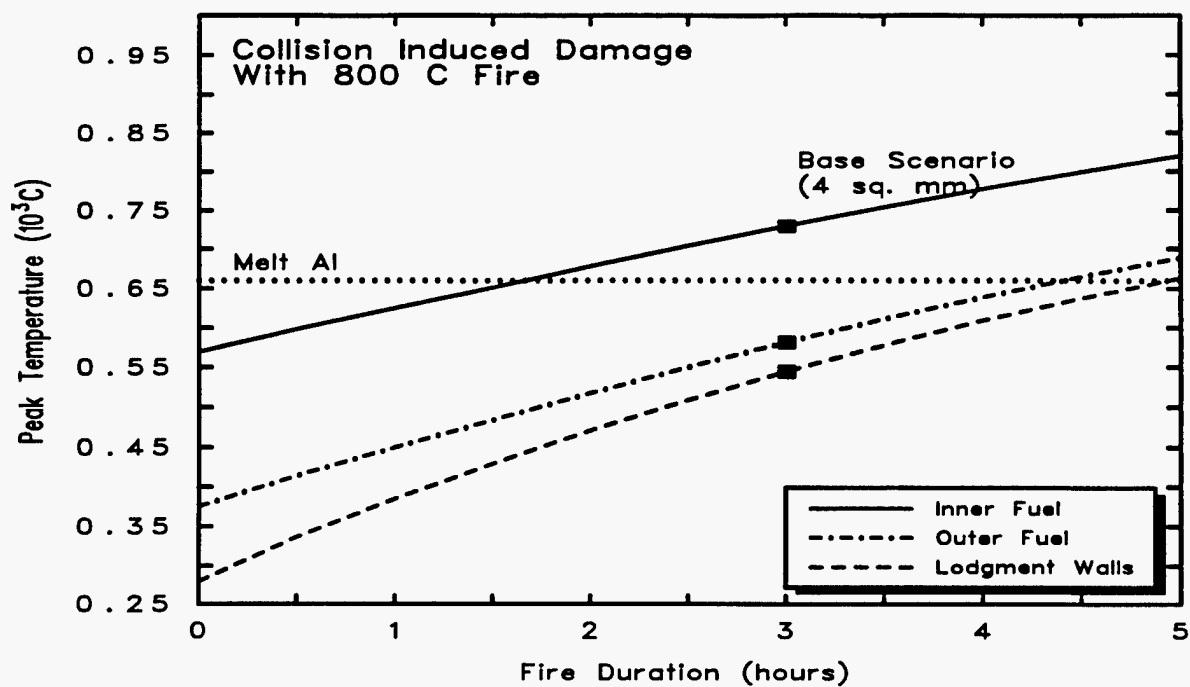


Figure 7-5a: Peak Cask Temperatures

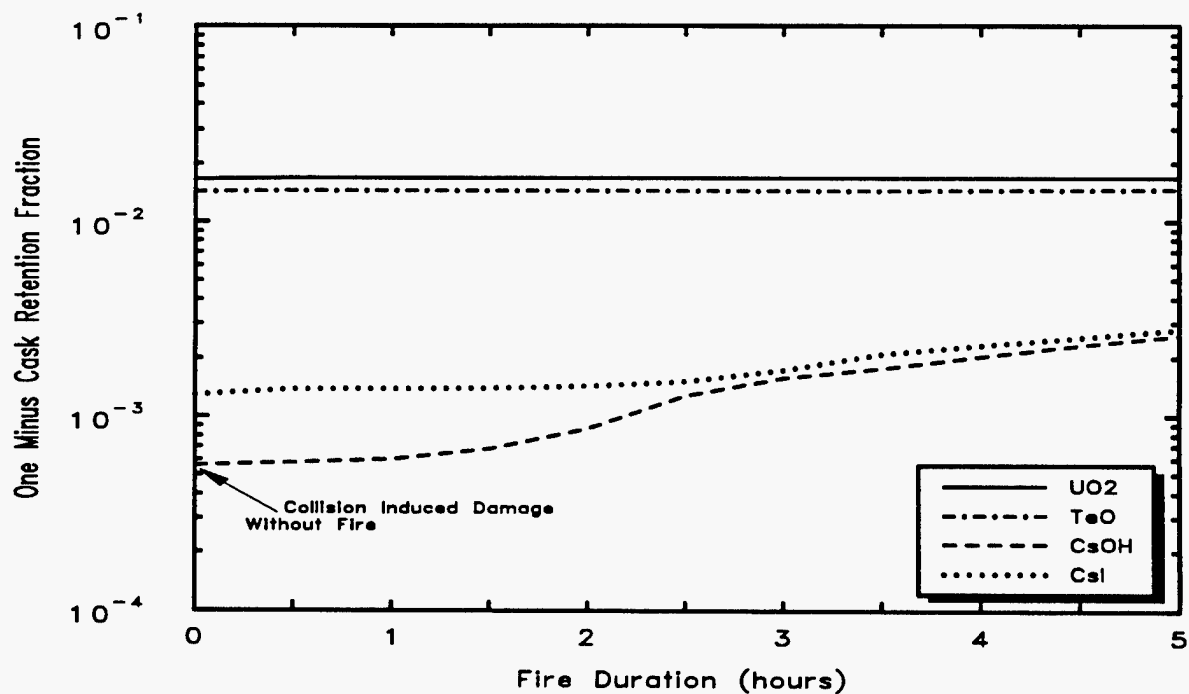


Figure 7-5b: Fire Enhancement of FP Transport

8.0 SUMMARY OF FINDINGS

The determination of risk associated with transporting spent PWR fuel in a TN-12 shipping cask includes the determination of the accident probability, fission product source term from the cask to the environment, and the consequences of that source term for a spectrum of accident scenarios. The key events associated with each accident scenario which govern the fission product source terms were the loss of integrity of the shipping cask, the extent of damage to the spent fuel rods, and the potential thermal challenge to the cask from a pool fire. Loss of integrity of the shipping cask would most likely come from the failure of the cask seal and the extent of that failure which was represented by the size of a postulated hole would strongly affect the magnitude of the fission product source term. The extent of damage to the spent fuel rods includes whether or not each of the 2448 fuel rods in a fully loaded cask fail by collision impact forces or thermally induced over pressurization and whether or not and to what extent the fuel pellets are fragmented by the collision forces. An accident involving a pool fire could enhance the fission product source term produced by the collision or the fire could directly cause the failure of the spent fuel rods by burst rupture and the loss of cask integrity by seal failure. The severity of the pool fire (i.e., fully or partial engulfing, temperature, and duration) are a function of the postulated accident conditions and therefore, are also probabilistic in nature. For example, a high temperature long duration fire may be possible for certain types of transportation accidents but also be extremely improbable.

The fission product source term for a given postulated accident scenario depends upon the spent fuel fission product inventory, the fraction of that inventory expelled from the fuel rods for each fission product species, the chemical forms of each species, and the fraction of each species expelled from the fuel rods that in turn escapes from the cask through the failed cask seal. The fission product inventory of a cask can be precisely calculated for aged spent fuel. The quantities of fission products that would be expelled from a ruptured fuel rod have been bounded reasonably well for spent fuel that has not been fragmented by collision impact forces but remains rather uncertain for spent fuel that is additionally fragmented by collision impact forces. In fact, the extent of any additional fragmentation depends upon the specific accident scenario postulated.

The subsequent transport of fission products from the shipping cask once expelled from the fuel rods was the primary focus of this study and the principal product of this study was insights into the ability of the shipping cask to retain these fission products after release to the cask interior from the rods. To achieve this goal, three basic accidents scenarios were postulated and the accident and transport modeling parameters most affecting the prediction of cask retention of fission products were varied to determine the effect of their uncertainty on the cask retention predictions.

These fission product transport insights generally indicate that a majority of the fission products, other than the noble gases, will likely remain within the cask except for some rather severe and improbable accident conditions that lead to catastrophic cask failures (large hole sizes). For accidents with only collision induced damage (i.e., no pool fire), a rather large sized failure of the cask seal was required to expel from the cask more than a few percent of the fission products that were expelled from the fuel rods into the interior of the cask. In addition, cask retention of fuel fines was not much increased by increased production of fuel fines by fragmentation of fuel during the collision. Retention of species (CsOH and CsI) that transported some significant fraction of the time as vapors was greater than that of fission products that transported (fuel fines) or almost always transported (TeO) as aerosols because deposition of these species when in vapor form onto cold surfaces was more efficient than deposition of aerosols onto all interior cask surfaces.

The transport of volatile forms of cesium from a cask where the integrity of the fuel rods and the cask was lost during a collision was enhanced by an accompanying pool fire but the enhanced cesium releases from the cask still did not exceed that of the fuel fines. The transport of fuel fines from the cask were not significantly affected by the postulated pool fire because the fines only existed as particulates.

The ability of the shipping cask to contain the volatile forms of cesium was greatly reduced when the failure of the cask was thermally induced by a postulated severe pool fire. This was shown by a base accident scenario that postulated that all of the fuel rods ruptured due to thermally induced overpressurization about 4 hours into the accident because of heating by a 1200 °C fully engulfing pool fire with a duration of 3 hours. The subsequent pressurization of the cask following the rupture of the rods was postulated to fail the cask seal that the heat from the

fire had thermally degraded. In this accident scenario, some 40% of volatile cesium was postulated to escape from the cask once expelled from the rods. However this scenario was not more severe than the collision scenarios because additional fragmentation of the fuel due to collision impact forces was not assumed to occur.

A potentially worst case but rather improbable scenario became apparent but not in time to be specifically included in the study. In this scenario, all of the spent fuel rods would be postulated to rupture and the fuel in the rods would sustain a high degree of additional fragmentation as a result of collision forces. But in contrast to the base collision scenarios studied, the shipping cask integrity would remain intact until the cask seal failed due to heating by a fire initiated by the collision. In this scenario, the volatile forms of cesium would be vaporized and exist as a gas in the cask atmosphere at the time the seal failed. Then, the depressurization of the cask would drive a large fraction of the cesium from the cask. This scenario could be much worse than the base scenario actually studied and discussed in the preceding paragraph because in this scenario, condensation of cesium species on cold cask surfaces is minimized and fuel fragmentation maximizes the amounts of aerosols available for release.

The final conclusion of this study was that for the most probable postulated transportation accident scenarios, most of the fission products expelled from the fuel rods would remain within the shipping cask should the integrity of the cask be compromised. At least one worst case scenario can be postulated for which the cesium source term to the environment could be rather severe, however the probability of this worst case scenario is likely rather small. Therefore its contribution to the overall transportation risk of transporting spent fuel would likely also be small.

9.0 REFERENCES

1. "TN-12 Safety Analysis Report", Transnuclear, Inc. Revision 1, April 30, 1979.
2. R. M. Summers, et. al., "MELCOR Computer Code Manuals," Volumes 1 and 2, NUREG/CR-6119, SAND93-2185, Sandia National Laboratories, September 1994.
3. B. E. Boyack, et. al., "MELCOR Peer Review," LA-12240, LANL, March 1992.
4. F. Gelbard, "MAEROS User Manual," NUREG/CR-1391, SAND80-0822, Sandia National Laboratories, December 1982.
5. H. Jordan, and M. R. Kuhlman, "TRAP-MELT2 Users Manual," NUREG/CR-4205, BMI-2124, May 1985.
6. T. L. Sanders, et. al., "A Method for Determining the Spent-Fuel Contribution to Transport Cask Containment Requirements," SAND90-2406, Sandia National Laboratories, November 1992.
7. "Zion Station Updated Final Safety Analysis Report," Commonwealth Edison Company, June 1992.
8. Code of Federal Regulations, Part 71, January 1, 1993.
9. N. R. Keltner, W. Gill, and L. A. Kent, "Simulating Fuel Spill Fires Under the Wing of an Aircraft," Fourth International Symposium on Fire Safety Science, Ottawa, Ontario, Canada, June 1994.
10. J. P. Holman, Heat Transfer, Second Edition, McGraw-Hill Book Company, 1963.
11. Chemical Engineering Handbook, John Perry Editor-in-Chief, 3rd Ed., 1950.
12. R. S. Siegel and J. R. Howell, Thermal Radiation Heat Transfer, Second Edition, McGraw-Hill Book Company, 1981.
13. L. E. Fischer, et. al., "Shipping Container Response to Severe Highway and Railway Accident Conditions," NUREG/CR-4829, UCID-20733, February 1987.
14. "Technical Basis for Estimating Fission Product Behavior During LWR Accidents," NUREG-0772, June, 1981.
15. G. W. Wilds, "Vaporization of Semi-Volatile Components from Savannah River Plant Waste Glass," DP-1504, August 1978.
16. R. C. Weast, Ed., Handbook of Chemistry and Physics, 56th Edition, CRC Press, 1975.
17. R. Lorenzelli, et. al., "Out of Pile Studies of Cesium With UO_2 , PuO_2 , and $(\text{U}, \text{Pu})\text{O}_2$," IAEA-SM-236/87, Translated from French by S. M. Kazed, Argonne National Laboratory, April 1979.
18. P. C. Reardon, Y. R. Rashid, and G. S. Brown, "On the Particle Size Distribution of Crushed Spent Fuel," Unpublished, Undated.
19. D. A. Powers, K. E. Washington, S. B. Burson, and J. L. Sprung, "A Simplified Model of Aerosol Removal by Natural Processes in Reactor Containments," NUREG/CR-6189, SAND94-0407, Sandia National Laboratories, July 1994.

ADDENDUM: REVISION TO RADIONUCLIDE SOURCE TIMING MODEL

Table of Contents

| | |
|--|------|
| AD.1 INTRODUCTION | AD-2 |
| AD.2 REVISED MODEL | AD-2 |
| AD.3 RESULTS OF REVISED BASE CASE CALCULATIONS | AD-4 |
| AD.4 RESULTS OF REVISED SENSITIVITY ANALYSES | AD-5 |
| AD.4.1 Sensitivity of Fuel Release Fraction | AD-5 |
| AD.4.2 Sensitivity of Cask Seal Failure Size | AD-5 |
| AD.5 CONCLUSIONS | AD-5 |

AD.1 INTRODUCTION

Several counterintuitive trends, discussed in Section 6.2, were discovered in the calculated results of this study, in particular, the cask retention of Kr was not the same as the cask retention of helium. It was determined that these trends were caused by the simplicity of the model used to introduce radionuclides into the calculation which simply introduced each radionuclide species into the fuel channels at uniform rate for a period of 100 seconds. This model was initially deemed adequate for calculations where the time required to depressurize the shipping cask was much greater than the time required to depressurize the fuel rods. Except for very large cask seal failures, the fuel rods would depressurize much faster than would the shipping cask.

The timing of radionuclide releases from breached fuel rods is not known, however, it is likely that the noble gases would be relatively uniformly mixed with the helium fill gas implying that the cask retention fractions for these two gases should be nearly identical. However the assumption that the other radionuclides, such as fuel fines, would be released in direct proportion with the helium gas is much less certain. Still, it would be more realistic and more intuitive to release all radionuclides in direct proportion with the helium gas than the uniform 100 second release model.

The fuel rod source term model was revised and implemented so that all radionuclide species were introduced into the fuel channels in direct proportion with the flow of helium through the rod breach. The three base cases and two of the single parameter sensitivity analyses were run again with the revised model. Project resources were not sufficient to rerun all of the calculations. In any case, the effect of the simplistic model did not have a major impact on the study conclusions.

AD.2 REVISED MODEL

The revised model introduces each radionuclide species into the fuel channels in direct proportion to the rate of helium flow from the fuel rod breach as shown by the following equation.

$$W_{RNi}(t) = \frac{W_{\text{helium}}(t)}{M_{\text{helium}}} \cdot M_{RNi}$$

where W_{RNi} = the time-dependent source rate for radionuclide species i,
 W_{helium} = the time-dependent rate at which helium purges from the failed fuel rods,
 M_{helium} = the total mass of helium purged from the failed fuel rods,
 M_{RNi} = the total mass of radionuclide species i sourced into the fuel channels.

The total helium purged from the failed fuel rods, as shown by the next equation, was determined using MELCOR, i.e., a preliminary run was made to determine the total helium purged which was then entered into the input model prior to running the actual calculation.

$$M_{\text{helium}} = \int_0^{\tau_{\text{end}}} W_{\text{helium}}(t) dt$$

The performance of the revised source model is compared to the original model in Figure AD-1. With the revised model, the bulk of the radionuclides are introduced into the calculation earlier than with the original model. Note that both curves in Figure AD-1 integrate to one.

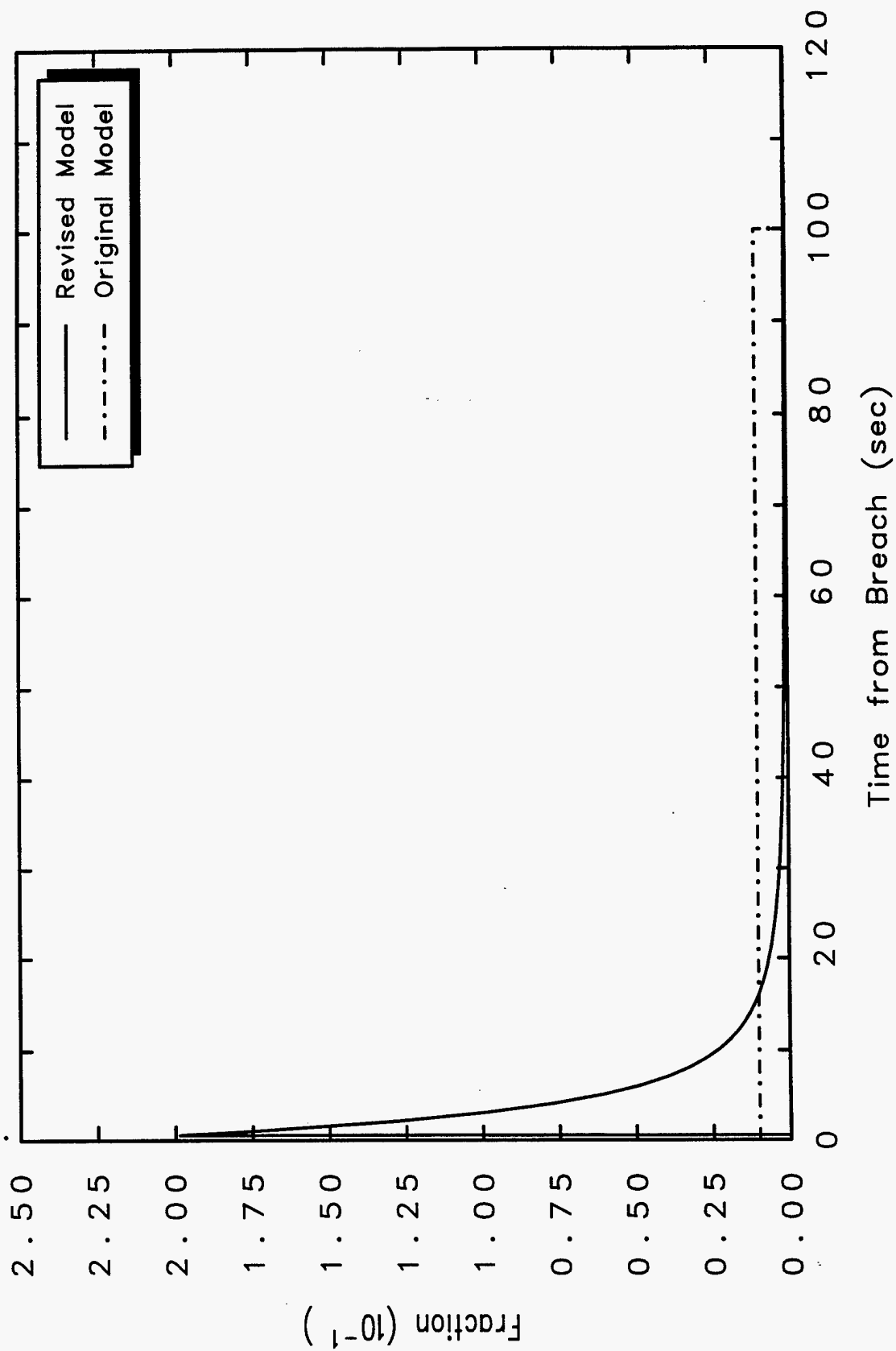


Figure AD-1: Normalized Radionuclide Source Rate

AD.3 RESULTS OF REVISED BASE CASE CALCULATIONS

The revised base case results are shown in Tables AD-1, AD-2, and AD-3 which replace the report Tables 6-2, 6-3, and 6-4, respectively. The revised results show a very close correlation between the cask retention for radioactive Kr and helium which was the primary objective of the model revision. Further, the effect of adding a fire to the collision scenario decreased Kr retention about the same for the 4mm² and the 100 mm² scenarios (~38% for both). Noting that the transport of radioactive Kr was predicted by the radionuclide transport models and the transport of helium was predicted by the thermal-hydraulic models, these results provide verification of the transport models as well as the input model for introducing radionuclide into the calculation.

Table AD-1: Base Scenario Results for a 4 mm² Cask Seal Leak Area

| FRACTIONS OF RADIONUCLIDES RETAINED WITHIN CASK | | | | | | |
|---|--------|--------|--------|--------|--------|------------|
| ACCIDENT SCENARIO | He | Kr | CsOH | CsI | TeO | Fuel Fines |
| Collision Without a Fire | 0.1882 | 0.1885 | 0.9986 | 0.9950 | 0.9577 | 0.9468 |
| Collision With a Fire | 0.1375 | 0.1374 | 0.9933 | 0.9894 | 0.9562 | 0.9458 |
| Fire Without a Collision | 0.1428 | 0.1406 | 0.6205 | 0.6130 | 0.6103 | 0.9220 |

Table AD-2: Base Scenario Results for a 100 mm² Cask Seal Leak Area

| FRACTIONS OF RADIONUCLIDES RETAINED WITHIN CASK | | | | | | |
|---|--------|--------|--------|--------|--------|------------|
| ACCIDENT SCENARIO | He | Kr | CsOH | CsI | TeO | Fuel Fines |
| Collision Without a Fire | 0.1935 | 0.1928 | 0.7686 | 0.7526 | 0.6895 | 0.6108 |
| Collision With a Fire | 0.1394 | 0.1390 | 0.7328 | 0.7201 | 0.6658 | 0.5835 |
| Fire Without a Collision | 0.1410 | 0.1400 | 0.3518 | 0.2992 | 0.2628 | 0.5672 |

Table AD-3: Base Scenario Fines Released to Environment

| FRACTIONS OF TOTAL FUEL MASS RELEASED TO ENVIRONMENT AS FINES | | |
|---|----------------------------------|------------------------------------|
| ACCIDENT SCENARIO | 4 mm ² Cask Seal Leak | 100 mm ² Cask Seal Leak |
| Collision Without a Fire | 1.06 x 10 ⁻⁵ | 7.78 x 10 ⁻⁵ |
| Collision With a Fire | 1.08 x 10 ⁻⁵ | 8.33 x 10 ⁻⁵ |
| Fire Without a Collision | 2.34 x 10 ⁻⁶ | 1.30 x 10 ⁻⁵ |

The cask retention of fuel fines decreased somewhat from the results using the original source model. About 3 times as many fuel fines were released to the environment for the 4 mm² cask leak and about 50% more were released for the 100 mm² leak. This decrease in cask retention due to the revised model was likely a result of more fines being transported from the fuel channels to the cask ends with initially rapid flow of helium. More fines in the cask upper end near the failed seal would result in more fines getting out.

AD.4 RESULTS OF REVISED SENSITIVITY ANALYSES

Two of the single parameter sensitivity analyses were run again to determine the effect of the revised model on these results. These sensitivity studies were: 1) the fraction of the fuel released from the rods into the cask as fuel fines, and 2) the size of hole in the failed cask seal.

AD.4.1 Sensitivity of Fuel Release Fraction

The revised results of the sensitivity of the fuel release fraction are shown in Figures AD-2a and AD-2b which can be directly compared to Figures 7-1a and 7-1b, respectively. The revised results are very similar to those of the original model, however, the plot scales were changed to accommodate the increased release of fuel fines to the environment.

AD.4.2 Sensitivity of Cask Seal Failure Size

The revised results of the sensitivity of the cask seal failure size are shown in Figure AD-3 which can be directly compared to Figures 7-2. Again the revised results are very similar to those of the original model. The upper end of the sensitivity range was increased to 1000 mm² compared to 100 mm² for the original study because of the expanded capability of the revised model. In the revised results, the curves for CsOH and CsI do not cross as they did in the original study, i.e., their crossing was an artifact of the simplicity of the original model.

AD.5 CONCLUSIONS

The revised results verify that the counterintuitive trends of the original calculations were generally caused by the over simplicity of the original source model. Although the results did change significantly in some specific numbers, the overall conclusions drawn from the original study remain valid. The trends shown in the sensitivity analyses not rerun are still valid although some of numbers would be expected to change. Thus, the study remains an effective demonstration of the ability of the shipping cask to retain a large fraction of the radionuclides purged from failed pressurized fuel rods.

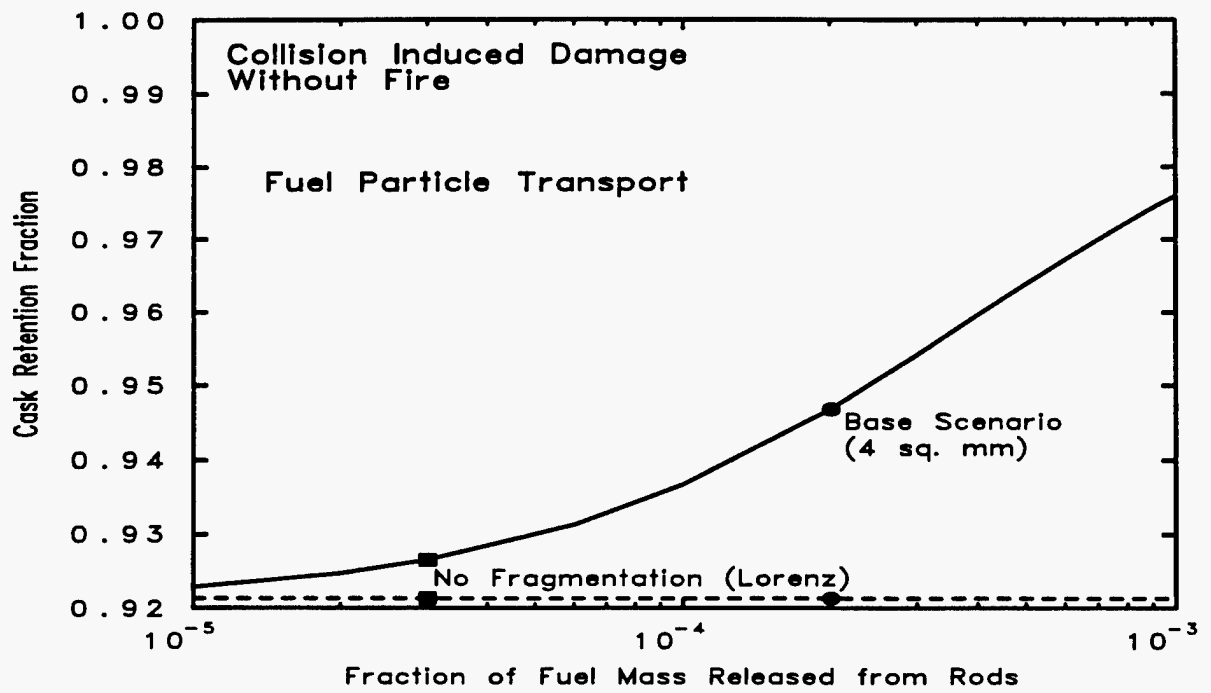


Figure AD-2a: Fuel Fragmentation Sensitivity

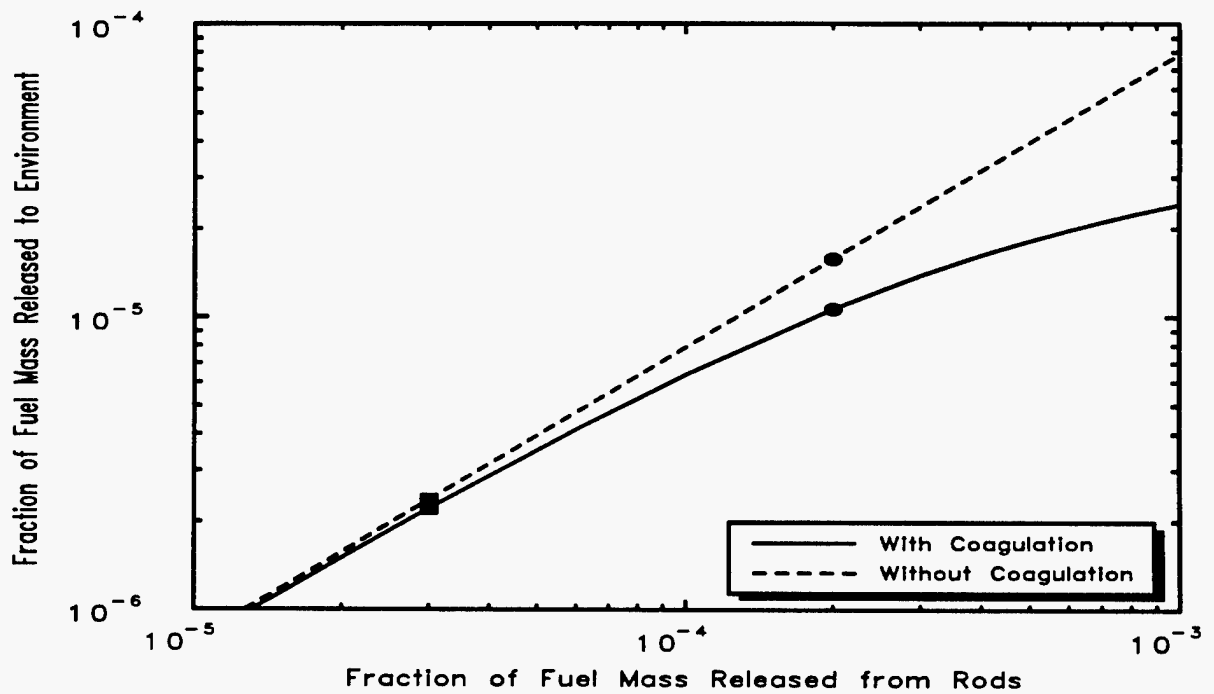


Figure AD-2b: Fuel Fragmentation Sensitivity

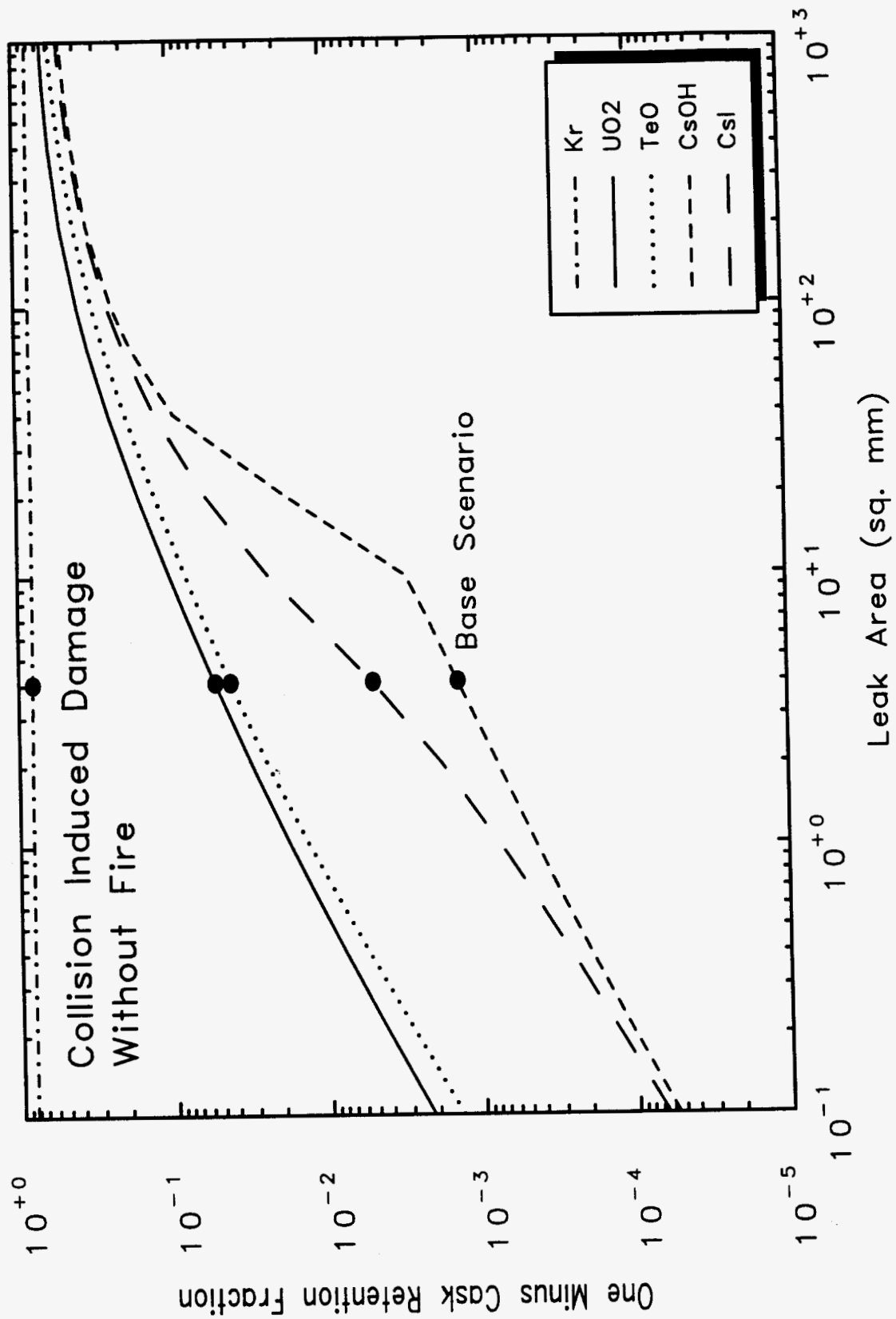


Figure AD-3: Cask Seal Failure Size Sensitivity

UNLIMITED RELEASE DISTRIBUTION

- 1 United States Department of Energy
Office of Scientific & Technical
Information
Attn: DOE/OSTI-4500-R74, UC722
Oak Ridge, TN 37830
- 1 United States Department of Energy
Attn: J. Sweeney, GC-51
1000 Independence SW
Washington, DC 20585
- 1 United States Department of Energy
Attn: C. Head, EM-60
1000 Independence SW
Washington, DC 20585
- 1 United States Department of Energy
Attn: D. Huizenga, EM-60
1000 Independence SW
Washington, DC 20585
- 1 United States Department of Energy
Attn: K. Chacey, EM-67
1000 Independence SW
Washington, DC 20585
- 3 United States Department of Energy
Attn: M. Keane, EM-76
K. Kelkenberg, EM-47
M. Wangler, EM-76
19901 Germantown Road
Germantown, MD 20874-1290
- 3 United States Department of Energy
Attn: J. Williams, RW-51
W. Lake, RW-45
C. Kouts, RW-45
Washington, DC 20545
- 6 United States Department of Energy
Albuquerque Operations Office
Albuquerque Headquarters
Attn: S. Hamp
B. Hermann
J. Holm
A. Kapoor
D. Krivitsky
M. Williams
P.O. Box 5400
Albuquerque, NM 87115
- 1 United States Department of Transportation
Hazardous Materials Safety
Attn: R. Boyle
Washington, DC 20590
- 1 United States Nuclear Regulatory
Commission
Nuclear Material Safety & Safeguards
Attn: E. Easton
11545 Rockville Pike
Rockville, MD 20852
- 1 International Atomic Energy Agency
Division of Radiation and Waste safety
Attn: Richard R. Rawl
Head, Transport safety Unit
Wagramerstrasse 5,
P.O. Box A-1400
Vienna
Austria
- 1 International Maritime Organization
Maritime Safety Division
Attn: Hartmut Hesse
Head, Cargoes and Facilitation Section
4 Albert Embankment
London, SE1 7SR
U. K.

- 1 British Nuclear Fuels Limited
Attn: Roger Cheshire
Senior manager, Terminals and Licensing
Risley
Warrington
Cheshire WA3 6AS
England
- 1 Edlow International Co.
Attn: Rod Fisk and Holly Tomasik
1666 Connecticut Avenue NW, Suite 201
Washington, DC 20009
- 1 Gesellschaft fur Anlagen und
Reaktorsicherheit (GRS) mbH
Attn: F. Lange
E. Hoermann
Schwertnergasse 1
D-50667 Koln
Germany
- 1 Hapag-Lloyd Container Linis GmbH
Attn: Christoph Zwanzleitner,
Containerservice Ballindamm 25
20095 Hamburg
Germany
- 1 MacGregor (USA) Inc.
Attn: Mike Jamer
20 Chapin Road, Unit 1012
Pine Brook, NJ
- 1 Nuclear Cargo & Service, GmbH and
Transkem Spedition GmbH
Attn: Holger Goncz
Rodenbacher Chaussee 6
D-63457 Hanau
Germany
- 1 Spliethoff's Bevrachtungskantoor B.V.
Attn: Hans Wouter Valk
Radarweg 36
1042 Amsterdam
Netherlands
- 3 Power Reactor and Nuclear Fuel
Development Corporation
Nuclear Material Control Division
Attn: T. Ito
K. Shibata
T. Yagi, Deputy Director
9-13, Akasaka, 1-Chome
Minato-Ku, Tokyo, 107-8445
Japan
- 1 Power Reactor and Nuclear Fuel
Development Corporation
Tokai Works
Technology Development Coordination
Division Nuclear Material Management
Section
Attn: T. Kitamura, General Manager
4-33 Muramatsu, Tokai
Ibaraki, 319-1112
Japan
- 1 F. Armingaud
ISPN/DSMR/SSTR
60-68, Av. du General Leclerc
B.P. No. 6
F-92265 Fontenay-aux-Roses
Cedex
France
- 1 A. J. Cappeto
Environmental Protection Specialist
Military Sealift Command, Atlantic
Military Ocean Terminal, Bldg. 42-4
Bayonne, NJ 07002
- 1 Nicole Dello
Department Etudes et Synthesis
Transnucleaire - Nusys
9, Rue Christoph Colomb
75008 Paris
France
- 1 B. Desnoyers
COGEMA
Service des Transport
B.P. No. 4
F-78141 Velizy Villacoublay
Cedex
France

- 1 Ann-Margret Ericsson
AMC Konsult AB
Kammakargatan 6
S-111 40 Stockholm
Sweden
- 1 B. Hall
Damage Control Officer
Military Sealift Command, Atlantic
Military Ocean Terminal, Bldg. 42-4
Bayonne, NJ 07002
- 1 M. Hussain
Nuclear Transport Limited
Risley, Warrington
Cheshire WA3 6AS
United Kingdom
- 1 Robert J. Heid
Engineering Computer Optecnomics, Inc.
1356 Cape St. Claire Road
Annapolis, MD 21401
- 1 E. P. Pfersich
Chief, Packaged Cargo Section
Hazardous Materials Branch
United States Coast Guard
2100 Second St. SW
Washington, DC 20593
- 1 P. C. Reardon
PCR Technologies
8416 Yeager Dr. NE
Albuquerque, NM 87109
- 1 R. C. Richards
U.S. Coast Guard R&D Center
1082 Shennecossett Road
Groton, CT 36615-1384
- 1 M. Claude Ringot
Cabinet d'Etudes Nucleaires
57 1, Les Monts Lories
91440 Bures-sur-Yvette
France

- 1 T. Schneider
CEPN
Service des Transport
B.P. No. 48
F-92263 Fontenay-aux-Roses
Cedex
France
- 1 Clinton J. Shaffer
ITS Corporation
6000 Uptown Blvd, NE, Suite 300
Albuquerque, NM 87110
- 1 Gheorghe Vieru
Institute for Nuclear Research
0300 Pitesti, P.O. Box 78
Romania
- 1 C. N. Young
Department of Transport
Floor 4/16
76 Marsham Street
London SW1P 4DR
United Kingdom

**SANDIA NATIONAL LABORATORIES,
INTERNAL DISTRIBUTION**

- | | |
|-----------|--|
| 1 MS0724 | J. B. Woodard, 6000 |
| 1 MS0715 | R. E. Luna, 6130 |
| 1 MS0766 | D. E. Ellis, 6300 |
| 1 MS0718 | F. L. Kanipe, 6341 |
| 1 MS0718 | G. S. Mills, 6341 |
| 1 MS0718 | S. K. Neuhauser, 6341 |
| 10 MS0718 | J. L. Sprung, 6341 |
| 1 MS0718 | R. F. Weiner, 6341 |
| 10 MS0718 | H. R. Yoshimura, 6341 |
| 1 MS0717 | D. J. Ammerman, 6342 |
| 1 MS0717 | G. F. Hohnstreiter, 6342 |
| 1 MS0717 | J. A. Koski, 6342 |
| 1 MS0977 | S. J. Bepalko, 6524 |
| 1 MS0977 | J. D. Smith, 6524 |
| 1 MS0720 | K. B. Sorenson, 6804 |
| 1 MS0720 | C. D. Massey, 6806 |
| 1 MS9018 | Central Technical Files, 8940-2 |
| 2 MS0899 | Technical Library, 4414 |
| 2 MS0619 | Review and Approval Desk, 12690, For DOE/OSTI |

M98005814



Report Number (14) SAND--98-117/2
TTC--1525/2

Publ. Date (11) 199805
Sponsor Code (18) DOE/EM, XF
UC Category (19) UC-2000, DOE/ER

ph

19980720 041

THIS QUALITY IMPROVED

DOE